

Towards Proactive Adaptive Vehicle Settings

Melman, T.

DOI

[10.4233/uuid:c6011a64-4c85-486c-abf7-bf4332543a16](https://doi.org/10.4233/uuid:c6011a64-4c85-486c-abf7-bf4332543a16)

Publication date

2022

Document Version

Final published version

Citation (APA)

Melman, T. (2022). *Towards Proactive Adaptive Vehicle Settings*. [Dissertation (TU Delft), Delft University of Technology]. <https://doi.org/10.4233/uuid:c6011a64-4c85-486c-abf7-bf4332543a16>

Important note

To cite this publication, please use the final published version (if applicable).
Please check the document version above.

Copyright

Other than for strictly personal use, it is not permitted to download, forward or distribute the text or part of it, without the consent of the author(s) and/or copyright holder(s), unless the work is under an open content license such as Creative Commons.

Takedown policy

Please contact us and provide details if you believe this document breaches copyrights.
We will remove access to the work immediately and investigate your claim.

TOWARDS PROACTIVE ADAPTIVE VEHICLE SETTINGS

- By Timo Melman

Towards proactive adaptive vehicle settings

by

Timo MELMAN

Towards proactive adaptive vehicle settings

Dissertation

for the purpose of obtaining the degree of doctor
at Delft University of Technology
by the authority of the Rector Magnificus, Prof. dr. ir. T.H.J.J. van der Hagen,
chair of the Board for Doctorates
to be defended publicly on
Friday 2 December 2022 at 12:30 o'clock

by

Timo MELMAN

Master of Science in Mechanical Engineering,
Technische Universiteit Delft, the Netherlands
born in De Ronde Venen, the Netherlands

This dissertation has been approved by the promotor.

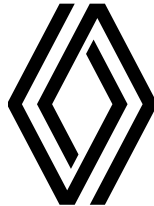
Composition of the doctoral committee:

Rector magnificus,	chairperson
Prof. dr. ir. D.A. Abbink,	Technische Universiteit Delft
Dr. ir. J.C.F. De Winter	Technische Universiteit Delft
Prof. dr. ir. A. Tapus,	ENSTA Paris

Independent members:

Prof. dr. O.M.J. Carsten,	Univeristy of Leeds
Prof. dr. D. de Waard,	Rijksuniversiteit Groningen
Prof. dr. ir. M.P. Hagenzieker,	Technische Universiteit Delft
Prof. dr. ir. M. Mulder,	Technische Universiteit Delft

Dr. X. Mouton of Groupe Renault has contributed greatly to the preparation of this dissertation.



Copyright © 2022 by T. Melman
An electronic version of this dissertation is available at
<http://repository.tudelft.nl/>

Cover and thesis design by Chardé Brouwer

TABLE OF CONTENTS

Summary / Samenvatting	8
CH 1. Introduction	16
Part 1. Improve the Fundamental Knowledge of Driver Adaptations	
CH 2. What Determines Drivers' Speed? A Replication of Three Behavioural Adaptation Experiments in a Single Driving Simulator Study	28
CH 3. How Road Narrowing Impacts the Trade-off Between Two Adaptation Strategies: Reducing Speed and Increasing Neuromuscular Stiffness	54
CH 4. Multivariate and Location-specific Correlates of Fuel Consumption: A Test Track Study	66
Part 2. Offline Changes in Vehicle Settings	
CH 5. How Do Driving Modes Affect the Vehicle's Dynamic Behaviour?	90
CH 6. Creating the Illusion of Sportiness: Evaluating Modified Throttle Mapping and Artificial Engine Sound for Electric Vehicles	108
CH 7. Do Sport Modes Cause Behavioral Adaptation?	132
Part 3. Online Changes in Vehicle Settings	
CH 8. Should Steering Settings be Changed by the Driver or by the Vehicle itself?	152
CH 9. A Proactive Method to Assist Eco-driving	168
CH 10. Conclusion and Discussion	186
Curriculum Vitae	198
List of Publications	200
Acknowledgements	202

Summary

In recent years cars are increasingly computerized, where the handling of the vehicle can be changed to accommodate individual needs. One specific feature in current vehicles that can alter the vehicle's dynamic behavior are driving modes: predetermined vehicle settings that drivers can select by the press of a button. Unfortunately user studies showed that the option to switch modes is underutilized. Possible explanations include mode confusion: drivers may not know when certain vehicle settings could be used best, or they may simply forget the current mode (or forget to change mode). Besides changing driving modes when the vehicle is stationary, driving modes offer the possibility to switch while driving. In theory, this could mean that during a sportier maneuver, such as curve driving or an overtaking maneuver, the driver benefits from dynamic vehicle settings. However, in practice, it is unlikely that drivers will select their preferred vehicle setting in dynamic driving situations or for short periods. A system that automatically changes the vehicle settings for the driver could potentially solve these issues.

The **aim of this dissertation** is to provide new quantitative and qualitative insights into the underlying principles to design a system with proactive adaptive vehicle settings: A system that automatically changes the vehicle settings to fit the individual and context-dependent needs of the driver.

Part 1. Improve the Fundamental Knowledge of Driver Adaptations

The first part of this thesis (Chap 2–4) investigates how people adapt to different road environments (road width and curvatures), task instructions, and car characteristics. This kind of knowledge would help to develop a system that adapts according to what the human driver would want when the location (where they drive), the target (i.e., eco vs. normal vs. sport), or the vehicle changes.

Chapter 2 conceptually replicates three highly-cited experiments on driver adaptations that could potentially predict speed adaptations following the introduction of changes to the road-vehicle-user system. In this study strong speed adaptations for varying road widths were found; however, none of the three well-cited homeostatic measures (i.e., experienced risk, experience effort, and safety margins) offered persuasive evidence for speed adaptation because they failed either the sensitivity criterion (i.e., the measure should increase/decrease if speed was held constant) or the constancy criterion (i.e., the measure should homeostatically be held constant if speed adaptations occurred).

Chapter 3 focuses on the potential interaction between two adaptation strategies when encountering a road narrowing: reducing speed or increasing neuromuscular stiffness of the arms. A trade-off between these two strategies was expected: for a short risk duration (operationalized by road narrowing length), drivers will favor increased neuromuscular stiffness over speed reduction; and vice versa for longer risk durations. The neuromuscular stiffness was quantified by measuring the grip force exerted by both hands. The results showed that all road narrowing conditions induced driver adaptations. However, the tested drivers did not consistently select the hypothesized different trade-offs for increasing duration of road narrowing: a low correlation was found between speed and grip force adaptations. Interestingly, individual trade-offs were consistent: the within-subject variability in speed-grip force adaptations was low across the tested risk durations.

Based on Chapters 2 and 3, it is likely that subjective measures (i.e., perceived risk) and physiological measures are too distant from the real driving task and generally suffer from a low signal-to-noise ratio to be practically useful. These results led to the notion that it is **important to measure driver adaptations** – rather than predicting using theories. **Chapter 4** gathers data for ninety-one drivers who drove a total of 4617 laps, in two vehicles (Renault Mégane or Renault Clio), on two test-track routes (a highway or a mountain road), and with two driving instructions (eco or sport). The results showed a strong predictive value for fuel

consumption for metrics related to speed, RPM, and throttle position; however, the largest variance was attributable to the route type. A subsequent location-specific analysis showed that the inter-driver variability in fuel consumption for the entire trip could already be predicted by measuring the instantaneous speed just after a single curve (i.e., the speed measured at a single curve had a good correlation with the fuel consumption of the total trip). Following this conclusion, throughout this thesis location-specific information has been accounted for in the analysis before investigating the intended effect of the conditions on driving behavior.

Part 2. Improve the Fundamental Knowledge of the Effect of Offline Vehicle Setting Changes on the Vehicle's Dynamic Behavior, Driving Behavior and Driver Experience.

The second part of the thesis (Chap 5–7) investigates how *offline* changes in vehicle settings (e.g., sound, powertrain settings, steering settings) affect the vehicle's dynamic behavior, driving behavior and driver experience. In this part, these questions are addressed for offline vehicle setting changes: changes that occur between driving trials and not while driving. In this way, transient effects in the data can be removed.

The current sport mode in the commercially available Renault Multi-Sense consists of several active components that jointly affect vehicle dynamic behavior. In literature their combined effect on the total vehicle's dynamic behavior for naturalistic driving on actual roads was unavailable. Therefore, **Chapter 5 provides empirical methodologies, metrics, and models to quantify this joint impact on longitudinal, lateral, and vertical vehicle dynamics.** The results showed strong vehicle dynamic behavioral differences in rear-wheel angle, engine torque, longitudinal acceleration, and vertical motion when driving with different vehicle settings. This goes beyond knowledge from literature, where the working principle of individual vehicle dynamical components is generally tested in a simulated environment or on test tracks but does not describe the actual effect on the vehicle's dynamic behavior for naturalistic driving, and for the vehicle dynamic components in congruence.

Chapter 6 and Chapter 7 systematically tested the effect on driving behavior and driver experience for various combinations of vehicle settings in an instrumented vehicle (Chap 7) and in a driving simulator study (Chap 6). Both chapters found increased sportiness perception when combining artificial engine sound and modified throttle mapping (a system that increases the acceleration performance given the driver's throttle input), and when presenting drivers with more agile four-wheel steering settings (a system that changes the steering responsiveness of the vehicle). Both in simulation and in the real world the increased sportiness perception did not result in any changes in speed. Other adaptations in driving behavior were observed, for example, drivers opportunistically used the increased available acceleration performance to accelerate more strongly to reach their target speed sooner (but the average speed remained the same).

Part 3. Improve the Fundamental Knowledge of the Effect of Online Vehicle Setting Changes on Driving Behavior and Driver Experience.

The final part of the thesis (Chap 8–9) combines all the learned principles from the previous chapters and investigates how *online* changes in vehicle settings affect driving behavior and driver experience.

Chapter 8 tests two interaction designs to adapt vehicle steering dynamics: (1) machine-initiated steering setting changes (i.e., proactively by the vehicle) and (2) driver-initiated steering setting changes (i.e., manually with a press of a button). This chapter showed that different driving situations (e.g., overtaking and curve driving vs. straight-line driving) require different steering dynamics. Both interaction designs objectively led to benefits for the driver over the entire route, compared to a non-adaptive, fixed steering sensitivity. Interestingly, even though the machine-initiated system resulted in less effort and

objectively higher performance increase than the driver-initiated system on average, some drivers still preferred the driver-initiated system. A likely explanation is that the driver-initiated condition gives drivers the freedom to choose, whereas they give away their freedom in the machine-initiated condition. In essence, if drivers want a fixed low (high) steering gain, they can select the low (high) steering gain setting at the start of their drive. That is, the driver-initiated condition can deliver what a fixed low and fixed high steering gain can deliver as well, whereas a machine-initiated system imposes the 'best' setting on the driver.

Chapter 9 combines all learned principles in a **patented proactive eco mode method**, which was implemented in a real vehicle and evaluated on a real road with expert drivers. This chapter describes the design and preliminary testing of a proactive eco mode that assists drivers in driving eco-friendly without being limited by the reduced acceleration performance to avoid turning off the eco mode (a commonly mentioned issue of the eco mode). This method used a pre-recorded database of location-specific driving behavior and road topology, in order to proactively switch mode at locations where acceleration is needed. Additionally, the system mitigates conflicts in case of misalignment with actual driver needs by overruling the proactive eco mode settings. The proactive eco mode was implemented in a Renault Talisman and tested with nine drivers driving on French roads. When driving with the proactive eco mode, the participants reached their target speed significantly faster while having similar energy consumption over the same distance compared to the non-adaptive eco mode. Moreover, all nine drivers rated the proactive eco mode as 'adding value' and rated the system as 'easier to reach a target speed' compared to the conventional non-adaptive eco mode. This chapter suggests that a proactive adaptive system can stimulate eco-driving (and its beneficial effects on energy consumption) by location-specific triggering of powertrain settings that facilitate acceleration.

Finally, this thesis contains multiple chapters, each of which describes its own individual scientific challenges, results, limitations, and conclusions. In **Chapter 10, the individual contributions are integrated towards overarching conclusions, limitations, and future work**. In short, five overarching conclusions were drawn:

1. Motivational driving models that use emotions or experiences as a construct are theoretically insightful but impractical; driving behavior could better be predicted by car state or location-specific variables.
2. A large part of the variability in driving behavior can be explained by location; location should be included in the design of an adaptive vehicle setting system.
3. The tested sport mode led to objectively more 'sporty' vehicle dynamics.
4. Sport mode settings are clearly perceived but do not cause speeding behavior.
5. Proactive adaptations of vehicle settings can objectively improve acceleration performance, lane-keeping, and steering performance, but are not always accepted by drivers.

Samenvatting

De laatste jaren worden auto's steeds geavanceerder, waarbij het rijgedrag van het voertuig kan worden aangepast aan individuele behoeften. In de huidige voertuigen is het mogelijk het dynamische gedrag van het voertuig aan te passen door verschillende rijmodussen: vooraf bepaalde voertuiginstellingen die bestuurders met één druk op de knop kunnen selecteren. Onderzoek onder gebruikers heeft helaas aangetoond dat de mogelijkheid om van modus te wisselen nauwelijks tot niet gebruikt wordt. Mogelijke verklaringen hiervoor zijn onder meer een 'modusverwarring' (oftewel: de onwetendheid over wanneer een bepaalde voertuiginstelling het beste kan worden gebruikt), het niet bewust zijn van de huidige rijmodus of het simpelweg vergeten aan te passen van de rijmodus. Rijmodussen bieden de mogelijkheid om zowel bij het stilstaan van het voertuig als tijdens het rijden van rijmodus te veranderen. In theorie zou dit kunnen betekenen dat de bestuurder tijdens een sportieve manoeuvre, zoals tijdens het rijden in bochten of bij het maken van een inhaalmanoeuvre, profiteert van dynamische voertuiginstellingen. Echter is het in de praktijk onwaarschijnlijk dat bestuurders hun favoriete voertuiginstelling zullen selecteren tijdens dynamische rijsituaties of voor een korte periode. Een systeem dat automatisch de voertuiginstellingen voor de bestuurder wijzigt, zou deze problemen mogelijk kunnen oplossen.

Het **doel van dit proefschrift** is om nieuwe kwantitatieve en kwalitatieve inzichten in beeld te brengen voor de onderliggende principes om een proactief adaptief systeem te ontwerpen: een systeem dat automatisch de voertuiginstellingen aanpast aan de individuele en contextafhankelijke behoeften van de bestuurder.

Deel 1. Het Verbeteren van de Fundamentele Kennis van Bestuurder Aanpassingen

Het eerste deel van dit proefschrift (hoofdstuk 2-4) onderzoekt hoe mensen zich aanpassen aan verschillende wegomgevingen (wegbreedte en bochten), taakinstructies en autokenmerken. Deze kennis draagt bij aan het ontwikkelen van een systeem dat zich aanpast aan de behoefte van de menselijke bestuurder wanneer de locatie (waar ze rijden), het doel (i.e., eco vs. normaal vs. sport) of het voertuig verandert.

Hoofdstuk 2 repliceert conceptueel drie veel geciteerde experimenten die mogelijke snelheidsaanpassingen zouden kunnen voorspellen na de introductie van veranderingen in de auto en/of weg. In deze studie werden sterke snelheidsaanpassingen gevonden voor verschillende wegbreedtes.

Geen van deze drie, tevens vaak naar gerefereerde, homeostatische signalen (i.e., experienced risk, experienced effort en safety margins) bood overtuigend bewijs voor snelheidsaanpassing. De verklaring hiervoor ligt bij het niet voldoen aan het 'gevoelheids criterium' (i.e., de waardes zou moeten toenemen/afnemen als de snelheid constant werd gehouden) of het 'constantheids criterium' (i.e., de waardes zouden homeostatisch constant moeten worden gehouden als snelheidsaanpassingen plaatsvonden).

Hoofdstuk 3 richt zich op de mogelijke interactie tussen twee aanpassingsstrategieën bij het tegenkomen van een wegversmalling: het verminderen van de snelheid of het vergroten van de neuromusculaire stijfheid van de armen. Aanvankelijk werd een interactie tussen deze twee strategieën verwacht: de bestuurders zullen voor korte duur (geoperationaliseerd door de lengte van de wegversmalling) de voorkeur geven aan verhoogde neuromusculaire stijfheid boven snelheidsvermindering; en vice versa voor langere duur. De neuromusculaire stijfheid werd gekwantificeerd door de grijpkracht van beide handen te meten. De resultaten toonden aan dat alle wegversmallingen leidden tot aanpassingen van de bestuurder. De proefpersonen kozen echter niet consequent voor de veronderstelde bestuurdersaanpassingen: er werd een lage correlatie gevonden in de aanpassingen in snelheid en grijpkracht. Opmerkelijk is de uitkomst dat de individuele compromissen consistent waren: de variabiliteit in snelheid/grijpkracht-aanpassingen onder de proefpersonen was laag in de geteste wegversmallingen.

Op basis van hoofdstukken 2 en 3 is het waarschijnlijk dat subjectieve signalen en fysiologische metrieken te ver verwijderd zijn van de werkelijke rijtaak en over het algemeen lijden aan een lage signaal-ruisverhouding om praktisch bruikbaar te zijn. Deze uitkomsten resulteerden in de gedachte dat het **essentieel is om aanpassingen van bestuurders te meten** in plaats van te voorspellen met behulp van theorieën. **Hoofdstuk 4** verzamelt gegevens van eenennegentig chauffeurs die in totaal 4617 rondes hebben gereden in twee voertuigen (Renault Mégane of Renault Clio), op twee testbaanroutes (een snelweg of een bergweg) en met twee rijmodussen (eco of sport). De resultaten toonden een duidelijk, voorspellend vermogen van het brandstofverbruik gebaseerd op snelheid, toerental en de stand van het gaspedaal; de grootste variatie was echter toe te schrijven aan het type route (snelweg vs. landweg). Een daaropvolgende, locatiespecifieke analyse toonde aan dat de variabiliteit in het brandstofverbruik tussen de bestuurders voor een gehele rit kon worden voorspeld door continu de snelheid net na een curve te meten (d.w.z. de gemeten snelheid van een enkele curve had een duidelijke correlatie met het brandstofverbruik van de totale rit). Gebaseerd op deze uitkomsten is in dit proefschrift bij het maken van analyses rekening gehouden met locatiespecifieke informatie, voordat het beoogde effect van de omstandigheden op het rijgedrag is onderzocht.

Deel 2. Het Verbeteren van de Fundamentele Kennis van het Effect van Offline Veranderingen in Voertuiginstellingen op het Dynamische Gedrag, het Rijgedrag en de Rijervaring van het Voertuig.

Het tweede deel van dit proefschrift (hoofdstuk 5-7) onderzoekt hoe *offline* veranderingen in voertuiginstellingen (bijv. geluid, motorinstellingen, of stuurinstellingen) het dynamische gedrag, het rijgedrag en de rijervaring van het voertuig beïnvloeden. In dit deel worden de vragen over offline wijzigingen in voertuiginstellingen behandeld: veranderingen die plaatsvinden tijdens testritten en niet tijdens het rijden. Hierdoor worden dynamische effecten die optreden tijdens een modusverandering niet meegenomen in de analyse.

De huidige sportmodus in de commercieel verkrijgbare Renault Multi-Sense bestaat uit meerdere actieve componenten die gezamenlijk het dynamische rijgedrag van de auto beïnvloeden. In de literatuur was er geen informatie beschikbaar over de invloed van de verschillende, gelijktijdig gebruikte systemen van het voertuig op het rijden op echte wegen. Om die reden biedt **Hoofdstuk 5 empirische methodologieën, metrieken en modellen om deze gezamenlijke impact op de longitudinale, laterale en verticale voertuigdynamica te kwantificeren**. De resultaten toonden sterke verschillen in achterwielhoeken, motorkoppel, longitudinale versnellingen en verticale bewegingen bij het rijden met verschillende voertuiginstellingen. Deze uitkomsten gaan verder dan de kennis vernomen uit de literatuur, waar het werkingsprincipe van individuele voertuigcomponenten over het algemeen wordt getest in een gesimuleerde omgeving of op een testbaan, maar waarin niet wordt beschreven wat het daadwerkelijke effect op het dynamische gedrag van het voertuig en samenhangende componenten bij het rijden op een echte weg is.

In **Hoofdstuk 6 en Hoofdstuk 7 is het effect van verschillende combinaties in voertuiginstellingen op rijgedrag en rijervaring systematisch getest** in zowel een geïnstrumenteerd voertuig (hoofdstuk 7) als in een rijimulatoronderzoek (hoofdstuk 6). Beide hoofdstukken vonden een verhoogde sportbeleving bij het combineren van kunstmatig motorgeluid en het aanpassen van de 'throttle mapping' (een aanpassing die de acceleratieprestatie van de auto verbeterd ten opzichte van de pedaalinput van de bestuurders) en bij het veranderen van de 'four-wheel steering'-instellingen (een systeem dat de stuurresponsie van het voertuig verandert). Zowel in simulatie als in de echte wereld resulteerde de toegenomen sportbeleving niet in snelheidsveranderingen. Er werden echter wel andere veranderingen in rijgedrag waargenomen, waaronder het opportunistische gebruik van bestuurders van de verhoogde beschikbare acceleratie prestaties om sterker te accelereren om hun beoogde

snelheid eerder te bereiken.

Deel 3. Verbeter de Fundamentele Kennis van het Effect van Online Wijzigingen in Voertuiginstellingen op het Rijgedrag en de Rijervaring.

Het laatste deel van dit proefschrift (hoofdstuk 8-9) brengt alle geleerde principes uit de vorige hoofdstukken samen en onderzoekt hoe *online* veranderingen in voertuiginstellingen het rijgedrag en de rijervaring beïnvloeden.

Hoofdstuk 8 test twee interactie ontwerpen van een systeem dat de stuurresponsie van het voertuig aanpast: (1) machine-geïnitieerde veranderingen in stuurinstellingen (d.w.z. proactief door het voertuig) en (2) bestuurder-geïnitieerde veranderingen in stuurinstellingen (d.w.z. handmatig met een druk op de knop). Dit hoofdstuk liet zien dat verschillende rijsituaties (bijvoorbeeld inhalen en rijden in bochten vs. rechtdoor rijden) verschillende stuurinstellingen vereisen. Beide interactieontwerpen leidden objectief tot voordelen voor de bestuurder over het gehele traject, vergeleken met een niet-adaptieve, vaste stuurinstelling. Interessant is dat hoewel het door de machine-geïnitieerde systeem gemiddeld tot minder inspanning en objectief hogere prestatie leidde dan het door de bestuurder-geïnitieerde systeem, sommige bestuurders toch de voorkeur aan het door de bestuurder-geïnitieerde systeem gaven. Een vermoedelijke verklaring is dat de bestuurder-geïnitieerde conditie bestuurders de vrijheid geeft om te kiezen, terwijl ze in een machine-geïnitieerde conditie deze vrijheid niet hebben. Als bestuurders een vaste lage (/hoge) stuurversterking wensen, kunnen ze in wezen de instelling voor lage (/hoge) stuurinstelling selecteren aan het begin van hun rit. Dat wil zeggen: de door de bestuurder-geïnitieerde conditie kan zowel een vast lage als een vast hoge stuurinstelling hebben, terwijl een door de machine-geïnitieerd systeem de bestuurder de 'beste' instelling oplegt.

Hoofdstuk 9 combineert alle geleerde principes in **een gepatenteerd proactieve eco-modus methode**, die werd geïmplementeerd in een echt voertuig en is geëvalueerd op een echte weg met deskundige chauffeurs. Dit hoofdstuk beschrijft het ontwerp en de voorlopige experimenten van een proactieve eco-modus, die bestuurders ondersteunt in milieuvriendelijk rijden zonder te worden beperkt door de verminderde acceleratieprestaties van het voertuig. De voornaamste reden hiervoor is het voorkomen dat de eco-modus wordt uitgeschakeld (dit is een vaak genoemd probleem van de eco-modus). Deze methode maakte gebruik van een vooraf opgenomen database van locatiespecifiek rijgedrag en weginformatie, om proactief van modus te wisselen op locaties waar acceleratie nodig is. Bovendien vermindert het systeem conflicten in het geval van een verkeerde afstemming op de werkelijke behoeften van de bestuurder door de proactieve instellingen voor de eco-modus te negeren. De proactieve eco-modus was geïmplementeerd in een Renault Talisman en is getest met negen chauffeurs rijdend op Franse wegen. Bij het rijden met de proactieve eco-modus bereikten de deelnemers hun doelsnelheid aanzienlijk sneller terwijl ze over dezelfde afstand een vergelijkbaar energieverbruik hadden in vergelijking met de niet-adaptieve eco-modus. Bovendien beoordeelden alle negen bestuurders de proactieve eco-modus als een 'toegevoegde waarde' en het 'vergemakkelijken van het bereiken van een snelheidsdoel' in vergelijking tot de conventionele, niet-adaptieve eco-modus. Dit hoofdstuk suggereert dat een proactief adaptief systeem eco-rijden kan stimuleren (en de gunstige effecten ervan op het energieverbruik) door middel van het veranderen van motorinstellingen gebaseerd op de locatie.

Tot slot bevat dit proefschrift meerdere hoofdstukken, die elk hun eigen individuele wetenschappelijke uitdagingen, resultaten, beperkingen en conclusies beschrijven. **In Hoofdstuk 10 worden de individuele bijdragen geïntegreerd in overkoepelende conclusies**, beperkingen en toekomstig werk. In het kort werden vijf overkoepelende conclusies getrokken:

-
1. 'Motivational driving models' die emoties of ervaringen als basis gebruiken, zijn theoretisch inzichtelijk maar onpraktisch; rijgedrag kan gerichter worden voorspeld door middel van voertuig variabelen of locatiespecifieke variabelen.
 2. Een groot deel van de variabiliteit in rijgedrag is te verklaren door de locatie. Locatie moet worden opgenomen in het ontwerp van een adaptief voertuigstelsel.
 3. De geteste sportmodus leidde tot objectief meer 'sportieve' voertuigdynamica.
 4. De instellingen van de sportmodus worden duidelijk waargenomen, maar veroorzaken geen snelheidsverhogingen.
 5. Proactieve aanpassingen van voertuiginstellingen kunnen objectief de acceleratieprestatie, lane-keeping en de stuurprestatie verbeteren, maar worden niet altijd geaccepteerd door de bestuurder.

Introduction



1.1. From Passive Vehicle Dynamics to Active Vehicle Dynamics

Since the first steam-powered automobile, manufacturers have attempted to improve driver comfort and vehicle stability. A substantial contribution was made in the early 1900s by the introduction of particular vehicle dynamics (VD) components, including the suspension system and power steering. For example, the suspension system, consisting of springs, dampers, and linkages, separates the car body from the wheel assembly, thereby reducing road vibrations in the car body and ensuring good contact between the tyres and road surface for the driver (Anubi, 2013; Savaresi et al., 2010).

At that time, all VD components were *passive*: mechanically determined and invariant. Passive vehicle dynamics components are designed to be functional in a wide range of driving situations and a wide variety of driving speeds. Although passive VD components have been a proven concept for many decades, this concept is not necessarily optimal. The main issue is that different driving situations may benefit from different behavior of the vehicle. For lateral vehicle dynamics behavior a speed-dependent trade-off exists: a low-gain steering system is preferable at high speeds, whereas at low speeds, a high-gain steering system is preferred to accommodate parking maneuvers (Reuter & Saal, 2017). Similarly, for vertical vehicle dynamics behavior, there is a trade-off between driver comfort and vehicle stability: soft suspension generally improves comfort while a hard suspension improves vehicle handling (Sekulić & Dedović, 2011; Sharp & Crolla, 1987).

To improve driver comfort and stability further for all situations, car manufacturers introduced *active VD components*. Active VD components allow the VD behavior to be changed while driving. Examples include the active suspension (i.e., springs and dampers), the active drivetrain, and the active steering system (Figure 1.1; Crolla, 1996; Shibahata, 2005). The active suspension utilizes variable damping and variable stiffness to change the vertical dynamic behavior of the vehicle. A number of current commercialized vehicles are equipped with active damping, while variable stiffness is a concept that is currently still in a research phase (Anubi, 2013; Morales et al., 2018). The active drivetrain may facilitate adjustments in engine characteristics, throttle mapping, and gear changing control to achieve better acceleration performance (Hosoda, 2010) at the cost of higher fuel consumption. The active steering system can enable speed-dependent change of a vehicle's lateral response, reduce steering effort, and increase stability (Abe, 2013; Cho et al., 2012; Huang & Pruckner, 2017; Klier et al., 2004). Several active steering systems exist including four-wheel steering (4WS), active front steering, steer-by-wire, and direct yaw control (Fahimi, 2013; Shibahata, 2005).

1.2. Driving modes: Predetermined Vehicle Settings the Driver can Select

Besides changing the VD settings as a function of driving speed and road surface, active VD components have opened the door to new possibilities where the handling of the vehicle can be adapted to accommodate individual needs. To this end, car manufactures have introduced driving modes: predetermined vehicle settings that drivers can select by the press on a button.

In general, four driving modes are considered: comfort mode, eco mode, sport/dynamic mode, and personal mode, where the latter mode allows the driver to set different combinations of vehicle settings (e.g., eco steering with a sport powertrain) (Sheller, 2004; Shibahata, 2005). According to manufacturers, the comfort mode “favours smooth steering” (Renault, 2022) and is developed for a “comfortable and economical driving style” (Mercedes-Benz, 2022), whereas the sport mode “permits an increased responsiveness from the engine and



Figure 1.1. Overview of active vehicle dynamic components that can alter the vehicle dynamics.

the gearbox” (Renault, 2022) for a “sporty driving style” (Mercedes-Benz, 2022). A detailed description is currently missing of how the active VD component parameters are affected by the current commercialized driving modes. Literature argues that a more sporty behavior could be achieved, for example, by adjusting the gear-changing map (Schoeggel et al., 2001), shortening the gear shifting period (Achleitner et al., 2005), and increasing the throttle responsiveness (Hosoda, 2010). Furthermore, the suspension dynamics are considered more sporty when they are stiffer along with stronger dampers (Hilgers et al., 2009; Kim et al., 2005; Wimmer et al., 2014), and the steering dynamics when the vehicle is more agile (Cho et al., 2012; Huang & Pruckner, 2017).

In addition to VD changes, the driving modes are complemented with changes in the cockpit ambience, such as changes in sound (e.g., engine sound enhancement in sport mode and noise canceling in comfort mode; Sontacchi et al., 2015), visuals (e.g., changes in ambient lighting and instrument cluster; Helander et al., 2013; Jindo & Hirasago, 1997), and haptics (e.g., changes in seat position and steering forces; Fankem & Müller, 2014; Kamp, 2012). It is possible that the psychological effects induced by cockpit ambience manipulations are equally important to the perception and the understanding of driving modes compared to the changes in vehicle behavior.

1.3. Underutilization of Driving Modes

Although driving modes offer the driver a level of personalization, user studies showed that the option to switch modes is underutilized. An internal report of Renault indicated that 34% of 300 Renault car drivers never switched driving modes. Possible explanations include mode confusion: drivers may not know when certain vehicle settings could be used best, or simply forget the current mode (or forget to change mode).

Besides changing driving modes when the vehicle is stationary, driving modes offer the possibility to switch *while* driving. In theory this would mean that during a sportier maneuver, such as curve driving or an overtaking maneuver, the driver might benefit from the dynamic vehicle behavior in sport mode. However, in practice it is unlikely that drivers will select their preferred driving mode in dynamic driving situations or for short periods. For example,

even though the sport mode might allow for faster and sportier driving during an overtaking maneuver, it is not easy or practical for drivers to switch mode while keeping their eyes on the road at the same time. This corresponds to results from the above mentioned Renault report, which indicated that 78% of the drivers do not use the ‘quick switch’ functionality—a functionality where two modes can be switched while driving.

In addition, the selected modes and the requirements for mode selection of such auto-adaptive systems are predefined and static; the vehicle settings adapted per mode are set beforehand and do not allow for within-mode personalization (e.g., do not allow the driver to choose a powertrain setting that is between the predefined ‘sport’ and ‘normal’ setting). It is likely that different drivers and different situations require different (combinations of) vehicle settings. For example, the agile vehicle – associated with the sport mode – could also be beneficial for city driving.

1.4. Automatically Selecting Driving Modes

The driving mode usability could be improved by automatically switching vehicle settings. Currently, systems are being developed that automatically switch between modes by BMW (Ilmberger, 2014), Audi (Schön, 2018), and Renault (Mouton et al., 2016). These systems propose a switch between driving modes based on the observed driving behavior in the past: if the driver’s recent behavior was ‘sporty’, the driving mode switches to a sport mode and if the driver is driving economically, an eco mode is selected.

While such systems may help drivers to select driving modes that fit their behavior, they act on the driver’s previous needs and might fail to take the driver’s needs in the near future into account and neither select combinations of vehicle settings. For example, the eco mode might lack the power to achieve the desired speed when merging into a highway. The driver might require a switch to a higher engine power just *before* and during the highway entrance to help accelerate, not after merging as current adaptive systems would recommend. In other words, the settings do not just need to adapt, but *proactively* adapt (i.e., based on the road ahead). Such a proactive principle of preview is a widely known concept in the field of driver modeling (e.g., Kolekar, 2021), path planning for autonomous vehicles (e.g., Rahiman & Zainal, 2013; Schwarting et al., 2018), and other advanced driver assistance systems such as lane-keeping assistance (e.g., Abbink et al., 2012). This thesis explores the potential for a so-called proactive adaptive vehicle setting, where the vehicle settings are automatically adapted to fit the individual and (future) context-dependent needs of the driver.

To successfully develop an adaptive system that is accepted by the driver, well-known challenges of human-centered adaptive automation – in which a human driver is still in the control loop – need to be addressed (Johnson et al., 2014; Kaber & Endsley, 2004; Kaber et al., 2001; Parasuraman, 2000). Inappropriate design of adaptive automation can negatively impact driver safety, efficiency, and driver acceptance (Byrne & Parasuraman, 1996; Parasuraman, 2000). Examples of inappropriate design include not keeping the driver engaged in the control loop, not informing the driver of the automation’s functioning, or not being responsive to the driver’s direct control input (Abbink et al., 2018; Melman et al., 2020). Russell et al. (2016) showed that automatically changing the VD behavior is challenging and does not come without risk. The authors showed that if the steering dynamics change without informing the driver, a substantial adaptation time is needed before they return to their previous steering behavior.

Another important design aspect is the way the switch is initiated. Miller and Parasuraman (2007) argued that there is a trade-off between human workload and unpredictability in machine-initiated and driver-initiated systems. Kidwell et al. (2012) showed that machine-initiated systems tend to reduce the human workload by decreasing the user involvement as a result of decreased responsibility in system control, but are also more unpredictable. On

the other hand, driver-initiated systems tend to increase the cognitive demand since there is an increase in the user's responsibility for system supervision.

1.5. Scientific Challenges for a Proactive Adaptive Vehicle Setting System

The scientific challenges to design a proactive adaptive vehicle setting system can be divided in three parts, and will be described in more detail below. The interplay of the parts is visualized in Figure 1.2.

Part 1: There is limited knowledge about the fundamental mechanisms of driver adaptations

What will happen when the vehicle settings continuously adapt to the driver and the environment? Before being able to address this question of a dynamically adapting system, we first need to understand the underlying mechanisms of driver adaptations to different environments (i.e., road width and curvatures), task instructions and vehicle characteristics. This kind of knowledge would help improve the understanding of why drivers drive as they do in case the location (where they drive), their target (i.e., eco vs. normal vs. sport) and the driving mode (sound, powertrain settings, steering settings) changes.

Several theories exist that aim to predict driver adaptations following the introduction of changes to the road-vehicle-user system. These theories postulate that drivers exhibit a trade-off between two conflicting motivations, namely arriving at a destination in time (efficiency) versus avoiding dangerous situations (safety), where the driver's level of subjective risk (Näätänen & Summala, 1974; Wilde, 1998), task difficulty (Fuller, 2005), or time/safety margins (Gibson & Crooks, 1938; Van Winsum et al., 2000) are regarded as important homeostatic variables. Melman et al. (2018) showed that these theories could be used to make predictions

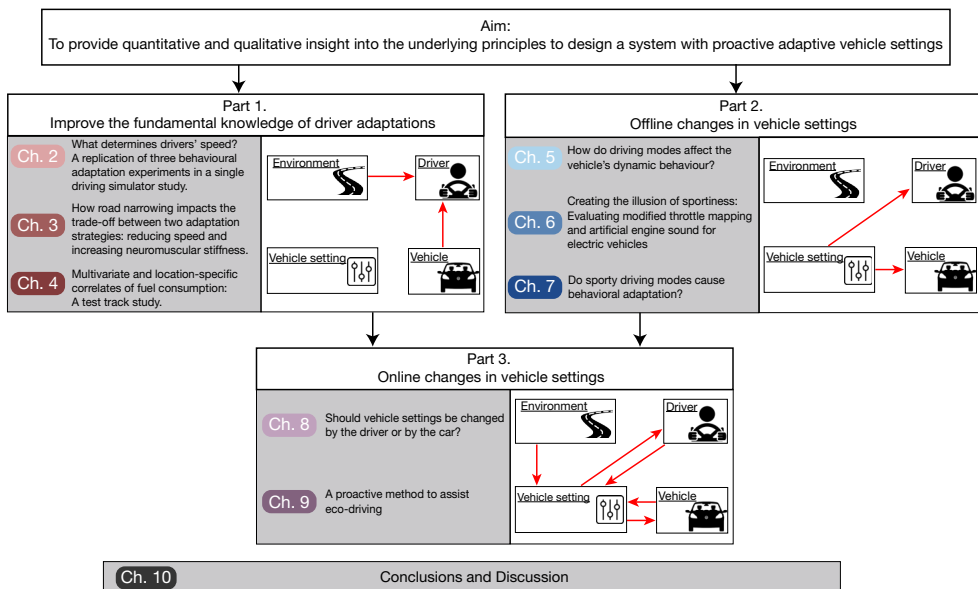


Figure 1.2. Schematic overview of the three main research parts of this thesis, and their respective chapters. Note that the theoretical and empirical knowledge obtained in Parts 1 and 2 was used to develop the prototypes in Part 3.

about speed adaptation for a well-defined driving situation, but it is unclear how accurate these theories are nor if these theories can practically be used for less controlled situations.

Besides predicting driver adaptations, it is important to understand how to capture driving behavior and at what time or location. It is essential to understand how to quantify driving behavior, and if this should be described on a trip level or on a meter-to-meter basis? If this is clear, the measured driving behavior has the potential to be used as a trigger for an adaptive algorithm.

Part 2: There is limited knowledge about the effect of offline vehicle setting changes on the vehicle's dynamic behavior, driving behavior and driver experience.

Even though driving modes exist in current vehicles, it is unclear how the underlying vehicle settings changes affect the vehicle's dynamic behavior and how drivers perceive and react to these dynamic changes. In literature, the working principle of individual VD components is generally tested in a simulated environment or on test tracks (Hilgers et al., 2009; Jeon et al., 2016). While these studies show the potential of these individual components in a controlled environment, the actual effect on the vehicle's dynamic behavior for naturalistic driving, and for the VD components in congruence, remains unclear.

From the driver perspective, it is unclear how important the contribution of the vehicle's behavioral changes are compared to the sound changes for the driving performance and driving experience. On top of this, it is unclear if the different vehicle settings cause drivers to adapt their behavior. In scientific literature, there are indications that drivers show adverse behavioral adaptations, when driving in more sportive conditions. For example, speeding has been found for sports cars that have a higher maximum engine power compared to vehicles with lower engine power (e.g., Horswill & Coster, 2002; Krahé & Fenske, 2002). Similarly, for the sport mode, it can be hypothesized that the increased perceived sportiness causes drivers to drive faster. On the other hand, it can be argued that sporty vehicle settings increase drivers' perceived danger due to the increased feedback received (e.g., increase in engine sound and vibrations), and hence, cause a reduction in driving speed.

Part 3. There is limited knowledge about the effect of online changes in vehicle settings on driving experience and driving behavior.

Third, and finally, the complex question of online adaptive systems, in which vehicle settings proactively change while driving, need to be considered. Currently, there is no information about the transient effects of changing vehicle settings on the closed-loop driver-vehicle behavior. Do proactive adaptive vehicle settings improve driver acceptance, safety and performance compared to the non-adaptive vehicle settings? Should changes in vehicle settings be made by the driver or automatically by the car? What will happen if you allow drivers to make their own manual switches in vehicle settings and give them proper instructions on how to switch: will drivers switch?

1.6. Thesis Aim

This dissertation aims to provide new quantitative and qualitative insights into the underlying principles to design a system with proactive adaptive vehicle settings: A system that automatically changes the vehicle settings to fit the individual and context-dependent needs of the driver.

1.7. Context and Approach

This dissertation is a collaboration between Group Renault, ENSTA Paris and the Delft University of Technology. In this collaboration, I made use of TU Delft's lab experiments and Renault's test facilities, vehicles and driving modes. The driving mode, highlighted in this dissertation, is Renault's Multi-Sense®. The Multi-Sense modes (i.e., comfort, sport, eco, MySense) impact not only parameters concerning the vehicle dynamics (e.g., adaptations in rear-wheel steering, drivetrain, and dampers), but also cockpit ambience (e.g., engine sound enhancement, color of ambient lighting, and dashboard interface) (Renault, 2022).

This dissertation is divided according to the three scientific challenges described in Section 1.5.

Since this thesis aims to develop a system that adapts according to what the human driver would want, the first step is to understand how and why humans adapt their driving behavior. For this reason, Part 1 (Chap 2–4) aims to get a better understanding of the fundamental mechanisms behind driver adaptations to environmental changes and to vehicle characteristics.

- **Chapter 2** conceptually replicates three highly cited experiments on driver adaptations.
- **Chapter 3** focuses on the interaction between two adaptation strategies when encountering a road narrowing (i.e., reducing speed or increasing neuromuscular stiffness of the arms).
- **Chapter 4** looks into how people adapt to instructions that correspond to mode changes. More specifically, we instructed drivers to adopt a normal or eco driving style and probed which metrics were able to capture this behavior best. This chapter investigated triggers that are suited for offline mode changes (advice that is based on the trip level or based on the driver's profile), but also for online mode changes (i.e., calculated on a meter-to-meter basis).

Part 2 (Chap 5–7) depicts the effect of offline changes in vehicle settings on the vehicle's dynamic behavior, driving behavior and driver experience. In this part, these questions are addressed for offline vehicle setting changes: changes that occur between driving trials and not while driving. In this way, transient effects in the data can be removed.

- **Chapter 5** provides quantitative insight into the extent to which the Multi-Sense driving modes impact the vehicle's lateral, longitudinal and vertical dynamic behavior. These results combined with the analysis method may help guide the future driving mode design explained in the following chapters.
- **Chapter 6** looks into how modified throttle mapping and artificial engine sound enhancement impact drivers' sportiness perception and driving behavior. A fixed-based driving simulator was used to test the effect in a controlled environment.
- **Chapter 7** builds on the experimental protocol used in *Chapter 6*. This chapter investigates the effect of different combinations of sport mode settings on driving behavior and driver experience. Specifically, it is hypothesized that the sport mode increases perceived sportiness and encourages faster driving. Oppositely, the sport mode may increase drivers' perceived danger, causing them to homeostatically drive more slowly. These hypotheses were tested using an instrumented vehicle on a test track.

Finally, Part 3 (Chap 8, Chap 9) combines all the learned principles and investigates the effect of online changes in vehicle settings on driving behavior and driver experience.

- **Chapter 8** tests two interaction designs to adapt vehicle steering dynamics: machine-initiated steering setting changes (i.e., proactively by the vehicle) and driver-initiated steering setting changes (i.e., manually with a press on a button).

- **Chapter 9** combines all learned principles in a patented proactive eco mode method, which was implemented in a real vehicle and evaluated on a real road with expert drivers.

Of note, except for the introduction and discussion, each chapter contains a paper that is either submitted or published, and they have been preserved in their original format. Therefore, the earlier published papers (Chap 2–5) are written in British English, whereas the later published papers are written in American English (Chap 1, Chap 6–10).

References

- Abbink, D. A., Carlson, T., Mulder, M., de Winter, J. C. F., Aminravan, F., Gibo, T. L., & Boer, E. R. (2018). A Topology of Shared Control Systems—Finding Common Ground in Diversity. *IEEE Transactions on Human-Machine Systems*, *48*, 509–525.
- Abbink, D. A., Mulder, M., & Boer, E. R. (2012). Haptic shared control: smoothly shifting control authority?. *Cognition, Technology & Work*, *14*, 19–28.
- Abe, M. (2013). Trends in Intelligent Vehicle Dynamics Controls and Their Future. *NTN Technical Review*, *81*, 2–10.
- Achleitner, A., Glück, H., Hähle, R., Krickelberg, T., Morbitzer, U., & Schätzle, M. (2005). The new Porsche 911 Carrera. *ATZ worldwide*, *107*, 15–19.
- Anubi, O. M. (2013). *Variable stiffness suspension system*. University of Florida.
- Byrne, E. A., & Parasuraman, R. (1996). Psychophysiology and adaptive automation. *Biological psychology*, *42*, 249–268.
- Cho, W., Choi, J., Kim, C., Choi, S., & Yi, K. (2012). Unified chassis control for the improvement of agility, maneuverability, and lateral stability. *IEEE Transactions on vehicular Technology*, *61*, 1008–1020.
- Crolla, D. A. (1996). Vehicle dynamics—theory into practice. *Proceedings of the Institution of Mechanical Engineers, Part D: Journal of Automobile Engineering*, *210*, 83–94.
- Fahimi, F. (2013). Full drive-by-wire dynamic control for four-wheel-steer all-wheel-drive vehicles. *Vehicle System Dynamics*, *51*, 360–376.
- Fankem, S., & Müller, S. (2014). A new model to compute the desired steering torque for steer-by-wire vehicles and driving simulators. *Vehicle System Dynamics*, *52*, 251–271.
- Fuller, R. (2005). Towards a general theory of driver behaviour. *Accident Analysis & Prevention*, *37*, 461–472.
- Gibson, J. J., & Crooks, L. E. (1938). A theoretical field-analysis of automobile-driving. *The American journal of psychology*, *51*, 453–471.
- Helander, M. G., Khalid, H. M., Lim, T. Y., Peng, H., & Yang, X. (2013). Emotional needs of car buyers and emotional intent of car designers. *Theoretical Issues in Ergonomics Science*, *14*, 455–474.
- Hilgers, C., Brandes, J., Ilias, H., Oldenettel, H., Stiller, A., & Treder, C. (2009). Active air spring suspension for greater range between adjusting for comfort and dynamic driving. *ATZ Worldwide*, *111*, 12–17.
- Horswill, M. S., & Coster, M. E. (2002). The effect of vehicle characteristics on drivers' risk-taking behaviour. *Ergonomics*, *45*, 85–104.
- Hosoda, M. (2010). *Power train for a new compact sporty hybrid vehicle* (No. 2010-01-1095). SAE Technical Paper.
- Huang, P. S., & Pruckner, A. (2017). Steer by wire. In *Steering Handbook* (pp. 513–526). Springer, Cham.
- Ilmberger, H. (2014). *Verfahren und Vorrichtung zum automatischen Auswählen von Fahrmodi*. (Germany Patent No. DE102014215258A1). Deutsches Patent- und Markenamt. <https://patents.google.com/patent/DE102014215258A1/de>
- Jeon, B. W., Kim, S. H., Jeong, D., & Chang, J. Y. I. (2016). *Development of Smart Shift and Drive Control System Based on the Personal Driving Style Adaptation* (No. 2016-01-1112). SAE Technical Paper.
- Jindo, T., & Hirasago, K. (1997). Application studies to car interior of Kansei engineering. *International journal of industrial ergonomics*, *19*, 105–114.
- Johnson, M., Bradshaw, J. M., Feltovich, P. J., Jonker, C. M., Van Riemsdijk, M. B., & Sierhuis, M. (2014). Coactive Design: Designing Support for Interdependence in Joint Activity. *Journal of Human-Robot Interaction*, *3*, 43.
- Kaber, D. B., & Endsley, M. R. (2004). The effects of level of automation and adaptive automation on human performance, situation awareness and workload in a dynamic control task. *Theoretical Issues in Ergonomics Science*, *5*, 113–153.
- Kaber, D. B., Riley, J. M., Tan, K. W., & Endsley, M. R. (2001). On the design of adaptive automation for complex systems. *International Journal of Cognitive Ergonomics*, *5*, 37–57.
- Kamp, I. (2012). The influence of car-seat design on its character experience. *Applied ergonomics*, *43*, 329–335.
- Kidwell, B., Calhoun, G. L., Ruff, H. A., & Parasuraman, R. (2012). Adaptable and adaptive automation for supervisory control of multiple autonomous vehicles. *Proceedings of the Human Factors and Ergonomics Society Annual Meeting*, *56*, 428–432.
- Kim, W., Lee, J., Yoon, S., & Kim, D. (2005). *Development of Mando's new continuously controlled semi-active suspension system* (No. 2005-01-1721). SAE Technical Paper.
- Klier, W., Reimann, G., & Reinelt, W. (2004). *Concept and functionality of the active front steering system* (No. 2004-21-0073). SAE

Technical Paper.

- Kolekar, S. B. (2021). Driver's risk field: A step towards a unified driver model (Doctoral dissertation). <https://doi.org/10.4233/uuid:a118e35c-dec9-4c1f-9ed7-8b65a5ca77a3>
- Krahé, B., & Fenske, I. (2002). Predicting aggressive driving behavior: The role of macho personality, age, and power of car. *Aggressive Behavior: Official Journal of the International Society for Research on Aggression*, 28, 21–29.
- Melman, T., Beckers, N., & Abbink, D. (2020). Mitigating undesirable emergent behavior arising between driver and semi-automated vehicle. *arXiv*. <https://arxiv.org/abs/2006.16572>
- Melman, T., De Winter, J. C. F., & Abbink, D. A. (2018). Does haptic steering guidance instigate speeding? A driving simulator study into causes and remedies. *Accident Analysis & Prevention*, 98, 372–387.
- Mercedes-Benz. (2022). Driving modes. https://moba.i.daimler.com/markets/ece-row/baix/cars/177.0_mbox-high_2020_a/en_GB/page/ID_9ec704d53993f553354ae365263f0b2f1d3ef3273993f563354ae36502733902-en-GB.html
- Miller, C. A., & Parasuraman, R. (2007). Designing for flexible interaction between humans and automation: Delegation interfaces for supervisory control. *Human factors*, 49, 57-75.
- Morales, A. L., Nieto, A. J., Chicharro, J. M., & Pintado, P. (2018). A semi-active vehicle suspension based on pneumatic springs and magnetorheological dampers. *Journal of Vibration and Control*, 24, 808-821.
- Mouton, X., Catherine, J., & Benedicte, N. (2016). *Method and system for managing a change in driving mode of a motor vehicle*. (France Patent No. FR3035054B1). Renault SAS. <https://patents.google.com/patent/FR3035054B1/>
- Näätänen, R., & Summala, H. (1974). A model for the role of motivational factors in drivers' decision-making. *Accident Analysis & Prevention*, 6, 243-261.
- Parasuraman, R. (2000). Designing automation for human use: empirical studies and quantitative models. *Ergonomics*, 43, 931-951.
- Rahiman, W., & Zainal, Z. (2013, June). An overview of development GPS navigation for autonomous car. In *2013 IEEE 8th Conference on Industrial Electronics and Applications (ICIEA)* (pp. 1112-1118). IEEE.
- Renault. (2022). Multi-sense. <https://gb.e-guide.renault.com/eng/easy-link/MULTI-SENSE>
- Reuter, M., & Saal, A. (2017). Superimposed Steering System. In *Steering Handbook* (pp. 469–492). Springer, Cham.
- Russell, H. E., Harbott, L. K., Nisky, I., Pan, S., Okamura, A. M., & Gerdes, J. C. (2016). Motor learning affects car-to-driver handover in automated vehicles. *Science Robotics*, 1,
- Savaresi, S. M., Pousset-Vassal, C., Spelta, C., Sename, O., & Dugard, L. (2010). *Semi-active suspension control design for vehicles*. Elsevier.
- Schoegg, P., Ramschak, E., & Bogner, E. (2001). *On-board optimization of driveability character depending on driver style by using a new closed loop approach* (No. 2001-01-0556). SAE Technical Paper.
- Schön, T. (2018). *Method for predicting at least one function setting of at least one motor vehicle component of a motor vehicle and prediction device*. (Germany Patent No. DE102018208431A1). Deutsches Patent- und Markenamt. <https://patents.google.com/patent/DE102018208431A1/en>
- Schwarting, W., Alonso-Mora, J., & Rus, D. (2018). Planning and decision-making for autonomous vehicles. *Annual Review of Control, Robotics, and Autonomous Systems*, 1, 187-210.
- Sekulić, D., & Dedović, V. (2011). The effect of stiffness and damping of the suspension system elements on the optimisation of the vibrational behaviour of a bus. *International Journal for Traffic & Transport Engineering*, 1, 231-244.
- Sharp, R. S., & Crolla, D. A. (1987). Road vehicle suspension system design-a review. *Vehicle System Dynamics*, 16, 167-192.
- Sheller, M. (2004). Automotive emotions: Feeling the car. *Theory, Culture & Society*, 21, 221-242.
- Shibahata, Y. (2005). Progress and future direction of chassis control technology. *Annual Reviews in Control*, 29, 151-158.
- Sontacchi, A., Frank, M., & Höldrich, R. (2015). In-car Active Sound Generation for enhanced feedback in vehicles with combustion engines or electric engines. In *Workshop on In-Vehicle Auditory Interactions at the 21st International Conference on Auditory Display (ICAD-2015)*.
- Van Winsum, W., Brookhuis, K. A., & de Waard, D. (2000). A comparison of different ways to approximate time-to-line crossing (TLC) during car driving. *Accident Analysis & Prevention*, 32, 47-56.
- Wilde, G. J. (1998). Risk homeostasis theory: An overview. *Injury Prevention*, 4, 89–91.
- Wimmer, C., Felten, J., & Odenthal, D. (2014). The electronic chassis of the new BMW i8–influence and characterization of driving dynamics. *5th International Munich Chassis Symposium 2014* (pp. 57-73). Springer Vieweg, Wiesbaden.

PART

2

3

4

***IMPROVE THE
FUNDAMENTAL
KNOWLEDGE OF DRIVER
ADAPTATIONS***

**What Determines Drivers'
Speed? A Replication of
Three Behavioural Adaptation
Experiments in a Single Driving
Simulator Study**



We conceptually replicated three highly cited experiments on speed adaptation, by measuring drivers' experienced risk (galvanic skin response; GSR), experienced task difficulty (self-reported task effort; SRTE) and safety margins (time-to-line-crossing; TLC) in a single experiment. The three measures were compared using a nonparametric index that captures the criteria of constancy during self-paced driving and sensitivity during forced-paced driving. In a driving simulator, 24 participants completed two forced-paced and one self-paced run. Each run held four different lane width conditions. Results showed that participants drove faster on wider lanes, thus confirming the expected speed adaptation. None of the three measures offered persuasive evidence for speed adaptation because they failed either the sensitivity criterion (GSR) or the constancy criterion (TLC, SRTE). An additional measure, steering reversal rate, outperformed the other three measures regarding sensitivity and constancy, prompting a further evaluation of the role of control activity in speed adaptation.

Published as:

Melman, T., Abbink, D. A., Van Paassen, M. M., Boer, E. R., & De Winter, J. C. F. (2018). What determines drivers' speed? A replication of three behavioural adaptation experiments in a single driving simulator study. *Ergonomics*, 61, 966–987. <https://doi.org/10.1080/00140139.2018.1426790>

2.1. Introduction

2.1.1. The Effects of Speed on Road Safety

Worldwide, 1.3 million people die in traffic each year, making road traffic accidents the eighth leading cause of death (Lozano et al., 2013). Excessive speed has long been considered a primary cause of traffic accidents (Aarts & Van Schagen, 2006; Elvik et al., 2004; Treat et al., 1979). An increase of speed does not only relate to an increased probability of being involved in an accident, it also aggravates the severity of accidents (Elvik et al., 2004).

When considering the aforementioned dangers of speeding, it is disconcerting that drivers tend to drive faster when receiving technological support or when encountering a less demanding environment. For example, drivers have been found to drive with higher speeds on well-lit roads than on reference roads without lighting (Assum et al., 1999), as a result of which the attainable safety benefit (i.e. safer driving due to better visibility) is partially negated by the risks of increased driving speed. Such decreases in safety as a result of a higher adopted speed are manifestations of a more general phenomenon called behavioural adaptation (Elvik, 2013; Hiraoka et al., 2010; OECD, 1990; Oviedo-Trespalacios et al., 2017; Saad, 2006; Sullivan et al., 2016). Although behavioural adaptation manifested as speeding has often been found (e.g. Dragutinovic et al., 2005; Janssen & Nilsson, 1993), the underlying psychological mechanisms of speed adaptation are still poorly understood (Vaa, 2007).

2.1.2. The Need For Understanding Behavioural Adaptation

There are several reasons why the determinants of speed adaptation need to be understood. First, a good understanding is important for designing effective educational and enforcement measures. Second, knowledge about speed adaptation may benefit the design of new ADAS to strike a more favourable balance between technology mediated safety improvement and motivationally inspired consumption of the offered safety. For example, we have previously shown that haptic steering feedback does not yield speed adaptation if the system disables itself when driving above a threshold speed (Melman et al., 2017). A good understanding of behavioural adaptation may allow for improvements of the algorithms and threshold settings of such technology. Third, knowledge of the determinants of speed choice may prove useful in the design of automated driving technology that behaves in a human-like (anthropomorphic) manner, rather than to adhere rigidly to a particular speed limit. It is expected that automated driving systems are better accepted if they behave anthropomorphically (e.g. Elbanhawi et al., 2015; Kolekar et al., 2017; Waytz et al., 2014).

2.1.3. Three Previous Experiments on Speed Adaptation

A large number of motivational theories of behavioural adaptation have been proposed, but the impact of three theories has been particularly large (Vaa, 2007): (1) the risk homeostasis theory (Wilde, 1982), (2) the task difficulty homeostasis theory (Fuller, 2005) and (3) the field of safe travel theory (Gibson & Crooks, 1938). These three theories, in turn, have received support from three well-cited experiments, respectively: (1) Taylor (1962), (2) Fuller et al. (2008) and (3) Van Winsum and Godthelp (1996). In each of these three experiments, it is was found that an internal or external variable is sensitive to changes in driving speed, or alternatively, remains constant if drivers' change their speed. These three experiments, which are the focus of the present study, are detailed below.

Experiment 1: constancy of galvanic skin response (GSR) in self-paced driving (Taylor, 1964)

Taylor (1962, 1964) proposed that experienced risk (i.e., anxiety level or tension) is the variable being regulated by drivers. In his research, Taylor measured the galvanic skin response (GSR, also known as electrodermal activity, as an indicator for experienced risk) of 12 participants

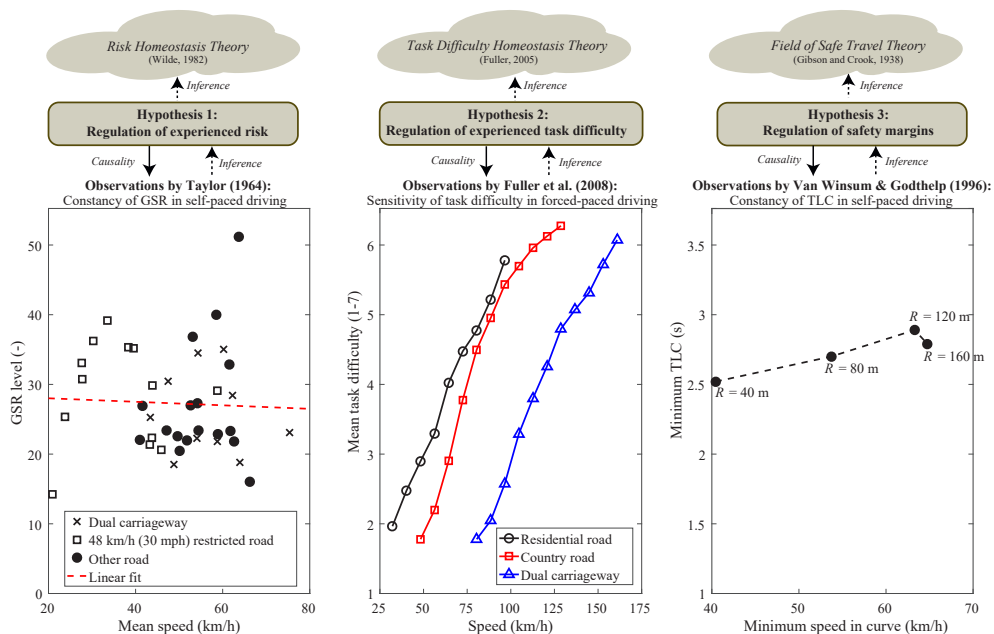


Figure 2.1. Relationship between speed adaptation theory (i.e. a non-operationalised set of statements), testable hypotheses and experimental observations (framework based on Meehl, 1990) Left = Experiment 1: Mean GSR level as a function of average speed on 40 road segments. Data from Taylor (1962). Middle = Experiment 2: Mean ratings of task difficulty (1 = extremely easy, 7 = extremely difficult) as a function of driving speed in videos. Data from Fuller et al. (2008, Figure 6, assuming $N = 40$). Right = Experiment 3: Mean minimum TLC as a function of mean minimum speed in curves of different radius (Van Winsum and Godthelp 1996). Speed increased substantially (60%) with increasing curve radius, while TLC showed only a moderate increase of 14% between the minimum and maximum curve radii.

who each drove 100 km on roads near London. Results showed that the mean GSR level per road segment did not exhibit a substantial correlation ($r = -0.04$) with the mean speed per road segment (Figure 2.1, left). In other words, the mean GSR was about the same regardless of whether participants were driving slowly in a busy shopping area with a high police-recorded accident rate per kilometre, or fast in a country road with a low accident rate per kilometre. These findings together with the fact that the mean GSR did correlate with driver experience (i.e. novice drivers had a higher mean GSR rate), led Taylor (1962) to conclude ‘that drivers adjust their speed so that the apparent accident risk, as indicated by their rate of production of the GSR, tends to remain constant whatever the conditions’. The work of Taylor has been influential. For example, in a review, Vaa (2007) discussed Taylor’s ‘GSR-constancy’ principle, whereas Wilde (1982, 2009) used Taylor’s findings to support his risk homeostasis theory (Figure 2.1, left). Indeed, according to Wilde (1982), ‘these findings were very instrumental in the development of the theory’.

Experiment 2: sensitivity of self-reported task difficulty in forced-paced driving (Fuller et al., 2008)

In a more recent paper, Fuller (2005) introduced ‘task difficulty homeostasis’ as a key sub-goal in driving, stating that ‘what drivers attempt to maintain is a level of task difficulty’ (p. 461). Fuller pointed out that task difficulty is equivalent to the construct mental workload, as can be measured using self-reports such as the six-item NASA-TLX or the unidimensional

Rating Scale Mental Effort (RSME). Fuller further argued that speed is the primary means for drivers to keep their experienced task difficulty at a desired level, and found support for this theory in two experiments in which participants watched videos played at different speeds (Fuller et al., 2008). In one of these experiments, forty participants answered after each video ‘How difficult would you find it to drive this section of road at this speed?’ on a scale from 1 (extremely easy) to 7 (extremely difficult). The results of this forced-paced (i.e. non-interactive) task showed a sensitivity to different road types, and a monotonic relationship between video speed and participants’ ratings of task difficulty (Figure 2.1, middle). More recently, Lewis-Evans and Rothengatter (2009) replicated the results of Fuller (2005) in a driving simulator, in which participants steered themselves and the results showed a similar but non-linear association between speed and reported task difficulty.

Experiment 3: constancy of time-to-line crossing in self-paced driving (Van Winsum & Godthelp, 1996)

In 1938, Gibson and Crooks defined a ‘field of safe travel’ that defines the possible paths that the car may take without being obstructed. Gibson and Crooks argued that drivers attempt to control their car to keep it in the middle of this field. In the 1930s, the field of safe travel was not operationalised, but recently, time-based safety margins have been proposed as a suitable candidate. In a review, Summala (2007) explained: ‘Gibson and Crooks (1938) ... demonstrate how roadway, obstacles and other road users modify this space – safety zone. They also implied that safety zone – and stopping distance within it – is an objectively measurable concept’. One time-based operationalisation of this field is the measure time-to-line-crossing (TLC), defined as the time it takes for the vehicle to cross the lane markers if holding the steering wheel in a steady position at the same speed (Summala, 2007; Van Winsum et al., 2000). Put differently, TLC represents the amount of time a driver has for ‘error neglecting’ (Godthelp, 1988) or ‘satisficing’ (Goodrich & Boer, 2000; Summala, 2007) until a corrective action is needed. Van Winsum and Godthelp (1996) showed in a driving simulator study that the minimum TLC in curves remained approximately constant with curve radius (see Figure 2.1, right), and they suggested ‘TLC to be a regulating mechanism that determines how speed is controlled’ (p. 439).

2.1.4. Present Study

As explained above, three influential speed adaptation theories have received corroboration from three now-classic experiments (Figure 2.1). In the present paper, we are not concerned with evaluating these three *theories* per se. Rather, our aim is to systematically test the three corresponding *hypotheses* in one single experiment.

The three experiments (Figure 2.1) were concerned with either constancy or sensitivity. We argue that a measure purporting to describe speed adaptation should meet both criteria. That is, the measure under consideration needs to remain *constant* when task demands change during *self-paced* driving (i.e. when speed adaptation is an option). This criterion was satisfied for GSR and TLC in Figure 2.1 left and right, respectively, as these variables remained approximately constant when the task demands (speed) changed. Second, the measure needs to be *sensitive* when task demands change during *forced-paced* driving (i.e. when speed is fixed and speed adaptation is not an option). Sensitivity was demonstrated for self-reported reported task difficulty in Figure 2.1 (middle), where speed adaptations were restricted.

Sensitivity alone is insufficient to validate a measure of speed adaptation, because sensitivity is uninformative about whether drivers actually use the variable to adjust their speed in self-paced conditions. Constancy alone is insufficient, as even random data or an entirely irrelevant measure would satisfy this criterion. This latter point was already recognised by Taylor (1962), who admitted that his results are ‘of course consistent with the

radically different assumption that the time rate of production of GSR is constant because it has nothing to do with the risk of driving'.¹

The present study examined which of the three hypotheses [(1) regulation of experienced risk, (2) regulation of experienced task difficulty or (3) regulation of safety margins] provides the most appropriate description of speed adaptation, in terms of both sensitivity and constancy. We performed a driving simulator experiment in which participants drove on a road with cones demarcating the entire driving lane. Participants completed two forced-paced runs (i.e. fixed speed of 90 and 130 km/h, respectively) and one self-paced drive, each run at four different lane widths. We selected lane width as independent variable because lane width is a salient indicator of task demand, which, by virtue of the speed-accuracy trade-off, was expected to exhibit a strong relationship with self-paced driving speeds (De Vos et al., 1999; Lewis-Evans & Charlton, 2006; Liu et al., 2016; Zhai et al., 2004).

Participants reported every 20 s how much effort their current task took (cf. Fuller et al., 2008), and we measured their TLC (cf. Van Winsum & Godthelp, 1996) as well as their GSR (cf. Taylor, 1964) while driving. Other psychophysiological measures (i.e. heart rate and heart rate variability) were recorded as well. The measures were compared with each other regarding constancy and sensitivity. Because different measures have different scale characteristics (e.g. self-reported task difficulty ranges from 0 to 10, while TLC can range from 0 to infinity on a straight road) and can be expected to respond nonlinearly to changes in lane width or speed (Lewis-Evans et al., 2011), we introduce a purely nonparametric method to compare the measures.

2.2. Methods

2.2.1. Participants

Twenty-four participants (17 male, 7 female) between 19 and 31 years old ($M = 24.6$, $SD = 2.4$) with normal or corrected-to-normal vision volunteered for this study. In response to the question of how often they drove in the past 12 months, one participant reported to drive every day, four drove 4–6 days a week, six drove 1–3 days per week, seven drove once a month and six drove less than once a month. Regarding mileage in the past 12 months, the most frequently selected answers were 1001–5000 km (8 respondents) and 1–1000 km (8 respondents), followed by 10,001–15,000 km (4 respondents), 5001–10,000 km (3 respondents) and 20,001–25,000 km (1 respondent). Twenty participants reported prior experience in a driving simulator, with a mean among all 24 participants of 5.3 times ($SD = 10.6$ times). All participant held a valid driver's licence ($M = 5.8$ years, $SD = 2.5$).

No exclusion criteria were applied regarding behaviours that are known to influence heart rate variability (HRV) and GSR, such as coffee consumption less than 2 h before the start of the experiment (11 participants), or being a smoker (2 participants) (Barutcu et al., 2005; Manzano et al., 2011; Villarejo et al., 2012). However, it was not permitted to smoke or drink coffee in between the experimental sessions.

2.2.2. Apparatus

Participants drove in a fixed-base simulator at the Control and Simulation Department at the faculty of Aerospace Engineering, Delft University of Technology (Figure 2.2). Self aligning torques of the steered front wheels were provided by a MOOG FCS ECol8000 S steering motor running at 2,500 Hz. A single-track model (heavy sedan of 1.8 m wide) was used to simulate the vehicle dynamics. The simulated vehicle had an automatic gearbox and its maximum attainable speed was 210 km/h. The environment was shown using three DLP projectors (BenQ W1080ST 1080p Full HD), together providing a horizontal and vertical field-of-view of, respectively, 180° and 40°. The images were displayed with a frame rate of 60 Hz, whereas the simulation and data logging were updated at 100 Hz. The front of the driver's



Figure 2.2. The fixed-based driving simulator used for the experiment.

car was visualised to facilitate more accurate perception of the car's position relative to the road boundaries. Constant car vibrations ('road rumble') were simulated with a seat shaker implemented in the driver's seat.

The GSR and electrocardiographic (ECG) data were measured at 1,000 Hz using a wireless hub (Plux Wireless Biosignals S.A., Portugal). The physiological sensors were synchronised with the simulator using a 5-volt synchronisation pulse, which was initiated by the simulator at the start of each run. For the GSR measurement, one pregelled Ag/AgCl electrode was placed inside the hand palm and one on the side of the wrist (see also Strong, 1970). The ECG local triode configuration was placed on the middle of the left chest.

2.2.3. Speed Conditions

All participants completed three runs, each run in a different speed condition:

1. A forced-paced condition in which the driving speed was fixed at 90 km/h (FP90).
2. A forced-paced condition in which the driving speed was fixed at 130 km/h (FP130).
3. A self-paced condition in which participants could adjust their speed by means of the gas and brake pedals (SP).

These conditions were counterbalanced across participants.

2.2.4. Lane Width Conditions and Road Environment

All participants drove each of the three runs on a single-lane 25-km long road. During each run, the participant encountered four segments of 6 km, each having a different lane width: 3.6, 2.8, 2.4 and 2.0 m. Cones were placed on the white lines to avoid that drivers would use the area outside the white lines or the hard shoulders. The lane widths allowed for a lateral deviation from the lane centre of 0.9, 0.5, 0.3 and 0.1 m, respectively, on each side of the 1.8-m-wide car before a line crossing. The lane width order was counterbalanced between runs, such that each of the 24 runs had a unique lane width order.

Each lane width segment (6 km long) consisted of five curves with 750-m inner radius and two curves with 500-m inner radius, yielding a curve/straight distance ratio of 32/68 per segment. Segments 1–4 were identical, except that the curves of Segments 1 and 3 were left/right mirrored with respect to the curves in Segments 2 and 4. A transition of lane width took place in a curve of 750-m radius. A road sign was placed 20 m before the lane-width transitions to support driver's awareness of the upcoming transition (Figure 2.3). Trees and cones were placed alongside the road to enhance participants' perception of speed. The cones were placed with a distance of 8 m between cones. A cone hit (defined as an incidence where the lateral error become greater than 0.9, 0.5, 0.3 or 0.1 m, depending on road width)

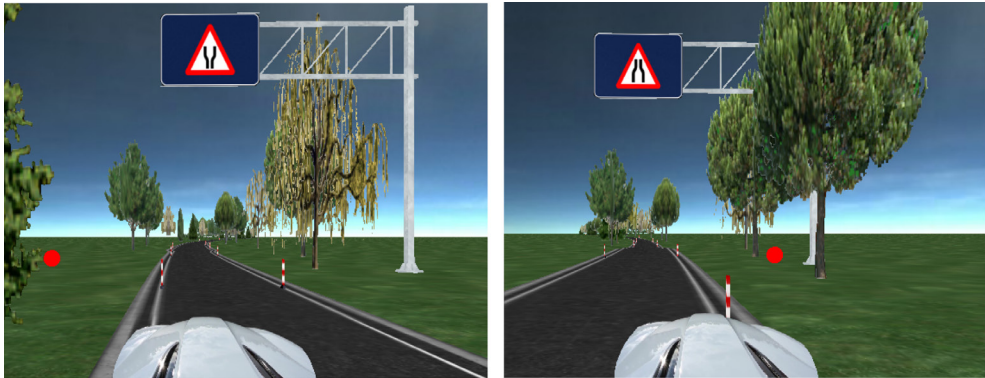


Figure 2.3. Simulator environment including the car front, transition signs and cone hit warning (i.e. red dot accompanied by a sound of 82 dB).

was both visualised (i.e. red dot on the side where the car hit the cone) and made audible (a loud tone was played). No on-road obstacles and no traffic were simulated.

In order to make the driving task more challenging, the simulated car was subjected to a lateral force perturbation, applied to the car's centre of gravity. This lateral force was an unpredictable multi-sine signal consisting of five frequencies ranging from 1/15 to 1/4 Hz, and having maximum amplitude of 1000 N for the summed signal. The lateral force ensured participants needed to steer actively also on straight segments, but was not consciously noticed by most of the participants (the experimenter asked this after the experiment).

2.2.5. Procedures

Participants read and signed an informed consent form, which explained the purpose, instructions and procedures of the study. The consent form stated that 'the purpose of this driving-simulator study is to investigate driving behaviour, subjective experience, physiological activity, workload and comfort while driving under different task demands (i.e. lane widths)'. Participants were asked to keep both hands on the steering wheel in a ten-to-two position at all times, and were instructed to minimise the number of cone hits. The consent form further stated that every 20 s a beep would be produced to indicate that the participant had to orally report a number to the following question: 'From 0 to 10, how much effort does the current driving task takes you?', where 0 is *No effort*, 5 is *Moderate effort* and 10 is *A lot of effort*. The answers were audio-recorded and typed down by the experimenter during the experiment. The instructions (driving task and effort question) were also orally explained to ensure that all participants understood this. No speed advice was provided and participants' questions regarding speed were not answered. The speedometer was visible to the participants (see Figure 2.2).

Before entering the driving simulator, participants completed a questionnaire regarding their driving experience as well as a Driver Behaviour Questionnaire (DBQ) consisting of seven violation items (De Winter & Dodou, 2016). A previous meta-analysis indicated that the DBQ violations scale has a moderately strong relationship ($r = 0.24$) with recorded measures of speed and speeding (De Winter et al., 2015). After completing the questionnaires, the GSR and ECG electrodes were placed and a 1-min 'rest' state was measured for the physiological variables (i.e. GSR and ECG).

Prior to the experiment, participants were familiarised with the simulator by means of a forced-paced training run followed by a self-paced training run. In the forced paced training run, the speed was fixed at 110 km/h, the average speed of the two forced-paced test

conditions. During the second training run, a beep was played every 20 s in order to familiarise the participant with answering the 'effort' question. The roads of the two familiarisation runs (3.7 km each) contained the same curves and lane widths as the experimental runs. In both training runs, the four lane widths were presented in ascending order. This allowed the participants to get an indication of the range of lane widths in order to calibrate their self-reported effort ratings.

The main experiment consisted of three runs, one speed condition per run. The three speed conditions and the four lane widths were counterbalanced across participants. After each run, the participant was informed about the number of cone hits and requested to step out of the simulator for a 10-min break and to complete two questionnaires: a NASA Task Load Index (NASA-TLX) (Hart & Staveland, 1988) to assess workload, the short version of the Dundee Stress State Questionnaire (DSSQ) to assess stress and fatigue (Matthews et al., 1999), and a simulator sickness item. In the latter, participants indicated whether they were feeling simulator sickness on a scale from 1 to 6 (1 = not experiencing any nausea, no sign of symptoms, 2 = arising symptoms [like a feeling in the abdomen], but no nausea, 3 = slightly nauseous, 4 = nauseous, 5 = very nauseous, retching, 6 = vomiting). The experimenters would ask the participant to leave the experiment in case that he or she provided a response of 4 or higher. The entire experiment, including placing the electrodes and completing all questionnaires, took approximately 1.5 h per participant.

2.2.6. Dependent Measures

Measures per lane width

The data corresponding to the first 500 m and last 400 m of each lane width segment of 6 km were discarded in order to exclude transition effects (i.e. accelerations and decelerations) between lane widths. The following measures were calculated per lane width across 5.1 km of driving per segment.

Speed and accuracy

- *Mean Speed (km/h)*.
- *Percentage Time Off-Road (%)*. This is the percentage of time that the car drove outside the cone boundaries.
- *Mean and Maximum Absolute Lateral Error (m)*. The absolute lateral error was defined as the distance between the middle of the car and the centre of the lane. The absolute lateral error and percentage time off-road are measures of lane-keeping accuracy.

Regulation of experienced effort

Mean Self-Reported Task Effort (SRTE) (0–10). Participants reported every 20 s how much effort the current task takes from 0 (No effort) to 10 (A lot of effort). Note that we did not use Fuller et al. (2008) original wording ('How difficult would you find it to drive this section of road at this speed?') because (a) Fuller's specific wording does not apply to a self-paced task and (b) our observations from a pilot test suggested that participants tended to interpret the word 'difficult' in relation to the *objective* task demands (i.e. the lane width) rather than *subjective* experience. In order to better comply with Fuller's hypothesis, we used the word 'effort', which appears to be more in line with how difficult the participants subjectively experience the task at a particular moment (and see Kahneman, 1973, for a treatise of the effort construct).

Regulation of safety margins

- *Median Time-to-Line-Crossing (TLC) (s)*. The TLC was computed using a trigonometric method (Van Winsum et al., 2000). TLC represents the time it would take for part of the vehicle to leave the lane under the assumption of constant speed and constant

steering wheel angle. The TLC was assumed to be 0 s when driving outside the lane boundaries.

- *15th percentile of Time-to-Line-Crossing (TLC15th) (s)*. This measure represents the 15th percentile of the raw TLC values (Godthelp et al., 1984). A low TLC15th or low median TLC means that drivers adopted small safety margins.

Regulation of experienced risk

- *Mean Galvanic Skin Response (GSR) (μ S)*. The raw GSR signal from the left and right hands was averaged. This averaged signal was filtered using a low-pass filter (cut-off frequency of 5 Hz) to reduce extraneous noise.
- *Mean GSR Rate (μ S/min)*. The rate was obtained by subtracting two adjacent sampling points of the combined mean GSR signal (explained above), taking the absolute value, and dividing this by the time step in minutes (cf. Taylor, 1964). The mean GSR may be regarded as a measure of the tonic level of the skin response, changing within tens of seconds to minutes. The mean GSR rate is a measure of the faster phasic response (Alberdi et al., 2016; Figner & Murphy, 2011; Nagai et al., 2004).
- *Mean Heart Rate (HR) (bpm)*.
- *SDNN (ms)*. This time-domain heart rate variability measure is defined as the standard deviation of the normal-to-normal (NN) intervals in the ECG signal. A low SDNN is indicative of high workload (Fallahi et al., 2016; Heikooop et al., 2017).
- *LF/HF Ratio*. This frequency-domain heart rate variability measure is defined as the ratio between the low frequencies and high frequencies of the NN intervals in the ECG signal, and offers information about sympathetic and parasympathetic activity (Berntson et al., 1997). An increase in the LF/HF ratio is indicative of increased workload (Hayashi et al., 2009; Hjortskov et al., 2004). The LF/HF ratio and SDNN were calculated after applying an NN artefact filter using software provided by Vollmer (2016).

Auxiliary measures

- *Steering Reversal Rate (reversals/s)*. This is the frequency with which the steering wheel reversed direction. It was calculated by determining the local minima and maxima of the steering wheel angle; if the difference between two adjacent peaks was greater than 2 deg, it was counted as a reversal. The steering wheel angle was first filtered with a low-pass Butterworth filter with a cut-off frequency of 2 Hz.

Measures per speed condition

The following measures were calculated per speed condition.

- *NASA-TLX (%)*. After each run, participants were asked to indicate their perceived workload for the entire run on six items: Mental Demand, Physical Demand, Temporal Demand, Performance, Effort and Frustration. Items were scored on a 21-point scale from *Very low* (0%) to *Very high* (100%), except for Performance, which ranged from *Perfect* (0%) to *Failure* (100%). The overall workload was calculated as the arithmetic mean of the six items (Byers et al., 1989).
- *Dundee Stress State Questionnaire (DSSQ)*. The short multidimensional DSSQ is an operationalisation of stress and fatigue. Thirty statements were asked regarding engagement, distress and worry (Matthews et al., 1999). Items were scored from 0 (*Definitely false*) to 4 (*Definitely true*). The overall engagement, distress and worry scores ranged from 0 (minimum possible) to 32 (maximum possible).

2.2.7. Statistical Analyses for Assessing the Effect of Lane Width and Speed

For each dependent measure and for each of the three speed conditions, a matrix of 24×4 numbers was computed (24 participants \times 4 lane width conditions). This matrix was rank transformed according to Conover and Iman (1981) to account for possible violations of the assumption of normality. The rank-transformed matrix, consisting of numbers from 1 to 96, was submitted to a repeated measures ANOVA with lane width as within-subject factor. Similarly, for each of the dependent measures, the scores for FP90 and FP130 were rank transformed according to Conover and Iman (1981). The resulting matrix, consisting of numbers from 1 to 48 (24 participants \times 2 speed conditions), was submitted to a repeated measures ANOVA with the two speed conditions as within-subject factor.

2.2.8. Nonparametric Index Design to Evaluate Speed Adaptation

We defined the amount of speed adaptation explained by a given measure using Kendall's coefficient of concordance (W), which ranges from 0 to 1 (Kendall & Smith, 1939). A perfect measure of speed adaptation meets the following four criteria:

Constancy

1. $W_{SP} = 0$: no concordance during self-paced driving. For example, for SRTE, $W_{SP} = 0$ means that participants rated the SRTE of the 2.0-, 2.4-, 2.8- and 3.6-m-wide lanes in no consistent order, and thus lane width had no consistent effect on SRTE.

Sensitivity

2. $W_{FP90} = 1$: full concordance during forced-paced driving at 90 km/h. For example, for SRTE, $W_{FP90} = 1$ means that participants driving in the FP90 condition unanimously rated the 2.0-, 2.4-, 2.8- and 3.6-m-wide lanes in the same order. That is, for SRTE, all participants found the 2.0-m lane more effortful than the 2.4-m lane, the 2.4-m lane more effortful than the 2.8-m lane and the 2.8-m-wide lane more effortful than the 3.6-m lane.
3. $W_{FP130} = 1$: full concordance during forced-paced driving at 130 km/h.
4. $W_{\Delta FP} = 1$: full concordance between FP130 and FP90. For example, for SRTE, $W_{\Delta FP} = 1$ means that all participants regarded FP130 as more effortful than FP90.

The above four concordance values were used to calculate an overall speed adaptation (OSA) score (Equation 2.1), which applies equal weight to sensitivity (W_{FP130} , W_{FP90} & $W_{\Delta FP}$) and constancy (W_{SP}). OSA can range between -1 (i.e. poorest possible speed adaptation measure with constancy 1 and sensitivity 0) and 1 (i.e. perfect speed adaptation measure with constancy 0 and sensitivity 1). A score of 0 occurs if the measure were uncorrelated with the experimental conditions (e.g. if totally random data were measured) or if the measure were equally sensitive during SP and FP.

$$OSA = \frac{W_{FP130} + W_{FP90} + W_{\Delta FP}}{3} - W_{SP} \quad (2.1)$$

2.3. Results

All participants finished the experiment; none of the participants responded a score of 3 (slightly nauseous) or higher for the simulator sickness item. Specifically, from 72 responses (24 participants \times 3 runs), there were 68 responses 'Not experiencing any nausea', and 4 responses of 'Arising symptoms'.

2.3.1. Descriptive Statistics and Effects of Lane Width

Tables 2.1–2.3 show the means and standard deviations per lane width and per dependent measure, for the FP130, FP90 and SP conditions, respectively. These tables also contain the results of the repeated measures ANOVAs regarding lane width.

Tables 2.1–2.3 show that the wider the lane, the higher the mean absolute lateral error and maximum lateral error. Lane width also had strong effects on the TLC measures and on SRTE. For the five physiological measures (mean GSR, mean GSR rate, HR, SDNN, LF/HF ratio), the effect of lane width was substantially weaker. Only the effects of SDNN were statistically significant in all three speed conditions, with the 3.6-m-wide lane yielding higher SDNN (indicative of lower workload) than the 2.0-m-wide lane.

Figure 2.4 shows (1) the mean speed, (2) the cumulative number of cone hits, (3) the mean SRTE, (4) the mean TLC and (5) the mean GSR as a function of travelled distance. It can be seen that over the entire trajectory, participants adopted a higher mean speed for the wider lanes. Furthermore, for the three widest lanes (i.e. 3.6, 2.8 m and 2.4 m) participants had similar mean acceleration (on straight segments) and deceleration (before curved segments) patterns. For the 2.0-m-wide lane, however, participants adopted a relatively constant mean speed across the 5.1-km-long segment. Figure 2.4 and Tables 2.1–2.3 further show that substantially more cones were hit for the 2.0-m-wide lane than for the three wider lanes.

Figure 2.4 shows that GSR does not clearly differentiate between the different lane widths, nor between the three speed conditions. The TLC and SRTE, however, are both clearly sensitive to lane width, with wider lanes yielding higher TLC and lower SRTE. Furthermore, SRTE shows to be a measure of speed adaptation. To illustrate, for the narrowest road (blue lines), SRTE was *higher* for FP130 than for SP, whereas for the widest road (red lines), SRTE was *lower*. Put differently, it appears that participants in the SP condition, to some extent, homogenised their own task demands. A similar pattern is seen for the median TLC across participants (Figure 2.4). These speed adaptations are described in further detail in the following section.

2.3.2. Comparing the Speed Adaptation Measures

Tables 2.1–2.3 and Figure 2.4 described the sensitivity of the measures to lane width, for

Table 2.1. Means (*M*), standard deviations (*SD*), and results of the repeated measures ANOVA (*p*, *F*) per dependent measure and lane width, for the self-paced condition (SP).

Dependent measures	Lane width				<i>p</i> value, <i>F</i> (3,69)
	2.0 m <i>M</i>	2.4 m <i>M</i>	2.8 m <i>M</i>	3.6 m <i>M</i>	
Mean speed (km/h)	91.7 (21.1)	123.5 (15.7)	135.3 (16.9)	148.4 (18.6)	<i>p</i> = 7.27e-24 <i>F</i> = 90.49
Percentage time off-road (%)	15.64 (7.48)	1.69 (1.54)	0.25 (0.64)	0.31 (0.77)	<i>p</i> = 2.17e-28 <i>F</i> = 130.65
Mean absolute lateral error (m)	0.057 (0.012)	0.097 (0.017)	0.116 (0.027)	0.203 (0.046)	<i>p</i> = 1.73e-36 <i>F</i> = 241.07
Maximum absolute lateral error (m)	0.305 (0.166)	0.391 (0.092)	0.439 (0.138)	0.781 (0.358)	<i>p</i> = 2.17e-28 <i>F</i> = 130.65
Self-reported task effort (0-10)	6.99 (1.35)	3.81 (1.48)	3.30 (1.54)	2.32 (1.38)	<i>p</i> = 9.50e-24 <i>F</i> = 89.61
Median TLC (s)	1.24 (0.46)	2.15 (0.43)	2.57 (0.60)	2.96 (0.67)	<i>p</i> = 7.94e-25 <i>F</i> = 98.04
TLC15th (s)	0.23 (0.33)	1.14 (0.22)	1.39 (0.26)	1.65 (0.30)	<i>p</i> = 1.42e-30 <i>F</i> = 154.81
Mean GSR (μS)	7.38 (3.34)	7.70 (3.32)	7.62 (3.21)	7.74 (3.44)	<i>p</i> = 0.664 <i>F</i> = 0.530
Mean GSR rate (μS/min)	8.73 (8.57)	8.71 (8.18)	8.75 (6.07)	9.75 (8.82)	<i>p</i> = 0.550 <i>F</i> = 0.71
Mean HR (bpm)	79.73 (11.61)	78.49 (10.63)	78.54 (11.70)	78.94 (11.11)	<i>p</i> = 0.282 <i>F</i> = 1.30
SDNN (ms)	47.43 (16.20)	51.97 (17.31)	55.92 (20.30)	55.46 (22.75)	<i>p</i> = 0.047 <i>F</i> = 2.79
LF/HF ratio (ms)	1.09 (0.39)	1.09 (0.45)	1.07 (0.40)	1.10 (0.45)	<i>p</i> = 0.935 <i>F</i> = 0.142
Steering reversal rate (deg/s)	0.79 (0.24)	0.63 (0.19)	0.63 (0.20)	0.61 (0.18)	<i>p</i> = 1.34e-05 <i>F</i> = 10.10

Table 2.2. Means (*M*), standard deviations (*SD*) and results of the repeated measures ANOVA (*p*, *F*) per dependent measure and lane width, for the forced-paced condition at 90 km/h (FP90).

Dependent measures	Lane width				<i>p</i> value, <i>F</i> (3,69)
	2.0 m <i>M</i>	2.4 m <i>M</i>	2.8 m <i>M</i>	3.6 m <i>M</i>	
Mean speed (km/h)	90 (0)	90 (0)	90 (0)	90 (0)	
Percentage time off-road (%)	16.62 (7.37)	0.79 (1.00)	0.05 (0.15)	0.02 (0.08)	<i>p</i> = 1.01e-28 <i>F</i> = 134.07
Mean absolute lateral error (m)	0.059 (0.011)	0.091 (0.020)	0.112 (0.025)	0.179 (0.047)	<i>p</i> = 2.10e-29 <i>F</i> = 141.43
Maximum absolute lateral error (m)	0.294 (0.114)	0.331 (0.063)	0.386 (0.084)	0.547 (0.151)	<i>p</i> = 1.02e-28 <i>F</i> = 134.07
Self-reported task effort (0-10)	6.73 (1.77)	3.31 (1.39)	1.76 (1.27)	0.86 (0.97)	<i>p</i> = 6.81e-29 <i>F</i> = 135.91
Median TLC (s)	1.15 (0.28)	2.77 (0.37)	3.76 (0.50)	4.88 (0.60)	<i>p</i> = 5.65e-55 <i>F</i> = 884.63
TLC15th (s)	0.17 (0.25)	1.53 (0.20)	2.12 (0.17)	2.75 (0.22)	<i>p</i> = 5.04e-62 <i>F</i> = 1430.17
Mean GSR (μS)	7.86 (4.52)	7.56 (4.29)	7.70 (4.34)	7.76 (4.14)	<i>p</i> = 0.200 <i>F</i> = 1.59
Mean GSR rate (μS/min)	7.51 (6.99)	6.81 (5.85)	6.55 (4.81)	6.57 (4.22)	<i>p</i> = 0.74 <i>F</i> = 0.42
Mean HR (bpm)	77.62 (11.31)	78.22 (11.50)	76.80 (9.68)	77.22 (11.19)	<i>p</i> = 0.661 <i>F</i> = 0.53
SDNN (ms)	49.92 (23.59)	64.05 (37.46)	60.83 (28.75)	58.35 (18.50)	<i>p</i> = 1.90e-4 <i>F</i> = 7.57
LF/HF ratio (ms)	1.08 (0.43)	1.22 (0.45)	1.18 (0.56)	1.27 (0.42)	<i>p</i> = 0.005 <i>F</i> = 4.65
Steering reversal rate (deg/s)	0.78 (0.21)	0.53 (0.17)	0.45 (0.15)	0.41 (0.16)	<i>p</i> = 9.12e-21 <i>F</i> = 69.21

Table 2.3. Means (*M*), standard deviations (*SD*), and results of the repeated measures ANOVA (*p*, *F*) per dependent measure and lane width, for the forced-paced condition at 130 km/h (FP130).

Dependent measures	Lane width				<i>p</i> value, <i>F</i> (3,69)
	2.0 m <i>M</i>	2.4 m <i>M</i>	2.8 m <i>M</i>	3.6 m <i>M</i>	
Mean speed (km/h)	130 (0)	130 (0)	130 (0)	130 (0)	
Percentage time off-road (%)	25.99 (11.03)	2.76 (2.41)	0.28 (0.44)	0.03 (0.12)	<i>p</i> = 1.47e-37 <i>F</i> = 260.62
Mean absolute lateral error (m)	0.075 (0.022)	0.106 (0.020)	0.123 (0.023)	0.197 (0.042)	<i>p</i> = 2.88e-30 <i>F</i> = 151.21
Maximum absolute lateral error (m)	0.411 (0.199)	0.448 (0.149)	0.467 (0.106)	0.643 (0.132)	<i>p</i> = 5.81e-12 <i>F</i> = 28.02
Self-reported task effort (0-10)	7.77 (1.54)	4.46 (1.53)	3.26 (1.69)	1.41 (1.16)	<i>p</i> = 5.83e-32 <i>F</i> = 172.10
Median TLC (s)	0.65 (0.28)	2.00 (0.42)	2.72 (0.43)	3.53 (0.56)	<i>p</i> = 5.66e-48 <i>F</i> = 545.73
TLC15th (s)	0.02 (0.07)	0.95 (0.19)	1.43 (0.17)	1.88 (0.15)	<i>p</i> = 1.60e-55 <i>F</i> = 918.50
Mean GSR (μS)	7.56 (3.08)	7.40 (3.00)	7.35 (3.14)	7.43 (3.44)	<i>p</i> = 0.787 <i>F</i> = 0.35
Mean GSR rate (μS/min)	7.92 (5.44)	6.71 (4.15)	7.38 (5.90)	8.33 (7.16)	<i>p</i> = 0.446 <i>F</i> = 0.90
Mean HR (bpm)	79.49 (12.57)	77.50 (11.43)	77.45 (11.50)	77.14 (11.82)	<i>p</i> = 0.152 <i>F</i> = 1.82
SDNN (ms)	52.92 (25.86)	54.61 (19.53)	51.48 (19.04)	61.92 (28.92)	<i>p</i> = 0.029 <i>F</i> = 3.19
LF/HF ratio (ms)	1.09 (0.49)	1.13 (0.47)	1.05 (0.32)	1.14 (0.33)	<i>p</i> = 0.265 <i>F</i> = 1.35
Steering reversal rate (deg/s)	0.93 (0.28)	0.67 (0.24)	0.58 (0.20)	0.50 (0.18)	<i>p</i> = 8.40e-19 <i>F</i> = 57.83

each speed condition. However, to assess speed adaptation, the effect sizes for a measure need to be evaluated for the forced-paced conditions *relative* to the self-paced condition, as shown in Table 2.4. Here, the index of interest is the overall speed adaptation (OSA) score, as defined in Equation 2.1.

Table 2.4 shows that both the SRTE and median TLC are somewhat successful in describing speed adaptation, with OSA scores for these measures being greater than 0

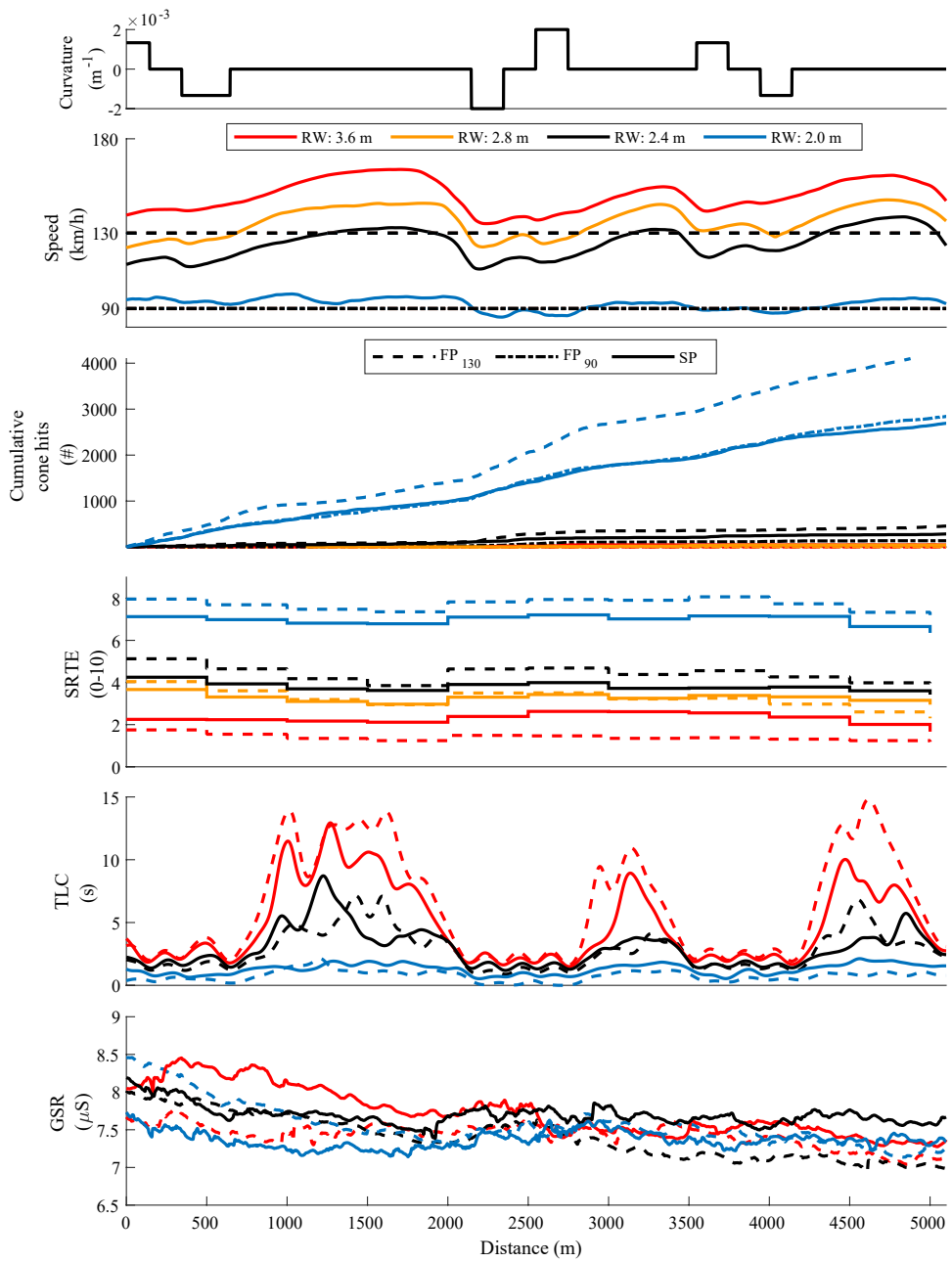


Figure 2.4. Selected variables as a function of travelled distance per lane width. Colours correspond to the four lane widths, and line styles correspond to the three speed conditions (for clarity, the bottom three plots do not show the FP90 condition, and the bottom two do not show the 2.8 m lane width). From top to bottom: (1) curvature (1/curve radius), (2) mean speed across participants, (3) cumulative number of cone hits summed across, (4) mean self-reported task effort (SRTE) across participants (sampled every 20 seconds), and (5) median TLC across participants. For visualization purposes, the median TLC was low pass filtered with a cut-off frequency of 0.005/m, (6) mean galvanic skin response (GSR) across participants.

(0.06 and 0.17, respectively). However, the GSR and GSR rate do not perform much better than random chance, with OSA values of 0.01 and 0.03, respectively. The measures of heart rate variability (SDNN, LF/HF ratio) yield OSA values greater than 0 as well (0.07 and 0.09, respectively). It is noteworthy that the highest OSA among all measures (0.43) occurred for the steering reversal rate (Table 2.4).

Figure 2.5 shows the means across participants per lane width and per speed condition for six selected measures. In agreement with Table 2.4 and Figure 2.4, SRTE is a relatively successful measure of speed adaptation (i.e. OSA > 0) as it dropped less strongly with lane width for SP than for FP. Similarly, the increase of TLC with lane width was less steep for SP than for FP. Figure 2.5 further shows that the GSR measures were insensitive to lane width in all three speed conditions. Overall, steering reversal rate is the most successful measure of speed adaptation, as SRR remained relatively constant in the SP condition (i.e. low W_{SP}), while being sensitive to lane width (i.e. high W_{FP130} and W_{FP90}) (Table 2.4).

2.3.3. Supplementary Analyses

As shown above, the physiological measures exhibit low sensitivity to lane width, which may suggest that these measures are statistically unreliable. However, this was clearly not the case. Figure 2.6, for example, illustrates that the heart rate reliably reflected individual differences ($\rho = 0.90$). Furthermore, a temporal effect can be distinguished: the mean heart rate decreased from Run 1 ($M = 80.6$ bpm, $SD = 11.3$) to Run 3 ($M = 76.5$, $SD = 10.8$). This run effect was further analysed by submitting a 24×3 (24 participants \times 3 speed conditions)

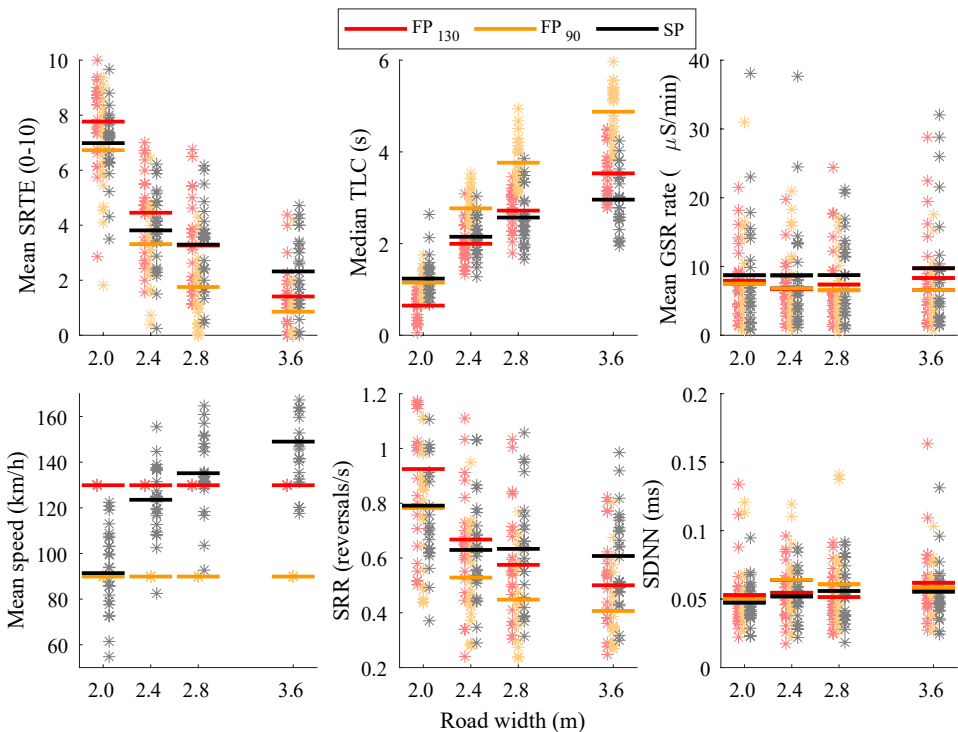


Figure 2.5. Scores of participants (asterisks) and means across participants (horizontal lines) per lane width (x-axis) and per speed condition (colour). Top left: self-reported task effort (SRTE); Top middle: median time-to-line-crossing (TLC); Top right: galvanic skin response rate (GSR rate); Bottom left: mean speed; Bottom middle: steering reversal rate (SRR); Bottom right: heart rate variability (SDNN).

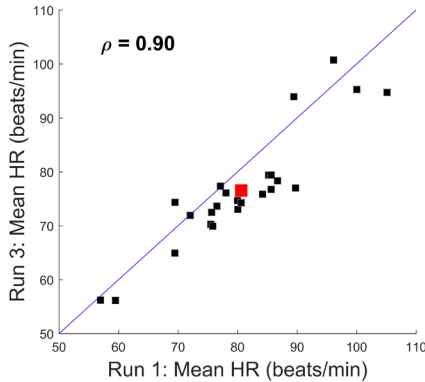


Figure 2.6. Mean heart rate during Run 1 versus Run 3. The markers represent values per participant (small squares) and means across 24 participants (large square).

matrix with rank-transformed numbers to a repeated-measures ANOVA, but now with the run number as within-subject factor. The results, which can be found in the supplementary materials, show that from the 17 measures, the mean HR and DSSQ Worry are significantly different between Run 1 and Run 3.

Finally, the correlation matrices in the supplementary material reveal several noteworthy patterns. In particular, participants with a higher mean HR tend to have a lower SDNN and a higher LF/HF ratio. Additionally there are strong correlations between mean GSR and mean GSR rate, as well as between DSSQ Distress and the NASA TLX (ρ between 0.61 and 0.84). In addition, driving experience (yearly mileage) correlated with the NASA TLX ($\rho = -0.35, -0.17, -0.48$ for SP, FP90 and FP130, respectively). Low correlations were found between the physiological measures and mileage ($|\rho| < 0.15$).

2.4. Discussion

2.4.1. Main Findings Regarding the Three Speed Adaptation Hypotheses

We aimed to test which of three regulatory hypotheses [(1) experienced risk, (2) experienced task difficulty or (3) safety margins] best describes the phenomenon that drivers adopt a higher speed when task demands are lowered. The three hypotheses were tested on both constancy: does the corresponding measure (i.e. GSR, SRTE, TLC) remain constant during self-paced driving?, and sensitivity: does the corresponding measure change as a function of lane width (4 lane widths) and imposed speed (2 fixed speeds) forced-paced driving? Previous research on this topic never tested the constancy criterion (GSR and TLC) and the sensitivity criterion (SRTE) in a single experiment, and compared the results.

Our driving simulator experiment showed that the task demand manipulation was successful in evoking speed adaptation: participants drove faster when the lane was wider. This effect, which is represented by a Kendall W of 0.81 (Table 2.3), serves as a useful confirmation that speed adaptation occurs when task demands are lowered Lewis-Evans and Charlton 2006).

Because the dependent measures respond non-linearly to changes in task demands (see Figure 2.5, for an illustration), a purely nonparametric index, called overall speed adaptation (OSA), was used. The OSA score can range between -1 and 1, where positive values mean that speed adaptation is captured by the measure; that is, the sensitivity to changes in task demand in forced paced driving conditions is greater than the sensitivity to task demand under self-paced conditions. Table 2.4 showed positive scores of 0.01, 0.06 and 0.17

for GSR, SRTE and TLC, respectively, which are still far from the perfect OSA = 1 score. Thus, results show that SRTE and TLC describe some speed adaptation, but none of the three tested measures provides a persuasive description of speed adaptation. The tested regulatory hypotheses failed either the criterion of sensitivity or the criterion of constancy.

2.4.2. Insufficient Sensitivity of GSR

The mean GSR and mean GSR rate exhibited clear individual differences (as evidenced by the test–retest correlations exceeding 0.80, see Table 2D in Supplementary material), but did *not* significantly co-vary with lane width or with the imposed speed in the forced-paced conditions. This lack of sensitivity may have several causes.

First, the GSR signal exhibited large fluctuations that were uncorrelated with the experimental conditions. This suggests that GSR reflects high-frequency dynamics of the sympathetic nervous system, which may have overwhelmed the subtle changes in driver tension in response to lane width. The measurement instruments themselves may have also been a factor here. Although we did follow Taylor's (1964) method of measuring GSR on the hands, it is possible that turning of the steering wheel may have interfered with the GSR and ECG recordings (Bernardi et al., 1996; Sun et al., 2012). Thus, within-subject noise may have been an important factor reducing sensitivity. Future research could place the electrodes on other locations of the body, such as the neck (Wen et al., 2017).

Second, it is possible that GSR does not reflect changes in driver tension in simulated driving. Taylor (1962) measured drivers' GSR during real-world driving and found that GSR exhibited a strong correlation with participants' age ($\rho = -0.64$) and years since obtaining the first driver's licence ($\rho = -0.85$), but such strong correlations were not found in this study ($|\rho| < 0.15$ between participants' GSR levels and mileage).

Third, the GSR may have operated at a different time scale than the time scale with which lane width and speed were manipulated. In our study, all measures were calculated per 5.1-km segment of driving of which the first 500 m and last 400 m of each lane width were discarded to exclude transition effects. The GSR rate may have a more phasic characteristic and could therefore be especially responsive during these transition period only (e.g. Christie, 1981). Future research could examine how drivers respond to transitions in task demands.

Fourth, it could be argued that GSR is not a sensitive proxy of experienced risk (e.g. Kinnear et al., 2013), and that Taylor's (1964) hypothesis, which states that drivers regulate their level of experienced risk, is false.

2.4.3. Insufficient Constancy of TLC and SRTE

Although TLC and SRTE were highly sensitive to both lane width and imposed speed, these measures were not constant during self-paced driving. Participants reported that wide lanes were less effortful to drive on (i.e. lower SRTE) than narrow lanes, even though participants drove considerably faster on the wider lanes. Here, it is possible that participants reported in congruence to what they saw (i.e. lane width itself) rather than what they subjectively experienced (i.e. experienced effort), or it is possible that Fuller et al. (2008) was wrong in the sense that drivers do not regulate their experienced task difficulty.

Similarly, we found that the wider the lane, the higher the observed TLC, which may be due to the causal relationship between speed and TLC (see also the observed correlation between speed and median TLC: $\rho = -0.51$ in the Supplementary material). If maintaining the same driving path, infeasible high speeds of 350–800 km/h (exceeding the maximum vehicle speed of 210 km/h) would have to be adopted on the widest lanes in order to acquire the same TLC as on the narrowest lane (estimated using data in Table 2.1). Thus, although TLC may be kept constant in some cases, such as when drivers adapt their speed to different curve radii (Van Winsum & Godthelp, 1996), it failed the constancy criterion when it came to lane width.

2.4.4. A Promising Alternative Measure of Speed Adaptation: Steering Reversal Rate

The three behavioural adaptation hypotheses, compared in this paper, focus on subjective effort and physiological stress as well as objective risk in the form of TLC. None of the hypotheses targets objective effort. The steering reversal rate (SRR), a widely used measure of steering activity (McLean & Hoffmann, 1975; Östlund et al., 2005), which may be seen as an *objective* measure of effort (Boer & Ward, 2003), had the highest OSA score (0.43) of the included measures.

SRR Yielded High Sensitivity for Forced-Paced Driving

During forced-paced driving, participants exhibited a higher SRR when the lane was narrower (i.e. W_{FP90} & W_{FP130} were high, see Table 2.4) and a higher SRR when the imposed speed was higher (i.e. $W_{\Delta FP}$ was high). These findings replicate early on-road research by McLean and Hoffmann (1972) which concluded that ‘the proportion of high-frequency (>0.4 Hz) steering control movements increases with increasing speed and decreasing lane width, that is, increases as the driving situation becomes ‘tighter’ (435).

The high sensitivity of SRR to lane width (i.e. high W_{FP90} & W_{FP130}) can be explained by the fact that a larger absolute lateral error is permitted on a wider lane, and thus less frequent steering input is needed to stay in the lane. Second, a decrease of lane width is accompanied by an increase of visual saliency and thus perceptual accuracy of the vehicle state relative to the environmentally imposed constraints; that is, the distance and splay angles to the lane edges are more clearly visible when the lane is narrower (Li & Chen, 2010). Indeed, steering activity is closely related to maintaining a certain vehicle state in response to perturbations such as external forces on the vehicle and perceptual inaccuracies (e.g. Van Leeuwen et al., 2015). Third, the cone warnings provided salient feedback to the driver that he or she had to make a steering correction; these cone warnings occurred more frequently on the narrower lanes (see Tables 2.1–2.3).

The high sensitivity of SRR to imposed speed (i.e. high $W_{\Delta FP}$) can be explained by visual cues as well: differences in heading angles are better detectable at a higher speed due to the effects of optic flow (see Crowell & Banks, 1993), thus providing incentives for steering corrections. Furthermore, a higher driving speed demands more frequent steering input due to the approximately quadratic increase in lateral displacement as a function of speed, as occurs with any vehicle (Wohl, 1961).

SRR Yielded High Constancy for Self-Paced Driving

In the self-paced condition, drivers kept a relatively constant SRR for different lane widths (i.e. WSP was low). The relatively high OSA score (0.43) suggest that drivers attempt to regulate a certain control activity by means of adjusting their speed. The role of control activity in speed adaptation deserves further investigation, for example, in future experiments with a greater range of physical steering demands (e.g. sharp curves) and different task demands (e.g. higher traffic density).

2.4.5. Measurement Considerations and Temporal Effects

We found that some of the dependent measures were highly correlated (see supplementary material), which indicates that a common factor may be extracted. Thus, speed adaptation may best be explained using multiple measures simultaneously. Visual scanning activity, which was not included in the present study, may be a fruitful additional measure of speed adaptation. To illustrate, it is possible that participants adapted to a decrease in task demands (i.e. increase in lane width, or a reduction in imposed speed) by engaging in extra visual scanning or by engaging in a visually distractive non-driving task. When a higher driving demand is short lived as in a slow sharp curve or a brief narrowing of a lane, drivers

may temporarily increase their vigilance and posture to compensate the increased demand with increase capability. In this context, the objective measure of risk as with TLC shows an increase in risk but the perceived risk is constant because more mental effort is invested temporarily. Future research could use eye-trackers, postural sensors or brain imaging, to try to obtain a more complete picture of how drivers respond to changes in task demands.

In our study, temporal effects, in terms of the run order, were found for some measures (self-reported worry, mean heart rate). It may be argued that these temporal effects are themselves triggers of speed adaptation. On a longer time scale, it has been found that drivers' conviction rates rise in the first few years after obtaining a driver's licence (Bjørnskau & Sagberg, 2005; Harrington, 1972), which may be an adaptation to an increasing fearlessness while driving. Studies in which drivers' feelings and physiological measurements are recorded across multiple months are recommended to gain insight into speed adaptation during a learning process. Of course, it is also possible that the observed run order effects in our experiment simply reflect that participants became accustomed to the experimental apparatus.

2.4.6. Theoretical Implications

We conceptually replicated three experiments that have been important in shaping extant behavioural adaptation theories (Figure 2.1). The fact that none of the three regulatory hypotheses convincingly described speed adaptation in our relatively simple experiment raises doubts about the validity of the three corresponding theories.

One may argue that the theories in Figure 2.1 are oversimplifications of actual driving and that more sophisticated theories exist nowadays. Indeed, in recent years, the theories reported in Figure 2.1 have been substantially revised. For example, Fuller's (2005) task difficulty homeostasis theory has been extended into a Risk Allostasis Theory by including drivers' dispositions to comply with the speed limit (Fuller, 2011). Based on work of Fuller (2005), Kinnear and Helman's (2011) proposed a revised task-capability interface, a diagram with 28 blocks that are interconnected with arrows. Similar extensions also exist for Gibson and Crooks' field of safe travel (Papakostopoulos et al., 2017). One can argue that these sophisticated theories are more correct than the theories reported in Figure 2.1, because they include more factors that are known to influence driver behaviour. Although adding blocks and arrows may indeed provide a better fit to observed driving behaviour, such complexity is not necessarily theoretically convincing due to the risk of overfitting (Box, 1976; Preacher, 2003; Roberts & Pashler, 2000). According to the well-known principle of parsimony, a theory/model should be as simple as possible, not any simpler. We recommend that researchers first determine which regulatory mechanisms occur in car driving, before devising complex models. Our findings concerning steering reversal rate calls for more research into its possible role in speed adaptation.

2.4.7. Experimental Validity

The task demands in our driving simulator experiment were manipulated by changing the road width and imposed speed. It is possible to devise other types of task demand manipulations, including changes in traffic characteristics, weather conditions and road infrastructure (e.g. intersections, road signage). Also, our participants were mostly university students, which may hamper the generalisability of the present findings.

Another limitation is that driving in a fixed-base simulator may not sufficiently trigger driver behavioural adaptation, even though our simulator provided a large visual field of view (which improves speed perception), and incentives (task instructions, audio-visual feedback) were offered to minimise the number of cone hits. The lack of physical crash risk in a simulator could have induced a lower variety of tension levels as compared to an on-road research (e.g. see Healey & Picard, 2005 for an on-road measurement of GSR). Participants in our simulator did drive considerably faster on wide lanes than on narrow lanes. On-road

experiments, in which tension variability is higher, are likely to result in even greater range of speeds. Nevertheless, there are clear advantages of using a driving simulator. In particular, a simulator allows for accurate measurements of vehicle state, and for limiting the number of confounding variables. As pointed out by Taylor (1962), traffic jams or other events beyond a driver's control may prevent drivers from adopting their preferred speed (see also De Winter et al., 2007, showing that traffic turns a self-paced task into a forced-paced one). Participants in the simulator all drove in an identical environment, and could drive at a speed they preferred without being impeded.

In hindsight, we can conclude that the driving condition with the narrowest lane clearly evoked different driving behaviour than the other three lane widths, with participants barely accelerating on the straights, presumably in an attempt to minimise the number of cone hits (Figure 2.4). Additionally, participants experienced substantially more cone hits in the 2.0-m lane width condition than with the other three lane widths. Although our nonparametric OSA index can deal with nonlinearities, it would be worth exploring whether ceiling/floor effects or threshold effects occur at the extreme ranges of speed and road widths (see Lewis-Evans, 2012 for an extensive treatise on nonlinear effects in self-reported measures during driving). Thus, whether the lane width of 2.0 m should be regarded as an outlier, or whether it is part of the full spectrum of task demand conditions, is a topic for further research. Also, participants were required to report their experienced effort every 20 s. It is possible that this secondary task itself required some effort or caused some tension and that may have manifested mostly in the 2-m-wide lane, which was already so narrow that the small amount of cognitive distraction may have been detrimental.

Lastly, this experiment was conducted with a relatively small sample size of 24 participants. Whether the SRR is truly a superior measure of speed adaptation needs to be verified in future on-road experiments with larger samples. Based on our results it is concluded that TLC and SRTE can describe some of the observed speed adaptation. The steering reversal rate shows promise in capturing speed adaptation, prompting further research into the role of conservation of control activity in car driving.

Note

1. It is noted that Taylor (1962, 1964) presented some evidence that his GSR recordings were sensitive to task demands. For example, he showed that GSR exhibited a strong negative correlation with participants' age and years of licensure ($\rho = -0.64$ and -0.85 , respectively, based on data reported in Taylor, 1962; Figures 5 and 6). Taylor (1962) also noted that participants' GSR was elevated during certain events, such as when trying to 'squeeze' their vehicle between other moving vehicles. These findings suggested that GSR is a reliable and sensitive measure of experienced risk. However, the correlation with years of licensure was based on a small sample of drivers ($N = 12$), while no quantitative data were provided regarding sensitivity to the external events.

References

- Aarts, L., & Van Schagen, I. (2006). Driving speed and the risk of road crashes: A review. *Accident Analysis and Prevention*, *38*, 215–224.
- Alberdi, A., Aztiria, A., & Basarab, A. (2016). Towards an automatic early stress recognition system for office environments based on multimodal measurements: A review. *Journal of Biomedical Informatics*, *59*, 49–75.
- Assum, T., Bjørnskau, T., Fosser, S., & Sagberg, F. (1999). Risk compensation—the case of road lighting. *Accident Analysis & Prevention*, *31*, 545–553.
- Barutcu, I., Esen, A. M., Kaya, D., Turkmen, M., Karakaya, O., Melek, M., ... & Basaran, Y. (2005). Cigarette smoking and heart rate variability: dynamic influence of parasympathetic and sympathetic maneuvers. *Annals of noninvasive electrocardiology*, *10*, 324–329.
- Bernardi, L., Valle, F., Coco, M., Calciati, A., & Sleight, P. (1996). Physical activity influences heart rate variability and very-low-frequency components in Holter electrocardiograms. *Cardiovascular research*, *32*, 234–237.
- Berntson, G. G., Thomas Bigger Jr., J., Eckberg, D. L., Grossman, P., Kaufmann, P. G., Malik, M., ... & Van der Molen, M. W. (1997). Heart rate variability: origins, methods, and interpretive caveats. *Psychophysiology*, *34*, 623–648.
- Bjørnskau, T., & Sagberg, F. (2005). What do novice drivers learn during the first months of driving? Improved handling skills or improved road user interaction? In *Traffic and Transport Psychology, Theory and Application* (Ed. G. Underwood) (pp. 129–140). London: Elsevier
- Boer, E. R., & Ward, N. J. (2003). Event-based driver performance assessment. *Proceedings of the Second International Driving Symposium on Human Factors in Driver Assessment, Training and Vehicle Design*, 119–124.
- Box, G. E. (1976). Science and statistics. *Journal of the American Statistical Association*, *71*, 791–799.
- Byers, J. C., Bittner, A. C., & Hill, S. G. (1989). Traditional and raw task load index (TLX) correlations: Are paired comparisons necessary? *Advances in Industrial Ergonomics and Safety*. A. Mital (Ed.) Taylor & Francis., 481–485
- Christie, M. J. (1981). Electrodermal activity in the 1980s: a review. *Journal of the Royal Society of Medicine*, *74*, 616–622.
- Conover, W. J., & Iman, R. L. (1981). Rank transformations as a bridge between parametric and nonparametric statistics. *The American Statistician*, *35*, 124–129.
- Crowell, J. A., & Banks, M. S. (1993). Perceiving heading with different retinal regions and types of optic flow. *Perception & Psychophysics*, *53*, 325–337.
- De Vos, A. P., Godthelp, J., & Käppler, W. D. (1999). Subjective and objective assessment of manual, supported, and automated vehicle control. In J. P. Pauwelussen (Ed.), *Vehicle Performance: Understanding Human Monitoring and Assessment* (pp. 97–120). Lisse, the Netherlands: Swets & Zeitlinger.
- De Winter, J. C. F., & Dodou, D. (2016). National correlates of self-reported traffic violations across 41 countries. *Personality and Individual Differences*, *98*, 145–147.
- De Winter, J. C. F., Dodou, D., & Stanton, N. A. (2015). A quarter of a century of the DBQ: Some supplementary notes on its validity with regard to accidents. *Ergonomics*, *58*, 1745–1769.
- De Winter, J. C. F., Wieringa, P. A., Kuipers, J., Mulder, J. A., & Mulder, M. (2007). Violations and errors during simulation-based driver training. *Ergonomics*, *50*, 138–158.
- Dragutinovic, N., Brookhuis, K. A., Hagenzieker, M. P., & Marchau, V. A. (2005). Behavioural effects of advanced cruise control use: A meta-analytic approach. *European journal of transport and infrastructure research*, *5*, 267–280.
- Elbanhawi, M., Simic, M., & Jazar, R. (2015). In the passenger seat: investigating ride comfort measures in autonomous cars. *IEEE Intelligent Transportation Systems Magazine*, *7*, 4–17.
- Elvik, R. (2013). 20 Impact of behavioural adaptation on cost-benefit analyses. In C. M. Rudin-Brown & S. L. Jamson (Eds.), *Behavioural adaptation and road safety: Theory, evidence and action* (pp. 371–384). Boca Raton, FL: CRC Press.
- Elvik, R., Christensen, P., & Amundsen, A. (2004). *Speed and road accidents: An evaluation of the Power Model* (TOI report 740). Oslo, Norway: Institute of Transport Economics. Retrieved from <http://www.trg.dk/elvik/740-2004.pdf>
- Falahi, M., Motamedzade, M., Heidari-moghadam, R., Soltanian, A. R., & Miyake, S. (2016). Effects of mental workload on physiological and subjective responses during traffic density monitoring: A field study. *Applied Ergonomics*, *52*, 95–103.
- Figner, B., & Murphy, R. O. (2011). Using skin conductance in judgment and decision making research. In M. Schulte-Mecklenbeck, A. Kuehberger, & R. Ranyard (Eds.), *A handbook of process tracing methods for decision research* (pp. 163–184). New York, NY: Psychology Press.
- Fuller, R. (2005). Towards a general theory of driver behaviour. *Accident Analysis & Prevention*, *37*, 461–472.
- Fuller, R. (2011). Driver control theory: From task difficulty homeostasis to risk allostasis. *Handbook of Traffic Psychology*, 13–26.
- Fuller, R., McHugh, C., & Pender, S. (2008). Task difficulty and risk in the determination of driver behaviour. *Revue Européenne de Psychologie Appliquée/European Review of Applied Psychology*, *58*, 13–21.
- Gibson, J. J., & Crooks, L. E. (1938). A theoretical field-analysis of automobile-driving. *The American Journal of Psychology*, *51*, 453–471
- Godthelp, H. (1988). The limits of path error-neglecting in straight line driving. *Ergonomics*, *31*, 609–619.
- Godthelp, H., Milgram, P., & Blaauw, G. J. (1984). The development of a time-related measure to describe driving strategy. *Human Factors*,

- 26, 257–268.
- Goodrich, M. A., & Boer, E. R. (2000). Designing human-centered automation: Trade-offs in collision avoidance system design. *IEEE Transactions on Intelligent Transportation Systems*, 1, 40–54.
- Harrington, D. M. (1972). The young driver follow-up study: An evaluation of the role of human factors in the first four years of driving. *Accident Analysis and Prevention*, 4, 191–240.
- Hart, S. G., & Staveland, L. E. (1988). Development of NASA-TLX (Task Load Index): Results of empirical and theoretical research. In P. A. Hancock & N. Meshkati (Eds.), *Human mental workload* (Vol. 1, pp. 139–183). Amsterdam, the Netherlands: North Holland Press.
- Hayashi, T., Okamoto, E., Nishimura, H., Mizuno-Matsumoto, Y., Ishii, R., & Ukai, S. (2009). Beta activities in EEG associated with emotional stress. *International Journal of Intelligent Computing in Medical Sciences & Image Processing*, 3, 57–68.
- Healey, J. A., & Picard, R. W. (2005). Detecting stress during real-world driving tasks using physiological sensors. *IEEE Transactions on Intelligent Transportation Systems*, 6, 156–166.
- Heikoop, D. D., De Winter, J. C. F., Van Arem, B., & Stanton, N. A. (2017). Effects of platooning on signal-detection performance, workload, and stress: A driving simulator study. *Applied Ergonomics*, 60, 116–127.
- Hiraoka, T., Masui, J., & Nishikawa, S. (2010). Behavioral adaptation to advanced driver-assistance systems. *Proceedings of SICE Annual Conference 2010* (pp. 930–935). IEEE.
- Hjortskov, N., Rissén, D., Blangsted, A. K., Fallentin, N., Lundberg, U., & Søgaard, K. (2004). The effect of mental stress on heart rate variability and blood pressure during computer work. *European Journal of Applied Physiology*, 92, 84–89.
- Janssen, W., & Nilsson, L. (1993). Behavioural effects of driver support. In A. M. Parkes & S. Franzen (Eds.), *Driving Future Vehicles* (pp. 147–155). London – Washington DC: Taylor & Francis
- Kahneman, D. (1973). *Attention and effort*. Englewood Cliffs, NJ: Prentice-Hall.
- Kendall, M. G., & Smith, B. B. (1939). The problem of m rankings. *The Annals of Mathematical Statistics*, 10, 275–287.
- Kinney, N., Kelly, S. W., Stradling, S., & Thomson, J. (2013). Understanding how drivers learn to anticipate risk on the road: A laboratory experiment of affective anticipation of road hazards. *Accident Analysis & Prevention*, 50, 1025–1033.
- Kinney, N. A. D., & Helman, S. (2011). Updating risk allostasis theory to better understand behavioural adaptation. In C. Rudin-Brown, & S. Jamson (Eds.), *Behavioural Adaptation and Road Safety* (pp. 87–110). CRC Press.
- Kolekar, S., De Winter, J. C. F., & Abbink, D. A. (2017). A human-like steering model: Sensitive to uncertainty in the environment. *IEEE International Conference on Systems, Man, and Cybernetics*.
- Lewis-Evans, B. (2012). *Testing models of driver behaviour* (Doctoral dissertation), University of Groningen
- Lewis-Evans, B., & Charlton, S. G. (2006). Explicit and implicit processes in behavioural adaptation to road width. *Accident Analysis & Prevention*, 38, 610–617.
- Lewis-Evans, B., De Waard, D., & Brookhuis, K. A. (2011). Speed maintenance under cognitive load—Implications for theories of driver behaviour. *Accident Analysis & Prevention*, 43, 1497–1507.
- Lewis-Evans, B., & Rothengatter, T. (2009). Task difficulty, risk, effort and comfort in a simulated driving task—Implications for Risk Allostasis Theory. *Accident Analysis & Prevention*, 41, 1053–1063.
- Li, L., & Chen, J. (2010). Relative contributions of optic flow, bearing, and splay angle information to lane keeping. *Journal of Vision*, 10(11):16, 1–14,
- Liu, S., Wang, J., & Fu, T. (2016). Effects of lane width, lane position and edge shoulder width on driving behavior in underground urban expressways: a driving simulator study. *International Journal of Environmental Research and Public Health*, 13, 1010.
- Lozano, R., Naghavi, M., Foreman, K., Lim, S., Shibuya, K., Aboyans, V., ... & Remuzzi, G. (2013). Global and regional mortality from 235 causes of death for 20 age groups in 1990 and 2010: a systematic analysis for the Global Burden of Disease Study 2010. *The Lancet*, 380, 2095–2128.
- Manzano, B. M., Vanderlei, L. C. M., Ramos, E. M., & Ramos, D. (2011). Acute effects of smoking on autonomic modulation: analysis by Poincaré plot. *Arquivos Brasileiros de Cardiologia*, 96, 154–160.
- Matthews, G., Joyner, L., Gilliland, K., Campbell, S., Falconer, S., & Huggins, J. (1999). Validation of a comprehensive stress state questionnaire: Towards a state “Big Three”? In I. Mervielde, I. J. Deary, F. de Fruyt, & F. Ostendorf (Eds.), *Personality psychology in Europe* (Vol. 7) (pp. 335–350). Tilburg: Tilburg University Press.
- McLean, J. R., & Hoffmann, E. R. (1972). The effects of lane width on driver steering control and performance. *6th Australian Road Research Board (ARRB) Conference*, Canberra (Vol. 6, No. 3).
- McLean, J. R., & Hoffmann, E. R. (1975). Steering reversals as a measure of driver performance and steering task difficulty. *Human Factors*, 17, 248–256. Retrieved from <http://www.ingentaconnect.com/content/hfes/hf/1975/00000017/00000003/art00004>
- Melman, T., De Winter, J. C. F., & Abbink, D. A. (2017). Does haptic steering guidance instigate speeding? A driving simulator study into causes and remedies. *Accident Analysis and Prevention*, 98, 372–387.
- Nagai, Y., Critchley, H. D., Featherstone, E., Trimble, M. R., & Dolan, R. J. (2004). Activity in ventromedial prefrontal cortex covaries with sympathetic skin conductance level: a physiological account of a “default mode” of brain function. *Neuroimage*, 22, 243–251.
- OECD. (1990). Behaviour adaptations to changes in the road transport system. Paris: OECD.
- Östlund, J., Peters, B., Thorslund, B., Engström, J., Markkula, G., Keinath, A., ... & Foehl, U. (2005). *Driving performance assessment—methods and metrics*. http://www.aide-eu.org/pdf/sp2_deliv_new/aide_d2_2_5.pdf

- Oviedo-Trespalacios, O., Haque, M. M., King, M., & Washington, S. (2017). Effects of road infrastructure and traffic complexity in speed adaptation behaviour of distracted drivers. *Accident Analysis & Prevention*, *101*, 67–77.
- Papakostopoulos, V., Marmaras, N., & Nathanael, D. (2017). The “field of safe travel” revisited: interpreting driving behaviour performance through a holistic approach. *Transport Reviews*, *37*, 695–714.
- Preacher, K. J. (2003). *The role of model complexity in the evaluation of structural equation models* (Doctoral dissertation), The Ohio State University.
- Roberts, S., & Pashler, H. (2000). How persuasive is a good fit? A comment on theory testing. *Psychological Review*, *107*, 358–367.
- Saad, F. (2006). Some critical issues when studying behavioural adaptations to new driver support systems. *Cognition, Technology and Work*, *8*, 175–181.
- Strong, P. (1970). Biophysical measurements. *Tektronix Measurement Series*. Beaverton, OR: Tektronix Inc.
- Sullivan, J. M., Flannagan, M. J., Pradhan, A. K., & Bao, S. (2016). *Literature review of behavioral adaptations to advanced driver assistance systems*. Washington.
- Summala, H. (2007). Towards understanding motivational and emotional factors in driver behaviour: comfort through satisficing. In P. C. Cacciabue (Ed.), *Modelling driver behaviour in automotive environments* (pp. 189–207). London, UK: Springer.
- Sun, F. T., Kuo, C., Cheng, H. T., Buthpitiya, S., Collins, P., & Griss, M. (2012). Activity-aware mental stress detection using physiological sensors. *Mobile computing, applications, and services*, 211–230.
- Taylor, D. H. (1962). *A study of drivers' galvanic skin response and the risk of accident* (Report No. LN/26/DHT). Road Research Laboratory: Department of Scientific and Industrial Research.
- Taylor, D. H. (1964). Drivers' galvanic skin response and the risk of accident. *Ergonomics*, *7*, 439–451.
- Treat, J. R., Tumbas, N. S., McDonald, S. T., Shinar, D., & Hume, R. D. (1979). *Tri-level study of the causes of traffic accidents. Executive summary* (Report No. DOT HS 805 099). Washington, DC: National Highway Traffic Safety Administration.
- Vaa, T. (2007). Modelling driver behaviour on basis of emotions and feelings: intelligent transport systems and behavioural adaptations. In P. C. Cacciabue (Ed.), *Modelling driver behaviour in automotive environments* (pp. 208–232). London, UK: Springer.
- Van Leeuwen, P. M., Gómez i Subils, C., Ramon Jimenez, A., Happee, R., & De Winter, J. C. F. (2015). Effects of visual fidelity on curve negotiation, gaze behavior, and simulator discomfort. *Ergonomics*, *58*, 1347–1364.
- Van Winsum, W., Brookhuis, K., & de Waard, D. (2000). A comparison of different ways to approximate time-to-line crossing (TLC) during car driving. *Accident Analysis & Prevention*, *32*, 47–56.
- Van Winsum, W., & Godthelp, H. (1996). Speed choice and steering behavior in curve driving. *Human Factors*, *38*, 434–441.
- Villarejo, M. V., Zapirain, B. G., & Zorrilla, A. M. (2012). A stress sensor based on galvanic skin response (GSR) controlled by ZigBee. *Sensors*, *12*, 6075–6101.
- Vollmer, M. (2016). A robust, simple and reliable measure of heart rate variability using relative RR intervals. *Computing in Cardiology*, *42*, 609–612.
- Waytz, A., Heafner, J., & Epley, N. (2014). The mind in the machine: Anthropomorphism increases trust in an autonomous vehicle. *Journal of Experimental Social Psychology*, *52*, 113–117.
- Wen, W., Tomoi, D., Yamakawa, H., Hamasaki, S., Takaku-saki, K., An, Q., Tamura, Y., Yamashita, A., & Asama, H. (2017). Continuous estimation of stress using physiological signals during a car race. *Psychology*, *8*, 978–986.
- Wilde, G. J. (1982). The theory of risk homeostasis: implications for safety and health. *Risk Analysis*, *2*, 209–225.
- Wilde, G. J. (2009). *Risk homeostasis: theory, evidence and practical implications. Invited lecture at the Road Safet Advance Course*, Department of Civil Engineering, University of Palermo, Italy.
- Wohl, J. G. (1961). Man-machine steering dynamics. *Human Factors*, *3*, 222–228.
- Zhai, S., Accot, J., & Woltjer, R. (2004). Human action laws in electronic virtual worlds: an empirical study of path steering performance in VR. *Presence: Teleoperators and Virtual Environments*, *13*, 113–127.

Appendix 2 – Correlation matrices

Table 2A. Spearman rank-order correlation matrix for the self-paced condition (SP).

Dependent measures	1	2	3	4	5	6	7	8	9	10	11	12	13	14	15	16	17	18	
1. Mean speed	1.00																		
2. Percentage time off-road	0.24	1.00																	
3. Mean absolute lateral error	0.10	0.75	1.00																
4. Maximum absolute lateral error	0.24	0.48	0.60	1.00															
5. Self-reported task effort (SRTE)	-0.08	-0.22	-0.32	-0.23	1.00														
6. Median TLC	-0.50	-0.73	-0.45	-0.41	-0.10	1.00													
7. TLC15th	-0.63	-0.78	-0.51	-0.43	-0.08	0.91	1.00												
8. Mean GSR	-0.01	-0.31	-0.19	-0.15	-0.15	0.37	0.32	1.00											
9. Mean GSR rate	0.14	-0.01	-0.06	0.13	0.07	-0.04	-0.11	0.74	1.00										
10. Mean HR	-0.01	-0.31	-0.40	-0.11	0.25	0.34	0.17	0.10	0.10	1.00									
11. SDNN	0.01	0.28	0.33	0.18	0.04	-0.33	-0.16	-0.14	-0.13	-0.58	1.00								
12. LF/HF ratio	0.08	-0.14	-0.21	0.09	0.25	0.09	-0.08	0.03	0.16	0.44	-0.52	1.00							
13. Steering reversal rate	0.08	0.24	-0.05	-0.06	0.33	-0.64	-0.41	-0.11	0.13	-0.30	0.37	-0.13	1.00						
14. Overall NASA TLX	-0.49	0.18	0.19	-0.02	0.31	0.06	0.07	-0.05	-0.06	0.07	0.05	-0.23	0.11	1.00					
15. DSSQ Engagement	0.14	0.02	0.07	0.11	0.02	-0.24	-0.07	-0.28	-0.16	-0.27	0.05	0.16	0.30	0.00	1.00				
16. DSSQ Distress	-0.46	0.11	0.04	-0.16	0.31	0.15	0.12	-0.07	-0.18	0.30	-0.03	-0.13	-0.09	0.84	-0.26	1.00			
17. DSSQ Worry	-0.52	-0.15	0.04	-0.02	0.27	0.38	0.39	0.05	-0.10	0.41	0.06	-0.11	-0.23	0.51	-0.32	0.66	1.00		
18. DBQ	0.25	0.04	-0.29	-0.50	0.18	-0.11	-0.14	-0.02	-0.06	0.14	-0.08	0.01	0.15	-0.21	-0.05	-0.10	-0.30	1.00	
19. Mileage	0.58	0.02	0.04	0.09	0.02	-0.25	-0.27	0.06	0.15	-0.07	0.14	0.09	0.11	-0.35	0.33	-0.32	-0.47	0.24	1.00

Note. $p < 0.05$ for $|\rho| \geq 0.41$, $p < 0.01$ for $|\rho| \geq 0.52$ and $p < 0.001$ for $|\rho| \geq 0.63$.

Table 2B. Spearman rank-order correlation matrix for the forced-paced condition at 90 km/h (FP90).

Dependent measures	1	2	3	4	5	6	7	8	9	10	11	12	13	14	15	16	17	18	
1. Mean speed																			
2. Percentage time off-road		1.00																	
3. Mean absolute lateral error		0.70	1.00																
4. Maximum absolute lateral error		0.48	0.76	1.00															
5. Self-reported task effort (SRTE)		-0.23	-0.26	-0.35	1.00														
6. Median TLC		-0.75	-0.40	-0.34	-0.18	1.00													
7. TLC15th		-0.81	-0.57	-0.49	-0.05	0.93	1.00												
8. Mean GSR		-0.31	-0.14	-0.09	-0.22	0.44	0.31	1.00											
9. Mean GSR rate		-0.09	-0.11	-0.05	-0.12	0.15	0.01	0.82	1.00										
10. Mean HR		-0.45	-0.20	-0.26	0.15	0.38	0.35	0.27	0.16	1.00									
11. SDNN		0.40	0.01	-0.03	-0.13	-0.27	-0.30	-0.08	-0.03	-0.41	1.00								
12. LF/HF ratio		-0.31	-0.15	-0.19	0.02	0.35	0.31	-0.03	0.03	0.45	-0.41	1.00							
13. Steering reversal rate		0.39	0.07	0.16	0.20	-0.71	-0.66	-0.09	0.16	-0.37	0.36	-0.12	1.00						
14. Overall NASA TLX		0.43	0.27	0.08	0.24	-0.45	-0.44	0.09	0.19	0.28	0.13	0.00	0.25	1.00					
15. DSSQ Engagement		0.23	0.25	0.19	-0.13	-0.07	-0.19	-0.19	-0.11	-0.14	0.14	0.16	0.17	-0.02	1.00				
16. DSSQ Distress		0.04	-0.15	-0.12	0.33	-0.19	-0.05	0.20	0.13	0.33	0.00	-0.18	0.12	0.71	-0.36	1.00			
17. DSSQ Worry		-0.14	-0.06	-0.36	-0.07	0.38	0.32	0.40	0.13	0.26	0.27	0.04	-0.12	0.15	0.01	0.18	1.00		
18. DBQ		-0.05	-0.37	-0.45	0.28	-0.14	-0.08	-0.14	0.07	0.30	-0.14	0.09	0.08	0.07	-0.06	0.07	-0.13	1.00	
19. Mileage		-0.14	-0.15	-0.01	0.02	0.22	0.17	-0.05	0.05	-0.03	0.07	0.00	-0.06	-0.17	0.23	-0.26	-0.09	0.24	1.00

Note. $p < 0.05$ for $|\rho| \geq 0.41$, $p < 0.01$ for $|\rho| \geq 0.52$ and $p < 0.001$ for $|\rho| \geq 0.63$. For FP90 no speed correlations are shown because the speed was fixed, and thus no correlations are applicable.

Table 2C. Spearman rank-order correlation matrix for the forced-paced condition at 130 km/h (FP130)

Dependent measures	1	2	3	4	5	6	7	8	9	10	11	12	13	14	15	16	17	18	
1. Mean speed	1.00																		
2. Percentage time off-road	0.75	1.00																	
3. Mean absolute lateral error	0.64	0.78	1.00																
4. Maximum absolute lateral error	-0.06	-0.18	0.05	1.00															
5. Self-reported task effort (SRTE)	-0.76	-0.59	-0.57	-0.02	1.00														
6. Median TLC	-0.78	-0.67	-0.63	0.05	0.91	1.00													
7. TLC15th	-0.26	-0.35	-0.28	-0.05	0.32	0.31	1.00												
8. Mean GSR	0.08	-0.17	0.01	0.01	-0.05	0.04	0.72	1.00											
9. Mean GSR rate	-0.19	-0.22	-0.15	0.03	0.30	0.21	0.07	-0.06	1.00										
10. Mean HR	0.04	-0.01	0.05	-0.05	-0.24	-0.06	0.33	0.30	-0.51	1.00									
11. SDNN	-0.43	-0.35	-0.23	0.07	0.39	0.37	0.12	0.11	0.62	-0.33	1.00								
12. LF/HF ratio	0.30	0.02	0.15	0.13	-0.73	-0.65	-0.09	0.18	-0.16	0.19	-0.08	1.00							
13. Steering reversal rate	0.50	0.22	0.46	0.40	-0.48	-0.47	-0.12	0.11	-0.01	-0.17	-0.19	0.34	1.00						
14. Overall NASA TLX	-0.28	-0.16	-0.02	0.08	-0.02	0.02	-0.34	-0.16	0.01	-0.09	0.25	0.32	-0.03	1.00					
15. DSSQ Engagement	0.12	-0.16	0.14	0.46	-0.13	-0.03	-0.05	0.13	0.02	-0.23	0.07	0.14	0.61	-0.01	1.00				
16. DSSQ Distress	0.09	0.13	0.32	0.15	0.05	0.05	0.00	-0.05	0.09	-0.06	0.10	0.01	-0.09	-0.14	0.11	1.00			
17. DSSQ Worry	-0.06	-0.10	-0.25	-0.07	-0.06	-0.10	0.05	-0.01	0.33	0.01	0.15	0.23	-0.31	-0.17	-0.37	-0.08	1.00		
18. DBQ	-0.34	-0.14	-0.19	-0.28	0.26	0.21	0.10	0.02	-0.02	0.08	-0.03	-0.12	-0.48	0.17	-0.51	-0.27	0.24	1.00	
19. Mileage																			1.00

Note. $p < 0.05$ for $|\rho| \geq 0.41$, $p < 0.01$ for $|\rho| \geq 0.52$ and $p < 0.001$ for $|\rho| \geq 0.63$. For FP130 no speed correlations are shown because the speed was fixed, and thus no correlations are applicable.

Table 2D. The results of the repeated measures ANOVA (p , F), Spearman correlation coefficient (ρ) between Run 1 and 3, and Means (M) per dependent measures with the session order as within-subjects factor.

Dependent measures	p -value	$F(2,46)$	ρ Run 1-3	M Run 1	M Run 2	M Run 3
Mean speed (km/h)	0.955	0.05		113.9	115.5	114.9
Percentage time off-road (%)	0.279	1.31	0.41	6.24	4.85	5.01
Mean absolute lateral error (m)	0.026	3.98	0.69	0.123	0.112	0.119
Maximum absolute lateral error (m)	0.157	1.93	0.39	0.492	0.433	0.435
Self-reported task effort (0-10)	0.407	0.92	0.33	3.73	4.00	3.76
Median TLC (s)	0.892	0.12	-0.05	2.50	2.56	2.53
TLC15th (s)	0.678	0.39	-0.34	1.25	1.28	1.28
Mean GSR (μ S)	0.955	0.05	0.81	7.68	7.48	7.61
Mean GSR rate (μ S/min)	0.209	1.62	0.86	8.70	7.37	7.36
Mean HR (bpm)	$5.14 \cdot 10^{-5}$	12.33	0.90	80.62	77.14	76.52
SDNN (ms)	0.851	0.16	0.75	56.61	53.48	56.13
LF/HF ratio (ms)	0.905	0.10	0.92	1.15	1.11	1.12
Steering reversal rate (deg/sec)	0.923	0.08	0.63	0.66	0.61	0.61
Overall NASA TLX (%)	0.849	0.16	0.27	50.80	51.77	50.24
DSSQ Engagement (0-32)	0.711	0.34	0.67	23.54	24.04	24.83
DSSQ Distress (0-32)	0.152	1.96	0.31	12.71	13.04	10.79
DSSQ Worry (0-32)	$5.50 \cdot 10^{-3}$	8.88	0.73	7.88	5.54	5.21

**How Road Narrowing Impacts
the Trade-off Between Two
Adaptation Strategies:
Reducing Speed and Increasing
Neuromuscular Stiffness**



When drivers encounter a road narrowing two potential adaptation strategies come into play that may increase safety margins: decreasing speed and increasing neuromuscular stiffness of the arms. These two adaptation strategies have so far been studied in isolation. We expect that there is a trade-off between these two strategies, and that risk duration would impact a driver's selection of the trade-off. Specifically, we hypothesized that for a short risk duration, drivers will favour increased neuromuscular stiffness over speed reduction; and vice versa for longer risk durations. Twenty-six participants drove in a driving simulator and encountered different risk durations; realized by road narrowings (from 3.6 m to 2.2 m) of varying lengths (10 m, 100 m, 250m, and 500 m). The neuromuscular stiffness was quantified by measuring the grip force exerted by both hands. The results show that all road narrowing conditions successfully induced driver adaptations, as a significant reduction in speed and increase in grip force was observed. However, the tested drivers did not consistently select the hypothesized different trade-offs for increasing duration of road narrowing: a low correlation was found between speed and grip force adaptations. Interestingly, individual trade-off were consistent: the within-subject variability in speed-grip force adaptations was low across the tested risk durations. Future research should further elucidate the underlying motivations for these individual adaptation strategies.

Published as:

Melman, T., Kolekar, S. B., Hogerwerf, E. W. M., & Abbink, D. A. (2020). How road narrowing impacts the trade-off between two adaptation strategies: Reducing speed and increasing neuromuscular stiffness. *Proceedings of the 2020 IEEE International Conference on Systems, Man, and Cybernetics* (pp. 3235–3240). Toronto, Canada. <https://doi.org/10.1109/SMC42975.2020.9283172>

3.1. Introduction

The ability to adapt is intrinsic to humans and imperative to cope with events in the driving scene. Literature provides evidence for different adaptation strategies across different experimental conditions, such as adapting speed, neuromuscular properties, and steering strategy when driving on different lane widths (McLean & Hoffmann, 1972; Melman et al., 2018; Pronker et al., 2017; Van der Wiel et al., 2015), adapting speed when approaching a curve (Van Winsum & Godthelp, 1996) or a one-lane bridge (Charlton & Starkey, 2016); adapting time headway and speed when driving in fog (Brooks et al., 2011) or behind a lead vehicle (Saffarian et al., 2012) and adapting steering strategy when perturbed by lateral wind gusts (Wierwille et al., 1983). These voluntary adaptations to changes in driving scene and task demand can be accompanied by involuntary adaptations such as an increase in galvanic skin response (i.e., sweat production), heart rate, respiratory rate, pupil diameter, and eye scanning behavior (Heikoop et al., 2018; Rendon-Velez et al., 2016).

The psychological mechanisms behind driver adaptations are yet to be elucidated. As Melman et al. (2018) argued, several theories have postulated that drivers exhibit a trade-off between two conflicting motivations, namely arriving at a destination in time (efficiency) versus avoiding dangerous situations (safety), where the driver's level of subjective risk (Näätänen & Summala, 1974; Wilde, 1998), task difficulty (Fuller et al., 2008), or time/safety margins (Gibson & Crooks, 1938; Van Winsum et al., 2000) are regarded as important homeostatic variables.

As indicated above, many researchers have shown the existence of steady-state driver adaptations, but few take the non-steady state and interaction between different driver adaptations into account. For example, a driving simulator study by Van der Wiel et al. (2015) showed an increase in neuromuscular stiffness to reducing road width (2.5 m and 4.5 m) while driving at two different fixed speeds (70 and 120 km/hr). The authors of that paper suggested that in real life, it would be likely that drivers prefer to reduce speed and thereby reduce the need for the energy-consuming increase in neuromuscular stiffness. Although fixing the driving speed can be beneficial to reduce between-driver variability, it inhibits a realistic understanding of the interaction between driver adaptations. Additionally, most studies (e.g., McLean & Hoffmann, 1972; Melman et al., 2018; Pronker et al., 2017; Van der Wiel et al., 2015) use fixed lengths of narrow road sections which only allows for investigation of steady-state driver adaptations due to fixed risk durations. In this paper, we aim to investigate the non steady state interaction between two commonly found adaptations strategies: speed and neuromuscular stiffness adaptations for different risk durations.

Speed adaptation has strong implications on road safety. In essence, higher speed reduces a driver's time to respond in an emergency scenario, increases the severity of the impact, and the probability of being involved in a crash (Aarts & Van Schagen, 2006; Elvik, 2013; Elvik et al., 2004; Hedlund, 2000). Adapting the neuromuscular stiffness improves robustness to perturbations but is an energy-consuming strategy (Gribble et al., 2003). Previous studies have estimated neuromuscular stiffness by adding perturbations on the steering wheel (Abbink et al., 2011; Antonin et al., 2015; Van der Wiel et al., 2015), or by measuring EMG signals which are intrusive and generally have low signal to noise ratio (Pick & Cole, 2006). Previous studies reported an inverse relation between neuromuscular stiffness and grip force during driving (Kuchenbecker et al., 2003; Nakamura et al., 2011; Pronker et al., 2017), allowing for a non-obtrusive measurement with a good signal to noise ratio. These findings motivated us to use grip force measurements.

In this study, a decrease in road width was utilized to induce speed and neuromuscular stiffness adaptations, as a change in road width is known to cause drivers to adjust their driving speed (Charlton & Starkey, 2016; McLean & Hoffmann, 1972) and neuromuscular stiffness (Pronker et al., 2017; Van der Wiel et al., 2015). To investigate the interaction between speed and neuromuscular stiffness adaptations, we created different risk durations

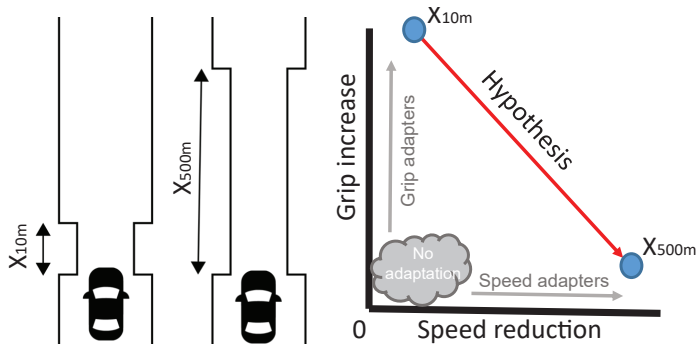


Figure 3.1. The hypothesized impact of the length of the narrow road section (x) on speed adaptation and grip force adaptation.

by exposing the driver to four different lengths of road narrowing.

In summary, this study examines to what extent the duration of increased risk (i.e., the length of a road narrowing) influences the drivers' speed and neuromuscular stiffness strategy (measured by grip force). We expect that there is a trade-off between these two strategies, and that risk duration would impact a driver's selection of the trade-off. Specifically, we hypothesized that for a short risk duration, drivers will favour increased neuromuscular stiffness over speed reduction; and vice versa for longer risk durations (Figure 3.1).

3.2 Method

3.2.1. Participants

Twenty-six participants (9 female) 20 to 32 years old ($M = 25.9$, $SD = 3.2$) volunteered in this study. All participants had normal or corrected to normal eyesight and had a valid driver's license for at least one year ($M = 6.5$, $SD = 3.4$).

3.2.2. Apparatus

The experiment was conducted in a fixed-based driving simulator. The scenery was visualized using three LCD projectors with a horizontal and vertical field-of-view of 180° and 40° . The simulation data was logged at 100 Hz. Vehicle dynamics were simulated with a single-track model (heavy sedan of 1.8 m wide), with an automatic gearbox and self-aligning torques were imposed on the steering wheel. Car vibrations ("road rumble") were simulated with a seat shaker implemented in the driver's seat. During the experiment, participants could control the speed of the vehicle, and the speedometer was displayed on the dashboard.

The grip force was measured using Tekscan 4256E pressure sensors attached to gloves (Figure 3.2). The sensor consists of 349 sensils (i.e., individual pressure-sensing locations) with a spatial resolution of 7.1 sensors/cm². During this study, the total sum of all sensils for the left and right hand were recorded. The grip force data was logged at 20 Hz and synchronized with the simulator data.

3.2.3. Road Conditions and Environment

During the experiment, participants drove 35 kilometres on a 3.6 m wide road. Participants encountered four different straight road-narrowing lengths (10 m, 100 m, 250 m, and 500 m). For each road-narrowing length, the road width reduced from 3.6 m to 2.2 m, allowing 0.9 m and 0.2 m lateral deviation on either side of the car, respectively (Figure 3.2). Every participant drove the four road-narrowing lengths eight times, which were presented in a



Figure 3.2. The used grip force sensors (left), and the simulator environment (right) for the 500m road narrowing including the car front.

3

counterbalanced order. All road-narrowings occurred on a straight road section, and were preceded and succeeded by a 200 m wide section. The road narrowing sections were separated by straights and curves sections to allow the drivers to reach their preferred speed. Speed perception was enhanced by means of trees alongside the road. Cones were placed along the entire road, and a car front was visualized to facilitate perception of the car's position relative to the road boundaries. A vibration that mimicked rumble strips was implemented on the steering wheel to give additional feedback to the driver when the car was outside the lane boundary. A multi-sine torque perturbation consisting of 6 low frequencies (ranging from 0.25 to 18 Hz) was applied to the steering wheel to mimic environmental disturbances (e.g., wind) that require the participants to steer even on long straight sections. The total multi-sine was scaled to low torques ($M = 0$, $SD = 0.13$ Nm) to ensure that the driver was not disrupted during driving due to the perturbation.

3.2.4. Experimental Procedure

Before the start of the experiment, the grip sensors were calibrated using a bulb shaped dynamometer, which ensured a good pressure distribution over all sensils. Participants were instructed to apply a force of 5 kg, 10 kg, 15 kg and a maximum force to the hand dynamometer. To get familiar with the driving simulator, each participants performed a training trial of 7 minutes on the wide road with no lane narrowing. During the experiment participants were instructed to drive as they normally would do while not hitting any cones, and to keep their hands in a 10-to-2 position. The experimenter stood next to the participants during the experiment and after each narrow section, the participants answered the question: '*How much effort did it cost you to successfully drive this section?*'. Participants responded with a number between 1 (*no effort*) and 10 (*a lot of effort*). In total the experiment took approximately 1 hour.

3.2.5. Dependent Measures

For all dependent measures, the wide section metric was calculated between 200 m to 150 m before the road narrowing starts. The narrow road is calculated over the middle 5 meters of the narrow road section.

Effect of road width

- *Mean speed (km/h)*. The mean speed was calculated over all 32 wide sections combined and over all 32 narrow sections combined.
- *Mean grip force (N)*. The mean grip force of both hands combined was calculated over all 32 wide sections combined and over all 32 narrow sections combined.

Effect of road width length

- *Delta speed (km/h; Δ Speed)*. The mean speed difference between the wide section relative to the narrow section.
- *Delta grip (N; Δ Grip force)*. The mean grip force difference between the wide section relative to the narrow section.
- *Self-reported task effort (1-10; SRTE)*. After each narrow section, the participants reported how much effort the current task takes from 0 (no effort) to 10 (a lot of effort).
- *Time off-road (s)*. The amount of time for which the car was outside the cone boundaries for then arrow road section.

3.2.6. Statistical Analysis

For each dependent measure, the mean of all eight repetitions was computed. These values were collected in a 26 x 4 matrix (26 participants and 4 road width lengths). First, the matrix was rank-transformed according to Conover and Iman (1981), to account for possible violations of the assumption of normality. This rank-transformed matrix with values ranging from 1 to 104 was submitted to a repeated-measures ANOVA with the four narrow-road lengths as a within-subject factor. A post-hoc paired t-test was performed with Bonferroni corrections applied to the six pairwise comparisons between the narrow road lengths. To investigate the effect of road width (section 3.2.5.), a paired t-test was used, after rank-transformation (i.e., with values ranging from 1-52).

3.3. Results

Figure 3.3 shows the lateral position, speed, and grip force averaged over all participants, for the entry (200 m before road narrowing), narrow section, and the exit (200 m after road narrowing). At the entry, the 10 m road narrowing results in slightly delayed and less speed reduction compared to the three longer narrow road lengths. An increase in grip force can be seen for all four conditions before entering the narrow section. Drivers maintain an almost constant speed, and a constant grip force over the entire narrow road section, with a small increase and decrease at the start and end of the section. At the exit, drivers increased speed and decreased grip force to approximately the speed at which they drove before they entered the entry section.

3.3.1. Effect of Road Width

The mean speed and mean grip force for all 32 wide combined and 32 narrow sections combined are shown in Figure 3.4. Participants drove with a lower mean speed and had a higher grip force on the narrow roads as compared to the wide roads. Confirming that road width reduction is indeed a good method to induce speed and grip force adaptations.

3.3.2. Effect of Narrow Road Length

Figure 3.5 visualizes the results for the four dependent measures, including the individual results for each participant averaged over eight repetitions. The results of the repeated-measures ANOVA show a significant effect for the narrow-road length for all four dependent measures. The post-hoc analysis identified a significantly smaller speed reduction for the 10 m compared to the 100 m section only. The grip force increment was lower for the 10 m than for the 100 m, 250 m and 500 m section. No significant differences were found for Δ Speed, Δ Grip force between the other narrow road lengths. The SRTE and time off-road progressively increased with narrow road lengths; between all narrow road lengths comparisons.

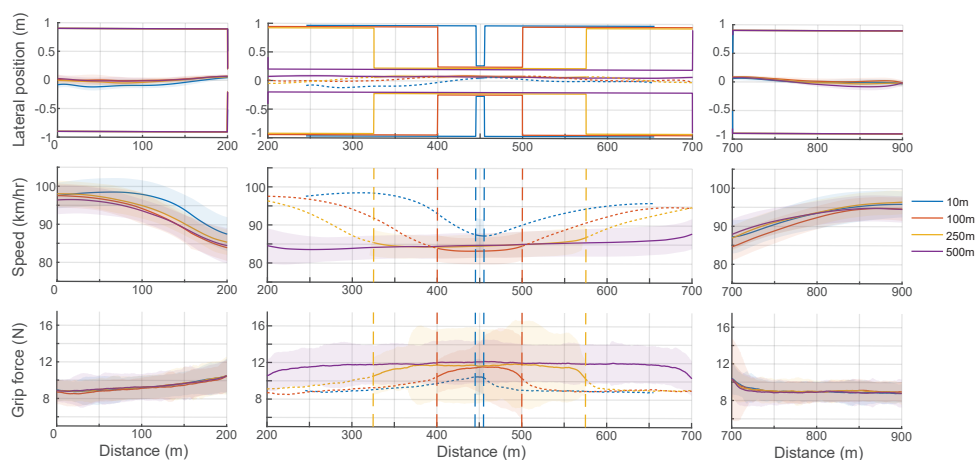


Figure 3.3. Mean results (solid), and standard deviation (transparent) for all participants for all four conditions as a function of the travelled distance. The top panels show the lateral position along with the lane width, the middle panels the speed and the bottom panels the grip force. The left panels show the entry section, the middle panels the narrow road section centred in the middle of each road narrowing and right panels the exit section.

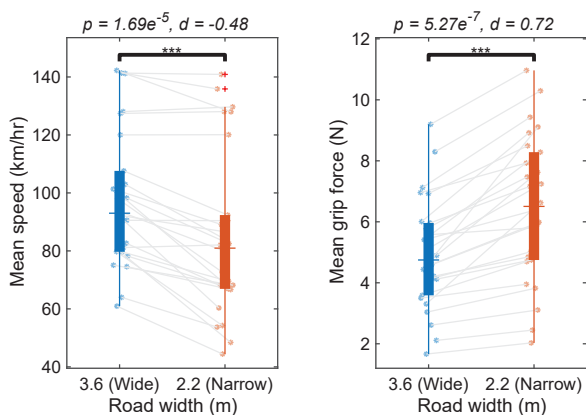


Figure 3.4. Mean speed (left) and mean grip force (right) effect for all participants (asterisks) for the wide and narrow sections (i.e., all four narrow road lengths combined). Where significant differences, ***: $p < 0.001$, and d : Cohen's d .

3.3.3. Interaction Between Speed and Grip Force Adaptation

Figure 3.6-left shows a scatter plot of Δ Speed and Δ Grip force. A small positive correlation ($\rho = 0.15$) was found, suggesting no trade-off between speed and grip force adaptations. Figure 3.6-middle visualizes the individual strategies adopted by all participants between 10 m and 500 m. Different individual strategies can be identified; for example, some drivers mainly adapted their speed (e.g., participant no. 4, 11, 26, 25; visualized with a red line in Figure 3.6-middle with an abs slope < 0.03), some adapt only grip force (e.g., participant no. 7, 15, 17, 21; visualized with a green line in Figure 3.6-middle with an abs slope > 0.5), adapt both speed and grip force (e.g., participant no. 13, 22, 16, 14), whereas others show minimal adaptation (e.g., participant no. 3, 5, 6, 10).

Figure 3.6-right shows the mean and the standard deviation (SD) over the eight repetitions

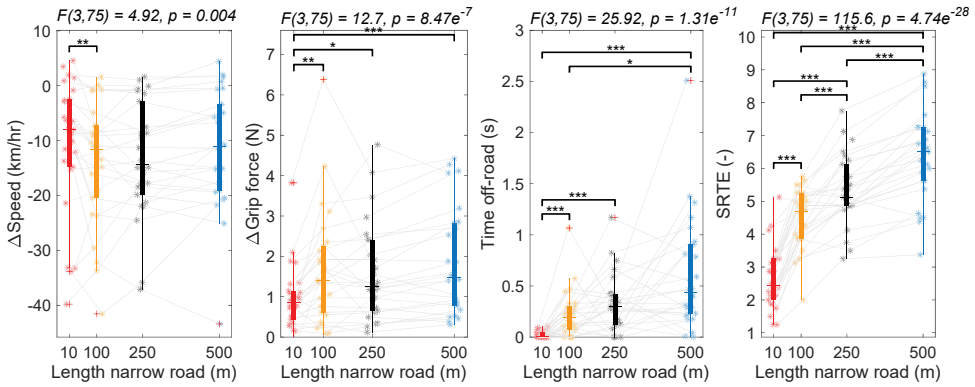


Figure 3.5. Boxplots for the four narrow road lengths for all participants (asterisks). From left to right: Δ Speed, Δ Grip force, time off-road and self-reported task effort (SRTE). Brackets indicate significant differences, *: $p < 0.05$; **: $p < 0.01$; ***: $p < 0.001$.

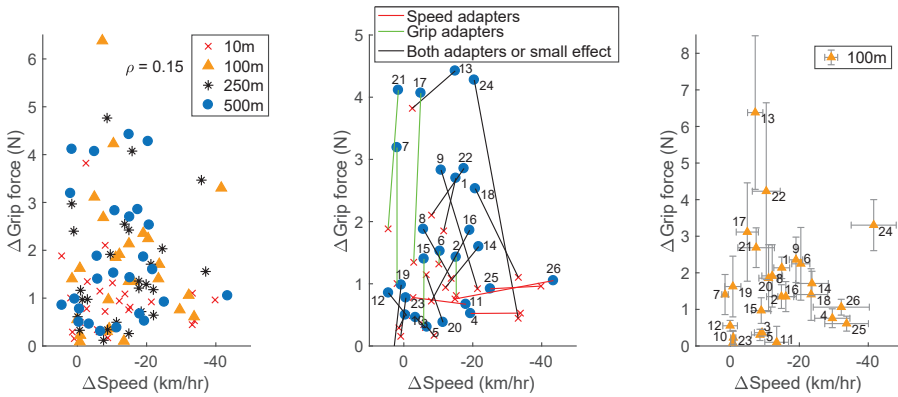


Figure 3.6. Left: a scatter plot of Δ Grip force and Δ Speed for the four different road narrowing lengths. Middle: visualizes the adaptation between the 100 m and 500 m narrow road length. Speed adapters and grip force adapters are visualized by red (abs slope < 0.03) and green lines (abs slope > 0.5), respectively. Right: The mean (triangle) and the standard deviation (error bars) over all the 8 repetitions on the 100 m section for each driver.

for the 100 m condition for each driver. Compared to the inter-subject variability (i.e., 100 m SD: Δ Speed = 11.3 km/hr, Δ Grip force = 1.42 N), a lower intra-subject variability was found (i.e., 100 m mean SD: Δ Speed = 6.7 km/hr, Δ Grip force = 1.25 N). This indicates that the individual participants adopted consistent strategies within themselves.

3.3.4. Learning Effect due to Repetitions

The effect of the repetition order of the experiment is shown in Figure 3.7 for the lateral position, speed and the grip force as a function of the travelled distance averaged over all participants for each repetition. When drivers become more familiar with a driving task they increased their speed and decreased their grip force. In the 10 m section, the highest speed is observed for the 8th repetition and the grip force decreases over the eight repetitions averaged over all participants, indicating a learning effect.

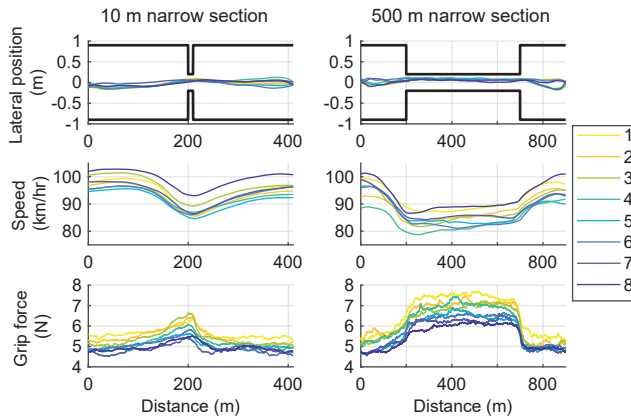


Figure 3.7. The lateral position, speed and grip force for each repetition averaged over all participants for the 10m (left), and the 500m narrow road section (right).

3.4. Discussion

In this driving simulator study, we expected that there would be a trade-off between two adaptation strategies (speed and neuromuscular stiffness), and that the risk duration would impact a driver's selection of the trade-off. Specifically, we hypothesized that for a short risk duration, drivers will favour increased neuromuscular stiffness (operationalized by grip force) over speed reduction; and vice versa for longer risk durations (Figure 3.1).

Our results showed that road width manipulation was successful in evoking speed and grip force adaptations: participants reduced speed and increased grip force when road width reduced (Figure 3.3 and Figure 3.5), which is in accordance to literature (Melman et al., 2018; Pronker et al., 2017; Van der Wiel et al., 2015). However, only a low positive correlation was found between the two adaptation strategies across drivers ($\rho = 0.15$), indicating that no trade-off exists. A possible reason for the apparent lack of trade-off may be due to the large variety in individual adaptation strategies that are consistently adopted by each driver. As visualized in Figure 3.6-middle some drivers adapt as hypothesized (Figure 3.1) with an increased speed and decreased grip force, whereas others adapt only speed, grip force or show minimal adaptation. Participants showed to be consistent within their own adaptation strategy, over the eight repetitions of each narrow road section (Figure 3.6-right). The large inter-driver variability and consistent intra-driver choice for adaptation strategies points towards an ecological fallacy (Selvin, 1958), indicating that conclusions about the behaviour of an individual should not be made based on the results of the entire group.

The results also showed that longer narrow road sections were subjectively perceived more effortful and objectively performed worse (i.e., higher time off-road; Figure 3.5). Interestingly, the adaptation strategies that could be utilized to reduce the task difficulty (i.e., reduce the speed) or to be more robust to perturbations (i.e., increase grip force), seem to have been sparingly employed by most drivers.

One could argue that the fact that this study was performed in a fixed-base driving simulator, which has the advantage of the ability to perform many repetitions in a consistent environment, but lacks physical risk and has limited speed and depth perception, might explain the limited effect of speed and grip force adaptations (Figure 3.5). However, this is unlikely, as strong speed and grip force adaptations (Figure 3.3) were found between the wide and narrow road sections. Similar adaptations were also found in on-road experiments (De Waard et al., 1995; Fitzpatrick et al., 2000). Additionally, the relative validity (i.e., the effect sizes between the pairwise comparisons) is high for simulators (Klüver et al., 2016).

We also reflected on whether the lengths of the narrow road section might have been

insufficient to investigate the trade-off. The average time a driver drove on the narrow section was approximately 25 s, which could have been insufficient to cause discomfort for the driver to stimulate a change in the adaptation strategy. This is supported by the observation in Figure 3.5, where the SRTE is still increasing and has not reached a steady-state value. This suggests that larger road narrowing lengths should be investigated to examine the trade-off hypothesis. The only difference in speed and grip force adaptations were found with respect to the 10 m section. Figure 3.4 and 3.5 revealed a different entrance strategy and less speed reduction and grip force increase, for the 10 m section compared to the longer road sections. This could suggest that drivers decide their strategy (positioning, speed, and grip force adaptation) before entering the narrow section and hence the length of the section had little effect on their adaptation behaviour.

Previous literature has shown that when drivers become more familiar with a driving task they increase their speed (Colonna et al., 2016). Such a learning effect in speed was found in this study, along with a reduction in the grip force over the eight repetitions averaged over all participants (Figure 3.7). A similar effect in neuromuscular property changes using electromyography (EMG) was observed in non-driving (Osu et al., 2002) and driving (Pick & Cole, 2007) tasks. However, the grip force sensor output degraded over time which could also have influenced the results (Brimacombe et al., 2009). In short, the grip force demonstrates itself to be a promising non-obtrusive method to capture neuromuscular adaptations as long as the sensor degradation is mitigated via calibration.

Although further investigation is needed to understand if longer narrow road sections were required to evoke a coherent trade-off across participants, the fact that participants adapted their speed and grip force to road narrowing, and adopted consistent individual strategies highlights the possibility of an ecological fallacy and the importance of investigating the interaction between adaptation strategies on an individual level. All-in-all the quest for better understanding steady-state and non-steady state driver adaptations, their interaction, and their underlying mechanisms continues.

3.5. Conclusions

- The interaction between different driver adaptation strategies is a seldom studied topic.
- Road narrowing is an effective method to induce speed and grip force adaptations (Figure 3.3).
- The twenty-six drivers did not consistently select the hypothesized trade-off for increasing duration of road narrowing: a low correlation was found between speed and grip force adaptations (Figure 3.6).
- Individual trade-offs were consistent: the within-subject variability in speed-grip force adaptations was low across the tested risk durations (Figure 3.6).
- Grip force measurement is a novel and non-obtrusive way to quantify neuromuscular stiffness adaptations.
- The results highlight the possibility of an ecological fallacy and the importance of investigating the interaction between adaptation strategies on an individual level.

References

- Aarts, L., & Van Schagen, I. (2006). Driving speed and the risk of road crashes: A review. *Accident Analysis and Prevention, 38*, 215–224.
- Abbink, D. A., Mulder, M., & Van Paassen, M. M. (2011, October). Measurements of muscle use during steering wheel manipulation. In *2011 IEEE International Conference on Systems, Man, and Cybernetics* (pp. 1652-1657). IEEE.
- Antonin, J., Zheng, R., & Kimihiko, N. (2015, October). A Scaling Method for Real-Time Monitoring of Mechanical Arm Admittance. In *2015 IEEE International Conference on Systems, Man, and Cybernetics* (pp. 1551-1556). IEEE.
- Brimacombe, J. M., Wilson, D. R., Hodgson, A. J., Ho, K. C., & Anglin, C. (2009). Effect of calibration method on Tekscan sensor accuracy. *Journal of Biomechanical Engineering, 131*, 1-4.
- Brooks, J. O., Crisler, M. C., Klein, N., Goodenough, R., Beeco, R. W., Guirl, C., ... & Beck, C. (2011). Speed choice and driving performance in simulated foggy conditions. *Accident Analysis & Prevention, 43*, 698-705.
- Charlton, S. G., & Starkey, N. J. (2016). Risk in our midst: Centrelines, perceived risk, and speed choice. *Accident Analysis & Prevention, 95*, 192-201.
- Colonna, P., Intini, P., Berloco, N., & Ranieri, V. (2016). The influence of memory on driving behavior: How route familiarity is related to speed choice. An on-road study. *Safety science, 82*, 456-468.
- Conover, W. J., & Iman, R. L. (1981). Rank transformations as a bridge between parametric and nonparametric statistics. *The American Statistician, 35*, 124-129.
- De Waard, D., Jessurun, M., Steyvers, F. J., Reggatt, P. T., & Brookhuis, K. A. (1995). Effect of road layout and road environment on driving performance, drivers' physiology and road appreciation. *Ergonomics, 38*, 1395-1407.
- Elvik, R. (2013). A re-parameterisation of the Power Model of the relationship between the speed of traffic and the number of accidents and accident victims. *Accident Analysis & Prevention, 50*, 854-860.
- Elvik, R., Christensen, P., & Amundsen, A. H. (2004). Speed and road accidents: an evaluation of the Power Model. *Transportøkonomisk Institutt*.
- Fitzpatrick, K., Carlson, P. J., Wooldridge, M. D., & Brewer, M. A. (2000). *Design factors that affect driver speed on suburban arterials* (No. FHWA/TX-00/1769-3).
- Fuller, R., McHugh, C., & Pender, S. (2008). Task difficulty and risk in the determination of driver behaviour. *Revue Européenne de Psychologie Appliquée, 58*, 13–21.
- Gibson, J. J., & Crooks, L. E. (1938). A theoretical field-analysis of automobile-driving. *The American Journal of Psychology, 51*, 453–471.
- Gribble, P. L., Mullin, L. I., Cothros, N., & Mattar, A. (2003). Role of cocontraction in arm movement accuracy. *Journal of neurophysiology, 89*, 2396-2405.
- Hedlund, J. (2000). Risky business: safety regulations, risk compensation, and individual behavior. *Injury prevention, 6*, 82-89.
- Heikoop, D. D., de Winter, J. C., van Arem, B., & Stanton, N. A. (2018). Effects of mental demands on situation awareness during platooning: A driving simulator study. *Transportation research part F: traffic psychology and behaviour, 58*, 193-209.
- Klüver, M., Herrigel, C., Heinrich, C., Schöner, H. P., & Hecht, H. (2016). The behavioral validity of dual-task driving performance in fixed and moving base driving simulators. *Transportation research part F: traffic psychology and behaviour, 37*, 78-96.
- Kuchenbecker, K. J., Park, J. G., & Niemeyer, G. N. (2003, January). Characterizing the human wrist for improved haptic interaction. In *ASME International Mechanical Engineering Congress and Exposition* (Vol. 37130, pp. 591-598).
- McLean, J. R., & Hoffmann, E. R. (1972). The effects of lane width on driver steering control and performance. In *6th Australian Road Research Board (ARRB) Conference, Canberra* (Vol. 6, No. 3).
- Melman, T., Abbink, D. A., van Paassen, M. M., Boer, E. R., & de Winter, J. C. (2018). What determines drivers' speed? A replication of three behavioural adaptation experiments in a single driving simulator study. *Ergonomics, 61*, 966-987.
- Näätänen, R., & Summala, H. (1974). A model for the role of motivational factors in drivers' decision-making. *Accident Analysis & Prevention, 6*, 243-261.
- Nakamura, H., Abbink, D., & Mulder, M. (2011, October). Is grip strength related to neuromuscular admittance during steering wheel control? In *2011 IEEE International Conference on Systems, Man, and Cybernetics* (pp. 1658-1663). IEEE.
- Osu, R., Franklin, D. W., Kato, H., Gomi, H., Domen, K., Yoshioka, T., & Kawato, M. (2002). Short-and long-term changes in joint co-contraction associated with motor learning as revealed from surface EMG. *Journal of neurophysiology, 88*, 991-1004.
- Pick, A. J., & Cole, D. J. (2006). Measurement of driver steering torque using electromyography. *Journal of Dynamic Systems, Measurement and Control, Transactions of the ASME, 128*, 960-968.
- Pick, A. J., & Cole, D. J. (2007). Driver steering and muscle activity during a lane-change manoeuvre. *Vehicle system dynamics, 45*, 781-805.
- Pronker, A. J., Abbink, D. A., Van Paassen, M. M., & Mulder, M. (2017). Estimating driver time-varying neuromuscular admittance through LPV model and grip force. *IFAC-PapersOnLine, 50*, 14916-14921.
- Rendon-Velez, E., Van Leeuwen, P. M., Happee, R., Horvath, I., van der Vegte, W. F., & de Winter, J. C. (2016). The effects of time pressure on driver performance and physiological activity: A driving simulator study. *Transportation research part F: traffic psychology and*

-
- behaviour*, 41, 150-169.
- Saffarian, M., Happee, R., & Winter, J. D. (2012). Why do drivers maintain short headways in fog? A driving-simulator study evaluating feeling of risk and lateral control during automated and manual car following. *Ergonomics*, 55, 971-985.
- Selvin, H. C. (1958). Durkheim's suicide and problems of empirical research. *American journal of sociology*, 63, 607-619.
- Van der Wiel, D. W., van Paassen, M. M., Mulder, M., Mulder, M., & Abbink, D. A. (2015). Driver adaptation to driving speed and road width: Exploring parameters for designing adaptive haptic shared control. In *2015 IEEE International Conference on Systems, Man, and Cybernetics* (pp. 3060-3065). IEEE.
- Van Winsum, W., Brookhuis, K., & de Waard, D. (2000). A comparison of different ways to approximate time-to-line crossing (TLC) during car driving. *Accident Analysis & Prevention*, 32, 47-56.
- Van Winsum, W., & Godthelp, H. (1996). Speed choice and steering behavior in curve driving. *Human Factors*, 38, 434-441.
- Wierwille, W. W., Casali, J. G., & Repa, B. S. (1983). Driver steering reaction time to abrupt-onset crosswinds, as measured in a moving-base driving simulator. *Human Factors*, 25, 103-116.
- Wilde, G. J. (1998). Risk homeostasis theory: an overview. *Injury prevention*, 4, 89-91.

**Multivariate and Location-specific
Correlates of Fuel Consumption:
A Test Track Study**



Current predictors of fuel consumption are typically based on computer simulations or data collections in real traffic, where the route and vehicle type are not under the researcher's control. Here, we predicted fuel consumption using test track data, an approach that allowed for location-specific predictions. Ninety-one drivers drove a total of 4617 laps, in two vehicles (Renault Mégane, Renault Clio), on two routes (highway and mountain), and with two eco-driving instructions (normal and eco). A multivariate analysis at the level of laps showed a strong predictive value for metrics related to speed, RPM, and throttle position, but with a considerable amount of variance attributable to route and vehicle type. A subsequent location-specific analysis showed that the predictive correlation of driving speed and throttle position fluctuated strongly during the lap and at some locations even became negative. We conclude that there is considerable potential in instantaneous location-specific prediction of fuel consumption.

Published as:

Melman, T., Abbink, D. A., Mouton, X., Tapus, A., & De Winter, J. C. F. (2021). Multivariate and location-specific correlates of fuel consumption: A test track study. *Transportation Research Part D: Transport and Environment*, 92, 102627. <https://doi.org/10.1016/j.trd.2020.102627>

4.1. Introduction

With the rise in CO₂ levels in the atmosphere, the reduction of fuel consumption is becoming an increasingly important topic. Under the pressure of strict regulations, car manufacturers are forced to produce increasingly efficient vehicles. Not only the vehicle technology itself but also the behaviour of the driver has a significant impact on fuel consumption. Studies show that eco-driving can reduce fuel consumption, and thereby pollutant emissions (Ho et al., 2015; Saboohi & Farzaneh, 2009), by 5% if compared to normal driving, or even more if compared to aggressive driving (for reviews about the effect of eco-driving on fuel efficiency, see Alam & McNabola, 2014; Huang et al., 2018; Xu et al., 2016).

Various authors have investigated optimal fuel-efficient driving through computer simulations. Maintaining a constant speed, shifting up early, and avoiding excessive pedal movements have been shown to be essential factors in minimising fuel consumption (Dib et al., 2014; Mensing et al., 2013; Saboohi & Farzaneh, 2009; Sarkan et al., 2019). Mensing et al. (2013) concluded through computer simulations that, for optimal eco-driving, drivers should accelerate quickly to a relatively low cruising speed. They also recommended early and gentle deceleration, followed by late and hard braking. Whether these optimal behaviours are realistic or desirable was not discussed in their research. For example, while extreme late braking can be optimal in terms of fuel consumption, it is not something drivers would normally do for safety and comfort reasons.

Although it is known how drivers should behave to drive ecologically, relatively little information is available about how ecologically-friendly drivers actually drive. Knowing how drivers drive is important for developing eco-driving feedback and training (Allison & Stanton, 2018; Caban et al., 2019; Sanguinetti et al., 2020). For example, drivers could receive an eco-score on their dashboard that reflects the impact of their current driving behaviour on fuel consumption (Sanguinetti et al., 2020; Vaezipour et al., 2015). Such an eco-score should be calibrated on realistic human driving behaviour, not based on modelled behaviour that may not be acceptable in the real world.

Real-world studies provide relevant insight into individual differences in ecological driving styles (Ericsson, 2001; Lois et al., 2019). Ericsson (2001), for example, investigated driving behaviour data for 19,230 driving periods collected in real traffic. A significant variation in fuel consumption was observed, with an average of 10 litres per km and a standard deviation of about 6 litres per km. Among other things, it was found that engine speeds above 3500 rpm explained part of the variance in fuel consumption. However, the strongest effect on fuel consumption was found for a “stop factor”, which was related to the number of stops per kilometre and the percentage of time the vehicle was stationary. This finding is not necessarily due to individual differences in driving behaviour, but rather due to traffic conditions such as the presence of traffic lights along the route. What this finding shows is that naturalistic driving studies inherently contain confounding factors that hamper understanding of what constitutes fuel-efficient driving behaviour. In particular, such studies do not control external factors that influence fuel consumption, such as the presence of curves, inclinations, traffic lights, and the impact of surrounding traffic.

As noted above, there is a paucity of research on how drivers drive ecologically. Although route selection and trip planning have been cited as an important factor in reducing fuel consumption (Sanguinetti et al., 2017; Sivak & Schoettle, 2012; Zhou et al., 2016), field studies typically do not control for it. This problem was also recognised by Lois et al. (2019), who stated: “to the best of our knowledge, there are no studies in the literature that analyse key factors for fuel consumption and eco-driving, controlling external factors.” In a field study, they measured the fuel consumption of 1156 trips from 24 drivers, and observed that external factors had a key role in fuel consumption. The authors created a statistical model in the form of a path analysis, which included two external factors that were found to be predictive of fuel consumption: road congestion and the slope of the road. Lois et al.’s method is a promising

approach to controlling for route-related effects. Still, this method is not entirely satisfactory for understanding the effects of external factors, because the control for external factors was applied in the form of a statistical correction rather than an experimental manipulation.

In our work, we have attempted to close this research gap by using instrumented vehicles on a test track. The availability of a test track makes it possible to expose drivers to a specific route, measure fuel consumption on a meter-to-meter basis, and remove the influence of uncontrolled traffic elements such as traffic lights and other road users. The instrumented vehicles recorded the vehicle location using GPS along with CAN bus data. Drivers were given the task of either complying with an eco-score or driving as they normally would, for two instrumented vehicle types and two route types with fundamentally different characteristics. The first route type was a sharply curved mountain route and the second route type was a highway.

The purpose of this paper is to predict fuel consumption from driving behaviour measurements, in order to allow informed design choices for eco-driving feedback and training applications. We use two methods of predicting fuel consumption: a multivariate analysis at the level of a trip (defined herein as a lap on the mountain or highway route in a given vehicle) and a location-specific method. We show, using the first method, that driving metrics have a strong predictive value for fuel consumption, and that a large part of the variance in the driving metrics is attributable to the route type and the vehicle type. These sources of variance would be a disturbance when predicting fuel consumption from driving metrics based on different routes and vehicles combined. Another limitation of trip-related metrics is that valuable information is lost due to the aggregation of, for example, driving behaviour on curves and straights. In the second part of this paper, we demonstrate that it is sensible to develop location-specific predictors of eco-driving. In this study, a location-specific predictor refers to driving behaviours (e.g., throttle position) at a specific travelled distance along the lap on the test track. More specifically, we correlated drivers' behaviours on a meter-to-meter basis with their fuel consumption for all other laps driven (leave-one-out validation). By means of a location-specific analysis, route features that can impact fuel consumption, such as curvature and road inclination, are implicitly controlled. Finally, we make conclusions and recommendations for location-specific fuel consumption predictions.

4.2. Method

This study uses data initially collected to monitor the wear of vehicle components. In this study, we use this data for the above-described purpose.

4.2.1. Participants

Ninety-one test drivers from Renault participated in this study. All participants regularly drove on the test track and were familiar with both routes (highway and mountain) and vehicle types (Renault Mégane and Renault Clio). These drivers were not professional test drivers; that is, their primary job did not consist of testing vehicle performance. Due to Renault's ethical and privacy protocols, driver-related information regarding age, gender, and yearly mileage cannot be made public.

4.2.2. Vehicles

Two vehicle types were used in this experiment: a Renault Mégane IV and Renault Clio IV (Table 4.1), both having a manual transmission. For each vehicle type, two identical vehicles were used for the experiment: one for eco-driving and one for normal driving, resulting in a total of four vehicles used in this experiment. These four vehicles were equipped with a GPS tracker and a CAN-bus that allowed for recording signals associated with vehicle motion, steering, and pedal movements at a sampling frequency of 100 Hz.

Table 4.1. Vehicle information for the two types of vehicles used in this experiment.

Vehicle type	Year of manufacture	Engine Model	Fuel type	Engine displacement (cm ³)	Max power (hp)	Curb weight (kg)	Emission legislation	Wheelbase length (mm)
Renault Clio	2017	K9K 628	Diesel	1461	90	1071	Euro 5	2589
Renault Mégane	2017	K9K 656	Diesel	1461	110	1205	Euro 6	2669

4.2.3. Route Types

This experiment was performed on Renault’s test circuit in Aubevoye, France. Two types of routes were used in this study: a 4.1 km long highway section containing a two-lane highway with a recommended speed of 100 km/hr, and a 5.7 km long two-lane mountain section with a maximum altitude difference of approximately 50 m. The highway sections and mountain sections were extracted from the total dataset using the recorded GPS locations, as shown in Figure 4.1. The routes did not feature intersections or traffic lights. Table 4.2 shows the total number of laps driven per task instruction, route type, and vehicle type. Appendix A provides an overview of the driven conditions for all 91 participants.

Table 4.2. The number of participants who drove with and without eco-score feedback, for the highway and mountain, and for the Mégane and the Clio.

	Normal				Eco-driving			
	Highway		Mountain		Highway		Mountain	
	Mégane	Clio	Mégane	Clio	Mégane	Clio	Mégane	Clio
Number of drivers	34	25	24	21	35	34	23	26
Total laps driven	665	585	449	481	784	665	536	452

4.2.4. Eco-Driving Training

In this experiment, two task instructions were given: an eco-instruction to drive as economically as possible, and a normal driving instruction. If drivers were assigned to the ‘normal’ task, they were asked to drive as they normally would. If drivers were assigned to the eco-driving task, they were asked to drive with an average Renault eco-score of at least 90% of 100%. The eco-score, ranging from 0% (non-eco) to 100% (eco), is a Renault in-house developed score, computed from longitudinal accelerations/decelerations, driving speed, and late gear changing behaviour (i.e., driving with a high engine RPM). A Renault expert trained five group leaders, who, in turn, trained the rest of the participants identically. During the two-hour training, the participants first drove on the test track with their own driving style. After this run, the eco-expert gave advice on speed, acceleration, braking, and shifting behaviour to optimise fuel consumption.

4.2.5. Experimental Protocol

The data were collected 24 hours a day over a period of 3.5 months. Every 8 hours, two drivers were assigned a vehicle and had to drive approximately 300 km. No specific instructions were given on where to drive. Drivers did not know that the highway and mountain sections were extracted and analysed separately. While driving, the average eco-score of the session was shown as a number on the display.

4.2.6. Part 1: Predicting Fuel Consumption From Lap-Level Metrics

Measured CAN-bus signals

From the CAN-bus data, 11 signals were obtained/derived. These signals reflect longitudinal driving behaviour (7 signals), lateral driving behaviour (3 signals), as well as fuel consumption (see Table 4.3, left column for the 10 longitudinal and lateral signals). The speed x longitudinal acceleration signal (va) is known to be predictive of fuel consumption (Ericsson, 2001) and is

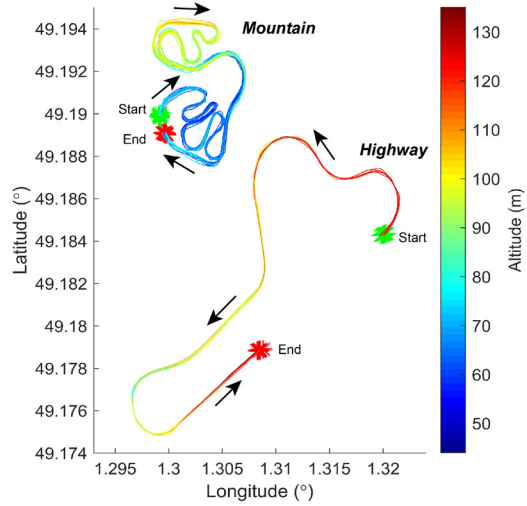
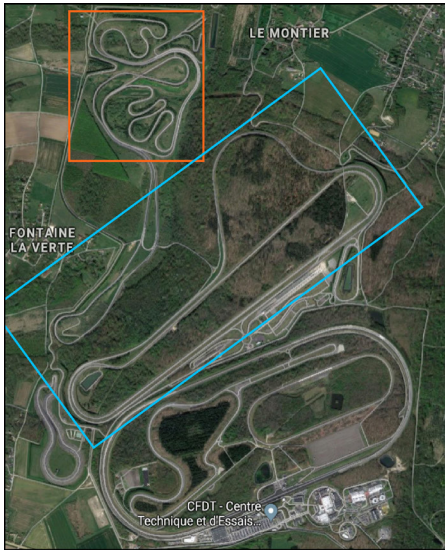


Figure 4.1. Left: top view of the route types (mountain and highway). Right: an example of the GPS data for the route types. The start and end-points are visualised with a green and red asterisk, respectively. The driving direction is indicated by arrows.

a surrogate for inertial power (Fomunung et al., 1999). We used va^2 to remove the distinction between negative and positive values. The raw measured fuel consumption had a minimum measurement step size of 80 ml, and an update rate that varied between 100 ms and a number of seconds. The cumulative fuel consumption data were interpolated to 100 Hz with trapezoids between connecting points. To calculate the instantaneous fuel consumption in cm^3/km (used in the location-specific analysis, see Section 4.2.7), the difference values of the cumulative fuel consumption were divided by the vehicle speed at every sampling point.

Tabel 4.3. The used signals (left column) and the 25 additional driving metrics calculated from these signals (right). For each longitudinal and lateral signal, the following metrics were calculated: mean, standard deviation, maximum, minimum, and 10th, 25th, 50th, 75th, 90th percentiles (see Appendix 4.2 for all 110 metrics).

Signal	Description
<i>Longitudinal signals</i>	
Speed (km/hr)	-
Longitudinal acceleration (m/s^2)	The 10 th , 25 th , 50 th , 75 th , 90 th percentiles of the absolute values of the signal. Number of times the absolute acceleration was greater than 1.5 m/s^2 Relative positive acceleration (m/s^2 ; RPA). The RPA correlates with fuel consumption (Ericsson, 2001), and is calculated as $\frac{1}{x} \int va^+ dt$, where x = total distance, v = speed, a^+ = positive accelerations count, negative ones are ignored.
Throttle position (%)	The percentage where no throttle was used.
Brake pressure (bar)	The number of brake presses (#).
Engine RPM (RPM)	-
Eco-score (%)	Number of times eco-score below 50 (#).
$(\text{Velocity} \cdot \text{longitudinal acceleration})^2 (va^2; \text{m}^2/\text{s}^3)$	-
<i>Lateral signals</i>	
Lateral acceleration (m/s^2)	The 10 th , 25 th , 50 th , 75 th , 90 th percentiles of the absolute values of the signal.
Steering wheel angle (SWA; deg)	The 10 th , 25 th , 50 th , 75 th , 90 th percentiles of the absolute values of the signal. Steering reversal rate (SRR). The steering reversal rate was defined as the number of times that the steering wheel was reversed (McLean and Hoffmann, 1975). It was calculated by determining the local minima and maxima of the steering wheel angle, and if the difference between two adjacent peaks was greater than 2 deg, it was counted as a reversal.
Steering wheel angle speed (deg/s)	The 10 th , 25 th , 50 th , 75 th , 90 th percentiles of the absolute values of the signal.

Calculated driving metrics

For each longitudinal and lateral signal, the following driving metrics were calculated per lap: mean, standard deviation, maximum, minimum, 10th, 25th, 50th, 75th, 90th percentiles (10 signals x 9 metrics = 90 in total). From the 90 metrics, 7 were removed because of a lack of variation (e.g., the minimum brake pressure). Twenty-five additional metrics were calculated from the longitudinal and lateral signals (see Table 4.3). Accordingly, a total 108 metrics of driving behaviour (90 – 7 + 25 = 108) were obtained, which were thought to be predictive of fuel consumption (based on Ericsson, 2001; Fomunung et al., 1999; Lois et al., 2019). From the fuel consumption signal, the mean fuel consumption per km (cm³/km), and the mean fuel consumption per second (cm³/s) were calculated (2 metrics). Appendix 2 provides the full list of all 110 metrics.

Principal component analysis

We performed a principal component analysis (PCA) on a matrix of 110 metrics x 4617 laps (all laps combined, see Table 4.2). A PCA extracts the major sources of variance in terms of component scores and loadings. The first principal component in our 110-dimensional dataset contains the direction with the largest variation, and the 110th component the smallest. The correlation between variables and factors is described by the component loadings, where 0 means no correlation and 1 means a perfect correlation with the principal component. Before conducting the PCA, all metrics were rank-transformed to create a uniform distribution. Oblique rotation of the loadings was performed to improve the interpretability of the components (Fabrigar et al., 1999).

Cohen's \bar{d} effect size to describe the effect of eco-driving, route type, and vehicle type

The impact of eco-driving, route type, and vehicle type for each driving metric was calculated using the average Cohen's \bar{d} effect size, according to Eqs. 4.1–4.4.

Effect of eco-driving instructions

$$\bar{d}(n - e) = \frac{d(n - e)_{Mégane,highway} + d(n - e)_{Mégane,mountain} + d(n - e)_{Clío,highway} + d(n - e)_{Clío,mountain}}{4} \quad (4.1)$$

with,

$$d(n - e) = \frac{M_{normal} - M_{eco}}{\sqrt{\frac{s_{normal}^2 + s_{eco}^2}{2}}} \quad (4.2)$$

where s is the pooled standard deviation, and M the mean of the score on the metric for the two compared conditions.

Effect of route type

$$\bar{d}(h - m) = \frac{d(h - m)_{normal,Mégane} + d(h - m)_{normal,Clío} + d(h - m)_{eco,Mégane} + d(h - m)_{eco,Clío}}{4} \quad (4.3)$$

with, h = highway, and m = mountain.

Effect of vehicle type

$$\bar{d}(M\acute{e} - C) = \frac{d(M\acute{e} - C)_{normal,highway} + d(M\acute{e} - C)_{normal,mountain} + d(M\acute{e} - C)_{eco,highway} + d(M\acute{e} - C)_{eco,mountain}}{4} \quad (4.4)$$

with, $M\acute{e}$ = *Mégane*, and C = *Clio*.

4.2.7. Part 2: Location-Specific Analysis

The location-specific analysis correlated the total fuel consumption of drivers with their driving behaviour for every 5 meters of the route along the track. The road location was computed using a combination of the GPS start location (Figure 4.1) and a distance meter that used wheel speed as input signal.

Spearman's leave-one-out correlation

The Spearman's leave-one-out correlation was calculated for all laps where drivers drove the same route at least twice in a given vehicle type and eco-driving condition. The correlation coefficient was calculated between (1) driving speed (km/hr), throttle position (%), or the current fuel consumption (cm^3/km) for each 5-m segment, and (2) the average fuel consumption over all the driver's laps in the same vehicle type and eco-driving condition, except for the lap used to calculate the value in (1). Speed and throttle position were selected because, in many studies, they are considered related to fuel consumption (e.g., Ma et al., 2015), whereas the current fuel consumption is the signal from which the total fuel consumption was constructed.

The location-specific correlation coefficient was computed for the highway route and mountain route separately. The computation of the location-specific correlation coefficient for the speed signal for the highway route can be illustrated as follows. Suppose a driver drove 30 laps on the highway with the *Mégane* in the eco-driving condition. One lap was used to record the speed every 5 meters, and the other 29 laps were used to calculate the driver's fuel consumption in cm^3/km . This procedure was repeated 30 times for this participant, with the next lap removed and the remaining 29 laps used to calculate average fuel consumption. Together this resulted in 30 data points of the mean speed every 5 m and the overall fuel consumption for this driver. This procedure was performed for all drivers and all four combinations of route type and eco-driving instructions (1. *Mégane* & eco, 2. *Mégane* & normal, 3. *Clio* & eco-driving, 4. *Clio* & normal), provided the driver had driven at least twice in that condition (i.e., 4 drivers were removed, see Appendix A). Accordingly, a total of 2697 data points were collected for every 5 m of the highway route. In turn, for every 5 m of the highway route, Spearman's rank-order correlation between speed and fuel consumption ($n = 2697$) was computed. A strong positive correlation would mean that drivers with a higher speed at that particular location had a higher overall fuel consumption.

The same procedure was followed for the throttle position and current fuel consumption as predictor signals. Also, the same procedure was used for computing the location-specific correlations for the mountain route (1915 data points from a total of 64 drivers).

4.3. Results

Figure 4.2 shows the mean fuel consumption, mean eco-score, and mean speed per eco-driving instruction, route type, and vehicle type. The mean eco-scores confirm that all drivers have fulfilled the task of having an average eco-score of at least 90% when driving in the eco-driving condition.

4.3.1. Part 1: Predicting Fuel Consumption From Lap-Level Metrics

Effect of eco-driving, route, and vehicle type on driving metrics

Eco-driving resulted in a lower fuel-consumption per km for both routes and both vehicles as compared to normal driving (Figure 4.2, left). The beneficial effect on eco-driving was greatest for eco-driving compared to normal driving ($\bar{d} = 3.05$; this corresponds to a 23.2% fuel reduction), followed by driving on the highway route versus the mountain route ($\bar{d} = -1.64$; 12.7% fuel reduction), and driving in the Clio instead of the Mégane ($\bar{d} = 0.48$; 3.4% fuel reduction).

Table 4.4 shows the Cohen's \bar{d} effect sizes for the eco-driving instructions, route type, and vehicle type, for the 50 metrics with the highest effect sizes for eco-driving instructions. Table 4.4 shows that both longitudinal and lateral metrics are affected by eco-driving (i.e., $\bar{d} > 2.0$). The strongest Cohen's \bar{d} values for eco-driving were found for the eco-score-related metrics, a result that can be explained by the task instructions given to participants. Furthermore, strong effects of eco-driving were found for longitudinal acceleration-related metrics (e.g., 90th percentile of the absolute value, maximum values, and the RPA), engine-RPM-related metrics (e.g., 90th percentile, 75th percentile, and maximum values), and throttle-related metrics (e.g., 90th and 75th percentiles), mean va^2 , and mean speed (see also Figure 4.2). As for lateral driving-related metrics, eco-driving had a large impact on the 50th percentile of absolute lateral acceleration, 50th percentile of the abs steering wheel angle (SWA), and mean SWA speed compared to normal driving. These results show that longitudinal and lateral driving metrics are highly indicative of fuel consumption.

Many of the metrics in Table 4.4 not only distinguish between eco-driving and normal driving, as described above, but are also sensitive to vehicle type, and especially to route type (with Cohen's \bar{d} values up to 20.12, see Appendix B for more detail about the route and vehicle Cohen's \bar{d} values). The strongest effects for route type were found for metrics

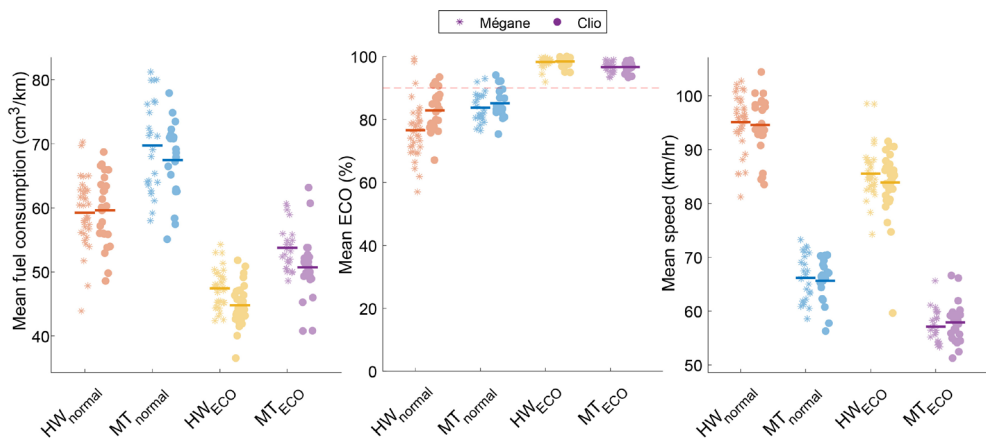


Figure 4.2. Mean fuel consumption per km (left), eco-score (middle), and driving speed (right) as a function of driving task, vehicle type, and route type. Each marker indicates, for one driver, the mean value averaged over all his/her driven laps.

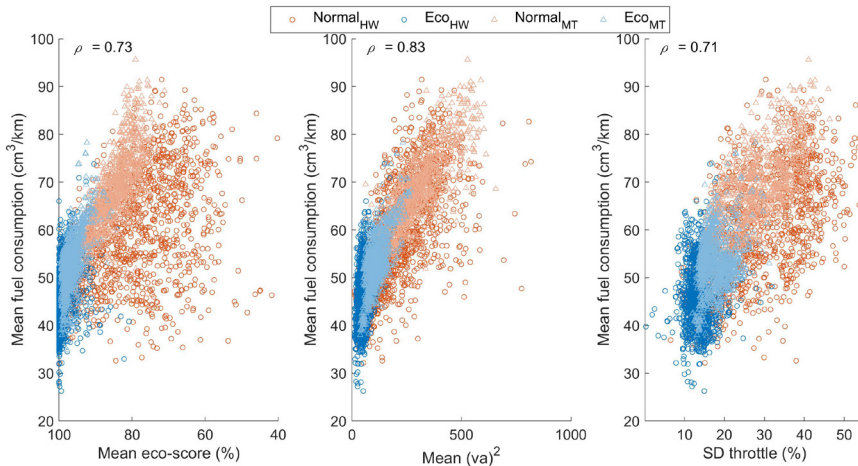


Figure 4.3. The Spearman's correlation (ρ) of the fuel consumption for three metrics (one marker represents one lap). No distinction is made between the Clio and Mégane.

calculated from lateral acceleration, steering wheel angle, steering wheel angle speed, and driving speed. The strongest effects for vehicle type were found for metrics calculated from the steering wheel angle, steering wheel angle speed, and the longitudinal acceleration.

Association between fuel consumption and driving metrics

Figure 4.3 shows examples of Spearman's rank-order fuel consumption correlations (which are also shown in Table 4.4) for three driving metrics: the eco-score, va^2 , and SD throttle position. A strong association between the eco-score and fuel consumption per km can be seen ($\rho = 0.73$). Interestingly, SD throttle position, a fairly simple metric, had a similar correlation with fuel-consumption ($\rho = 0.71$) as the Renault eco-score. The strongest correlation with fuel consumption (see also Table 4.4) was found for the va^2 metric ($\rho = 0.83$).

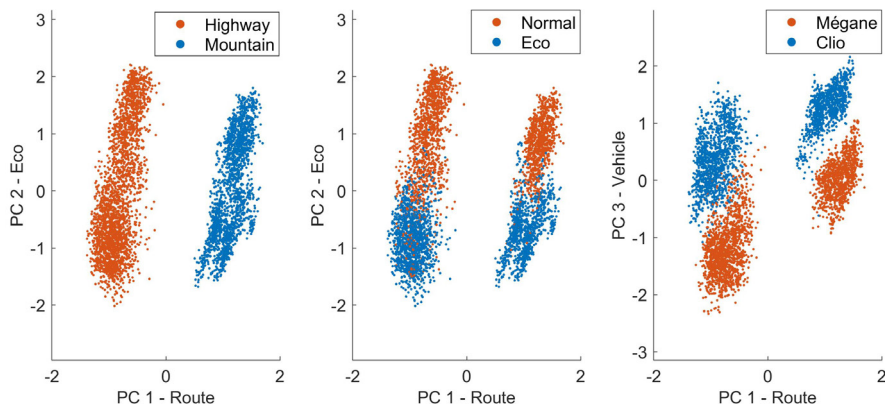


Figure 4.4. Scatter plot of the first two principal component scores (left and middle), and the first and third principal component scores (right) of all laps ($n = 4617$, one marker represents one lap). The colours indicate the route type (left), eco-driving condition (middle), and vehicle type (right).

Table 4.4. Fifty metrics with the highest Eco-driving Cohen's \bar{d} effect sizes, and the corresponding correlation with fuel consumption for all driven laps (4617 data points).

Rank	Signal name	Metric	Cohen's \bar{d}			Spearman's correlation with fuel consumption (4617 data points)
			Eco-driving instructions (normal-eco)	Route type (highway - mountain)	Vehicle type (Mégane - Clio)	
17	Fuel consumption per km	mean	3.05	-1.64	0.48	1.00
22	Fuel consumption per s	mean	2.86	1.92	0.33	0.67
49	Principal component 1	-	2.09	-15.30	1.57	0.57
2	Principal component 2	-	3.96	-0.31	0.08	0.80
81	Principal component 3	-	1.15	-3.88	-5.13	0.39
1	Eco	SD	4.18	-0.08	0.21	0.68
3	Eco	10 th perc	-3.90	-0.03	-0.20	-0.71
4	Eco	min	-3.81	1.03	0.00	-0.64
5	Eco	mean	-3.54	0.24	-0.31	-0.73
6	Engine RPM	max	3.48	-1.00	0.34	0.76
7	Eco	# times below 50	3.47	-1.78	0.30	0.74
8	Engine RPM	90 th perc	3.44	-0.10	0.38	0.71
9	Engine RPM	75 th perc	3.43	0.11	0.47	0.69
10	Longitudinal acceleration	90 th perc of abs	3.35	-5.98	-0.29	0.72
11	Engine RPM	mean	3.22	0.65	0.51	0.64
12	va^2	90 th perc	3.21	-1.78	-0.13	0.83
13	Throttle	max	3.18	-0.80	-0.64	0.68
14	Longitudinal acceleration	RPA	3.16	-3.89	-2.75	0.75
15	Longitudinal acceleration	SD	3.13	-5.22	-0.33	0.75
16	Engine RPM	SD	3.09	-1.98	0.17	0.72
18	Engine RPM	50 th perc	3.04	0.64	0.50	0.62
19	Longitudinal acceleration	75 th perc of abs	2.94	-5.51	-1.26	0.73
20	Eco	25 th perc	-2.93	0.22	-0.39	-0.75
21	Brake pressure	mean	2.88	-3.96	-0.81	0.67
23	Long acceleration	90 th perc	2.86	-4.57	-0.93	0.74
24	Brake pressure	SD	2.84	-3.69	-0.64	0.71
25	va^2	75 th perc	2.78	-1.33	-0.88	0.81
26	Longitudinal acceleration	max	2.77	-5.45	-0.98	0.62
27	va^2	mean	2.77	-1.52	-0.31	0.83
28	Speed	90 th perc	2.74	4.45	0.06	0.12
29	Engine RPM	25 th perc	2.72	1.22	0.56	0.52
30	Brake pressure	max	2.62	-3.16	-0.39	0.69
31	Speed	75 th perc	2.46	4.69	0.09	0.09
32	Longitudinal acceleration	10 th perc	-2.46	5.09	0.26	-0.59
33	Throttle	SD	2.46	-0.91	-0.90	0.71
34	Speed	max	2.45	3.80	0.04	0.14
35	Lateral acceleration	50 th perc of abs	2.39	-2.25	0.07	0.74
36	Throttle	90 th perc	2.37	-0.03	-0.99	0.67
37	Speed	SD	2.37	-1.99	0.08	0.78
38	Longitudinal acceleration	min	-2.34	3.38	0.13	-0.71
39	Engine RPM	10 th perc	2.33	1.64	0.55	0.40
40	va^2	50 th perc	2.32	-0.57	-1.76	0.67
41	Eco	50 th perc	-2.28	0.17	-0.42	-0.71
42	Longitudinal acceleration	50 th perc of abs	2.24	-4.09	-2.41	0.64
43	Longitudinal acceleration	75 th perc	2.24	-2.74	-3.11	0.64
44	Longitudinal acceleration	# of hard brakes	2.23	-4.01	-0.64	0.62
45	va^2	SD	2.21	-1.24	0.28	0.80
46	Steering wheel angle	50 th perc of abs	2.16	-8.55	1.59	0.64
47	Throttle	mean	2.15	1.14	-0.83	0.58
48	Speed	mean	2.11	6.31	0.08	0.05
50	Speed	50 th perc	2.05	6.27	0.11	0.04

Note. A larger than 0 means higher values for normal than eco, highway than mountain, and Mégane than Clio.

Principal component analysis (PCA)

Figure 4.4 shows the principal component scores for all laps ($n = 4617$) with colour markings for the route type (left), eco-driving (middle), and vehicle type (right). The first principal component is primarily composed of (i.e., high factor loadings) metrics that yielded strong Cohen's \bar{d} values for route type in Table 4.4 (i.e., speed, lateral accelerations, SWA, and SWA speed, see Appendix B for all factor loadings). Likewise, the second principal component is mainly composed of metrics that yielded strong Cohen's \bar{d} values for eco-driving in Table 4.4 (i.e., eco-score, speed, fuel consumption, throttle position, engine RPM, va^2). The third

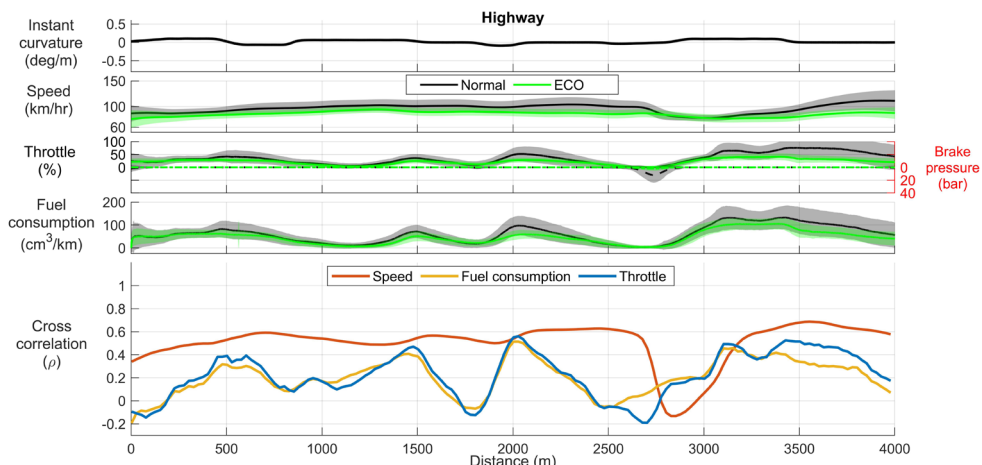


Figure 4.5. Location-specific results for the highway route for the normal ($n = 1250$, 53 drivers) and eco-driving ($n = 1449$, 54 drivers) conditions. The bottom figure shows the leave-one-out correlation ($n = 2697$, 84 drivers).

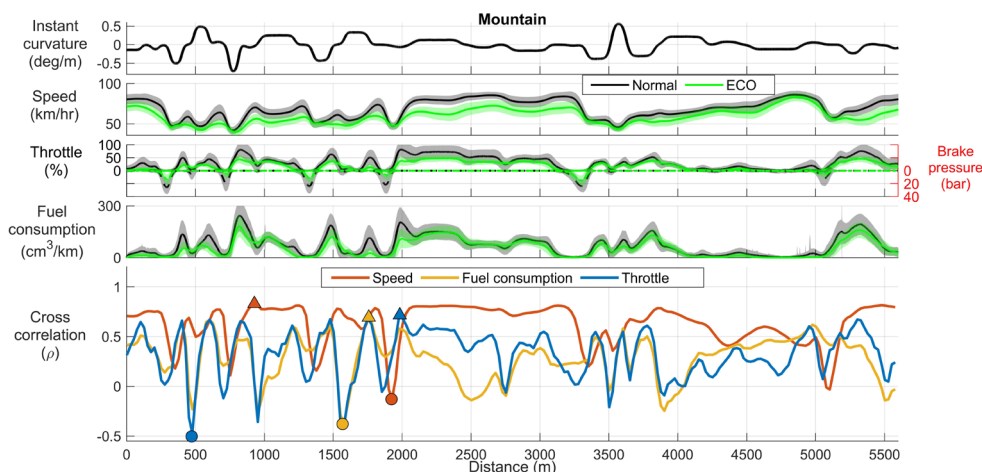


Figure 4.6. Location-specific results for the mountain route for the normal ($n = 930$, 38 drivers) and eco-driving ($n = 988$, 38 drivers) conditions. The bottom figure shows Spearman's leave-one-out correlation ($n = 1915$, 64 drivers).

principal component is composed of metrics that proved sensitive to vehicle type (i.e., SWA, va^2 , longitudinal acceleration). In total, the first three principal components captured 74.9% of the total variance (1. route: 45.7%, 2. eco-driving: 21.8%, 3. vehicle type: 7.4%).

4.3.2. Location-Specific Analysis

Figure 4.5 (highway) and Figure 4.6 (mountain) show the results of the location-specific analysis. These figures show the mean and standard deviation of recorded signals of all laps for both normal driving (highway: $n = 1250$, 53 drivers; mountain: $n = 930$, 38 drivers) and eco-driving (highway: $n = 1449$, 54 drivers; mountain: $n = 988$, 38 drivers) as a function of travelled distance for the two vehicles combined. In addition to the three selected predictor signals, we also visualised the instantaneous curvature (yaw rate/speed) to provide an insight

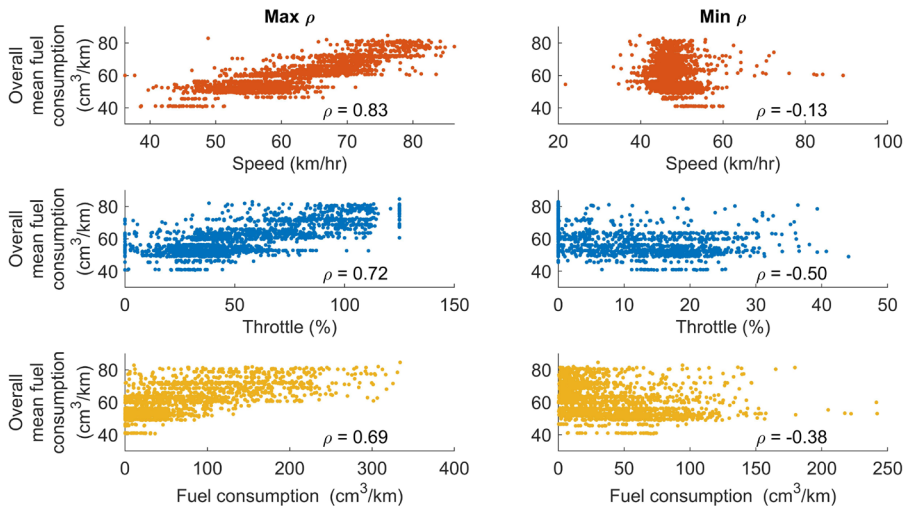


Figure 4.7. Scatter plots of the maximum (left) and minimum (right) Spearman's leave-one-out correlation between mean fuel consumption and three driving metrics. The triangles and circles in Figure 4.6 mark the location of the maximum and minimum, respectively.

into the sharpness of the curves, and the brake pedal position to provide a more complete picture of driving behaviour. The bottom panels of Figures 4.5 and 4.6 show the location-specific correlations between overall fuel consumption and driving speed, between overall fuel consumption and throttle position, and between overall fuel consumption and current fuel consumption, for the highway route ($n = 2697$, 84 drivers) and mountain route ($n = 1915$, 64 drivers), respectively.

The figures illustrate that, in the eco-driving condition, participants on average drove a substantially slower speed compared to normal driving, for most of the highway and mountain routes. For some sharp curves of the mountain road, the mean speeds in the two groups were equivalent. Lower and later throttle presses (positive values in the third subplot), and less braking (negative values in the third subplot) were found for eco-driving compared to normal-driving. Finally, when eco-driving a lower current fuel consumption was found compared to normal driving.

The bottom graphs of Figures 4.5 and 4.6, show that the correlation coefficient depends on the route and the location along the route. Higher peak correlations occur for driving speed (highway route: $\rho = 0.69$, mountain route: $\rho = 0.83$) than for fuel consumption (highway route: $\rho = 0.56$, mountain route: $\rho = 0.71$) and throttle position (highway route: $\rho = 0.56$, mountain route: $\rho = 0.72$). The throttle and fuel consumption exhibit a more volatile correlation with fuel consumption than the driving speed. The correlations for fuel consumption and throttle position decrease considerably, and even become negative, at the beginning of turns. Figure 4.7 shows a scatter plot for the maximum and minimum correlation of the mountain route (indicated with triangle and circles in Figure 4.6, respectively). A negative correlation for speed ($\rho = -0.13$), throttle ($\rho = -0.50$), or fuel consumption ($\rho = -0.38$) means that drivers with a higher driving speed, deeper throttle depression, and higher fuel consumption at that particular location had a lower overall fuel consumption.

4.4. Discussion

The purpose of this study was to predict fuel consumption from driving behaviour measurements, with the underlying motivation to allow improvements in eco-driving feedback and training applications. In the first part of the analysis, we correlated 110 driving metrics and three PCA components with fuel consumption at the level of laps on the test track. The goal of this analysis was to determine which metrics are most strongly associated with fuel use, to examine how these metrics are associated with each other, and to investigate how much these metrics are influenced by route and vehicle type. In the second part of the analysis, we examined which part of the route is predictive of fuel consumption by correlating driving behaviour at a large number of points along the route with drivers' fuel consumption for the entire route.

Part 1: Predicting fuel consumption from lap-level metrics

Compared to normal driving, eco-driving resulted in a 23.2% reduction in fuel consumption per kilometre, corresponding to a Cohen's \bar{d} of 3.05 (i.e., a large difference; more than 3 times the standard deviation). Compared to the literature, such fuel reduction benefits are on the higher side (see also Alam & McNabola, 2014; Huang et al., 2018; Xu et al., 2016), which can be explained by the eco-score received on the dashboard, the extensive eco-training received for all 91 drivers, and the lack of surrounding traffic and traffic lights. In summary, the experimental methods (i.e., the eco-driving training, and test track setting) were successful in eliciting vastly different driving styles and corresponding fuel consumption levels to be analysed further.

The metrics that proved to be most sensitive to the eco-driving instructions (i.e., metrics yielding the largest eco-driving Cohen's \bar{d}) were metrics associated with engine RPM, longitudinal acceleration, and throttle input. Note that a high eco-driving Cohen's \bar{d} for a particular metric does not imply that this metric is a practical index of eco-driving. In fact, the speed and longitudinal metrics had a high Cohen's \bar{d} for *eco-driving*, but an even higher Cohen's \bar{d} for *route type*, which indicates that these metrics are more influenced by the driven route than the adopted eco-driving style. We advocate that, ideally, an eco-score should correlate strongly with consumption and should be interpretable in different road environments and for different vehicles. In other words, when driving in an energy-demanding environment (e.g., mountain), drivers should not receive a notification that they drive eco-unfriendly. Of course, such information might still be valid if drivers need to be informed that they selected an eco-unfriendly route, but in practice, drivers may not be able to adjust their route. Similar statements were made by Andrieu and Saint Pierre (2012), Shi et al. (2015) and Dib et al. (2014), who proposed to normalise fuel consumption to the road environment.

The principal component analysis results complement the findings described above, where the largest part of the variance (45.7%) in the metrics was attributable to the route type. High component loadings were found for metrics related to speed, lateral acceleration, and steering wheel angle, suggesting that especially these metrics are impacted by route type (Appendix B). The second component showed high loadings for engine RPM, va^2 , throttle, speed, and eco-score metrics. It had a large correlation with fuel consumption, but a small correlation with route and vehicle type, making it interesting to be used as an eco-score in future research. Finally, for the third component (vehicle type), high loadings were obtained for the 10th percentile of the absolute longitudinal acceleration, the 10th percentile of va^2 , and the 75th percentile of the steering wheel angles. These effects may be attributable to vehicle-specific factors such as the steering wheel gain, pedal mapping, and engine type.

The first part concludes that driving metrics are highly predictive of fuel consumption but with a considerable amount of variance attributable to route and vehicle type. There is a substantial amount of literature on the effects of eco-driving behaviour, vehicle type, and route features on fuel consumption and driving metrics (Brundell-Freij & Ericsson, 2005; Ma

et al., 2015; Wang & Boggio-Marzet, 2018). Compared to the literature, our experimental protocol allowed for a more controlled investigation of eco-driving behaviour (participants were allocated to an eco-driving condition), vehicle type (in the real world, sporty drivers may choose to drive a sportier vehicle), and route (in the real world, drivers can determine their own route). The large influence of route and vehicle type on fuel consumption makes most of the metrics in their current form limitedly useful for providing drivers with advice on their driving style.

Part 2: Location-specific analysis

In the second part of this paper, we correlated driving behaviour along the lap with drivers' fuel consumption for all laps driven. We demonstrated that it makes sense to develop location-specific predictors of eco-driving, as high leave-one out correlations with fuel consumption were found for specific locations of the route. The highest correlation was found for driving speed, for both the highway route ($\rho = 0.69$) and the mountain route ($\rho = 0.83$). The correlations showed strong fluctuations along the route, with negative correlations when approaching particular curves. The negative correlations mean that, for that specific location, drivers who adopted a higher speed, throttle, or fuel consumption per km, ended up with lower fuel consumption over the entire route. Keeping momentum while approaching a curve is advantageous because, if a higher speed is maintained throughout the curve, less acceleration is needed after the curve. Our findings correspond to Ma et al. (2015), who showed that the largest fuel consumption differences between driving styles were found in the acceleration and deceleration phases.

Our findings emphasise the importance of developing location-specific fuel-consumption/driving style predictors. Currently, researchers employ artificial intelligence and large amounts of data to create increasingly accurate predictors (Martinez et al., 2017). We argue that, at one point, adding more trip-level data, or measuring for longer periods of time, will not improve the accuracy of fuel-economy predictions anymore, but including location-specific information could. Note that the Cohen's \bar{d} , calculated per lap, already corrects for route and vehicle type, but it is not location-specific. If fuel consumption predictions are conducted at a trip level, valuable location-specific information is lost due to the aggregation of data. This was clearly visible from the correlation between the mean speed and fuel consumption: with, on the one hand, a very weak correlation when computed per lap (i.e., combining all route, vehicle, and eco-driving instructions: $\rho = 0.05$; Table 4.4) and, on the other hand, the highest leave-one-out correlation (for the mountain route $\rho = 0.83$ and the highway route $\rho = 0.69$), along with a strong eco-driving Cohen's \bar{d} ($\bar{d} = 2.11$). The low mean speed correlation with fuel consumption when calculated per lap can be explained by a formal fallacy (also known as the Simpson's paradox; Simpson, 1951), where, in a given environment, driving faster normally increases fuel usage, while between environments, driving faster reduces fuel usage (i.e., highway driving yields better fuel economy than driving in the mountains). A location-specific eco-driving predictor would be able to resolve this fallacy. In theory, a location-specific predictor would not even need a (long) observation window, but allows for an almost immediate prediction of the driver's overall fuel consumption or driving style based on the driver's current behaviour. Extending our location-specific predictor with external information such as information about congestion (Lois et al., 2019), static traffic features (traffic signs, traffic lights, parked vehicles), and dynamic features (other road users) may lead to even more powerful predictions.

Future studies should investigate the robustness of a location-specific predictor for other types of environments, and determine general rules for the "best" location to create a location-predictor. Based on our results, we hypothesise that the acceleration and deceleration phases are particularly suitable because these are the periods where the standard deviation

of the fuel consumption is large between drivers (e.g., beginning and the end of a curve, or near traffic lights). To practically implement a real-world location-predictor in eco-feedback systems this would require a mapping of not only road type (e.g., curvature and slope), but also the location-specific driving behaviour of a variety of drivers (a “Tesla-like” approach). As an alternative to such an exhaustive mapping, a more general set of rules could be established: for example an average road curvature of 500-m has a correlation with driving metric and fuel consumption of Y1, whereas the acceleration phase at a traffic light has a correlation of Y2. The use of location-specific information with real-vehicle CAN-data would be feasible (Melman et al., 2021).

Although this test track study allowed for a controlled driving behaviour study with real vehicles, it lacks interaction with other road elements, such as other road users and traffic lights. Future studies should investigate how our results generalise to more realistic conditions. To maintain the high control that allows for the systematic analysis used in this study, we recommend that future research is conducted with surrounding vehicles traffic on a test track. It can be expected that drivers will change their eco-driving behaviour when driving in front of or behind other vehicles, such as during car following. Finally, we note that some of our effect sizes should be interpreted with caution, as correlation does not imply causation. For example, the high eco-driving Cohen’s d for the metric ‘50th percentile of the absolute steering wheel angle’ does not imply that drivers should be advised to steer less if they want to improve their fuel economy. This finding can be explained by an underlying cause known from vehicle dynamics: taking a turn at a lower driving speed requires a somewhat smaller steering wheel angle.

We conclude that driving metrics, when calculated per lap, are strongly correlated with fuel consumption in that lap. However, a large part of the variance in the driving metrics was attributable to the route type, making trip-level metrics less suitable for real-time driver feedback. We demonstrated that location-specific measurements offer powerful and near-instantaneous fuel consumption predictions for specific locations on the route. These findings may pave the way for new eco-driving applications.

References

- Alam, M. S., & McNabola, A. (2014). A critical review and assessment of Eco-Driving policy & technology: Benefits & limitations. *Transport Policy*, 35, 42-49.
- Allison, C., & Stanton, N. (2018). Eco-driving: the role of feedback in reducing emissions from everyday driving behaviours. *Theoretical Issues in Ergonomics Science*, 20, 85-104.
- Andrieu, C., & Saint Pierre, G. (2012). Using statistical models to characterise eco-driving style with an aggregated indicator. In *IEEE Intelligent Vehicles Symposium* (pp. 63-68).
- Brundell-Freij, K., & Ericsson, E. (2005). Influence of street characteristics, driver category and car performance on urban driving patterns. *Transportation Research Part D: Transport and Environment*, 10, 213-229.
- Caban, J., Vrabel, J., Šarkan, B., & Ignaciuk, P. (2019). About eco-driving, genesis, challenges and benefits, application possibilities. *Transportation Research Procedia*, 40, 1281-1288.
- Dib, W., Chasse, A., Moulin, P., Sciarretta, A., & Corde, G. (2014). Optimal energy management for an electric vehicle in eco-driving applications. *Control Engineering Practice*, 29, 299-307.
- Ericsson, E. (2001). Independent driving pattern factors and their influence on fuel-use and exhaust emission factors. *Transportation Research Part D: Transport and Environment*, 6, 325-345.
- Fabrigar, L. R., Wegener, D. T., MacCallum, R. C., & Strahan, E. J. (1999). Evaluating the use of exploratory factor analysis in psychological research. *Psychological Methods*, 4, 272.
- Fomunung, I., Washington, S., & Guensler, R. (1999). A statistical model for estimating oxides of nitrogen emissions from light duty motor vehicles. *Transportation Research Part D: Transport and Environment*, 4, 333-352.
- Ho, S. H., Wong, Y. D., & Chang, V. W. C. (2015). What can eco-driving do for sustainable road transport? Perspectives from a city (Singapore) eco-driving programme. *Sustainable Cities and Society*, 14, 82-88.
- Huang, Y., Ng, E. C., Zhou, J. L., Surawski, N. C., Chan, E. F., & Hong, G. (2018). Eco-driving technology for sustainable road transport: A review. *Renewable and Sustainable Energy Reviews*, 93, 596-609.
- Lois, D., Wang, Y., Boggio-Marzet, A., & Monzon, A. (2019). Multivariate analysis of fuel consumption related to eco-driving: Interaction of driving patterns and external factors. *Transportation Research Part D: Transport and Environment*, 72, 232-242.
- Ma, H., Xie, H., Huang, D., & Xiong, S. (2015). Effects of driving style on the fuel consumption of city buses under different road conditions and vehicle masses. *Transportation Research Part D: Transport and Environment*, 41, 205-216.
- Martinez, C. M., Heucke, M., Wang, F. Y., Gao, B., & Cao, D. (2017). Driving style recognition for intelligent vehicle control and advanced driver assistance: A survey. *IEEE Transactions on Intelligent Transportation Systems*, 19, 666-676.
- Melman, T., De Winter, J., Mouton, X., Tapus, A., & Abbink, D. (2021). How do driving modes affect the vehicle's dynamic behaviour? Comparing Renault's MultiSense sport and comfort modes during on-road naturalistic driving. *Vehicle System Dynamics*, 59, 485-503.
- Mensing, F., Bideaux, E., Trigui, R., & Tattgrain, H. (2013). Trajectory optimisation for eco-driving taking into account traffic constraints. *Transportation Research Part D: Transport and Environment*, 18, 55-61.
- Saboo, Y., & Farzaneh, H. (2009). Model for developing an eco-driving strategy of a passenger vehicle based on the least fuel consumption. *Applied Energy*, 86, 1925-1932.
- Sanguinetti, A., Kurani, K., & Davies, J. (2017). The many reasons your mileage may vary: Toward a unifying typology of eco-driving behaviors. *Transportation Research Part D: Transport and Environment*, 52, 73-84.
- Sanguinetti, A., Queen, E., Yee, C., & Akanesuvan, K. (2020). Average impact and important features of onboard eco-driving feedback: A meta-analysis. *Transportation Research Part F: Traffic Psychology and Behaviour*, 70, 1-14.
- Sarkan, B., Sermanova, S., Harantova, V., Stopka, O., Chovancova, M., & Szala, M. (2019). Vehicle fuel consumption prediction based on the data record obtained from an engine control unit. In *MATEC Web of Conferences* (Vol. 252, p. 06009). EDP Sciences.
- Shi, B., Xu, L., Hu, J., Tang, Y., Jiang, H., Meng, W., & Liu, H. (2015). Evaluating driving styles by normalising driving behavior based on personalised driver modeling. *IEEE Transactions on Systems, Man, and Cybernetics: Systems*, 45, 1502-1508.
- Simpson, E. H. (1951). The interpretation of interaction in contingency tables. *Journal of the Royal Statistical Society: Series B (Methodological)*, 13, 238-241.
- Sivak, M., & Schoettle, B. (2012). Eco-driving: Strategic, tactical, and operational decisions of the driver that influence vehicle fuel economy. *Transport Policy*, 22, 96-99.
- Vaezipour, A., Rakotonirainy, A., & Haworth, N. (2015). Reviewing in-vehicle systems to improve fuel efficiency and road safety. *Procedia Manufacturing*, 3, 3192-3199.
- Wang, Y., & Boggio-Marzet, A. (2018). Evaluation of eco-driving training for fuel efficiency and emissions reduction according to road type. *Sustainability*, 10, 3891.
- Xu, Y., Li, H., Liu, H., Rodgers, M. O., & Guensler, R. L. (2016). Eco-driving for transit: An effective strategy to conserve fuel and emissions. *Applied Energy*, 194, 784-797.
- Zhou, M., Jin, H., & Wang, W. (2016). A review of vehicle fuel consumption models to evaluate eco-driving and eco-routing. *Transportation Research Part D: Transport and Environment*, 49, 203-218.

Appendix 4A. Number of laps per participant and experimental condition

Table 4A. Number of laps each participant drove the highway section and mountain section for eco-driving and normal-driving and the two vehicle types.

Participant	Mégane				Clio			
	Normal		Eco		Normal		Eco	
	Highway	Mountain	Highway	Mountain	Highway	Mountain	Highway	Mountain
1	0	0	0	0	0	19	0	28
2	28	0	0	0	0	0	0	0
3	0	8	0	0	0	0	0	0
4	35	15	0	0	0	0	0	0
5	0	0	17	49	0	0	16	16
6	0	0	8	3	8	0	0	0
7	16	19	0	21	0	0	0	0
8	37	0	0	0	0	0	0	0
9	5	27	0	0	0	28	0	0
10	0	0	19	0	0	0	23	0
11	0	0	5	43	0	0	38	7
12	0	0	0	0	36	10	0	0
13	0	13	0	0	0	0	0	0
14	17	15	19	0	0	0	0	0
15	0	0	19	0	0	0	0	0
16	0	0	0	0	21	0	0	0
17	0	0	33	0	0	0	0	24
18	24	10	0	0	0	0	0	0
19	0	0	8	33	0	0	0	23
20	19	13	0	0	0	0	0	0
21	0	0	0	24	0	0	17	0
22	0	0	0	0	0	0	14	0
23	0	0	0	0	20	62	0	0
24	0	0	0	0	29	0	0	0
25	0	18	0	0	21	0	17	8
26	0	0	0	0	20	0	13	0
27	0	0	0	0	43	0	0	0
28	0	0	0	0	0	0	1	10
29	0	0	0	0	13	45	0	0
30	0	0	49	33	20	20	26	0
31	0	0	0	0	9	0	0	0
32	9	23	0	0	0	0	0	0
33	0	0	0	0	0	0	0	23
34	7	0	0	0	0	0	14	0
35	11	0	8	3	0	0	28	0
36	0	0	17	0	0	24	0	0
37	0	0	0	0	0	34	0	0
38	34	0	10	0	0	0	22	0
39	0	0	30	56	62	7	19	40
40	3	0	0	0	0	0	0	0
41	26	0	0	0	0	0	0	0
42	1	28	0	22	0	0	23	0
43	0	0	29	50	0	0	0	0
44	41	22	0	0	0	0	0	0
45	0	0	25	14	0	0	28	5
46	0	0	0	0	0	38	0	0
47	37	0	0	0	0	0	0	0
48	11	14	15	31	0	0	0	0
49	0	0	24	0	0	20	0	0
50	11	14	8	20	19	0	0	0
51	0	0	25	0	0	0	12	37
52	0	0	0	0	0	0	5	0
53	0	0	0	0	30	0	43	0
54	0	0	0	0	3	34	0	0

*(Continued on the next page)

Table 4A. (continued)

Participant	Mégane				Clio			
	Normal		Eco		Normal		Eco	
	Highway	Mountain	Highway	Mountain	Highway	Mountain	Highway	Mountain
55	0	0	14	0	0	0	0	0
56	0	0	0	13	0	0	13	0
57	0	0	14	15	25	1	0	0
58	0	4	0	0	26	1	0	0
59	0	0	24	0	0	0	0	0
60	0	0	0	11	0	0	6	21
61	0	0	34	0	0	0	32	7
62	0	0	0	27	0	0	3	40
63	12	24	20	0	0	20	0	0
64	11	0	0	0	0	0	0	0
65	5	3	0	0	16	0	0	0
66	0	0	0	0	11	0	0	0
67	0	0	20	0	0	0	0	3
68	31	0	0	0	22	0	15	0
69	0	0	22	0	0	0	0	0
70	0	0	0	0	33	0	18	2
71	36	38	0	0	0	0	16	9
72	20	42	0	0	0	15	0	0
73	16	7	0	0	0	0	0	0
74	0	0	0	0	0	0	34	0
75	0	0	68	0	0	0	15	16
76	73	0	28	17	0	0	0	6
77	3	0	0	0	42	0	0	0
78	0	0	0	0	0	0	23	29
79	0	22	0	0	0	0	0	0
80	0	0	32	25	0	0	0	0
81	0	0	0	0	20	31	0	0
82	20	20	0	0	0	10	0	0
83	0	0	0	0	0	0	11	19
84	3	15	0	0	14	13	0	23
85	13	0	27	10	0	0	0	5
86	29	0	29	0	0	0	17	0
87	3	35	52	15	22	18	12	32
88	0	0	0	0	0	0	25	11
89	18	0	3	1	0	0	40	8
90	0	0	14	0	0	0	0	0
91	0	0	15	0	0	31	26	0
# of different drivers	34	24	35	23	25	21	34	26
# of driving sections	665	449	784	536	585	481	665	452

Appendix 4B. List of all 110 driving metrics, PCA loadings and their corresponding analysis results

Table 4B. Cohen's d effect size, Spearman's correlation with fuel consumption, and the PCA loadings for all 110 driving metrics.

Rank	Driving metric	Cohen's d			Spearman's correlation with fuel consumption (4617 data points)	PCA loadings		
		Eco-driving instructions (normal-eco)	Route type (highway - mountain)	Vehicle type (Mégane - Clio)		PCA 1 Route	PCA 2 Eco	PCA 3 Vehicle
	Principal component 1	2.09	-15.3	1.57	0.57			
	Principal component 2	3.96	-0.31	0.08	0.8			
	Principal component 3	1.15	-3.88	-5.13	0.39			
1	Fuel consumption per km mean	3.05	-1.64	0.48	1	0.29	0.73	0.07
2	Fuel consumption per s mean	2.86	1.92	0.33	0.67	-0.41	0.91	-0.03
3	Eco mean	-3.54	0.24	-0.31	-0.73	-0.11	-0.86	0.01
4	Eco std	4.18	-0.08	0.21	0.68	0.05	0.84	-0.01
5	Eco min	-3.81	1.03	0	-0.64	-0.09	-0.78	0.01
6	Eco 10 th perc	-3.9	-0.03	-0.2	-0.71	-0.07	-0.85	0
7	Eco 25 th perc	-2.93	0.22	-0.39	-0.75	-0.21	-0.83	0.03
8	Eco 50 th perc	-2.28	0.17	-0.42	-0.71	-0.17	-0.83	0.08
9	Eco 75 th perc	-1.14	NaN	NaN	-0.46	0	-0.61	0.06
10	Eco 90 th perc	-0.41	-0.52	NaN	-0.2	0.11	-0.38	0.09
11	Eco # bellow eco 50	3.47	-1.78	0.3	0.74	0.35	0.73	-0.03
12	Speed mean	2.11	6.31	0.08	0.05	-0.83	0.62	-0.1
13	Speed std	2.37	-1.99	0.08	0.78	0.26	0.69	0.08
14	Speed max	2.45	3.8	0.04	0.14	-0.79	0.66	-0.06
15	Speed min	1.2	8.28	-0.21	-0.17	-0.81	0.41	-0.12
16	Speed 10 th perc	0.92	7.4	0.02	-0.11	-0.82	0.45	-0.12
17	Speed 25 th perc	1.47	7.21	0.08	-0.01	-0.83	0.55	-0.11
18	Speed 50 th perc	2.05	6.27	0.11	0.04	-0.84	0.6	-0.1
19	Speed 75 th perc	2.46	4.69	0.09	0.09	-0.82	0.64	-0.09
20	Speed 90 th perc	2.74	4.45	0.06	0.12	-0.81	0.67	-0.09
21	Long acc mean	0.14	3.76	-4.08	0.01	-0.88	0.15	0.63
22	Long acc std	3.13	-5.22	-0.33	0.75	0.63	0.46	0.21
23	Long acc max	2.77	-5.45	-0.98	0.62	0.65	0.26	0.27
24	Long acc min	-2.34	3.38	0.13	-0.71	-0.57	-0.53	-0.08
25	Long acc 10 th perc	-2.46	5.09	0.26	-0.59	-0.72	-0.21	-0.21
26	Long acc 25 th perc	-1.43	4.62	0.38	-0.42	-0.65	-0.09	-0.26
27	Long acc 50 th perc	0.49	1.8	-2.61	0.04	-0.82	0.1	0.72
28	Long acc 75 th perc	2.24	-2.74	-3.11	0.64	-0.02	0.42	0.72
29	Long acc 90 th perc	2.86	-4.57	-0.93	0.74	0.52	0.45	0.3
30	Long acc 10 th perc of abs	0.23	-2.34	-6.04	0.15	-0.17	-0.14	1
31	Long acc 25 th perc of abs	0.9	-3.4	-3.25	0.41	0.14	0.02	0.84
32	Long acc 50 th perc of abs	2.24	-4.09	-2.41	0.64	0.28	0.29	0.63
33	Long acc 75 th perc of abs	2.94	-5.51	-1.26	0.73	0.52	0.38	0.39
34	Long acc 90 th perc of abs	3.35	-5.98	-0.29	0.72	0.66	0.4	0.2
35	Long acc # of hard acc/dec	2.23	-4.01	-0.64	0.62	0.77	0.24	0.16
36	Long acc RPA	3.16	-3.89	-2.75	0.75	0.2	0.47	0.6
37	Throttle mean	2.15	1.14	-0.83	0.58	-0.48	0.82	0.25
38	Throttle std	2.46	-0.91	-0.9	0.71	0.03	0.74	0.36
39	Throttle max	3.18	-0.8	-0.64	0.68	0.02	0.75	0.26
40	Throttle min	NaN	NaN	NaN	-0.02	-0.01	0	-0.08
41	Throttle 10 th perc	NaN	0.86	NaN	-0.08	-0.22	0.02	-0.15
42	Throttle 25 th perc	0.1	3.24	-0.18	-0.15	-0.68	0.2	-0.17
43	Throttle 50 th perc	1.19	1.41	-0.37	0.37	-0.6	0.61	0.17
44	Throttle 75 th perc	1.72	-0.17	-0.87	0.72	-0.18	0.74	0.42
45	Throttle 90 th perc	2.37	-0.03	-0.99	0.67	-0.2	0.79	0.4
46	Throttle % no throttle	-0.54	-1.93	-0.11	0.13	0.65	-0.24	0.2
47	Brake pressure mean	2.88	-3.96	-0.81	0.67	0.61	0.4	0.19
48	Brake pressure std	2.84	-3.69	-0.64	0.71	0.55	0.49	0.16
49	Brake pressure max	2.62	-3.16	-0.39	0.69	0.52	0.54	0.11
50	Brake pressure 90 th perc	0.96	-1.37	-0.76	0.37	0.31	0.14	0.28
51	Brake pressure # of brakes	1.36	-3.93	0.1	0.51	0.82	0.12	0.08
52	Engine RPM mean	3.22	0.65	0.51	0.64	-0.09	0.96	-0.15
53	Engine RPM std	3.09	-1.98	0.17	0.72	0.35	0.64	0.11
54	Engine RPM max	3.48	-1	0.34	0.76	0.2	0.82	0.03
55	Engine RPM min	1.28	2.17	0.04	0.1	-0.56	0.51	-0.09
56	Engine RPM 10 th perc	2.33	1.64	0.55	0.4	-0.31	0.85	-0.25
57	Engine RPM 25 th perc	2.72	1.22	0.56	0.52	-0.21	0.92	-0.22
58	Engine RPM 50 th perc	3.04	0.64	0.5	0.62	-0.09	0.93	-0.17
59	Engine RPM 75 th perc	3.43	0.11	0.47	0.69	0.02	0.93	-0.12
60	Engine RPM 90 th perc	3.44	-0.1	0.38	0.71	0.06	0.91	-0.05
61	va2 mean	2.77	-1.52	-0.31	0.83	0.21	0.81	0.2
62	va2 std	2.21	-1.24	0.28	0.8	0.32	0.8	0.03

* (Continued on the next page)

Table 4B. (continued)

Rank	Driving metric	Cohen's <i>d</i>			Spearman's correlation with fuel consumption (4617 data points)	PCA loadings		
		Eco-driving instructions (normal-eco)	Route type (highway - mountain)	Vehicle type (Mégane - Clio)		PCA 1 Route	PCA 2 Eco	PCA 3 Vehicle
63	va2 max	1.89	-1.13	-0.16	0.73	0.3	0.73	0.09
64	va2 10 th perc	0.63	-0.27	-3.68	0.16	-0.42	-0.01	1.05
65	va2 25 th perc	1.33	-0.6	-2.53	0.43	-0.26	0.23	0.93
66	va2 50 th perc	2.32	-0.57	-1.76	0.67	-0.15	0.59	0.65
67	va2 75 th perc	2.78	-1.33	-0.88	0.81	0.09	0.75	0.38
68	va2 90 th perc	3.21	-1.78	-0.13	0.83	0.27	0.79	0.16
69	Lat acc mean	0	12.87	-1.1	-0.23	-0.94	0.26	0.08
70	Lat acc std	1.69	-3.63	0.13	0.66	0.75	0.38	0.03
71	Lat acc max	0.85	-2.63	-0.16	0.55	0.76	0.23	0.08
72	Lat acc min	-0.94	3.64	-0.08	-0.57	-0.76	-0.27	-0.04
73	Lat acc 10 th perc	-1.77	5.55	-0.42	-0.63	-0.82	-0.3	-0.01
74	Lat acc 25 th perc	-1.93	8.75	-2	-0.53	-0.98	-0.16	0.21
75	Lat acc 50 th perc	-0.33	15.02	-2.72	-0.33	-1.02	0.1	0.28
76	Lat acc 75 th perc	1.66	2.46	-0.15	0.2	-0.68	0.69	-0.04
77	Lat acc 90 th perc	1.59	-1.7	-0.02	0.7	0.44	0.6	0.05
78	Lat acc 10 th perc of abs	1	-1.43	-1.96	0.27	-0.06	0.03	0.66
79	Lat acc 25 th perc of abs	1.96	-3.56	-2.18	0.52	0.45	0.13	0.51
80	Lat acc 50 th perc of abs	2.39	-2.25	0.07	0.74	0.46	0.65	0.03
81	Lat acc 75 th perc of abs	1.77	-2.8	0.08	0.71	0.62	0.49	0.06
82	Lat acc 90 th perc of abs	1.34	-3.1	0.05	0.63	0.72	0.35	0.05
83	SWA mean	1.49	14.94	1.95	-0.17	-0.67	0.42	-0.41
84	SWA std	1.45	-17.48	2.11	0.57	1.02	0.2	-0.28
85	SWA max	0.92	-15.16	2.15	0.48	1.06	0.13	-0.34
86	SWA min	-0.6	20.12	-1.57	-0.5	-0.97	-0.09	0.18
87	SWA 10 th perc	-0.96	15.61	-1.04	-0.53	-0.9	-0.09	0.06
88	SWA 25 th perc	-0.02	15.3	-0.22	-0.33	-0.84	0.2	-0.12
89	SWA 50 th perc	1.23	6.51	1.33	-0.2	-0.72	0.37	-0.28
90	SWA 75 th perc	1.74	-0.25	2.2	0.42	0.36	0.65	-0.71
91	SWA 90 th perc	1.75	-10.85	2.6	0.54	1.04	0.2	-0.33
92	SWA 10 th perc of abs	0.96	-4.26	0.53	0.44	0.82	0.14	-0.08
93	SWA 25 th perc of abs	1.73	-9.06	1.11	0.5	0.92	0.14	-0.09
94	SWA 50 th perc of abs	2.16	-8.55	1.59	0.64	0.92	0.28	-0.13
95	SWA 75 th perc of abs	1.86	-12.75	2.33	0.58	1.01	0.23	-0.27
96	SWA 90 th perc of abs	1.31	-15.92	2.22	0.53	1.04	0.17	-0.32
97	SWA SRR	0.65	-2.11	0.61	0.41	0.75	0.17	-0.15
98	SWA speed mean	-0.11	-1.33	0.14	0.1	0.26	-0.08	0.05
99	SWA speed std	1.18	-7.8	0.99	0.54	0.95	0.17	-0.12
100	SWA speed max	0.41	-3.89	0.33	0.4	0.89	-0.02	-0.04
101	SWA speed min	-0.32	5.02	-0.45	-0.38	-0.89	0.05	0.03
102	SWA speed 10 th perc	-1.31	5.8	-0.67	-0.53	-0.9	-0.16	0.03
103	SWA speed 25 th perc	-0.9	3.63	7.27	-0.39	-0.54	-0.02	-0.34
104	SWA speed 50 th perc	NaN	NaN	NaN	-0.01	-0.02	0.02	0
105	SWA speed 75 th perc	0.76	-5.11	-5.71	0.35	0.59	-0.1	0.39
106	SWA speed 90 th perc	1.32	-6	0.76	0.53	0.91	0.15	-0.06
107	SWA speed 25 th perc of abs	NaN	NaN	NaN	0.15	0.13	0.01	0.24
108	SWA speed 50 th perc of abs	0.79	-5.1	-14.88	0.37	0.59	-0.07	0.38
109	SWA speed 75 th perc of abs	1.31	-5.69	0.89	0.53	0.96	0.16	-0.14
110	SWA speed 90 th perc of abs	1.34	-7.69	0.92	0.54	0.93	0.18	-0.09

PART



5

6

7

OFFLINE CHANGES IN VEHICLE SETTINGS

How Do Driving Modes Affect the Vehicle's Dynamic Behaviour?



Several modern vehicles provide the option to select a driving mode. However, the literature contains no empirical studies that investigate how driving modes affect the vehicle's dynamic behaviour in regular on-road driving. We examined for which CAN-bus signals the differences between Renault's Multi-Sense® comfort and sport modes are most apparent. We gathered data on a 26.3 km route containing a rural and highway section. A single person drove the route four times in comfort mode and four times in sport mode. By statistically analysing and ordering 887 CAN-bus signals, we found strong differences between the two modes for rear-wheel angle, engine torque, longitudinal acceleration, and vertical motion. Parameter identification of a quarter car model identified a 3.5 times higher damping coefficient for the sport mode compared to the comfort mode. Due to four-wheel steering, compared to the comfort mode, the sport mode yielded a higher lateral acceleration and yaw rate for a given steering wheel angle and driving speed. In conclusion, this study provides quantitative insight into the extent to which the Multi-Sense driving modes impact the vehicle's lateral, longitudinal, and vertical dynamic behaviour. The results and the analysis methods help guide future driving mode designs.

Published as:

Melman, T., De Winter, J. C. F., Mouton, X., Tapus, A., & Abbink, D. A. (2021). How do driving modes affect the vehicle's dynamic behaviour? Comparing Renault's MultiSense sport and comfort modes during on-road naturalistic driving, *Vehicle System Dynamics*, 59, 485–503. <https://doi.org/10.1080/00423114.2019.1693049>

5.1. Introduction

5.1.1. Driving Modes

In recent years, cars have evolved from vehicles having invariable characteristics to vehicles of which the dynamic characteristics can be changed using active springs, dampers, drivetrain, and steering systems (Crolla, 1996). These active dynamic components aim to improve comfort (e.g., by reducing vibrations in vehicle's body; Rajamani, 2011) and stability (Abe, 1999; Reuter & Saal, 2017; Yu et al., 2008). On top of this, some vehicle models offer the option to alter the parameters of the active dynamic components by selecting different driving modes (e.g., sport or comfort mode). These driving modes intend to offer distinct ride experiences, e.g., a comfort mode for a “smooth and silent ride” versus a sport mode for a “shaky adventurous ride” (Kissai et al., 2018; Sheller, 2004; Shibahata, 2005).

Nowadays, many car brands offer the driver the possibility to manually select one of the three basic driving modes such as Eco, Comfort, or Sport. One particular system, highlighted in this paper, is Renault's Multi-Sense®. The Multi-Sense modes (i.e., comfort, sport, eco, neutral) impact not only parameters concerning the vehicle dynamics (e.g., rear-wheel steering, drivetrain, and dampers), but also cockpit ambience (e.g., colour of ambient lighting, dashboard interface) (Renault, 2018).

A number of studies have examined the potential of driving modes in areas such as fuel/energy management (Chau et al., 2017; Jeon et al., 2002; Mohd et al., 2017), chassis control (Hilgers et al., 2009; Kim et al., 2005; Wimmer et al., 2014), or adaptation to personal driving styles (Jeon et al., 2016). The existing literature focuses on the functionality of individual active vehicle components, where a distinction can be made between active components that affect longitudinal/lateral (Section 5.1.2) and vertical vehicle dynamics (Section 5.1.3). However, to the best of our knowledge, no empirical studies in the current literature investigate differences in vehicle behaviour as a function of different driving modes.

5.1.2. Active Lateral and Longitudinal Vehicle Dynamics

The characteristics of the steering system are known to influence the subjective steering feel and comfort (Boller, 2017; Pfeffer et al., 2008; Tagesson, 2017) as well as lane-keeping performance (Nagai & Koike, 1994; Shyrokau et al., 2018). An important parameter is the steering ratio, which is the ratio between the driver's steering wheel angle and the front wheel angle. In most conventional cars, the steering ratio and turning radius are mechanically linked and invariant (Trzesniowski, 2017). Invariant steering systems allow drivers to develop a reliable mental model (Russell et al., 2016). However, invariant systems cannot accommodate differences in desired steering responsiveness for different driving situations. For example, at high speed (e.g., highway driving), a low-gain steering system may be preferred as the driver requires small steering angles and high accuracy. At low speed, accuracy and stability are less critical, and a high-gain steering system may be preferred to accommodate a parking manoeuvre (Reuter & Saal, 2017).

Various active steering systems exist, such as four-wheel steering (4WS), active front steering, steer-by-wire, and direct yaw control (Shibahata, 2005; Strandroth et al., 2012). These systems enable functionalities such as speed-dependent change of vehicle agility (faster lateral movement of the vehicle with the same steering input), manoeuvrability (change in turning radius), steering effort (lower steering torques to achieve a similar lateral response), and stability (active safety by superposition of the steering angles or rear wheel angle in case of 4WS) (Abe, 1999, 2013; Cho et al., 2012; Huang & Pruckner, 2017; Klier et al., 2004).

Four-wheel steering enables active rear-wheel steering in addition to the front axle (Fahimi, 2013). With 4WS, at low speed, the rear wheels countersteer the front wheels (Figure 5.1a), and at high speed, they are turned in the same direction (Figure 5.1b). Countersteering shortens the virtual wheelbase (see Figure 5.1b), resulting in a smaller turning radius compared to no 4WS, whereas parallel steering increases the virtual wheelbase (see Figure 5.1a). Thus,

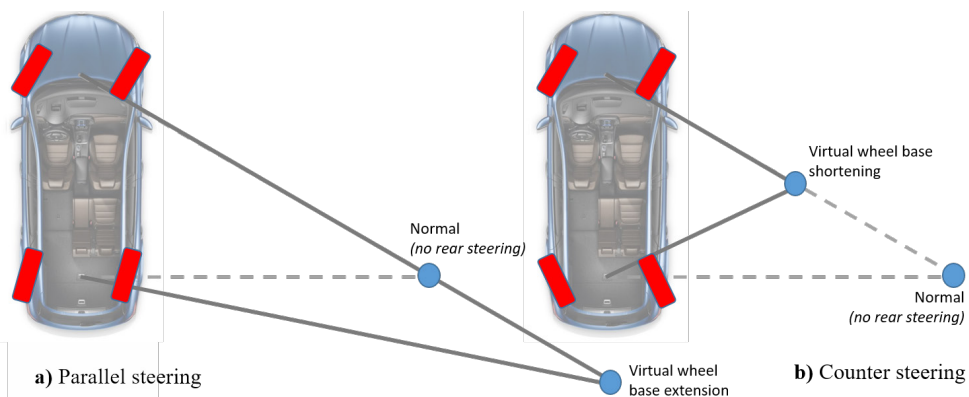


Figure 5.1. Steering configurations: a) Parallel steering; b) Countersteering. For a constant front steering angle, the turn radius is smaller for countersteering as compared to parallel steering (Herold & Wallbrecher, 2017).

for a constant steering wheel angle and constant speed, countersteering results in a higher steady-state yaw rate and lateral acceleration compared to parallel steering. Additionally, parallel steering results in a faster build-up of the lateral acceleration towards a target value as compared to regular front steering (Furukawa et al., 1989; Herold & Wallbrecher, 2017; Nalecz & Bindemann, 1988, 1989; Whitehead, 1988). For parallel steering, the transfer function of steering wheel angle to lateral acceleration has a low phase shift as the vehicle can generate rear-wheel slip angles without the need for a vehicle sideslip angle, reducing the time required to reach a steady-state condition.

Active longitudinal vehicle dynamics components include engine characteristics, throttle response, and gear switching control (Shinagawa et al., 2015).

5.1.3. Active Vertical Vehicle Dynamics

The suspension system includes the springs, dampers, and linkages that separate the car body (sprung mass) from the wheel assembly (unsprung mass). It has the function to improve the comfort of the vehicle occupants (i.e., reduce road vibrations in the car body) and to provide desirable handling specifications and contact between the tyres and road surface (Anubi, 2013; Savaresi et al., 2010). Where soft components, in general, improve ride comfort, a hard suspension improves handling specifications (Ikenaga, Lewis et al., 2000; Sekulić & Dedović, 2011; Sharp & Crolla, 1987; Yamashita et al., 1994). Passive suspension systems can only offer a compromise between these conflicting criteria (Els et al., 2007; Merker et al., 2002), resulting in sub-optimal vehicle characteristics.

Active suspension components enable online changes of the stiffness and damping settings. Current commercialised vehicles utilise variable damping in combination with passive springs but typically do not use variable stiffness, a concept that is currently in a research phase (Anubi, 2013; Morales et al., 2018; Sun et al., 2017). Besides variable damping and stiffness, active suspension mechanisms can apply control strategies to minimize the impact of braking and cornering on the body (active body control, active roll control) and to compensate for road irregularities (Furukawa et al., 1989; Trächtler, 2004; Wen et al., 2017). The performance of these components strongly depends on the implemented controller design (e.g., Choi et al., 2001; Guglielmino et al., 2008; Koch & Kloiber, 2014; Petek et al., 1995; Savaresi et al., 2010).

Driving modes could affect the functionality of these components (Hilgers et al., 2009; Kim et al., 2005). For example, for a sport driving mode, a higher variable damping parameter

could be utilised to feed more vibrations to the driver. For a comfort mode, softer damping would be used to remove these vibrations.

5.1.4. The need for understanding the impact of driving modes on the vehicle's dynamic behaviour

As pointed out above, a substantial body of literature exists on the behaviour of individual active components. However, no empirical studies investigate how these individual active components are affected by driving modes. Furthermore, for actual roads, the impact of driving modes on the vehicle's dynamic behaviour is unknown. In the present exploratory study, we aimed to quantify the vehicle's dynamic changes between the Renault Multi-Sense® comfort and sport modes. According to Renault (2018), the comfort mode 'favours smooth steering' and the sport mode 'permits an increased responsiveness from the engine and the gearbox.'. We aimed to make the dynamical effects of these modes transparent in the scientific literature. Accordingly, we gathered naturalistic driving data on a route containing a rural road and highway road section. A single driver drove the same route four times in comfort mode and four times in sport mode. Based on logged CAN-bus data (887 signals associated with rigid body motions, steering, and powertrain responses), we investigated which vehicle state variables discriminate the two modes, and used that selection to analyse the vehicle's longitudinal, lateral, and vertical dynamic behaviour in more detail. Changes in damping characteristics were quantified by identifying the damping coefficient in a simulation model of the suspension travel.

5

5.2. Experimental Design

5.2.1. Test Driver

One test driver (first author, male, 26 years old, eight years licensed to drive) participated in this study. In the past 12 months, the test driver drove 1 to 3 times a week, with a yearly mileage of about 10,000 to 15,000 km.

5.2.2. Apparatus

In the study, the test driver drove a 2015 Renault Talisman (Figure 5.2c) equipped with Multi-Sense and a CAN-bus for data gathering. The 887 CAN signals were recorded at frequencies ranging from 10 Hz to 100 Hz. The GPS location was recorded (sampled at 0.5 Hz) using an iPhone SE and the 'GPS tracker' application.

5.2.3. Road Trajectory

The driver drove on roads in France (near Versailles). The route consisted of a 9.1 km long rural road section (Figure 5.2a), and on a 14.5 km long highway road section (Figure 5.2b), which together are referred to as the *combined route* (23.6 km). The rural road section contained single-lane and two-lane sections, with very little traffic (< 2 cars per drive). The highway road section included two highway exits and two entries and had an advisory speed of 110 km/h. On the highway, low-density traffic was encountered.

5.2.4. Procedure

The driver was given the task to drive as he normally would, and with similar average speed for both the sport and comfort modes. The driver was familiar with the roads and with both modes before the start of the experiment. The two sections were driven on two separate days, with on the first day the rural road section was driven, and on a second day, the highway section was driven. Each road section was driven four times in sport mode and four times in

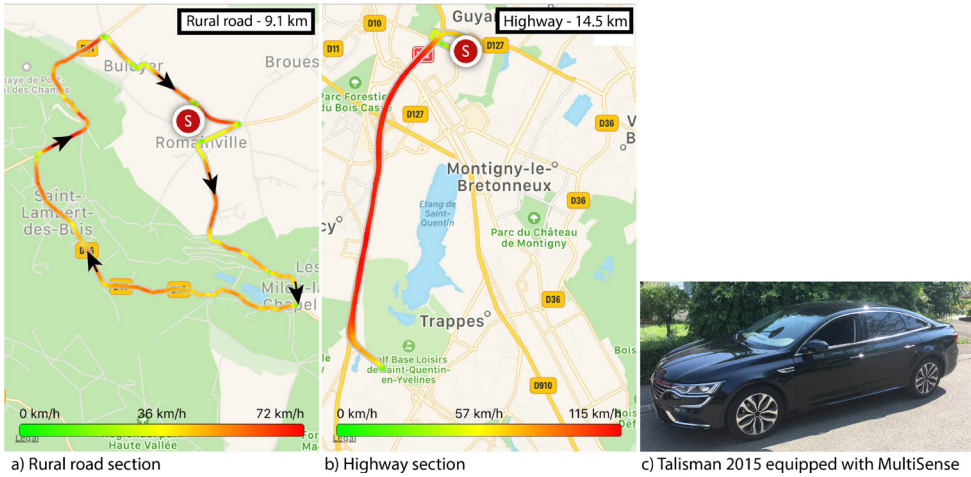


Figure 5.2. (a) rural road section (9.1 km), (b) highway section (14.5 km), (c) 2015 Renault Talisman equipped with Multi-Sense used in the experiment. The start/end is visualised with an S-sign, and the driven direction for the rural road is indicated with an arrow.

comfort mode in alternating order (starting with the sport mode for the rural road on day one and starting with comfort at the highway on day two). Between each driven section, there was a 5-minute break to mitigate fatigue. Furthermore, after the first four drives (2x sport and 2x comfort) there was a one-hour long break. For the highway road, the driver performed multiple overtaking manoeuvres. The combined route took 27 minutes (14 minutes for the rural road section, and 13 minutes for the highway road). On both days it was a clear day with an external temperature on day one (rural road) of 19°C and on day two (highway) of 21 °C. Finally, the first day there was 33 litre in the fuel tank at the start of the experiment, and on day two 27 litres.

5.2.5 Dependent Measures

Ordering the data

The following procedure was performed to find which measures discriminate between the comfort and sport modes. For each of the eight drives per road type (i.e., four drives in comfort mode & four drives in sport), we calculated for both sections (highway and rural road separately) and for all 887 CAN measures, the mean value of each of the signals, the standard deviation of each signal (a measure of variation), and the mean absolute successive difference of each signal (a measure of the amount of sample-to-sample fluctuations in the signal). Next, Cohen's d (Equation 5.1, Cohen, 1988) was computed as a measure of effect size between the four values for the sport mode and the four values for the comfort mode for the rural road and the highway separately. Cohen's d describes how much two samples (i.e., sport and comfort) differ from each other.

$$d = \frac{\mu_{sport} - \mu_{comfort}}{s}, \quad s = \sqrt{\frac{s_{sport}^2 + s_{comfort}^2}{2}} \quad (5.1)$$

With μ_k the sample mean of the four values of a particular mode, s the pooled standard deviation, and s_k the standard deviation of the four values of a particular mode. An illustration of the meaning of Cohen's d is provided in Appendix A.

5.2.6. Simulation Model

Quarter car model to identify the sprung damper coefficient

A quarter car linear oscillatory model of the suspension travel (Karnopp, 2009; Yoshimura et al., 2001) was used to estimate the sprung damper coefficient, b_s ($b_s > 0$). A constraint optimisation was performed to fit the model-based suspension travel on the empirically obtained suspension travel from the highway and rural road sections, per driving mode.

Table 5.1 provides the meaning and value of each parameter used in the simulation model. The values for the vehicle's sprung and unsprung mass and stiffness were obtained from Renault. These provided values yield a natural frequency for the sprung mass and unsprung mass of 1.48 Hz and 10.30 Hz, respectively. Using the equation of motion of this system, the transfer function can be derived for the suspension travel (i.e., the difference between sprung mass distance and unsprung mass distance ($X1 - X2$) as a response to the road disturbance frequency input D) (Equation 5.2). The road disturbance frequencies D (Hz) are linearly spaced between 0.47 Hz and 12 Hz.

$$H = \frac{X1 - X2}{D} = \frac{-m_s * b_u * s^3 - m_s * k_u * s^2}{(m_s * s^2 + b_s * s + k_s) * (m_u * s^2 + (b_s + b_u) * s + (k_s + k_u)) - (b_s * s + k_s) * (b_s * s + k_s)} \quad (5.2)$$

The power spectral density (PSD) of the suspension travel can be calculated using Equation 5.3.

$$\Phi_{(x1-x2)}(f) = |H(f)|^2 * \Phi_r(f) \quad (5.3)$$

where $H(f)$ is the complex frequency function from Equation 5.2, and $\Phi_r(f)$ is the PSD of the roughness of asphalt concrete pavement in good conditions, as a function of temporal excitation frequency (Equation 5.4; see Sekulić & Dedović, 2011; Wong, 2001, for a more detailed explanation).

$$\Phi_r(f) = \frac{C_{sp} * V^{N-1}}{f^N} \quad (5.4)$$

In Equation 5.4 a roughness coefficient (C_{sp}) of $7.5 \cdot 10^{-7}$ m was used for the rural road section, and $1.6 \cdot 10^{-7}$ m for the highway section. We assumed a fixed velocity (V) of 11 m/s, and 20 m/s for respectively the rural road, and the highway, and wavenumber (N) of 2.59 (rural road) and 2.32 (highway; which is, according to Wong, 2001, a value for a 'good pavement' condition).

5.3. Results

5.3.1. Driving Behaviour

Table 5.2 shows no substantial differences in mean speed (< 0.7 km/h), brake depression,

Table 5.1. Parameters used in the quarter car model. Numbers were provided by Renault. Parameter b_s was estimated using our model identification process.

Vehicle type	Year of manufacture	Engine Model	Fuel type	Engine displacement (cm3)	Max power (hp)	Curb weight (kg)	Emission legislation	Wheelbase length (mm)
Renault Clio	2017	K9K 628	Diesel	1461	90	1071	Euro 5	2589
Renault Mégane	2017	K9K 656	Diesel	1461	110	1205	Euro 6	2669

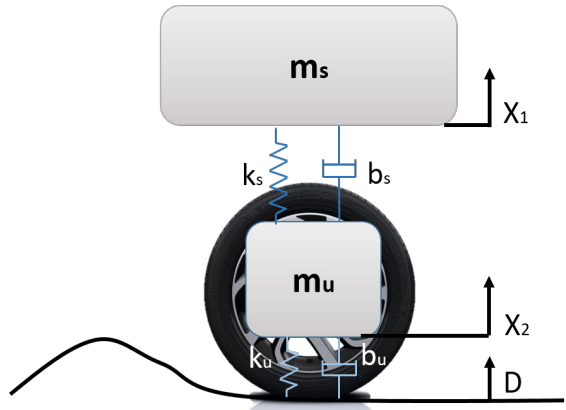


Figure 5.3. The quarter car linear oscillatory model used to model the suspension travel ($X_1 - X_2$) for different road disturbance frequencies (D).

and absolute yaw rate between the sport and comfort mode, for the combined route. For the sport mode, a substantially higher mean absolute rear-wheel angle, mean engine speed, mean gear number, mean throttle position, mean lateral and mean longitudinal acceleration, compared to the comfort mode.

Figures 5.4 and 5.5 show common driving-related measures as a function of travelled distance across all repetitions for the rural road and highway, separately. From top to bottom Figure 5.4 and 5.5 show among the four repetitions: (1) the mean speed, (2) the mean engine speed, (3) the mean brake pressure, (4) the mean steering wheel angle, (5) the mean yaw rate, and (6), the mean rear wheel angle for both comfort mode and sport mode. Over the entire route, no substantial difference in speed and brake pressure can be seen for the two modes. Regarding longitudinal dynamics, the engine speed was higher for sport as compared to comfort. In terms of lateral dynamics, the results show higher rear-wheel angles, but smaller steering wheel angles for the sport mode as compared to the comfort mode. No clear differences can be observed for the yaw rate. The differences in the vehicle’s vertical, lateral, and longitudinal dynamic behaviour will be analysed in more detail in Sections 5.3.2–5.3.5.

5.3.2. Most-Discriminating Measures Between Comfort and Sport Mode

The Cohen’s d effect sizes for the 30 most-discriminating measures (i.e., largest Cohen’s d values) for the rural road and the highway are shown in Figures 5.6 and 5.7 respectively. The largest differences in means occurred for engine speed (RPM), engine-torque related values, and throttle, mostly because the car drove longer at a lower gear in sport mode (see Table 5.2), resulting in a higher available torque (Table 5.2), and lower throttle input percentage (Table 5.2). The largest differences in standard deviations occurred for engine speed (RPM), throttle position, and rear-wheel angle. Finally, the largest differences in high-frequency variation (i.e., the mean absolute difference) were found for the suspension travel

Table 5.2. The mean and standard deviation (SD) results of the four repetitions for the comfort and sport for the combined route, rural road, and highway.

	Normal				Eco-driving			
	Highway		Mountain		Highway		Mountain	
	Mégane	Clio	Mégane	Clio	Mégane	Clio	Mégane	Clio
Number of drivers	34	25	24	21	35	34	23	26
Total laps driven	665	585	449	481	784	665	536	452

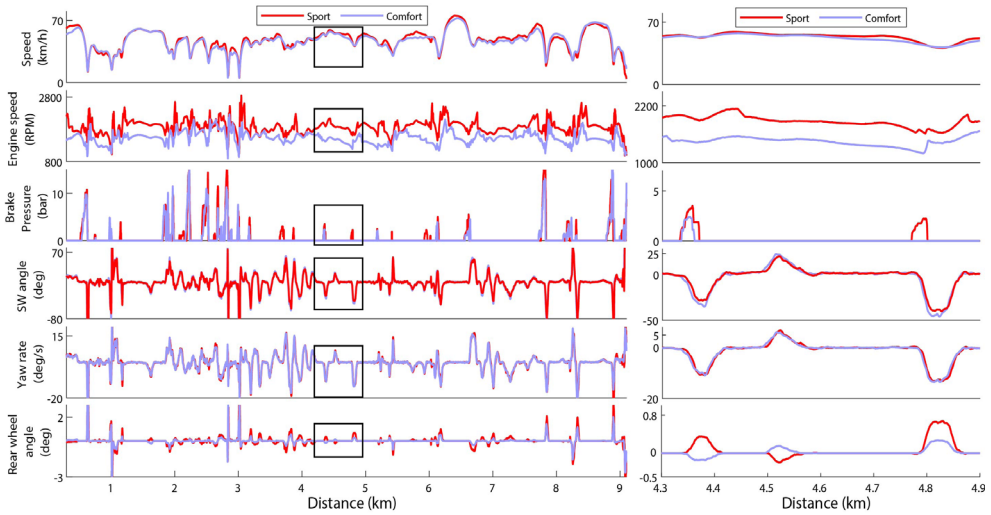


Figure 5.4. For the rural road section, six recorded variables averaged across four repetitions as a function of travelled distance (left) and for a selected travelled distance interval (right). From top to bottom: mean speed, mean engine speed, mean brake depression, mean steering wheel angle, mean yaw rate, and mean rear wheel angle.

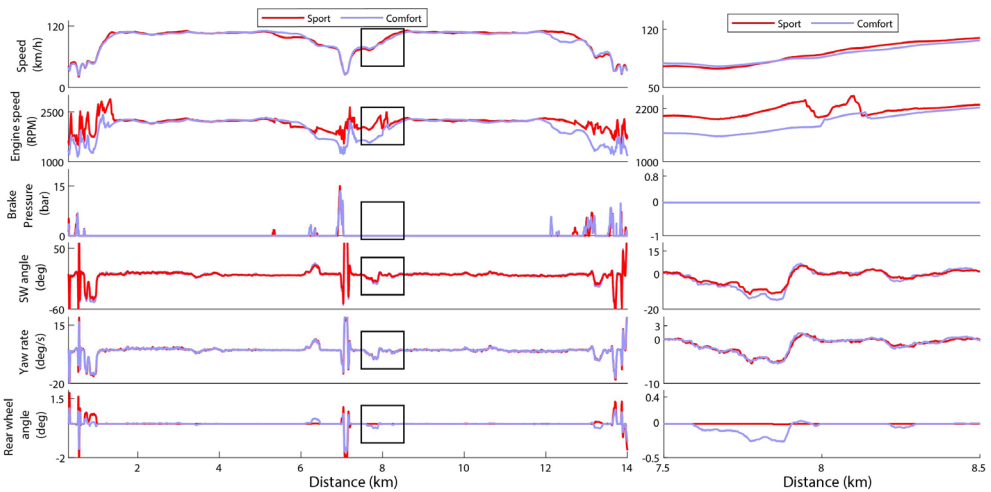


Figure 5.5. For the highway section, six recorded variables averaged across four repetitions as a function of travelled distance (left) and for a selected travelled distance interval (right). From top to bottom: mean speed, mean engine speed, mean brake depression, mean steering wheel angle, mean yaw rate, and mean rear wheel angle.

(described in more detail in Section 5.3.3) and rear-wheel angle (described in more detail in Section 5.3.4).

5.3.3. Vertical Dynamics

Power spectral density of suspension travel to identify the damping coefficient

The suspension travel time response of the four repetitions, for the rural road and highway separately, were combined in one data vector and submitted to MATLAB's p-Welch power

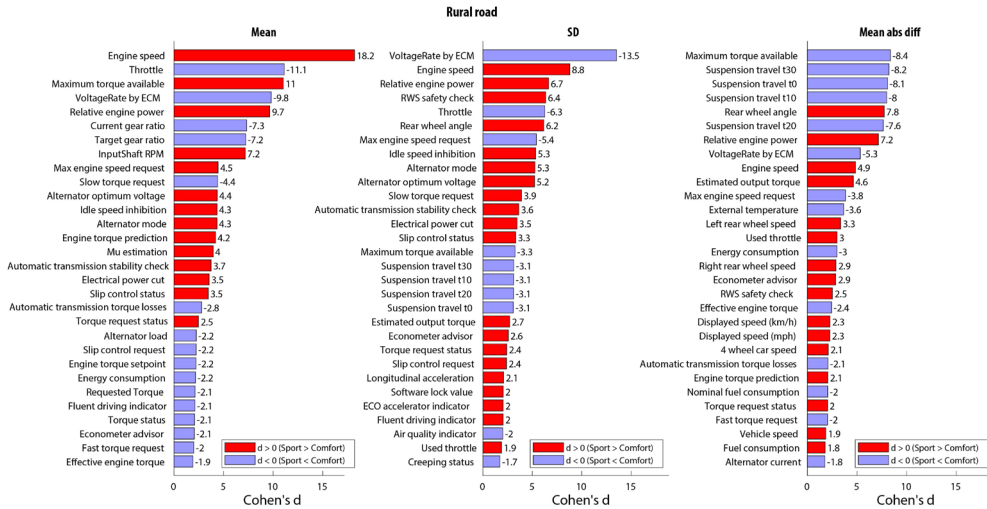


Figure 5.6. For the rural road section: the ranking of the absolute value of Cohen's d , i.e., the 30 most discriminative measures between the sport mode and comfort mode out of 887 measures. Left: mean of the signal, Middle: standard deviation of the signal, Right: mean absolute successive difference of the signal.

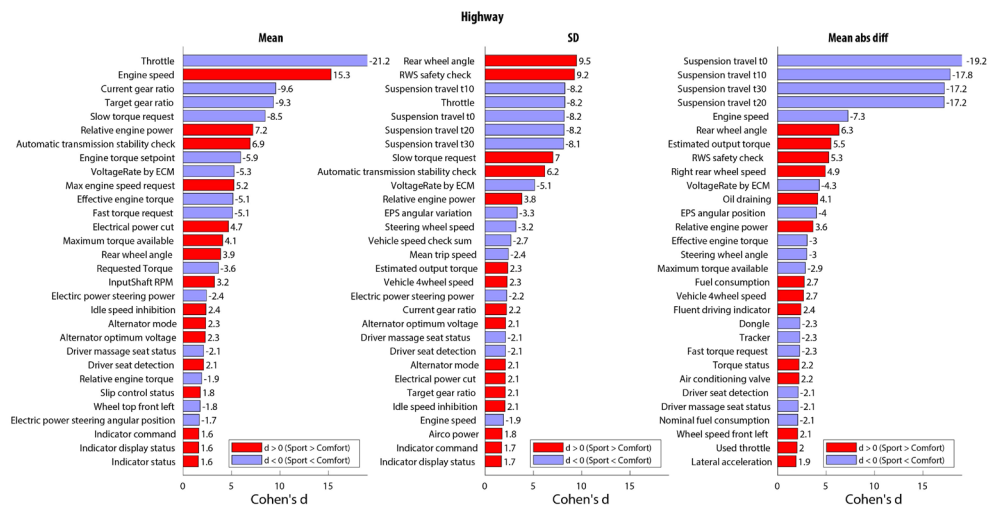


Figure 5.7. For the highway section: the ranking of the absolute value of Cohen's d , i.e., the 30 most discriminative measures between the sport mode and comfort mode out of 887 measures. Left: mean of the signal, Middle: standard deviation of the signal, Right: mean absolute successive difference of the signal.

spectral density estimator (Hayes, 2009; Stoica & Moses, 2005; Welch, 1967). Due to the high impact of the pavement roughness and vehicle speed, on the vehicle's oscillatory behaviour, the results were identified separately for both the highway (low pavement roughness and high speed) and rural road (high pavement roughness and low speed). The power spectral density estimate for the sport and comfort mode and the fitted quarter car model are shown in Figure 5.8. The constraint optimization, which fitted the model-based suspension travel on the observed data, identified a 3.38 x higher damper setting for sport (1585 Ns/m) than

for comfort (469 Ns/m) for the highway section and a 3.32 x higher damper setting for sport (1079 Ns/m) than for comfort (325 Ns/m) for the rural road section. A higher suspension travel power was found for comfort than sport around the natural frequencies of the sprung mass and unsprung mass of 1.48 Hz and 10.30 Hz, respectively. The natural frequencies locations are identical for sport and comfort mode.

5.3.4. Lateral Dynamics

Figure 5.9a, 5.10a, and 5.11a illustrate the impact of vehicle speed and steering wheel angle on the rear-wheel angle, yaw rate, and lateral acceleration. Figure 5.9b, 5.10b, and 5.11b show the slopes of fitted linear regression lines for speed bins of 5 km/h for a combination of the combined route and the four repetitions.

Figure 5.9a shows that between 20 and 30 km/h more countersteering is performed for the sport than for the comfort mode, whereas for speeds between 80 and 90 km/h more parallel steering is performed for comfort than for sport. This effect is visualised for all speeds ranges between 0 and 115 km/h in Figure 5.9b. More countersteering is executed (i.e., a stronger negative slope value of the rear wheel angle vs. steering wheel angle) for sport than compared to comfort mode for speeds between 15 and 80 km/h. Above 55 km/h parallel steering (positive slope) is exhibited for comfort mode, whereas no parallel steering is available for the sport mode.

Figure 5.10 shows that higher yaw rates are obtained for sport mode than for comfort mode. The yaw rate difference is especially visible when the parallel steering strategy is executed (i.e., speeds above 55 km/h).

Figure 5.11 illustrates the effect of vehicle speed on the lateral acceleration response to a steering wheel deviation. For the sport and comfort mode, the same steering wheel angle results in higher lateral accelerations when the speed becomes higher. Above 40 km/h, higher lateral accelerations are observed for the sport mode compared to the comfort mode.

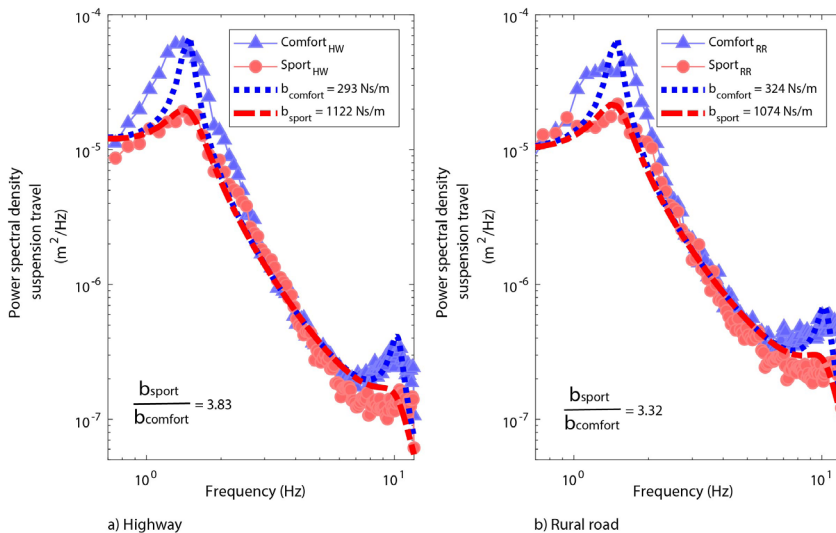


Figure 5.8. Power spectral density of the vibrations of the suspension travel for the highway section (a) and the rural road section.

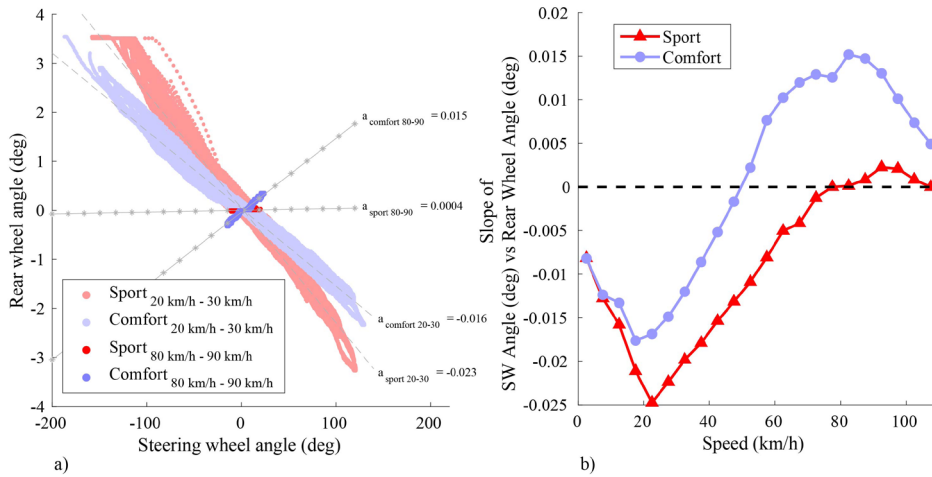


Figure 5.9. Rear-wheel angle as a function of steering wheel angle for the sport (red) and comfort mode (blue). (a) Steering wheel angle and rear wheel angle between 20 and 30 km/h (light) and 80 and 90 km/h (dark). (b) The slope of the linear regression between steering wheel angle and rear wheel angle per 5 km/h speed bin. Results are based on the combined route and the four repetitions combined.

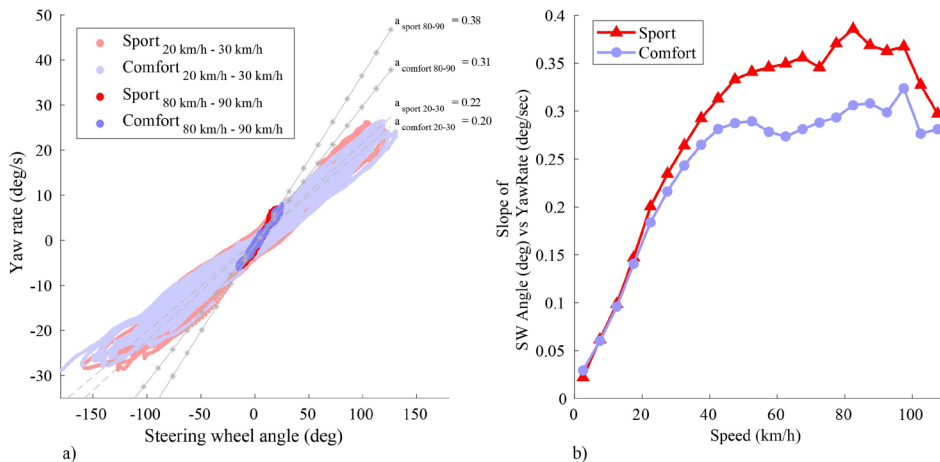


Figure 5.10. Yaw rate as a function of steering wheel angle for the sport (red) and comfort mode (blue). (a) Steering wheel angle and yawrate between 20 and 30 km/h (light) and 80 and 90 km/h (dark). (b) The slope of the linear regression between steering wheel angle and yaw rate per 5 km/h speed bin. Results are based on the combined route and the four repetitions combined.

5.3.5. Longitudinal Dynamics

Figure 5.12 shows the mean longitudinal acceleration (m/s^2) as a function of brake pressure input (bar) and throttle input (%) for the comfort and sport modes for the combined route and the four repetitions combined. The results show an increased longitudinal acceleration for sport mode than for comfort mode for throttle inputs between 20% and 40%. No clear differences can be seen for the decelerations in comfort mode.

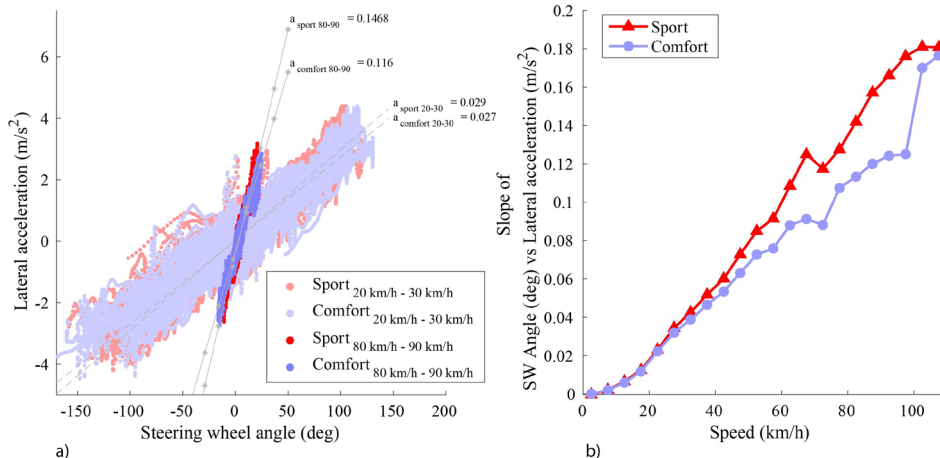


Figure 5.11. Lateral acceleration as a function of steering wheel angle for the sport (red) and comfort mode (blue). (a) Steering wheel angle and lateral acceleration between 20 and 30 km/h (light) and 80 and 90 km/h (dark). (b) The slope of the linear regression between steering wheel angle and lateral acceleration per 5 km/h speed bin. Results are based on the combined route and the four repetitions combined.

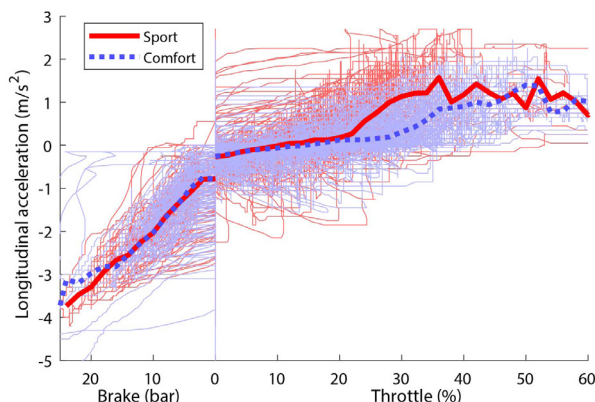


Figure 5.12. The raw (thin lines) and mean (thick lines) longitudinal acceleration as a function of the brake and throttle depression for the sport and comfort repetitions for the combined route.

5.4. Discussion

In this exploratory study, we aimed to quantify the differences in the vehicle’s dynamic behaviour between the Renault Multi-Sense sport mode and comfort mode in naturalistic driving conditions. We gathered driving data on a combined route (26.3 km) containing a rural road and highway section, using a single driver driving the same route four times in comfort mode and four times in sport mode. The data were analysed for differences between sport and comfort mode in three steps: (1) an analysis of 11 selected measures, to analyse differences in general driving behaviour, (2) an investigation of which vehicle state variables best discriminate between the two driving modes, based on calculating the Cohen’s *d* effect size of metrics (mean, standard deviation, and mean absolute difference) for all 887 CAN-bus

signals, and (3) a detailed analysis of the vehicle's lateral, longitudinal and vertical dynamic behaviour for the obtained signals in step 2.

In the first set of analyses, differences between sport and comfort modes were observed in RPM, rear-wheel angles, steering angle (for large steering angles). Important for this study, no substantial difference between sport and comfort mode in mean driving speed (< 0.7 km/h) was found, indicating a consistent driving speed across modes and repetitions, as was intended. Additionally, no substantial differences were found for the mean yaw rate, which is to be expected, since the same yaw rate is needed to drive the same route.

In the second set of analyses, the sorted Cohen's d effect sizes revealed strong differences for longitudinal variables (i.e., drivetrain related signals such as engine speed, engine torque, throttle, gear ratio), lateral dynamic behaviour variables (i.e., such as rear-wheel angles), and vertical dynamic variables (i.e., such as the suspension travel). The results contained several redundancies in CAN signals with the same meaning (e.g., vehicle speed in km/h, and vehicle speed in mph), or signals that are causally related (e.g., current gear ratio, and engine speed), or are unimportant to the present study (e.g., air-conditioning power). The inclusion of unimportant measures could have been prevented by manually selecting CAN signals, but would be at the cost of a lower generality.

In the third set of analyses, differences found in longitudinal, lateral, and vertical dynamic behaviour were further analysed. The longitudinal dynamic behavioural results showed that by shifting the car into sport mode, the car initiates a more aggressive throttle response especially for throttle inputs above 20%, and remaps its gear ratios so that the car will hold onto gears longer (i.e., higher maximum torque available and more relative engine power), with higher RPMs and a lower fuel efficiency compared to comfort mode. For the first time, these results provide evidence that the Multi-Sense sport and comfort modes substantially affect longitudinal dynamic behaviour.

For lateral dynamic behaviour, the sport mode resulted in a higher mean absolute rear-wheel angle, due to a difference in rear-wheel steering present above 20 km/h (Figure 5.9). Countersteering and parallel steering are widely proposed rear-wheel steering control strategies (Furukawa et al., 1989; Herold & Wallbrecher, 2017; Sano et al., 1986; Whitehead, 1988). In our study, a clear speed-dependent rear-wheel steering control strategy was observed, with at lower speeds (15–80 km/h) more countersteering for sport than comfort mode, and at higher speeds (> 50 km/h) parallel steering for comfort mode, and no rear-wheel steering for sport mode. For a given steering input at speeds above 40 km/h, the sport mode (which used no rear-wheel steering at high speeds), caused a higher yaw rate and a higher lateral acceleration compared to the comfort mode (which used parallel rear-wheel steering). These results are in line with literature showing that for a given steering input parallel steering results in a reduced steady-state yaw rate and reduced steady-state lateral acceleration (Nalecz & Bindemann, 1989). Our contribution is that we showed for the first time how the four-wheel steering strategy is utilized by different driving modes.

The quarter car model identified a 3.83 times (highway) and 3.32 times (rural road) higher damper value for the sport than for the comfort mode. Therefore, when driving in sport mode, the higher value of shock absorber damping provides lower oscillatory movements at exciting frequencies approximating the resonance frequencies, whereas the amplitudes of the driver's vertical acceleration are increased (Sekulić & Dedović, 2011). The manufacturer-provided sprung, and unsprung mass and stiffness resulted in an accurate estimate of the natural frequencies (Figure 5.8). A visual inspection of Figure 5.8 shows a broadening of the natural frequencies for the empirical data, a phenomenon that is not captured by the quarter car model. This broadening could be caused by energy losses due to the non-linearity of the damping, non-static parameters (mass, stiffness, and damping changes while driving), or one of the many assumptions in the quarter car model. Indeed many assumptions are made in the quarter car model (i.e., fixed speed, static model parameters, linear damping

approximation, only 1 wheel modelled, vertically aligned dampers, fixed asphalt roughness, equally distributed input frequencies), resulting in inaccuracies. Nevertheless, it needs to be noted that the quarter car model is an effective model to comprehend the order of difference between the average variable damping settings of the sport and comfort mode, and is widely used to model suspension dynamics (Karnopp, 2009; Sekulić & Dedović, 2011; Sharp & Crolla, 1987).

Limitations and Future work

Despite the 887 available CAN-bus signals, some vehicle-related signals (e.g., roll, pitch, sprung-mass acceleration, and wheel load) and driver-related signals (e.g., driver steering torque) were not part of the CAN-bus dataset. This makes it impossible, for example, to show the effect of driving mode on road holding (i.e., instantaneous wheel load) and vehicle comfort (i.e., sprung-mass vertical acceleration). For many of these signals, the effect can be deduced from the results in this paper. In this study, we investigated changes in vehicle dynamics measured by the CAN signals, using the built-in sensors of the vehicle. Future studies could add additional sensors to complement our analyses.

In this study, we used a data-driven approach to quantify the main dynamical differences between sport and comfort mode. It is, of course, true that the working mechanisms of the active components are known by Renault. However, these are merely software codes and hard to interpret. For actual roads, the impact of driving modes on the total vehicle's dynamic behaviour was not yet documented. That is, how much driving modes affect the vehicle's dynamic behaviour was previously unclear in the scientific literature. We aimed to make this effect transparent for the first time, and we showed, for example, for the lateral dynamics, not only the on-road control strategy (i.e., the rear wheel strategy), but also the effect of this control strategy on vehicle's dynamical behaviour (i.e., lateral acceleration and yaw rate).

We quantified the differences in vehicle dynamics between two given driving modes. Future research could use the opposite approach, namely, to develop new driving modes based on desired vehicle dynamics. For example, the quarter car model could be used to determine to what extent the damping coefficients should be adjusted for generating a driving mode with a particular ride height characteristic. Additionally, based on collected vehicle dynamics data, it should be possible to classify driving modes. For example, based on observed front and rear wheel angles as well as observed lateral accelerations and ride height fluctuations, the current vehicle dynamic behaviour could be classified as 'sport-like' or 'comfort-like'. Based on this classification, novel control strategies, such as model-predictive control techniques (e.g., Canale et al., 2006; Giorgetti et al., 2006) could be utilised to create desired vehicle behaviours. This approach would allow for comparisons of vehicle characteristics between different vehicle brands and types.

In this study, we aimed to constrain driving style by giving the driver the task to 'drive with the same speed'. This approach allowed for a valid comparison of the differences between the two modes, but it prevented behavioural adaptations on behalf of the driver. Previous studies have shown that changes in vehicle dynamics and assistance systems instigate driver adaptations such as driving with a higher speed or driving closer to a lead vehicle (Martens & Jenssen, 2012; Mehler et al., 2014; Melman et al., 2017; Saad, 2006). It can be hypothesized that drivers in sport mode will adapt their driving style towards sportier behaviour. During this experiment, one vehicle and one driver were used. Future research should investigate how the results relate to different vehicles, driving modes of different car brands, and a large pool of drivers.

Finally, the impact of Multi-Sense modes on subjective driving experience is a matter of future study. Besides changes in vehicle dynamics, changes in audio-visual cues can be expected to contribute to driving experience and system acceptance. The present results and analysis methods may help guide future studies that evaluate how drivers use and

experience different driving mode designs.

5.5. Conclusions

Before conducting this study, there was a lack of knowledge about how driving modes affect the vehicle's dynamic behaviour in normal driving conditions on real roads. In this study, we aimed to quantify the differences in vehicle dynamics between the sport and comfort mode of Renault's Multi-Sense®, by statistically analysing 887 CAN-bus signals. This study showed that during naturalistic driving:

- The driving modes affect lateral dynamics due to four-wheel steering. Compared to the sport mode, the comfort mode uses less countersteering at low speeds and more parallel steering at high speeds (> 50 km/h). The four-wheel steering strategy results in a higher steady-state lateral acceleration and yaw-rate for the sport mode compared to comfort mode.
- Driving modes affect the longitudinal dynamics due to changes in engine settings. In the sport mode, the car has a more sensitive throttle response for throttle inputs above 20%, holds onto gears longer, and maintains a higher torque and RPMs, at the expense of lower fuel efficiency, as compared to comfort mode.
- Driving modes affect the vertical dynamics due to different damping settings. An about 3.5 times higher damper coefficient was identified for the sport mode compared to the comfort mode.
- Driving modes are more than a 'gimmick' but substantially change how the vehicle responds to the driver's control input. Future studies are needed to investigate the impact of these changes on drivers' behaviour, acceptance, and safety.

References

- Abe, M. (1999). Vehicle dynamics and control for improving handling and active safety: from four-wheel steering to direct yaw moment control. *Proceedings of the Institution of Mechanical Engineers, Part K: Journal of Multi-body Dynamics*, 213, 87-101.
- Abe, M. (2013). Trends in Intelligent Vehicle Dynamics Controls and Their Future. *NTN Technical Review*, 81, 2-10.
- Anubi, O. M. (2013). *Variable stiffness suspension system*. University of Florida.
- Boller, A. (2017). STEERING FEEL AND STEER-BY-WIRE—Steering feel in heavy trucks—a driver-oriented approach to evaluate different configurations of steering support. *7th International Munich Chassis Symposium 2016* (pp. 575-594). Springer Vieweg, Wiesbaden.
- Canale, M., Milanese, M., & Novara, C. (2006). Semi-active suspension control using "fast" model-predictive techniques. *IEEE Transactions on Control Systems Technology*, 14, 1034-1046.
- Chau, C. K., Elbassioni, K., & Tseng, C. M. (2017). Drive mode optimization and path planning for plug-in hybrid electric vehicles. *IEEE Transactions on Intelligent Transportation Systems*, 18, 3421-3432.
- Cho, W., Choi, J., Kim, C., Choi, S., & Yi, K. (2012). Unified chassis control for the improvement of agility, maneuverability, and lateral stability. *IEEE Transactions on Vehicular Technology*, 61, 1008-1020.
- Choi, S. B., Lee, H. K., & Chang, E. G. (2001). Field test results of a semi-active ER suspension system associated with skyhook controller. *Mechatronics*, 11, 345-353.
- Cohen, J. (1988). *Statistical power analysis for the behavioral sciences* (2nd ed.). Hillsdale, NJ: Erlbaum
- Crolla, D. A. (1996). Vehicle dynamics—theory into practice. *Proceedings of the Institution of Mechanical Engineers, Part D: Journal of Automobile Engineering*, 210, 83-94.
- Els, P. S., Theron, N. J., Uys, P. E., & Thoresson, M. J. (2007). The ride comfort vs. handling compromise for off-road vehicles. *Journal of Terramechanics*, 44, 303-317.
- Fahimi, F. (2013). Full drive-by-wire dynamic control for four-wheel-steer all-wheel-drive vehicles. *Vehicle System Dynamics*, 51, 360-376.
- Furukawa, Y., Yuhara, N., Sano, S., Takeda, H., & Matsushita, Y. (1989). A review of four-wheel steering studies from the viewpoint of vehicle dynamics and control. *Vehicle System Dynamics*, 18, 151-186.
- Giorgetti, N., Bernporad, A., Tseng, H. E., & Hrovat, D. (2006). Hybrid model predictive control application towards optimal semi-active suspension. *International Journal of Control*, 79, 521-533.
- Guglielmino, E., Sireteanu, T., Stammers, C. W., Ghita, G., & Giudea, M. (2008). *Semi-active suspension control: improved vehicle ride and*

road friendliness. Springer Science & Business Media.

- Hayes, M. H. (2009). *Statistical digital signal processing and modeling*. John Wiley & Sons.
- Herold, P., & Wallbrecher, M. (2017). All-Wheel Steering. In *Steering Handbook* (pp. 493-512). Springer, Cham.
- Hilgers, C., Brandes, J., Ilias, H., Oldenettel, H., Stiller, A., & Treder, C. (2009). Active air spring suspension for greater range between adjusting for comfort and dynamic driving. *ATZ Worldwide*, *111*, 12-17.
- Huang, P. S., & Pruckner, A. (2017). Steer by Wire. In *Steering Handbook* (pp. 513-526). Springer, Cham.
- Ikenaga, S., Lewis, F. L., Campos, J., & Davis, L. (2000). Active suspension control of ground vehicle based on a full-vehicle model. *Proceedings of the American Control Conference*, *6*, 4019-4024.
- Jeon, B. W., Kim, S. H., Jeong, D., & Chang, J. Y. I. (2016). *Development of Smart Shift and Drive Control System Based on the Personal Driving Style Adaptation* (No. 2016-01-1112). SAE Technical Paper.
- Jeon, S. I., Jo, S. T., Park, Y. I., & Lee, J. M. (2002). Multi-mode driving control of a parallel hybrid electric vehicle using driving pattern recognition. *Journal of Dynamic Systems, Measurement, and Control*, *124*, 141-149.
- Karnopp, D. (2009). How significant are transfer function relations and invariant points for a car suspension model?. *Vehicle System Dynamics*, *47*, 457-464.
- Kim, W., Lee, J., Yoon, S., & Kim, D. (2005). *Development of Mando's new continuously controlled semi-active suspension system* (No. 2005-01-1721). SAE Technical Paper.
- Kissai, M., Mouton, X., Monsuez, B., Martinez, D., & Tapus, A. (2018, June). Optimizing Vehicle Motion Control for Generating Multiple Sensations. *IEEE Intelligent Vehicles Symposium*, 928-935.
- Klier, W., Reimann, G., & Reinelt, W. (2004). *Concept and functionality of the active front steering system* (No. 2004-21-0073). SAE Technical Paper.
- Koch, G., & Kloiber, T. (2014). Driving state adaptive control of an active vehicle suspension system. *IEEE Transactions on Control Systems Technology*, *22*, 44-57.
- Martens, M. H., & Jenssen, G. D. (2012). *Behavioral adaptation and acceptance* (pp. 117-138). Springer London.
- Mehler, B., Reimer, B., Lavallière, M., Dobres, J., & Coughlin, J. F. (2014). Evaluating technologies relevant to the enhancement of driver safety. AAA Foundation for Traffic Safety.
- Melman, T., De Winter, J. C. F., & Abbink, D. A. (2017). Does haptic steering guidance instigate speeding? A driving simulator study into causes and remedies. *Accident Analysis & Prevention*, *98*, 372-387.
- Merker, T., Girres, G., & Thriemer, O. (2002). *Active body control (ABC) the DaimlerChrysler active suspension and damping system* (No. 2002-21-0054). SAE Technical Paper.
- Mohd, T. A. T., Hassan, M. K., Aris, I., Azura, C. S., & Ibrahim, B. S. K. K. (2017). Application of fuzzy logic in multi-mode driving for a battery electric vehicle energy management. *International Journal on Advanced Science, Engineering and Information Technology*, *7*, 284-290.
- Morales, A. L., Nieto, A. J., Chicharro, J. M., & Pintado, P. (2018). A semi-active vehicle suspension based on pneumatic springs and magnetorheological dampers. *Journal of Vibration and Control*, *24*, 808-821.
- Nagai, M., & Koike, K. (1994). Theoretical study of vehicle wandering phenomenon induced by dented road cross profile. *International Journal of Heavy Vehicle Systems*, *1*, 182-194.
- Nalecz, A. G., & Bindemann, A. C. (1988). Analysis of the dynamic response of four wheel steering vehicles at high speed. *International journal of vehicle design*, *9*, 179-202.
- Nalecz, A. G., & Bindemann, A. C. (1989). *Handling properties of four wheel steering vehicles* (No. 890080). SAE Technical Paper.
- Petek, N. K., Romstadt, D. J., Lizell, M. B., & Weyenberg, T. R. (1995). Demonstration of an automotive semi-active suspension using electrorheological fluid. *SAE Transactions*, 987-992.
- Pfeffer, P. E., Harrer, M., & Johnston, D. N. (2008). Interaction of vehicle and steering system regarding on centre handling. *Vehicle System Dynamics*, *46*, 413-428.
- Rajamani, R. (2011). *Vehicle dynamics and control*. Springer Science & Business Media.
- Renault. (2018). *Renault TALISMAN Driver's handbook*. https://www.renaulteurodrive.com.au/resources/handbooks/TALISMAN_ESTATE_2018.pdf
- Reuter, M., & Saal, A. (2017). Superimposed Steering System. In *Steering Handbook* (pp. 469-492). Springer, Cham.
- Russell, H. E., Harbott, L. K., Nisky, I., Pan, S., Okamura, A. M., & Gerdes, J. C. (2016). Motor learning affects car-to-driver handover in automated vehicles. *Science Robotics*, *1*, eaah5682.
- Saad, F. (2006). Some critical issues when studying behavioural adaptations to new driver support systems. *Cognition, Technology & Work*, *8*, 175-181.
- Sano, S., Furukawa, Y., & Shiraiishi, S. (1986). Four wheel steering system with rear wheel steer angle controlled as a function of steering wheel angle. *SAE Transactions*, 880-893.
- Savaresi, S. M., Poussot-Vassal, C., Spelta, C., Sename, O., & Dugard, L. (2010). *Semi-active suspension control design for vehicles*. Elsevier.
- Sekulić, D., & Dedović, V. (2011). The effect of stiffness and damping of the suspension system elements on the optimisation of the vibrational behaviour of a bus. *International Journal for Traffic & Transport Engineering*, *1*, 231-244.

Sharp, R. S., & Crolla, D. A. (1987). Road vehicle suspension system design-a review. *Vehicle System Dynamics*, 16, 167-192.

Sheller, M. (2004). Automotive emotions: Feeling the car. *Theory, Culture & Society*, 21, 221-242.

Shibahata, Y. (2005). Progress and future direction of chassis control technology. *Annual Reviews in Control*, 29, 151-158.

Shinagawa, T., Kudo, M., Matsubara, W., & Kawai, T. (2015). *The new Toyota 1.2-liter ESTEC turbocharged direct injection gasoline engine* (No. 2015-01-1268). SAE Technical Paper.

Shyrokau, B., De Winter, J., Stroosma, O., Dijksterhuis, C., Loof, J., van Paassen, R., & Happee, R. (2018). The effect of steering-system linearity, simulator motion, and truck driving experience on steering of an articulated tractor-semitrailer combination. *Applied Ergonomics*, 71, 17-28.

Stoica, P., & Moses, R. L. (2005). *Spectral analysis of signals*. Upper Saddle River, NJ: Prentice-Hal

Strandroth, J., Rizzi, M., Olai, M., Lie, A., & Tingvall, C. (2012). The effects of studded tires on fatal crashes with passenger cars and the benefits of electronic stability control (ESC) in Swedish winter driving. *Accident Analysis & Prevention*, 45, 50-60.

Sun, S., Tang, X., Li, W., & Du, H. (2017). Advanced vehicle suspension with variable stiffness and damping MR damper. *2017 IEEE International Conference on Mechatronics (ICM)*, 444-448.

Tagesson, K. (2017). *Driver-centred Motion Control of Heavy Trucks* (Doctoral Thesis). Chalmers University of Technology.

Trächtler, A. (2004). Integrated vehicle dynamics control using active brake, steering and suspension systems. *International Journal of Vehicle Design*, 36, 1-12.

Trzesniowski, M. (2017). Steering Kinematics. In: Harrer M., Pfeffer P. (eds) *Steering Handbook*. Springer, Cham

Welch, P. (1967). The use of fast Fourier transform for the estimation of power spectra: a method based on time averaging over short, modified periodograms. *IEEE Transactions on Audio and Electroacoustics*, 15, 70-73.

Wen, S., Chen, M. Z., Zeng, Z., Yu, X., & Huang, T. (2017). Fuzzy control for uncertain vehicle active suspension systems via dynamic sliding-mode approach. *IEEE Transactions on Systems, Man, and Cybernetics: Systems*, 47, 24-32.

Whitehead, J. C. (1988). *Four wheel steering: Maneuverability and high speed stabilization* (No. 880642). SAE Technical Paper.

Wimmer, C., Felten, J., & Odenthal, D. (2014). The electronic chassis of the new BMW i8—Influence and characterization of driving dynamics. *5th International Munich Chassis Symposium 2014* (pp. 57-73). Springer Vieweg, Wiesbaden.

Wong, J. Y. (2001). *Theory of ground vehicles*. John Wiley & Sons, Inc., New York.

Yamashita, M., Fujimori, K., Hayakawa, K., & Kimura, H. (1994). Application of H ∞ control to active suspension systems. *Automatica*, 30, 1717-1729.

Yoshimura, T., Kume, A., Kurimoto, M., & Hino, J. (2001). Construction of an active suspension system of a quarter car model using the concept of sliding mode control. *Journal of Sound and Vibration*, 239, 187-199.

Yu, F., Li, D. F., & Crolla, D. A. (2008). Integrated vehicle dynamics control—State-of-the art review. *IEEE Vehicle Power and Propulsion Conference*.

Appendix 5A - Cohen's d visualised

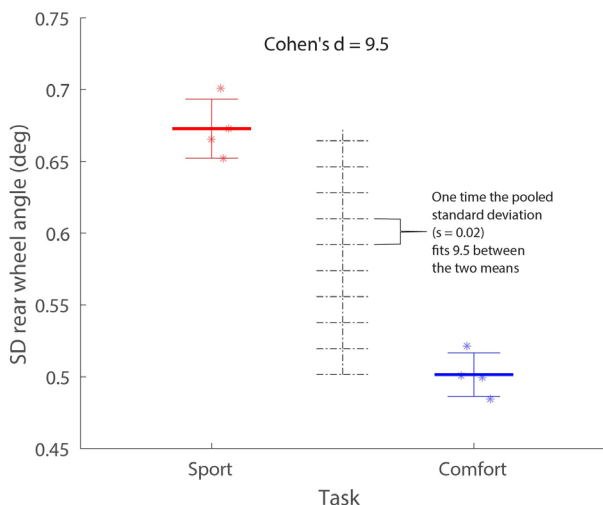


Figure 5A. The scores of the four repetitions (asterisks) and means of four repetitions (horizontal lines) for the sport and comfort mode. The whiskers represent the mean±1 standard deviation. Cohen's d represents the number of times the pooled standard deviations fits between the two means.

**Creating the Illusion of
Sportiness: Evaluating Modified
Throttle Mapping and Artificial
Engine Sound for Electric
Vehicles**



Modern computerized vehicles offer the possibility to change vehicle parameters with the aim of creating a novel driving experience, such as an increased feeling of sportiness. For example, electric vehicles can be designed to provide an artificial sound, and the throttle mapping can be adjusted to give drivers the illusion that they are driving a sports vehicle (i.e., without altering the vehicle's performance envelope). However, a fundamental safety-related question is how drivers perceive and respond to vehicle parameter adjustments. As of today, human-subject research on throttle mapping is unavailable, whereas research on sound enhancement is mostly conducted in listening rooms, which provides no insight into how drivers respond to the auditory cues. This study investigated how perceived sportiness and driving behavior are affected by adjustments in vehicle sound and throttle mapping. Through a within-subject simulator-based experiment, we investigated (1) Modified Throttle Mapping (MTM), (2) Artificial Engine Sound via a virtually elevated rpm (AES), and (3) MTM and AES combined, relative to (4) a Baseline condition, and (5) a Sports car that offered increased engine power. Results showed that, compared to Baseline, AES and MTM-AES increased perceived sportiness and yielded a lower speed variability in curves. Furthermore, MTM and MTM-AES caused higher vehicle accelerations than Baseline during the first second of driving away from a standstill. Mean speed and comfort ratings were unaffected by MTM and AES. The highest sportiness ratings and fastest driving speeds were obtained for the Sports car. In conclusion, the sound enhancement not only increased the perception of sportiness but also improved drivers' speed control performance, suggesting that sound is used by drivers as functional feedback. The fact that MTM did not affect the mean driving speed indicates that drivers adapted their 'gain' to the new throttle mapping and were not susceptible to risk compensation.

Published as:

Melman, T., Visser P. J. D., De Winter, J. C. F. (2021). Creating the Illusion of Sportiness: Evaluating Modified Throttle Mapping and Artificial Engine Sound for Electric Vehicles. *Journal of Advanced Transportation*, 2021, 4396401. <https://doi.org/10.1155/2021/4396401>

6.1. Introduction

Drivers use their vehicles as more than just a means to arrive at their destinations. As explained by Rothengatter (1988), road user behavior is to an extent governed by the “pleasure of driving fast” (p. 605). Indeed, a portion of road users appears to be attracted to sporty driving, as evidenced by the sales of sports cars or vehicle models that offer high engine power and agile handling characteristics (JATO, 2021). As an alternative, several manufacturers produce vehicles that can provide a sporty driving experience via a sport mode the driver can select. The sport mode has gained a substantial presence on the car market today (Audi, 2021; BMW, 2021; Mercedes-Benz, 2021; Porsche, 2021; Renault, 2021; Volvo, 2021).

According to manufacturers, the sport mode “permits an increased responsiveness from the engine and the gearbox” (Renault, 2021) and offers a “sporty driving style” (Mercedes-Benz, 2021). The Sport mode may encompass technology that increases the throttle sensitivity, road holding, and agility of the vehicle (De Novellis et al., 2015; Melman et al., 2021; Shibahata, 2005). This includes the active drivetrain (e.g., changes in engine mapping and gear shifting; Shinagawa et al., 2015; Wehbi et al., 2017), active suspension, and four-wheel steering (Furukawa et al., 1989; Herold & Wallbrecher, 2017). Additionally, sport modes can be accompanied by mechanical sound enhancement, which concerns the adjustment of physical elements of the drivetrain and the active control of valves that redirect the engine airflow and influence the exhaust sound (Ambrosino et al., 2011; Jackson, 2013)

In recent decades, several techniques have been developed to increase perceived sportiness without altering the vehicle dynamics and without requiring costly components or mechanical adjustments to the vehicle. Two of such techniques are Artificial Engine Sound and Modified Throttle Mapping.

6.1.1. Artificial Engine Sound (AES)

Artificial Engine Sound (AES) refers to a system that produces synthetic sounds through the cabin speakers. AES has been proposed for electric vehicles (e.g., Bräunl, 2012; Fang & Zhang, 2017; Govindswamy & Eisele, 2011; Min et al., 2018; Nyeste & Wogalter, 2008;). However, current research on sounds for electric vehicles mostly focuses on pedestrian safety (e.g., Faas & Baumann, 2021; Karaaslan et al., 2018). Considerably less research is available that focuses on the experience of drivers inside the electric vehicle.

Psychoacoustics research has shown that perceived sportiness can be increased by adjusting characteristics of the sounds, such as loudness, roughness, sharpness, and tonality (Krüger et al., 2004; Kwon et al., 2018). However, a limitation of psychoacoustics studies is that they are typically conducted in listening rooms. As Jennings et al. (2010) argued, “perception of the sounds of on-road cars is affected by stimuli for other senses (e.g., visual and vibrational), and the fact that an assessor is also concentrating on driving” (p. 1263). To illustrate, research in a listening room by Park et al. (2019) found that loudness was predictive of perceived sportiness ($r = 0.84$) but negatively predictive of perceived comfort ($r = -0.83$), consistent with the generally accepted “trade-off hypothesis of pleasantness and power” (Bisping, 1995, p. 1203). A driving simulator study by Hellier et al. (2011), however, found that drivers regarded no engine noise at all as uncomfortable. Hence, it appears that sound perception may be different in listening rooms as compared to active driving.

Very little research on perceived sportiness in real vehicles is available. An exception is Zeitler and Zeller (2006), who let acoustical experts rate the interior sounds of different vehicles on a test track. Their results showed that perceived sportiness was strongly correlated with the sound volume increase during engine load (i.e., while accelerating). However, engine performance (e.g., actual sportiness) and acoustic feedback were confounded; that is, the vehicles that delivered more power were also those that produced a sporty sound. In a follow-up experiment, they tried to disentangle these two effects using AES and found that vehicle sounds and engine torque independently contributed to perceived sportiness.

Apart from investigating the effects of AES on perceived sportiness, it is essential to examine the extent to which AES influences driving behavior. Previous research suggests that the presence and volume of vehicle sound affect driving speeds. More specifically, it has been found that a reduction in engine volume or the lack of engine sound causes drivers to drive faster (Hellier et al., 2011; Horswill & McKenna, 1999), underestimate their speed (Evans, 1970; Horswill & McKenna, 1999; Horswill & Plooy, 2008), and show poorer speed control (Denjean et al., 2012; McLane & Wierwille, 1975; Merat & Jamson, 2011). These findings are consistent with the notion that engine sound acts as an information source that facilitates perception and control, or as argued by Hellier et al. (2011): “engine noise can be characterised as ‘feedback’ rather than ‘noise’” (p. 598).

In summary, although the above-mentioned studies indicate that the presence and volume of sound affect driving behavior, there appears to be a lack of research about how drivers perceive and respond to sound enhancement techniques that could be applied in electric vehicles, such as AES. Furthermore, research on vehicle sound has to date been predominantly conducted in listening rooms, a setting which cannot provide information about drivers’ speed adaptation.

6.1.2. Modified Throttle Mapping (MTM)

A second approach that may increase perceived sportiness without requiring mechanical components is Modified Throttle Mapping (MTM). MTM is defined as the software-based adjustment of the relationship between the driver’s throttle input and the engine throttle input. Through MTM, for a given driver throttle input, the engine produces more torque while the maximum torque (i.e., the torque for 100% driver throttle input) remains the same. Note that MTM is not the same as modified ‘engine mapping’, i.e., the adjustment of engine characteristics through changes in fuel injection, air charge, ignition timing, and valve timing, and other factors that influence engine performance (Barker, 1982; Holliday et al., 1998).

Research describes different ways of changing the throttle mapping and the corresponding effect on vehicle performance (e.g., Hosoda, 2010; Melman et al., 2021; Schoeggel et al., 2001), but only a few studies have investigated the effects of MTM on driving behavior. The few studies that did investigate human-in-the-loop effects of MTM used intelligent controllers, such as a throttle pedal for regulating the desired engine torque and desired wheel torque (Boris et al., 2010) or a throttle pedal that caused the vehicle to decelerate more strongly upon releasing the pedal in critical car-following situations (Mulder et al., 2010).

6.1.3. Aim and Hypotheses

Little is known about how drivers perceive and respond to vehicle parameter adjustments that intend to provide a sporty driving experience for electric vehicles, such as MTM and AES technology. It is important to investigate this topic with a view to road safety. If such systems reduce vehicle controllability and increase driving speed, this could be seen as undesirable.

The current study aimed to investigate how drivers perceive and respond to AES and MTM—two systems that intend to provide a sporty driving experience for electric vehicles, and which do not change the vehicle’s performance envelope in any way. The individual and combined contributions of MTM and AES were compared to a Baseline condition and a vehicle that offered increased engine power (‘sports car’). The sports car was included to investigate how the results for AES and MTM compare to a car that offers actually increased sportiness. The combined condition (AES-MTM) was included to examine whether or not the effects of MTM and AES are additive.

The expected effects of MTM and AES can be explained using theory from the field of manual control (e.g., McRuer & Jex, 1967). Figure 6.1 shows a model of human driving behavior in a speed control task, based on Weir and Chao (2007) and McRuer et al. (1977). Here, the human outputs a foot movement (‘throttle driver’), which via the throttle mapping

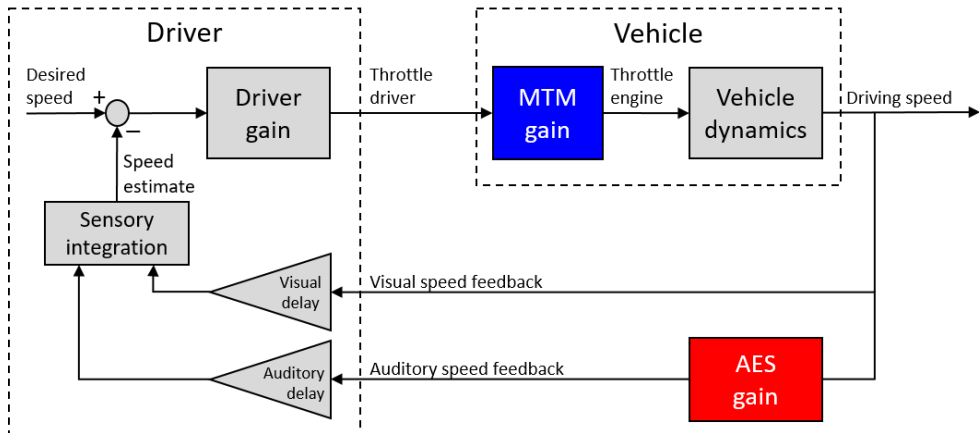


Figure 6.1. Schematic representation of a driver driving with Modified Throttle Modification (MTM) and Artificial Engine Sound (AES). This figure assumes a fixed-base driving simulator, which means that the driver is not provided with physical motion feedback.

(a variable gain, i.e., a multiplication factor) results in an input to the vehicle model ('throttle engine', describing how much torque is requested from the car). The car model outputs the current driving speed, which is fed back to the driver via visual and auditory pathways. The driver perceives these two feedback sources with a time delay. Additionally, the driver is represented by a gain, which describes how strongly the driver responds to the difference between the perceived speed and the desired speed. The desired speed represents the speed at which the driver wishes to drive at a particular moment; it is dependent on many factors, including the environment (road curvature, road width), the driver's personality, and the driver's risk assessment based on the visual and auditory information received.

If drivers apply a particular 'throttle driver', this will result in a higher 'throttle engine' when driving with MTM (i.e., high MTM gain) compared to without (i.e., low MTM gain). Accordingly, MTM was hypothesized to increase perceived sportiness and vehicle acceleration compared to without. However, it can be expected that the effect of MTM on driving speed is only short-lasting, as visual feedback is dominant in driving (e.g., Sivak, 1996). This hypothesis can be further motivated from the viewpoint of open-loop versus closed-loop control (Jagacinski & Flach, 2003). That is, MTM is expected to increase vehicle acceleration (and thus speed) for short-term 'open-loop' leg movements involved in pressing the pedal but will not affect 'closed-loop' driving speed. Note that Figure 6.1 depicts a closed-loop situation, where the driver uses auditory and visual feedback to control the car's speed. In the context of Figure 6.1, an increase of MTM gain is expected to result in a reciprocal decrease in the driver gain, so that the driving speed is unaffected.

In the current study, AES was implemented through an increase of the 'virtual rpm', where we assumed an electric vehicle that generated the sound of a combustion engine. When driving with AES enabled (i.e., high AES gain), fluctuations in driving speed result in larger fluctuations in engine sound pitch as compared to Baseline (i.e., a condition with a low AES gain). In other words, the enabling of AES can be expected to strengthen the auditory feedback loop, making drivers better aware of speed fluctuations, and thus contributing to a more accurate estimate of driving speed relative to the desired driving speed (see Hellier et al., 2011 for a similar argumentation regarding vehicle sound in general). It is noted that visual feedback is processed relatively slowly compared to the other sensory modalities (Hosman & Stassen, 1998). This may be especially true when it comes to the perception of longitudinal ego-speed, which requires the driver to extract (changes in) optical flow and edge rate

information (Larish & Flach, 1990) (but note that the speedometer provides a more direct indication of speed). Hence, auditory feedback may have an important role in speed control.

In addition to the mechanisms depicted in Figure 6.1, AES may influence the desired driving speed itself. As pointed out above, increasing the engine sound volume leads to a lower driving speed. In the same vein, the increased virtual rpm can be expected to result in lower driving speeds. This hypothesis is consistent with the phenomenon of risk compensation, which predicts that drivers increase their speed when provided with protective or assistive technology, or conversely reduce their speed when provided with technology that reduces protection or increases the perceived risk (Fuller, 2005; Melman et al., 2018; Wilde, 1998).

The hypothesized effects for MTM and AES are summarized in Table 6.1.

Table 6.1.

Hypothesized effects of the two systems on perceived sportiness and driving behavior relative to a Baseline condition

	Perceived sportiness	Driving speed
Artificial Engine Sound (AES)	Higher	Lower mean and lower variability
Modified Throttle Mapping (MTM)	Higher	Higher (short term)

6.2. Method

6.2.1. Participants

Thirty-two participants (6 females) between 19 and 35 years old ($M = 23.4$, $SD = 3.1$) with normal or corrected-to-normal vision volunteered for the driving simulator experiment. Regarding the question ‘On average, how often did you drive a vehicle in the last 12 months’, 3 participants reported every day, 5 reported 4 to 6 days a week, 12 reported 1–3 days a week, 11 reported once a month to once a week, and 1 never. Regarding mileage in the past 12 months, the most frequently selected response category was 1001–5000 km (14 respondents), followed by 5001–10000 km (7 respondents, 10001–15000 km (4 respondents), and 15001–20000 km (4 respondents). The research was approved by the Human Research Ethics Committee (HREC) of the Delft University of Technology, and all participants provided written informed consent.

6.2.2. Apparatus

The experiment was conducted in a fixed-base simulator (see Figure 6.2). The steering wheel and pedals used in the simulation were from a Sensodrive Senso-Wheel running at 1 kHz. The simulation was developed using JOAN (Beckers et al., 2021), an open-source software framework developed at the TU Delft that builds on the CARLA open-source simulator (Version 0.9.8; Dosovitskiy et al., 2017). The vehicle dynamics were simulated by the Unreal Engine using PhysX (Unreal, 2021). The scenery was shown via a 65-inch 4k TV with a 60 Hz refresh rate. The virtual camera settings provided a 90-deg horizontal field of view. The simulation and data logging were updated at 100 Hz. The sound of the vehicle’s engine was presented via Beyerdynamic DT-770 Pro 32 Ohm headphones. The car’s interior and bonnet were included in the visualization to enhance the perception of road position and vehicle speed and were the same for all conditions (Figure 6.2). The vehicle speed was shown digitally in light blue font above the bonnet.



Figure 6.2. The experimental environment with a participant driving in the fixed-based simulator. The digital speedometer can be seen in light blue font, just above the bonnet.

6.2.3. Independent Variables and Design

Participants drove five trials, one of the following five conditions per trial:

1. Baseline
2. Artificial engine sound (AES)
3. Modified throttle mapping (MTM)
4. Modified throttle mapping and artificial engine sound combined (MTM-AES)
5. Sports car

The five conditions were presented according to a balanced within-subject design (Williams design).

For the Baseline, AES, MTM, and MTM-AES conditions, the simulated vehicle was a 2-m wide sedan of 2316 kg. It had a maximum engine torque of 350 Nm, a maximum speed of 149 km/h, and a drag coefficient of 0.24. The vehicle was modeled after an electric vehicle, with a single-gear gearbox and a nearly constant engine torque for different speeds. The Sports car offered increased engine power. It was modeled after the same heavy sedan and visually identical to the other four conditions, but with an increased maximum torque of 550 Nm and a maximum speed of 203 km/h.

For the Baseline, AES, MTM, and MTM-AES conditions, the same interior sound of a vehicle driving at constant speed was used (Volkswagen Golf V 1.6 FSI running at 2140 rpm; Soundsnap, 2021a). This sound was looped, and the playback speed of the interior sound was slowed down or sped up depending on the vehicle speed and momentary engine torque ('throttle engine'), hence providing a virtual rpm. In this way, the vehicle sound was informative about vehicle speed and engine torque. The Sports car had a higher rpm and was based on another sound sample (Audi A4 B8 20TDI running at 3050 rpm; Soundsnap, 2021b), which produced a more racy sound at high virtual rpm. Figure 6.3 shows how the virtual rpm depended on vehicle speed and engine torque, for Baseline, AES, and the Sports car. The mapping shown in Figure 6.3 was based on extensive pilot testing, where it was made sure that the differences between conditions were noticeable and within a realistic rpm range.

The MTM condition changed the relationship between the driver's throttle depression ('throttle driver') and the normalized requested engine torque ('throttle engine'), without affecting the maximum engine power (Figure 6.4). For a 'throttle driver' value of 27%, the difference in 'throttle engine' between Baseline (15%) and MTM (49%) was maximal (34%).

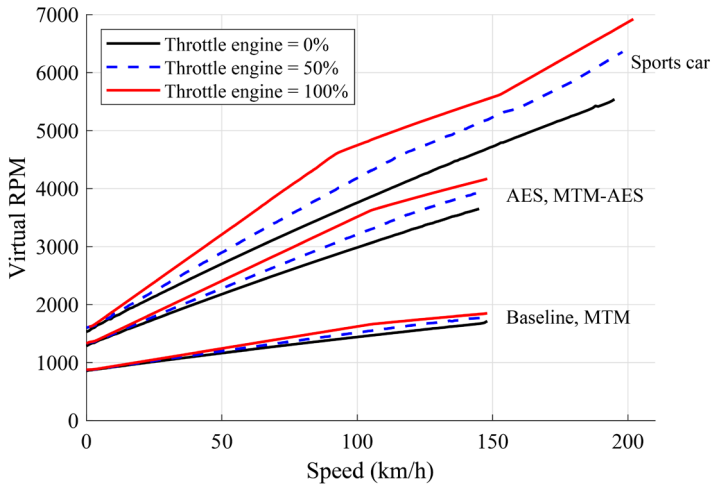


Figure 6.3. Virtual engine speed (rpm) as a function of vehicle speed and throttle engine. The data used to create this graph were obtained from the data recordings of the experiment.

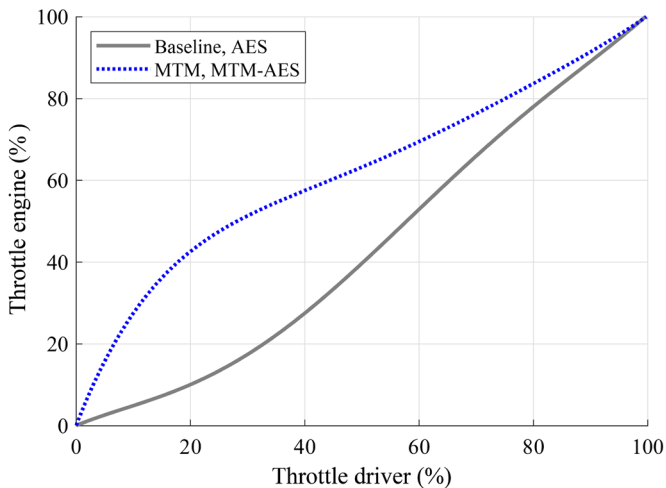


Figure 6.4. The modified throttle mapping. ‘Throttle driver’ was measured by a displacement sensor attached to the throttle pedal, whereas ‘throttle engine’ was determined by software. Note that ‘throttle driver’ could become slightly smaller than 0 when releasing the pedal or exceed 100% when fully depressing the pedal. In the analysis, all values above 100 and below 0 were rounded to 100 and 0, respectively. The ‘throttle driver’ range from 0 to 100% corresponded to a physical pedal depression of about 75 mm at an exerted force of about 35 N.

The throttle mappings were based on pilot tests, where it was made sure that the difference between Baseline and MTM was noticeable while retaining controllability. For the Sports car, a linear throttle mapping was used, where 0% ‘throttle driver’ corresponded to 0% ‘throttle engine’, and 100% ‘throttle driver’ corresponded to 100% ‘throttle engine’.

6.2.4. Road Environment

The participants drove five trials on the same single-lane road (3.6 m wide and 8.1 km long). Trees, buildings, landscapes, and guardrails were placed next to the road. The route was divided into an acceleration section, a straight section, and a curvy section (Figure 6.5).

The first 2.6 km consisted of an acceleration task where drivers were requested to accelerate four times to 60 km/h. The locations of the accelerations were indicated via stop signs and speed limit signs next to the road. The acceleration section was implemented to ensure that all drivers strongly accelerated at least four times per condition. The middle 2 km was a straight section where participants could choose a speed at which they felt comfortable. The straight allowed an investigation of the participants' speed choice.

The last 3.5 km consisted of a curvy section that contained curves with an inner radius of 100, 150, and 250 m. Each curve type appeared three times, and the curves were connected by straight sections with a length of 50 or 100 m. No traffic and no on-road obstacles were simulated. The curvy section allowed investigating naturalistic deceleration and acceleration for curves.

6.2.5. Procedure

Participants first read and signed a consent form and completed a questionnaire regarding their demographics and driving experience. Participants were asked to drive as they usually would and adhere to the traffic rules identified by road signs next to the road. Next, the participants were requested to sit in the simulator.

Before each condition, a three-minute training run was performed on a road consisting of straights and curves. During each training trial, the participants were asked to familiarize themselves with the upcoming condition by accelerating, decelerating, and curve driving.

In each experimental trial, participants drove in one of the five conditions (Baseline, MTM, AES, MTM-AES, or Sports car). After each trial, participants stepped out of the simulator and completed a questionnaire about their driving experience. The experiment took approximately 75 minutes per participant.

6.2.6. Dependent Measures

A distinction is made between self-reported experience and driving behavior.

Self-reported experience.

After each trial, participants completed a questionnaire containing 14 questions on a five-point Likert scale. The first four questions investigated drivers' perceived effort for Q1 braking, Q2 steering, Q3 accelerating, and Q4 maintaining speed, on a scale of *low* to *high*. This was followed by three questions regarding the perception of the vehicle: Q5 engine responsiveness (*low* to *high*), Q6 brake responsiveness (*high* to *low*), and Q7 engine sound of the vehicle (*high* to *low*).

Finally, seven questions were asked using a semantic differential scale. Participants had to answer whether they had experienced the vehicle as Q8 *sporty/not sporty*, Q9 *dangerous/safe*, Q10 *comfortable/not comfortable*, Q11 *undesirable/desirable*, Q12 *raising alertness/sleep-inducing*, Q13 *irritating/likable*, and Q14 *sluggish/quick*. In the analysis, answers to Q6, Q7, Q8, and Q10 were mirrored such that the results were expressed on a scale from low to high.

Of note, Q8 was the main question of interest in this research (i.e., perceived sportiness), whereas Q10, Q11, and Q13 assessed acceptance (Q11 and Q13 were from the satisfaction dimension of an acceptance survey of Van der Laan et al., 1997). Q1, Q2, and Q6 were negative control questions that were expected not to be affected by any of the experimental conditions, whereas Q3, Q5, Q7, and Q14 were positive control questions, expected to be

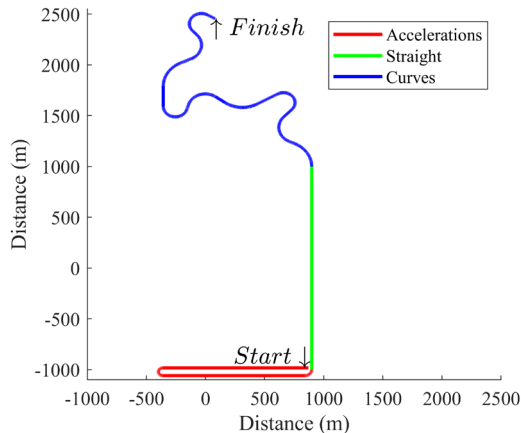


Figure 6.5. Top view of the 8.1 km driven route consisting of three sections: an acceleration section, a straight section, and a curvy section.

affected by at least one of the experimental conditions. Finally, Q4, Q9, and Q12 assessed additional experiences of interest, namely whether participants found it difficult to control the speed of the vehicle (Q4), whether they found the vehicle safe (Q9), and how the experimental conditions affected their overall arousal level (Q12).

Principal component analysis on the questionnaire results.

To identify underlying dependencies and to increase the interpretability of the 14 questionnaire items, a principal component analysis (PCA) was performed. A matrix with responses for 160 trials (32 participants x 5 trials per participant) and 14 items was normalized to a mean of 0 and a standard deviation of 1 and submitted to PCA. The first two components were retained, and component scores per participant and experimental condition were computed after oblique rotation (Promax).

Driving Behavior.

The driving behavior measures were calculated separately for the straight and curvy sections (Figure 6.5). For the straight section, the first 800 m and last 400 m were discarded to investigate steady-state driving. For the curvy section, the entire 3.5 km was used. The following measures were calculated:

- *Mean speed (km/h).* A measure for road safety: an increase in speed reduces a driver's time to respond in an emergency scenario and increases the probability of being involved in a crash (Aarts & Van Schagen, 2006; Pei et al., 2012).
- *Standard deviation (SD) of the speed (km/h).* A higher SD speed indicates that drivers were not able or willing to maintain a constant speed.
- *Mean absolute longitudinal acceleration (m/s^2).* This is a measure indicative of the 'fluency' and sportiness of driving. A high mean absolute longitudinal acceleration can be seen as sporty driving behavior (Ericsson, 2001; Martinez et al., 2018).
- *Mean throttle driver (%).* A measure of how deeply drivers pressed the accelerator on average.
- *Mean throttle engine (%).* This measure indicates how much engine torque was delivered on average. Together, 'throttle driver' and 'throttle engine' allowed examining how drivers adapted to the MTM condition.
- *Throttle driver released time (%).* In the literature, this measure is also referred to as

coasting. Coasting has been interpreted as indicative of uncertainty or a delay in decision-making (Houtenbos et al., 2017; Yeo et al., 2010). It can also be seen as a consequence of having accelerated too much, resulting in an overshoot of speed and a subsequent throttle release.

Additionally, an analysis was performed for the acceleration section, where the first second of the four acceleration phases (i.e., accelerating from standstill) was averaged per experimental condition. The start of each trial was determined based on the moment the throttle position exceeded 0%.

6.2.7. Statistical Analyses

For each measure, a matrix of 32 x 5 numbers was obtained (32 participants and 5 conditions). For each condition in this matrix, the mean, standard deviation (*SD*), and 95% within-subject confidence interval (*CI*) were computed. The 95% within-subject confidence intervals were calculated according to Morey (2008), where the matrix was normalized by subtracting for each participant the mean of all conditions from the five condition observations before using the standard method for determining the 95% *CI*. The *CI* was adjusted with a correction factor based on the number of experimental conditions (Morey, 2008). According to Cumming and Finch (2005), non-overlapping *CI*s correspond to a *p*-value smaller than 0.006.

6.3. Results

6.3.1. Self-Reported Experience

Figure 6.6 shows the means and within-subject 95% confidence intervals for the 14 questionnaire items. Compared to Baseline, AES and MTM-AES resulted in increased perceived sportiness (Q8), perceived engine responsiveness (Q5), and perceived quickness (Q14). Furthermore, AES and MTM-AES were clearly perceived overall (Q7), whereas desirability (Q11) and likability (Q13) did not show significant differences from Baseline.

MTM-AES resulted in an increased self-reported effort to maintain speed compared to AES, and a similar trend was evident for MTM versus Baseline (Q4). The effects of MTM on the other questionnaire items, including sportiness (Q8), were not significant. For the three negative control questions (brake effort [Q1], steering effort [Q2], and brake response [Q6]), no significant differences were observed between the five conditions.

The Sports car yielded lower acceleration effort (Q3), higher perceived engine responsiveness (Q5), and higher perceived sportiness (Q8) than the other four conditions. Additionally, the Sports car was regarded as less sleep-inducing (Q12) and quicker (Q14). Finally, the Sports car was liked (Q13) and regarded as desirable (Q11).

The principal component analysis loadings are shown in Table 6.2. The first principal component is primarily composed of questions related to sportiness and acceleration of the vehicle. The second principal component is mainly composed of questions that correspond to comfort, safety, likability, and desirability. In total, the first two principal components captured 53.2% of the variance (PC1–Sportiness; 36.8%, PC2–Positive Affect: 16.4%).

The mean PC1–Sportiness scores (95% *CI*) for Baseline, MTM, AES, MTM-AES, and Sports car were -0.813, [-1.083, -0.543], -0.542 [-0.824, -0.261], 0.000 [-0.256, 0.256], 0.201 [-0.078, 0.480], and 1.153 [0.874, 1.432]. The mean PC2–Positive affect scores (95% *CI*) for Baseline, MTM, AES, MTM-AES, and Sports car were 0.078 [-0.291, 0.447], -0.156 [-0.542, 0.230], 0.196 [-0.167, 0.559], -0.187 [-0.513, 0.139], and 0.069 [-0.198, 0.336]. Thus, the PC1–Sportiness scores were substantially elevated for the Sports car, as well as the AES and MTM-AES conditions, whereas no clear differences between the five conditions were found in PC2–Positive Affect.

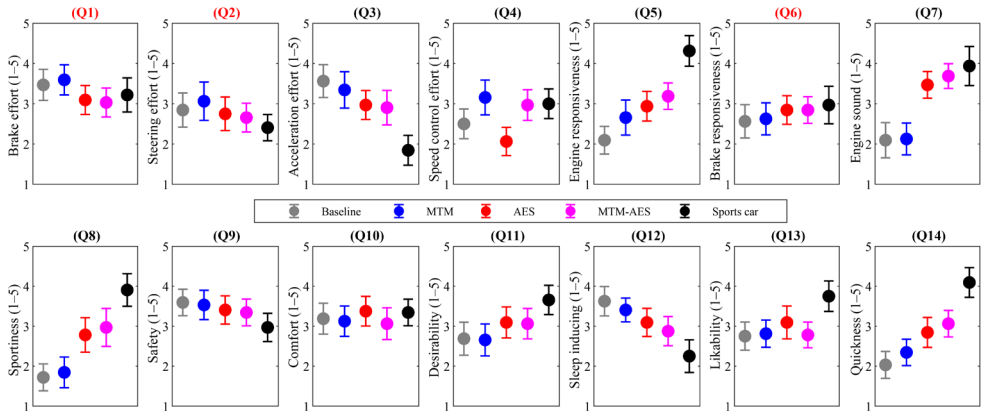


Figure 6.6. The questionnaire results for the 14 questions for the five conditions. The figure depicts the means (circles) and within-subject 95% confidence intervals (whiskers). The questionnaire numbers for the negative control questions (Q1, Q2, Q6) are indicated in red.

Table 6.2. Promax-rotated PCA loadings for the first two principal components (PC)

	PC1 Sportiness	PC2 Positive Affect
Q1. Brake effort	0.00	-0.26
Q2. Steering effort	-0.16	-0.52
Q3. Acceleration effort	-0.78	-0.15
Q4. Speed control effort	0.09	-0.62
Q5. Engine responsiveness	0.83	0.02
Q6. Brake responsiveness	-0.08	0.01
Q7. Engine sound	0.5	-0.24
Q8. Sportiness	0.83	0.08
Q9. Safety	-0.35	0.72
Q10. Comfort	0.02	0.77
Q11. Desirability	0.41	0.64
Q12. Sleep inducing	-0.78	0.19
Q13. Likability	0.44	0.64
Q14. Quickness	0.87	0.13

6.3.2. Driving Behavior

Figure 6.7 shows the road curvature, driving speed, throttle driver, and throttle engine, averaged over all participants as a function of traveled distance. It can be seen that participants adhered to the traffic signs and accelerated four times to 60 km/h (in accordance with the instructions), and adopted an average speed during the straight section of 115–120 km/h. In the subsequent curvy section, drivers can be seen to slow down more for sharper curves. Over the entire track, drivers adopted lower throttle inputs when driving with MTM and MTM-AES compared to Baseline and AES.

Effects of MTM (MTM vs. Baseline & MTM-AES vs. AES)

Table 6.3 shows the means, standard deviations, and non-overlapping confidence intervals for the driving behavior measures. Figure 6.7 and Table 6.3 show that for both sections, participants applied a significantly lower ‘throttle driver’ for MTM compared to Baseline and AES, whereas no significant differences were found for ‘throttle engine’. In other words, participants adapted to the MTM condition by pressing the throttle less deeply. Furthermore,

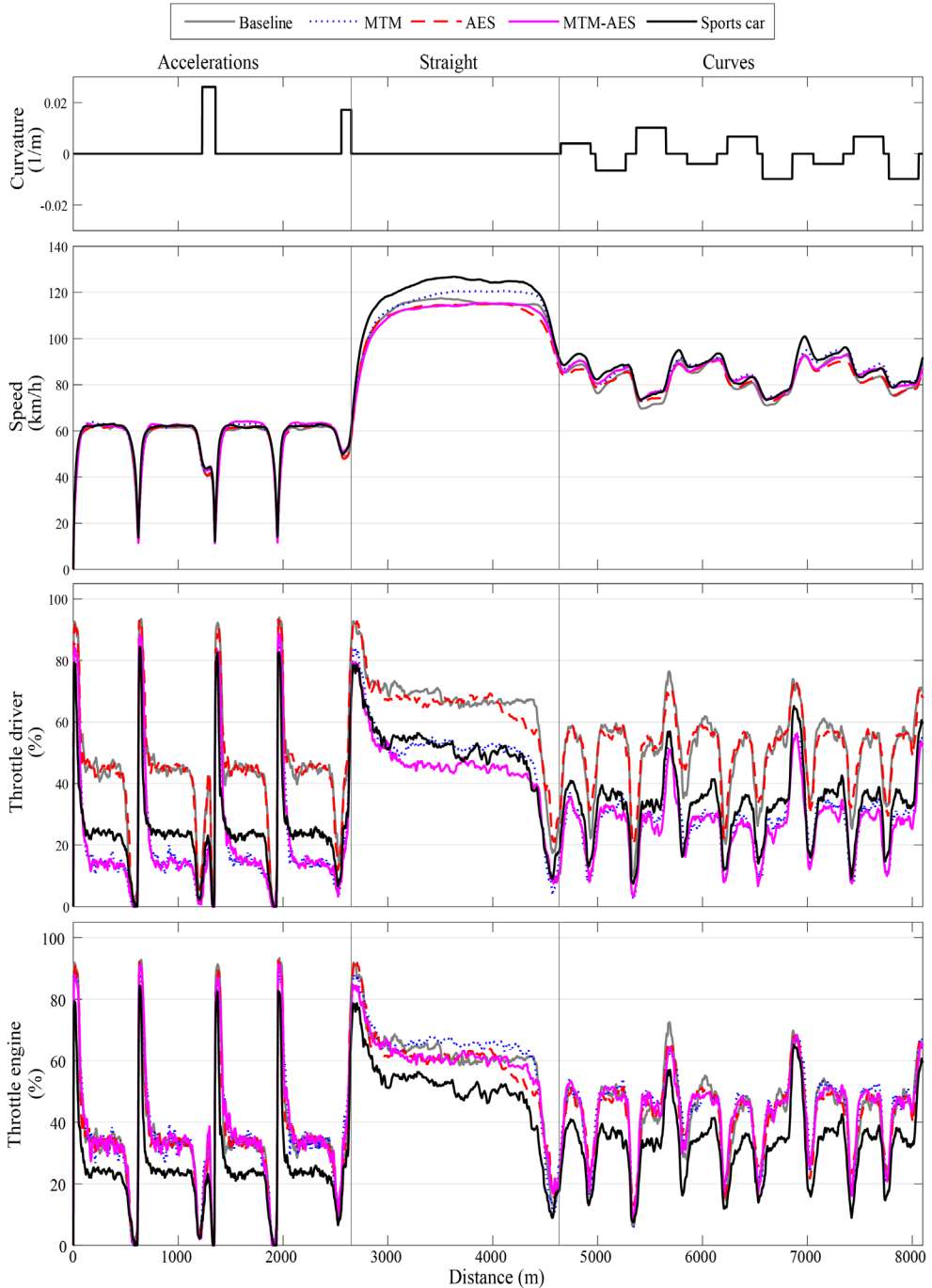


Figure 6.7. The mean driving behavior per condition averaged over all 32 participants; from top to bottom: road curvature, speed, acceleration, throttle driver, and throttle engine. The vertical lines demarcate the acceleration, straight, and curvy sections. Note that the vehicle speed does not drop to exactly 0 km/h during the acceleration section; this is because participants stopped their vehicle at slightly different distances on the road.

Table 6.3. Mean (*M*) and standard deviation (*SD*) for each dependent measure, and the within-subject 95% confidence interval comparison. Non-overlapping confidence intervals are denoted by 'x'

	Conditions					Confidence interval (x = non-overlapping)										
	Baseline	MTM	AES	MTM-AES	Sports car											
	(1) <i>M</i> (<i>SD</i>)	(2) <i>M</i> (<i>SD</i>)	(3) <i>M</i> (<i>SD</i>)	(4) <i>M</i> (<i>SD</i>)	(5) <i>M</i> (<i>SD</i>)	1-2	1-3	1-4	1-5	2-3	2-4	2-5	3-4	3-5	4-5	
Acceleration section																
Mean acceleration during the first second (m/s ²)	1.10 (0.45)	1.37 (0.35)	1.06 (0.37)	1.36 (0.33)	1.70 (0.71)	x		x	x	x			x	x	x	x
Straight section																
Mean speed (km/h)	115.71 (22.02)	120.28 (22.27)	114.64 (23.27)	114.73 (23.08)	124.98 (29.86)										x	x
<i>SD</i> speed (km/h)	2.37 (3.48)	1.41 (1.16)	2.39 (2.46)	1.84 (1.37)	5.40 (5.94)										x	x
Mean abs acceleration (m/s ²)	0.14 (0.17)	0.09 (0.07)	0.16 (0.18)	0.11 (0.09)	0.29 (0.25)				x						x	x
Mean throttle driver (%)	66.59 (17.05)	52.07 (29.84)	66.22 (15.49)	45.17 (27.18)	50.10 (22.16)	x		x	x	x					x	x
Mean throttle engine (%)	60.63 (20.48)	65.49 (21.14)	60.28 (18.86)	60.51 (19.14)	50.10 (22.15)					x					x	x
Throttle driver released time (%)	0 (0)	0.22 (0.83)	0.02 (0.11)	0.44 (2.04)	1.67 (5.50)											
Curvy section																
Mean speed (km/h)	81.44 (15.54)	84.42 (15.20)	81.72 (16.89)	83.54 (15.35)	84.93 (15.95)											
<i>SD</i> speed (km/h)	8.91 (2.75)	8.06 (2.28)	7.71 (2.76)	7.34 (2.19)	8.65 (3.03)			x	x							x
Mean abs acceleration (m/s ²)	0.54 (0.26)	0.50 (0.21)	0.45 (0.21)	0.44 (0.19)	0.57 (0.30)			x	x						x	x
Mean throttle driver (%)	50.88 (5.73)	28.22 (9.28)	51.56 (6.33)	26.85 (9.27)	32.77 (6.28)	x		x	x	x					x	x
Mean throttle engine (%)	43.01 (7.56)	44.62 (7.13)	43.29 (8.26)	44.01 (7.30)	32.76 (6.27)					x					x	x
Throttle driver released time (%)	4.84 (5.39)	8.68 (5.86)	3.09 (4.02)	6.95 (5.63)	7.53 (7.91)	x		x	x	x					x	x

for MTM and MTM-AES, the throttle-released time was about twice as high as Baseline and AES. The results for the first second of the acceleration phase (i.e., accelerating from standstill) showed a higher mean acceleration for MTM and MTM-AES compared to Baseline and AES.

Figure 6.8 depicts the distribution for 'throttle driver' and 'throttle engine' for all participants combined for the curvy section. It can again be seen that, compared to Baseline and AES, MTM and MTM-AES resulted in substantially lower 'throttle driver' values (Figure 6.8, top). For 'throttle engine', the mean was equivalent between conditions (see Table 6.3), but the distribution of 'throttle engine' (Figure 6.8, bottom) showed clear differences between conditions. More specifically, for MTM and MTM-AES, low 'throttle engine' levels (5–40%) were underrepresented, and high 'throttle engine' levels (40–75%) were overrepresented compared to Baseline and AES. For the Sports car, a lower 'throttle engine' was found compared to the other conditions. This can be explained by the fact that the Sports car had more engine power, and thus a lower 'throttle engine' was needed to drive at a particular speed (see also Table 6.3).

Figure 6.9 shows the participants' mean acceleration during the first 3 s after driving away. It shows that drivers adopted significantly higher accelerations when driving with MTM and MTM-AES than Baseline and AES. The increased acceleration for MTM compared to Baseline, which was described above, is clearly visible. After about 1.5 s, the accelerations were equivalent for Baseline, MTM, AES, and MTM-AES conditions.

Effects of AES (AES vs. Baseline & AES vs. MTM)

Table 6.3 shows that no significant effects of AES on mean driving speed were found. However, AES resulted in a decreased *SD* speed and decreased mean absolute acceleration while driving through curves. In other words, AES induced more fluent driving behavior compared to Baseline.

Effects of Sports car

Compared to the other four conditions, the Sports car yielded a high mean speed (on the straight section, not in the curvy section), a high *SD* speed, and a high mean absolute acceleration. The highest mean acceleration during the 1-s acceleration phase was found for the Sports car. In other words, the Sports car resulted in sporty driving behavior.

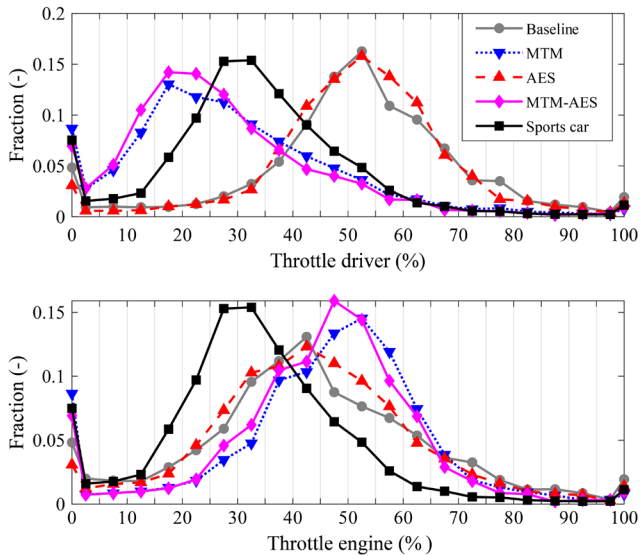


Figure 6.8. ‘Throttle driver’ and ‘throttle engine’ distribution of all participants for the curvy section. The fraction is plotted in the middle of each bin. The bin width is 5%, where the first bin includes the scalar 0, the second bin includes values greater than 0 and less than or equal to 5, and so on. The last bin contains the scalar value 100. The sum of all fractions equals 1 for each condition.

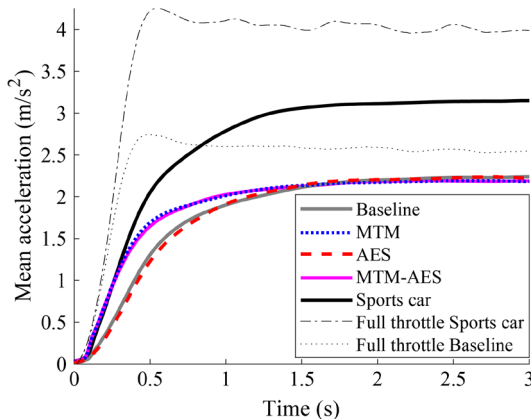


Figure 6.9. Mean vehicle acceleration for 0–60 km/h acceleration phases, averaged over repetitions and participants during the first 3 s. The ‘full throttle’ lines are added as a reference.

6.4. Discussion

This study investigated the effects on perceived sportiness and driving behavior of Modified Throttle Mapping (MTM) and Artificial Engine Sound (AES) relative to a vehicle without these systems (Baseline) and a vehicle that offered increased engine power together with a sporty engine sound (Sports car). Below we discuss the results using the framework presented in Figure 6.1.

6.4.1. Artificial Engine Sound (AES)

On a scale of 1 to 5, the mean perceived sportiness ratings for Baseline, MTM, AES, MTM-AES, and Sports car were 1.72, 1.84, 2.78, 2.97, and 3.91, confirming the hypothesis that AES has a positive effect on perceived sportiness. AES was also clearly noticed and yielded high ratings of vehicle quickness and responsiveness. However, AES did not increase perceived sportiness to the extent of driving the Sports car. The principal component analysis complemented these findings, where a strong effect of AES and MTM-AES compared to Baseline was found on the PC1–Sportiness dimension, whereas PC2–Positive Affect scores were relatively unaffected by the experimental conditions. In other words, AES increased perceived sportiness without compromising comfort.

Regarding driving behavior, the AES and MTM-AES conditions yielded improved speed control (i.e., lower *SD* speed) while driving through curves compared to Baseline. In other words, AES induced fluent rather than sporty driving behavior. These results can be interpreted using Figure 6.1. That is, a plausible explanation would be that due to the more rapid change in virtual rpm for AES compared to Baseline, changes in engine torque were more readily noticed via the auditory feedback loop, which in turn improved speed control. These effects may be especially manifest in our fixed-base simulator, which did not provide vestibular feedback. Several previous studies agree on the importance of sound in vehicle speed control, but these studies typically investigated the impact of sound in driving tasks where the speedometer was not visible, possibly increasing the impact of auditory feedback (Denjean et al., 2012). Merat and Jamson (2011) found an increase in speed variability compared to a baseline condition, especially for a ‘no sound & no speedometer’ condition’. We found improvements in speed control even though the speedometer was permanently visible to the driver. With the presence of a speedometer, visual feedback delays can be expected to be smaller compared to when no speedometer is available, as the speedometer provides a direct reading. Note that the speed variability benefits were statistically significant only for the curvy section, possibly because the visual demands from the roadway were higher during curve driving, as a result of which participants were unable to glance at the speedometer. In summary, the results indicate that AES increased perceived sportiness and improved speed control performance.

AES and MTM-AES did not significantly affect participants’ mean driving speed relative to Baseline. This finding is inconsistent with the risk compensation mechanism outlined in the Introduction, based on which we hypothesized that the elevated virtual rpm would entice drivers to drive more slowly. Previous research has found that drivers slow down when provided with a more demanding environment (e.g., narrower lanes; Melman et al., 2020; driving in fog; Brooks et al., 2011) or when driver assistance systems are disabled (e.g., Janssen & Nilsson, 1993; Melman et al., 2017). According to Elvik et al. (2009), the degree of risk compensation can be predicted by the noticeability of the intervention and the ‘size of the engineering effect’ of the intervention, where the latter is defined as the safety benefits caused by the intervention if the driver would *not* change his behavior. Although AES was clearly noticeable in our study according to the questionnaire outcomes, there was no engineering effect since AES did not affect the vehicle dynamics. In other words, AES did not offer a safety benefit, nor did it instigate drivers to drive faster.

Although no speed increase was found for MTM and AES, the Sports car did induce

higher driving speeds and higher mean absolute acceleration than the other conditions. Put differently, the Sports car resulted in sporty driving behavior. This finding is not entirely self-evident. Previous cross-sectional research indicates that sporty vehicles are driven in a more risky manner than non-sporty vehicles, but the causal direction of this association remained unproven (Horswill & Coster, 2002). The present study showed that the Sports car yielded a 10 km/h higher mean speed on the straight than MTM-AES, confirming that the availability of more engine power caused drivers to drive faster.

Earlier psychoacoustics research showed a decrease in comfort and acceptance for more sporty (rough, loud) sounds (Krüger et al., 2004; Kwon et al., 2018; Wang et al., 2014), whereas we found no significant effects of comfort and acceptance for AES compared to Baseline. In fact, the Sports car yielded the *highest* self-reported desirability and likeability among the five conditions. The difference between our findings and previous research may have arisen because our participants were driving on a challenging trajectory that included curves. The sound, therefore, had a functional role (e.g., to aid in speed perception, see Figure 6.1), which may have contributed to improved comfort and acceptance (as also pointed out by Hellier et al., 2011). Furthermore, our sample consisted of predominantly young males, who may be accepting of sporty sounds.

6.4.2. Modified Throttle Mapping (MTM)

MTM caused substantially higher vehicle accelerations than Baseline, but this was not reflected in ratings of sportiness, quickness, acceleration effort, or engine responsiveness. These findings are inconsistent with our hypothesis that stated that MTM would increase perceived sportiness. The absence of effects of MTM in the self-report questionnaire suggests that participants may have hardly been aware of the altered throttle mapping. As pointed out above, in fixed-base simulators, accelerations can be sensed via the auditory and visual senses only (Boer et al., 2000; De Groot et al., 2011; Greenberg et al., 2003). It is recommended that future studies on the perception of MTM are conducted in a real vehicle, allowing for vestibular feedback. In reference to Figure 6.1, this would require an additional feedback loop in the form of motion feedback (McRuer & Weir, 1969, and for state-of-the-art manual control models incorporating vestibular motion feedback, see Mulder et al., 2017).

Consistent with our hypothesis, participants adapted to the MTM by pressing the throttle less deeply in such a way that their mean driving speed was unaffected. In the context of Figure 6.1, drivers quickly adapted their ‘driver gain’ to the increase in ‘MTM gain’. Previous research concurs that human operators can adapt to different control gains (De Winter & De Groot, 2012; Jenkins & Connor, 1949). An early review by McRuer and Jex (1967) showed that the range of optimum gains is wide, with only small deviations in self-reported handling qualities for 300–400% changes in the gain of the controlled vehicle. These findings are consistent with our study, which showed that drivers appeared to have hardly noticed the MTM.

Although MTM yielded the same mean ‘throttle engine’ as the Baseline condition, it yielded a different ‘throttle engine’ distribution. These findings can be explained directly by the throttle mapping, as depicted in Figure 6.4. For example, for the MTM condition, ‘throttle engine’ values between 0 and 40% were obtained for only a small range of ‘throttle driver’ (0–18%).

Of note, MTM yielded a relatively high self-reported effort for speed control and throttle-release times that were about twice as high as the Baseline condition. It seems that the sensitive MTM pedal led to high pedal movements, as characterized by overshoot (i.e., high ‘throttle engine’) and subsequent releasing of the pedal. A likely explanation is that high control gains amplify the influence of motor noise, so that higher gain requires more corrective effort (Chapanis & Kinkade, 1972; De Winter & De Groot, 2012; Jenkins & Connor, 1949). In other words, when driving with MTM, drivers fully adapted their ‘throttle engine’ to

achieve the same mean speed as Baseline, but at the cost of corrective pedal adjustments and effort. On the flipside, the advantage of a higher gain is that the required amplitude of limb movement is smaller.

6.4.3. MTM and AES Combined

A visual inspection of the results in Figure 6.6 and Table 6.3 reveals no clear MTM x AES interaction effects. For example, the results for perceived sportiness (Q8) suggest that the effects of MTM and AES are additive, with ‘the whole’ (i.e., effects of MTM-AES vs. Baseline) being approximately equal to the ‘sum of its parts’ (i.e., MTM vs. Baseline and AES vs. Baseline). The lack of interaction is supported by two-way repeated-measures ANOVAs using the results for Baseline, MTM, AES, and MTM-AES conditions as input. All 27 ANOVAs revealed a non-significant MTM x AES interaction effect ($p > 0.05$ for each of the dependent variables, i.e., 14 self-reports and 13 performance measures). This lack of interaction may be surprising because the MTM-AES system is interactive in nature, as AES allows for a more direct perception of engine torque (see Figure 6.3). For example, MTM yielded higher throttle-released times than Baseline, something that should theoretically be better audible to participants when AES is enabled compared to when AES is disabled. Future research should employ larger sample sizes to be able to detect MTM x AES interactions that may exist.

6.4.4. Practical Implications and Recommendations

The current MTM implementation is easily translated to a real vehicle as it is based on a commercially available product that performs the same digital manipulation (DTE Systems, 2021). Similarly, electric vehicles could be equipped with an AES system similar to the one in this study. It should not be forgotten that a driving simulator itself provides only an illusion of driving (Hancock, 2009). In real electric vehicles, there is also ambient sound (e.g., tires, wind) and vibrations, which may require active sound cancellation to provide a veridical synthetic sound. Furthermore, as recommended above, research in real vehicles is still needed.

It is noted that the current implementations of AES and MTM, although justified based on pilot testing, represent only one point in the large design space that exists. The current study involved pitch adjustments in engine sound, tested in acceleration, straight driving, and curve driving tasks. Other options would be to apply continuous auditory feedback to support braking, lane-keeping, car-following, or automation mode awareness (e.g., Bazilinsky et al., 2019; Bringoux et al., 2017).

Apart from investigating other sounds and throttle mappings, it would be interesting to investigate how other technologies affect perceived sportiness and driving behavior. Sport modes commonly use red ambient light (Helander et al., 2013; Nieke et al., 2016; Renault, 2021) and a sporty instrumented cluster (e.g., see Jindo & Hirasago, 1997; Jung et al., 2010; Petiot et al., 2015). Other techniques to increase perceived sportiness are to increase steering torques and center point emphasis of the steering system (Fankem & Müller, 2014), shortening the gear shift stroke (Hosoda, 2010), changing the seat so that it has high side supports (Kamp, 2012), and recreating the road feedback between front-wheel slip and steering force that has been lost due to power steering (Uselmann et al., 2015).

6.5. Conclusions

This study was concerned with examining how drivers perceive and respond to electric-vehicle parameter adjustments that intend to provide a sporty driving experience. Modified Throttle Mapping (MTM) and Artificial Engine Sound (AES) were tested—systems that affect the ‘gain’ of the accelerator pedal and the auditory feedback provided to drivers, respectively, and which do not enhance the car’s performance envelope. The results showed the following effects relative to the Baseline condition:

- AES increased perceived sportiness, whereas MTM did not.
- AES and MTM did not affect perceived comfort.
- AES yielded improved speed control in curves.
- MTM increased vehicle acceleration from a standstill.
- AES and MTM yielded average driving speeds that were comparable to Baseline.
- No AES x MTM interaction effects were found.

These novel findings may have utility for vehicle manufacturers. Throttle mapping (i.e., MTM gain as depicted in Figure 6.1) is a component of every vehicle, but so far, no research seems to have examined its effects on driving behavior and perception. Research into the effects of sound on driving behavior has so far mainly focused on the presence/absence or volume of sound and not on sound enhancement as could be applied in electric vehicles. Furthermore, research on vehicle sound has to date been predominantly conducted in listening rooms, a setting which, as argued in the Introduction, is not realistic. In listening rooms, sporty sounds tend to be perceived as uncomfortable, whereas in our study, sporty sounds were not seen as uncomfortable but rather contributed to improved speed control performance.

In addition to its applied value, this study offers fundamental insights into human perception and behavior. The current findings were interpreted using principles from manual control theory, as shown in Figure 6.1, where we highlighted the role of driver adaptation (drivers fully adapted their own gain to the increased MTM gain) and feedback loops (drivers used the artificial sound as a feedback channel that aided in speed control). Furthermore, no risk compensation occurred, i.e., in the context of Figure 6.1, the ‘desired speed’ remained unaffected.

In more general terms, our study indicates that findings from complex tasks, such as driving, can be interpreted with the help of qualitative representations from control theory, a notion emphasized by several psychologists and human factors scientists before (Flach, 1990; Jagacinski, 1977; Sheridan, 2004) but which is still undervalued (Mansell & Marken, 2015).

Supplementary Material

The data, analysis scripts, and videos of the experiment can be downloaded via the following link <https://doi.org/10.4121/16644697>

References

- Aarts, L., & Van Schagen, I. (2006). Driving speed and the risk of road crashes: A review. *Accident Analysis & Prevention*, 38, 215–224.
- Ambrosino, M., Lubrano, L., Sciacca, F., Giorgi, P., & Ferla, L. (2011). *DualMode sporty exhaust development* (Technical Paper No. 2011-01-0926). SAE International.
- Audi. (2021). Driving dynamic. Audi drive select. <https://ownersmanuals2.com/audi/q7-2020-owners-manual-75410/page-110>
- Barker, T. D. (1982). Engine mapping techniques. *International Journal of Vehicle Design*, 3, 142–152.
- Bazilinskyy, P., Larsson, P., Johansson, E., & De Winter, J. C. F. (2019). Continuous auditory feedback on the status of adaptive cruise control, lane deviation, and time headway: An acceptable support for truck drivers? *Acoustical Science and Technology*, 40, 382–390.
- Beckers, N., Siebinga, O., Giltay, J., & Van der Kraan, A. (2021). JOAN, a human-automated vehicle experiment framework (Version 1.0) [Computer software]. <https://github.com/tud-hri/joan>
- Bisping, R. (1995). Emotional effect of car interior sounds: Pleasantness and power and their relation to acoustic key features. *SAE Transactions*, 104, 2207–2213.
- BMW. (2021). Drive modes in detail. <https://ownersmanuals2.com/bmw-auto/x5-2021-owners-manual-80671/page-161>
- Boer, E. R., Girshik, A. R., Yamamura, T., & Kuge, N. (2000). Experiencing the same road twice: A driver centered comparison between simulation and reality. *Proceedings of the Driving Simulation Conference Europe*. Paris, France.
- Boris, R., Vermillion, C., & Butts, K. (2010). A comparative analysis of electronic pedal algorithms using a driver-in-the-loop simulator and system identification of driver behavior. *Proceedings of the 2010 American Control Conference* (pp. 682–687). Baltimore, MD.
- Bräunl, T. (2012). Synthetic engine noise generation for improving electric vehicle safety. *International Journal of Vehicle Safety*, 6, 1–8.
- Bringoux, L., Monnoyer, J., Besson, P., Bourdin, C., Denjean, S., Dousset, E., Goulon, C., Kronland-Martinet, R., Mallet, P., Marqueste, T., Martha, C., Roussarie, V., Sciabica, J.-F., & Stratulat, A. (2017). Influence of speed-related auditory feedback on braking in a 3D-driving simulator. *Transportation Research Part F: Traffic Psychology and Behaviour*, 44, 76–89.
- Brooks, J. O., Crisler, M. C., Klein, N., Goodenough, R., Beeco, R. W., Guiri, C., Tyler, P. J., Hilpert, A., Miller, Y., Grygier, J., Burroughs, B., Martin, A., Ray, R., Palmer, C., & Beck, C. (2011). Speed choice and driving performance in simulated foggy conditions. *Accident Analysis & Prevention*, 43, 698–705.
- Chapanis, A., & Kinkade, R. G. (1972). Design of controls. In H. P. van Cott & R. G. Kinkade (Eds.), *Human engineering guide to equipment design* (pp. 345–379). Washington, DC: American Institute for Research.
- Cumming, G., & Finch, S. (2005). Inference by eye: Confidence intervals and how to read pictures of data. *American Psychologist*, 60, 170–180.
- De Groot, S., De Winter, J. C. F., Mulder, M., & Wieringa, P. A. (2011). Nonvestibular motion cueing in a fixed-base driving simulator: Effects on driver braking and cornering performance. *Presence: Teleoperators and Virtual Environments*, 20, 117–142.
- Denjean, S., Roussarie, V., Kronland-Martinet, R., Ystad, S., & Velay, J. L. (2012). How does interior car noise alter driver's perception of motion? Multisensory integration in speed perception. *Proceedings of the Acoustics 2012 Nantes Conference*, ed. S. F. d'Acoustique. Nantes, France.
- De Novellis, L., Somiotti, A., & Gruber, P. (2015). Driving modes for designing the cornering response of fully electric vehicles with multiple motors. *Mechanical Systems and Signal Processing*, 64–65, 1–15.
- De Winter, J. C. F., & De Groot, S. (2012). The effects of control-display gain on performance of race car drivers in an isometric braking task. *Journal of Sports Sciences*, 30, 1747–1756.
- Dosovitskiy, A., Ros, G., Codevilla, F., Lopez, A., & Koltun, V. (2017). CARLA: An open urban driving simulator. *Proceedings of the 1st Annual Conference on Robot Learning*, 1–16. Retrieved from <http://proceedings.mlr.press/v78/dosovitskiy17a/dosovitskiy17a.pdf>
- DTE Systems. (2021). The PedalBox: The throttle response. <https://www.pedalbox.com/en/product/response>
- Elvik, R., Høy, A., Vaa, T., & Sørensen, M. (2009). Basic concepts of road safety research. *The Handbook of road safety measures* (pp. 81–98). Emerald Group Publishing Limited.
- Ericsson, E. (2001). Independent driving pattern factors and their influence on fuel-use and exhaust emission factors. *Transportation Research Part D: Transport and Environment*, 6, 325–345.
- Evans, L. (1970). Speed estimation from a moving automobile. *Ergonomics*, 13, 219–230. Faas, S. M., & Baumann, M. (2021). Pedestrian assessment: Is displaying automated driving mode in self-driving vehicles as relevant as emitting an engine sound in electric vehicles? *Applied Ergonomics*, 94, 103425.
- Fang, Y., & Zhang, T. (2017). Sound quality investigation and improvement of an electric powertrain for electric vehicles. *IEEE Transactions on Industrial Electronics*, 65, 1149–1157.
- Fankem, S., & Müller, S. (2014). A new model to compute the desired steering torque for steer-by-wire vehicles and driving simulators. *Vehicle System Dynamics*, 52, 251–271.
- Flach, J. M. (1990). Control with an eye for perception: Precursors to an active psychophysics. *Ecological Psychology*, 2, 83–111.
- Fuller, R. (2005). Towards a general theory of driver behaviour. *Accident Analysis & Prevention*, 37, 461–472.
- Furukawa, Y., Yuhara, N., Sano, S., Takeda, H., & Matsushita, Y. (1989). A review of four-wheel steering studies from the viewpoint of vehicle dynamics and control. *Vehicle System Dynamics*, 18, 151–186.
- Govindswamy, K., & Eisele, G. (2011). Sound character of electric vehicles (No. 2011-01-1728). *SAE Technical Paper*.

- Greenberg, J., Artz, B., & Cathey, L. (2003). The effect of lateral motion cues during simulated driving. *Proceedings of DSC North America*. Dearborn, MI.
- Hancock, P. A. (2009). The future of simulation. In D. Vincenzi, J. Wise, M. Mouloua, & P. A. Hancock (Eds.), *Human factors in simulation and training* (pp. 169–186). Boca Raton, FL: CRC Press, Taylor & Francis.
- Helander, M. G., Khalid, H. M., Lim, T. Y., Peng, H., & Yang, X. (2013). Emotional needs of car buyers and emotional intent of car designers. *Theoretical Issues in Ergonomics Science*, *14*, 455–474.
- Hellier, E., Naweed, A., Walker, G., Husband, P., & Edworthy, J. (2011). The influence of auditory feedback on speed choice, violations and comfort in a driving simulation game. *Transportation Research Part F: Traffic Psychology and Behaviour*, *14*, 591–599.
- Herold, P., & Wallbrecher, M. (2017). All-wheel steering. In M. Harrer & P. Pfeffer (Eds.), *Steering handbook* (pp. 493–512). Cham: Springer.
- Holliday, T., Lawrance, A. J., & Davis, T. P. (1998). Engine-mapping experiments: A two-stage regression approach. *Technometrics*, *40*, 120–126.
- Horswill, M. S., & Coster, M. E. (2002). The effect of vehicle characteristics on drivers' risk-taking behaviour. *Ergonomics*, *45*, 85–104.
- Horswill, M. S., & McKenna, F. P. (1999). The development, validation, and application of a video-based technique for measuring an everyday risk-taking behavior: Drivers' speed choice. *Journal of Applied Psychology*, *84*, 977–985.
- Horswill, M. S., & Plooy, A. M. (2008). Auditory feedback influences perceived driving speeds. *Perception*, *37*, 1037–1043.
- Hosman, R., & Stassen, H. (1998). Pilot's perception and control of aircraft motions. *IFAC Proceedings Volumes*, *31*, 311–316.
- Hosoda, M. (2010). Power train for a new compact sporty hybrid vehicle (Technical Paper No. 2010-01-1095). *SAE International*.
- Houtenbos, M. D., De Winter, J. C. F., Hale, A. R., Wieringa, P. A., & Hagenzieker, M. P. (2017). Concurrent audio-visual feedback for supporting drivers at intersections: A study using two linked driving simulators. *Applied Ergonomics*, *60*, 30–42.
- Jackson, A. P. (2013). A comparison between active and passive approaches to the sound quality tuning of a high performance vehicle (Technical Paper No. 2013-01-1878). *SAE International*.
- Jagacinski, R. J. (1977). A qualitative look at feedback control theory as a style of describing behavior. *Human Factors*, *19*, 331–347.
- Jagacinski, R. J., & Flach, J. M. (2003). *Control theory for humans – Quantitative approaches to modeling performance*. Mahwah, NJ: Lawrence Erlbaum.
- Janssen, W., & Nilsson, L. (1993). *An experimental evaluation of in-vehicle collision avoidance systems* (GIDS Deliverable MAN2). Haren, Netherlands: Traffic Research Centre, University of Groningen.
- JATO. (2021). *European new car market starts 2021 with record market share for SUVs*. <https://www.jato.com/european-new-car-market-starts-2021-with-record-market-share-for-suvs>
- Jenkins, W. L., & Connor, M. B. (1949). Some design factors in making settings on a linear scale. *Journal of Applied Psychology*, *33*, 395–409.
- Jennings, P. A., Dunne, G., Williams, R., & Giudice, S. (2010). Tools and techniques for understanding the fundamentals of automotive sound quality. Proceedings of the Institution of Mechanical Engineers, *Part D: Journal of Automobile Engineering*, *224*, 1263–1278.
- Jindo, T., & Hirasago, K. (1997). Application studies to car interior of Kansei engineering. *International Journal of Industrial Ergonomics*, *19*, 105–114.
- Jung, G., Kim, S. M., Kim, S. Y., Jung, E. S., & Park, S. (2010). Effects of design factors of the instrument cluster panel on consumers' affection. *Proceedings of the International MultiConference of Engineers and Computer Scientists*, Vol. 3. Hong Kong.
- Kamp, I. (2012). The influence of car-seat design on its character experience. *Applied Ergonomics*, *43*, 329–335.
- Karaaslan, E., Noori, M., Lee, J., Wang, L., Tatari, O., & Abdel-Aty, M. (2018). Modeling the effect of electric vehicle adoption on pedestrian traffic safety: An agent-based approach. *Transportation Research Part C: Emerging Technologies*, *93*, 198–210.
- Krüger, J., Castor, F., & Müller, A. (2004). Psychoacoustic investigation on sport sound of automotive tailpipe noise. *Fortschritte der Akustik-DAGA* (pp. 233–234). Strasbourg, France.
- Kwon, G., Jo, H., & Kang, Y. J. (2018). Model of psychoacoustic sportiness for vehicle interior sound: Excluding loudness. *Applied Acoustics*, *136*, 16–25.
- Larish, J. F., & Flach, J. M. (1990). Sources of optical information useful for perception of speed of rectilinear self-motion. *Journal of Experimental Psychology: Human Perception and Performance*, *16*, 295–302. <https://doi.org/10.1037/0096-1523.16.2.295>
- Mansell, W., & Marken, R. S. (2015). The origins and future of control theory in psychology. *Review of General Psychology*, *19*, 425–430.
- Martinez, C. M., Heucke, M., Wang, F. Y., Gao, B., & Cao, D. (2018). Driving style recognition for intelligent vehicle control and advanced driver assistance: A survey. *IEEE Transactions on Intelligent Transportation Systems*, *19*, 666–676.
- McLane, R. C., & Wierwille, W. W. (1975). The influence of motion and audio cues on driver performance in an automobile simulator. *Human Factors*, *17*, 488–501.
- McRuer, D. T., Allen, R. W., Weir, D. H., & Klein, R. H. (1977). New results in driver steering control models. *Human Factors*, *19*, 381–397.
- McRuer, D. T., & Jex, H. R. (1967). A review of quasi-linear pilot models. *IEEE Transactions on Human Factors in Electronics*, *HFE-8*, 231–249.
- McRuer, D. T., & Weir, D. H. (1969). Theory of manual vehicular control. *Ergonomics*, *12*, 599–633.
- Melman, T., Abbink, D. A., Van Paassen, M. M., Boer, E. R., & De Winter, J. C. F. (2018). What determines drivers' speed? A replication of three behavioural adaptation experiments in a single driving simulator study. *Ergonomics*, *61*, 966–987.

- Melman, T., De Winter, J., Mouton, X., Tapus, A., & Abbink, D. (2021). How do driving modes affect the vehicle's dynamic behaviour? Comparing Renault's MultiSense sport and comfort modes during on-road naturalistic driving, *Vehicle System Dynamics*, 59, 485–503.
- Melman, T., De Winter, J. C. F., & Abbink, D. A. (2017). Does haptic steering guidance instigate speeding? A driving simulator study into causes and remedies. *Accident Analysis & Prevention*, 98, 372–387.
- Melman, T., Kolekar, S., Hogerwerf, E., & Abbink, D. (2020). How road narrowing impacts the trade-off between two adaptation strategies: Reducing speed and increasing neuromuscular stiffness. *Proceedings of the 2020 IEEE International Conference on Systems, Man, and Cybernetics* (pp. 3235–3240). Toronto, Canada.
- Merat, N., & Jamson, H. (2011). A driving simulator study to examine the role of vehicle acoustics on drivers' speed perception. *Proceedings of the Sixth International Driving Symposium on Human Factors in Driver Assessment, Training and Vehicle Design* (pp. 226–232). Lake Tahoe, California. <https://doi.org/10.17077/drivingassessment.1401>
- Mercedes-Benz. (2021). Driving modes. https://moba.i.daimler.com/markets/ece-row/baix/cars/177.0_mbox-high_2020_a/en_GB/page/ID_9ec704d53993f553354ae365263f0b2f-1d3ef3273993f563354ae36502733902-en-GB.html
- Min, D., Park, B., & Park, J. (2018). Artificial engine sound synthesis method for modification of the acoustic characteristics of electric vehicles. *Shock and Vibration*, 2018. <https://doi.org/10.1155/2018/5209207>
- Morey, R. D. (2008). Confidence intervals from normalized data: A correction to Cousineau (2005). *Tutorial in Quantitative Methods for Psychology*, 4, 61–64. <https://doi.org/10.20982/tqmp.04.2.p061>
- Mulder, M., Pauwelussen, J. J., Van Paassen, M. M., Mulder, M., & Abbink, D. A. (2010). Active deceleration support in car following. *IEEE Transactions on Systems, Man, and Cybernetics-Part A: Systems and Humans*, 40, 1271–1284. <https://doi.org/10.1109/TSMCA.2010.2044998>
- Mulder, M., Pool, D. M., Abbink, D. A., Boer, E. R., Zaal, P. M., Drop, F. M., Van der El, K., & Van Paassen, M. M. (2017). Manual control cybernetics: State-of-the-art and current trends. *IEEE Transactions on Human-Machine Systems*, 48, 468–485. <https://doi.org/10.1109/THMS.2017.2761342>
- Nieke, M., Mauro, J., Seidl, C., & Yu, I. C. (2016). User profiles for context-aware reconfiguration in software product lines. In T. Margaria & B. Steffen (Eds.), *Leveraging applications of formal methods, verification and validation: Discussion, dissemination, applications. ISoLA 2016. Lecture Notes in Computer Science*, vol 9953 (pp. 563–578). Cham: Springer. https://doi.org/10.1007/978-3-319-47169-3_44
- Nyeste, P., & Wogalter, M. S. (2008). On adding sound to quiet vehicles. *Proceedings of the Human Factors and Ergonomics Society Annual Meeting*, 52, 1747–1750. <https://doi.org/10.1177/154193120805202112>
- Park, D., Park, S., Kim, W., Rhiu, I., & Yun, M. H. (2019). A comparative study on subjective feeling of engine acceleration sound by automobile types. *International Journal of Industrial Ergonomics*, 74, 102843. <https://doi.org/10.1016/j.ergon.2019.102843>
- Pei, X., Wong, S. C., & Sze, N. N. (2012). The roles of exposure and speed in road safety analysis. *Accident Analysis & Prevention*, 48, 464–471. <https://doi.org/10.1016/j.aap.2012.03.005>
- Petiot, J. F., Francisco, C. C., & Ludivine, B. (2015). A comparison of conjoint analysis and interactive genetic algorithms for the study of product semantics. *Proceedings of the 20th International Conference on Engineering Design (ICED 15) Vol 5: Design Methods and Tools-Part 1*. Milan, Italy.
- Porsche. (2021). Model overview. Panamera models. <https://www.porsche.com/usa/models/panamera/panamera-e-hybrid-models/drivechassis/sport-mode>
- Renault. (2021). Multi-sense. <https://gb.e-guide.renault.com/eng/easy-link/MULTI-SENSE>
- Rothengatter, T. (1988). Risk and the absence of pleasure: a motivational approach to modelling road user behaviour. *Ergonomics*, 31, 599–607. <https://doi.org/10.1080/00140138808966702>
- Schoegg, P., Ramschack, E., & Bogner, E. (2001). *On-board optimization of driveability character depending on driver style by using a new closed loop approach* (No. 2001-01-0556). SAE Technical Paper. <https://doi.org/10.1016/j.aap.2012.03.005>
- Sheridan, T. B. (2004). Driver distraction from a control theory perspective. *Human Factors*, 46, 587–599. <https://doi.org/10.1518/hfes.46.4.587.56807>
- Shibahata, Y. (2005). Progress and future direction of chassis control technology. *Annual Reviews in Control*, 29, 151–158. <https://doi.org/10.1016/j.arcontrol.2004.12.004>
- Shinagawa, T., Kudo, M., Matsubara, W., & Kawai, T. (2015). *The new Toyota 1.2-liter ESTEC turbocharged direct injection gasoline engine* (Technical Paper No. 2015-01-1268). SAE International. <https://doi.org/10.4271/2015-01-1268>
- Sivak, M. (1996). The information that drivers use: is it indeed 90% visual? *Perception*, 25, 1081–1089. <https://doi.org/10.1068/p251081>
- Soundsnap. (2021a). Volkswagen Golf V 1.6 FSI engine regular driving with slow acceleration mono. https://www.soundsnap.com/volkswagen_golf_v_1_6_fsi_engine_regular_driving_with_slow_acceleration_mono_wav
- Soundsnap. (2021b). Audi A4 B8 20TDI engine 3k RPM loop mono. https://www.soundsnap.com/audi_a4_b8_20tdi_engine_3k_rpm_loop_mono_wav
- Unreal. (2021). Unreal Engine 4 documentation. <https://docs.unrealengine.com/en-US/index.html>

-
- Uselmann, A., Krüger, K., Bittner, C., & Rivera, G. (2015). Innovative software functions to operate electric power steering systems in sports cars – Unterstützungskraftregelung (UKR). In P. Pfeffer (Ed.), *6th International Munich Chassis Symposium 2015. Proceedings* (pp. 423–441). Wiesbaden: Springer Vieweg. https://doi.org/10.1007/978-3-658-09711-0_28
- Van der Laan, J. D., Heino, A., & De Waard, D. (1997). A simple procedure for the assessment of acceptance of advanced transport telematics. *Transportation Research Part C: Emerging Technologies*, 5, 1–10. [https://doi.org/10.1016/S0968-090X\(96\)00025-3](https://doi.org/10.1016/S0968-090X(96)00025-3)
- Volvo. (2021). V90 cross country. Drive modes. <https://www.volvocars.com/en-th/support/manuals/v90-cross-country/2019w17/starting-and-driving/drive-modes/drive-modes>
- Wang, Y. S., Shen, G. Q., & Xing, Y. F. (2014). A sound quality model for objective synthesis evaluation of vehicle interior noise based on artificial neural network. *Mechanical Systems and Signal Processing*, 45, 255–266. <https://doi.org/10.1016/j.ymssp.2013.11.001>
- Wehbi, K., Bestle, D., & Beilharz, J. (2017). Automatic calibration process for optimal control of clutch engagement during launch. *Mechanics Based Design of Structures and Machines*, 45, 507–522. <https://doi.org/10.1080/15397734.2016.1250221>
- Weir, D. H., & Chao, K. C. (2007). Review of control theory models for directional and speed control. In P. Cacciabue (Ed.), *Modelling driver behaviour in automotive environments: Critical issues in driver interactions with intelligent transport systems* (pp. 293–311). New York, NY: Springer. https://doi.org/10.1007/978-1-84628-618-6_17
- Wilde, G. J. (1998). Risk homeostasis theory: an overview. *Injury Prevention*, 4, 89–91. <https://doi.org/10.1136/ip.4.2.89>
- Yeo, H., Shladover, S. E., Krishnan, H., & Skabardonis, A. (2010). Microscopic traffic simulation of vehicle-to-vehicle hazard alerts on freeway. *Transportation Research Record*, 2189, 68–77. <https://doi.org/10.3141/2189-08>
- Zeitler, A., & Zeller, P. (2006). *Psychoacoustic modelling of sound attributes* (No. 2006-01-0098). SAE Technical Paper. <https://doi.org/10.4271/2006-01-0098>

Do Sport Modes Cause Behavioral Adaptation?



A key question in transportation research is whether drivers show behavioral adaptation, that is, slower or faster driving, when new technology is introduced into the vehicle. This study investigates behavioral adaptation in response to the sport mode, a technology that alters the vehicle's auditory, throttle-mapping, power-steering, and chassis settings. Based on the literature, it can be hypothesized that the sport mode increases perceived sportiness and encourages faster driving. Oppositely, the sport mode may increase drivers' perceived danger, homeostatically causing them to drive more slowly. These hypotheses were tested using an instrumented vehicle on a test track. Thirty-one drivers were asked to drive as they normally would with different sport mode settings: Baseline, Modified Throttle Mapping (MTM), Artificial Engine Sound enhancement (AESe), MTM and AESe combined (MTM-AESe), and MTM, AESe combined with four-wheel steering, increased damping, and decreased power steering (MTM-AESe-4WS). Post-trial questionnaires showed increased perceived sportiness but no differences in perceived danger for the three MTM conditions compared to Baseline. Furthermore, compared to Baseline, MTM led to higher vehicle accelerations and, with a smaller effect size, a higher time-percentage of driving above the 110 km/h speed limit, but not higher cornering speeds. The AESe condition did not significantly affect perceived sportiness, perceived danger, and driving speed compared to Baseline. These findings suggest that behavioral adaptation is a functional and opportunistic phenomenon rather than mediated by perceived sportiness or perceived danger.

Published as:

Melman, T., Tapus, A., Jublot, M., Mouton, X., Abbink, D. A., & De Winter, J. C. F. (2022). Do sport modes cause behavioral adaptation? *Transportation Research Part F: Traffic Psychology and Behaviour*. <https://doi.org/10.1016/j.trf.2022.07.017>

7.1. Introduction

The ability to adapt to changing circumstances is essential when it comes to driving through traffic. For example, experienced drivers are able to anticipate hazards and decelerate in time where necessary (Underwood et al., 2011; Vlakoveld, 2011). However, sometimes drivers adapt in a way that is unexpected, a phenomenon referred to as behavioral adaptation (OECD, 1990). More specifically, behavioral adaptation has been defined as “*those behaviors which may occur following the introduction of changes to the road-vehicle-user system and which were not intended by the initiators of the change*” (OECD, 1990, p. 23). Behavioral adaptation may manifest itself as a “*continuum of effects ranging from a positive increase in safety to a decrease in safety.*” The term risk compensation (Elvik et al., 2009) is often used to describe behavioral adaptation that results in decreased safety, such as faster driving or driving with shorter headways.

Concerns about behavioral adaptation are frequently raised when introducing advanced driver assistance systems (ADAS) (for reviews, see Rudin-Brown & Jamson, 2013; Saad, 2006; Sullivan et al., 2016). Specific examples include adopting shorter headways when driving with a forward collision warning system (Reinmueller et al., 2020) and driving faster when using a lane-keeping assistance system (Melman et al., 2017). In these cases, the intended safety benefits of ADAS are not realized to the fullest extent because drivers take more risks when receiving assistance. It should be emphasized that behavioral adaptation is not necessarily a negative occurrence. Cocron et al. (2011), for example, noted that drivers of electric vehicles are aware of the fact that their vehicles emit little noise and therefore report driving more cautiously in the vicinity of pedestrians and cyclists.

Behavioral adaptation may also occur when the vehicle’s capabilities themselves are changed. In a cross-sectional study, Horswill and Coster (2002) showed positive correlations between observed vehicle speed and physical characteristics of the vehicle, such as engine power. Other examples of behavioral adaptation are vehicles that are driven faster in the snow when fitted with studded tires (Rumar et al., 1976) or shorter gaps that are accepted when vehicles have better acceleration capabilities (Evans & Herman, 1976).

Understanding behavioral adaptation is increasingly relevant now that a growing number of vehicles allow the vehicle’s characteristics to be adjusted through so-called driving modes, such as the sport or eco mode (for examples of this technology, see Audi, 2021; BMW, 2021; Mercedes-Benz, 2021; Porsche, 2021; Renault, 2021; Volvo, 2021). Through the press of a button, driving modes aim to offer a different driving experience through adjustments in auditory, visual, and haptic feedback. In the sport mode, for example, the vehicle settings are altered to create a more sportive experience. This includes adjustments in the powertrain settings such as a sportier throttle mapping (i.e., a more sensitive throttle pedal) and a more aggressive gear-changing strategy (i.e., staying longer in lower gears), but also adjustments that do not affect vehicle handling but aim to change the driver’s perception, such as artificial engine sound enhancement and dashboard lighting.

According to Elvik et al. (2009), the degree of behavioral adaptation depends on whether road users experience a benefit in changing behavior, such as time gain. In the above-mentioned examples of vehicle modifications, this is clearly the case. For example, vehicles fitted with studded tires allow for a higher cornering speed than vehicles with regular tires. Sport modes do not affect the theoretical performance envelope of the vehicle (i.e., maximum engine power and maximum tire grip remain the same) but increase the effective performance envelope (i.e., make it less effortful to accelerate) and intend to create the subjective experience of sportiness. So far, no research in real vehicles seems to exist that has examined its effects on driving behavior. Although it may be expected that drivers exploit the sport mode to accelerate to a cruising speed more quickly, whether the sport mode also causes behavioral adaptation in the form of driving fast through curves or speeding is unknown.

Two alternative mechanisms may explain drivers' choice of speed when driving in a sport mode. On the one hand, it can be hypothesized that sportier auditory, visual, and haptic feedback encourages drivers to *increase* driving speed because drivers associate a sportier vehicle with a more sportive driving style. In the literature, speeding has been found for sports cars that have a higher maximum engine power (and thus higher maximum speed) compared to vehicles with lower engine power (e.g., Horswill & Coster, 2002; Krahe & Fenske, 2002; Melman et al., 2021b). Similarly, for the sport mode, it can be hypothesized that the increased perceived sportiness causes drivers to drive faster.

On the other hand, sporty vehicle settings can be argued to increase drivers' perceived danger due to the increased feedback received (e.g., increase in engine sound and vibrations), and hence, cause a *reduction* in driving speed, a mechanism consistent with the risk homeostasis theory (Wilde, 1998). In the same vein, it has been argued that older models of cars are driven at a slower speed than modern cars, speculatively because these cars provide a more dangerous experience, with more noise and vibrations (Fosser & Christensen, 1998). Previous psychoacoustic studies concur that increased engine volume or the presence of engine sound causes drivers to drive slower (Hellier et al., 2011; Horswill & McKenna, 1999) and more accurately estimate their speed (Evans, 1970; Horswill & Plooy, 2008). Note that the risk homeostasis theory has been extensively criticized, primarily because it seems to suggest that any safety-related intervention will fail to have an effect on accident rates, something that is clearly incompatible with the available evidence (Evans, 1986; Vaa, 2007). At the same time, there is much support for the notion that drivers adapt their driving speed to the situation in conjunction with the risk they perceive (e.g., Kolekar et al., 2021; Trimpop, 1996; Wilde, 2013).

As literature provides us with two competing hypotheses, we decided to examine the effect of sport mode settings on drivers' speed. The present study measured behavioral adaptation operationalized as driving speed in an instrumented vehicle while driving the same test-track route for different combinations of active components used in a commercial sport driving mode. More specifically, we tested five conditions: (1) Baseline (equivalent to Renault's eco mode), (2) Modified Throttle Mapping (MTM), (3) Artificial Engine Sound enhancement (AESe), (4) MTM and AESe combined (MTM-AESe), and (5) MTM, AESe combined with four-wheel steering, increased variable damping, and decreased power steering assistance (MTM-AESe-4WS). The settings of each system are the same as the one used in Renault's MultiSense sport mode and were previously described in Melman et al. (2021a). Condition 5 (MTM-AESe-4WS) is identical to Renault's sport mode (i.e., it incorporates all systems used in sport mode except the cockpit lighting color adjustments and dashboard interface), whereas Condition 4 (MTM-AESe) is the combination of Condition 2 (MTM) and Condition 3 (AESe). In the analysis, we investigated the effects of the systems on longitudinal driving behavior (i.e., speed and acceleration), combined with a location-specific analysis to discover where on the test track differences between the conditions emerged.

Apart from measuring driving speed and other vehicle-state variables, a post-trial questionnaire was used to measure the two constructs underlying our hypotheses: perceived sportiness and perceived danger. Several additional items were included that could help clarify why or how drivers adapt their behavior. More specifically, we queried the extent to which participants noticed relevant vehicle characteristics (see Elvik et al., 2009, who pointed out that the degree of behavioral adaptation depends on the noticeability of the feedback), and we measured the perceived effort in steering and accelerating (see Fuller, 2005; Melman et al., 2018, who noted that perceived effort might govern behavioral adaptation).

The current study is a conceptual replication of a fixed-base simulator study (Melman et al., 2021b) that investigated how perceived sportiness and driving behavior are affected by artificial engine sounds and modified throttle mapping (i.e., a more sensitive throttle pedal). In that study, the enhanced engine sound was simulated via a virtually elevated rpm,

whereas the current study amplifies the natural engine sounds through the in-cabin speakers. The modified throttle mapping was similar in both studies. The elevated rpm sound led to increased perceived sportiness as assessed through self-reports, whereas no statistically significant increase or decrease in driving speed was observed, i.e., behavioral adaptation did not occur. The same study also showed that modified throttle mapping only led to higher vehicle accelerations just after driving away from a standstill, while cruising speed was unaffected, which again indicates that behavioral adaptation did not occur. However, whether these results replicate in a production vehicle is still unknown. Human perception is substantially different in a real vehicle than in the driving simulator that was used because the driving simulator produced no vibratory or vestibular feedback, and drivers in simulators do not experience physical risk (De Winter & De Groot, 2012; Melman et al., 2021b).

7.2. Methods

7.2.1. Participants

Thirty-one participants (29 males, 1 female, 1 ‘preferred not to say’) between 20 and 59 years old ($M = 44.3$, $SD = 10.6$) volunteered for the test track experiment. The participants were all employees of Renault, Paris, and the majority were engineers and technicians. In response to the question ‘On average, how often did you drive a vehicle in the last 12 months’, 9 participants reported every day, 14 reported 4 to 6 days a week, 7 reported 1–3 days a week, and 1 reported once a month to once a week. Regarding mileage in the past 12 months, 2 reported 1001–5000 km, 5 reported 5001–10000 km, 9 reported 10001–15000 km, 8 reported 15001–20000 km, 2 reported 20001–25000 km, 2 reported 25001–30000 km, and 3 reported 35001–50000 km. To the question ‘How often do you drive on the CTA track?’ (i.e., the test track of Renault), 6 drivers reported never having driven it, 5 reported less than once a month, 10 reported between once a week and once a month, 5 reported once a week, and 5 reported 1–3 times a week. All participants reported having heard of the eco, comfort, and sport modes. Twenty-four participants had driven the sport mode at least once. The research was approved by Renault, and all participants provided written informed consent.

7.2.2. Experimental vehicle

The instrumented vehicle used in the current study was a Renault Talisman Phase 2 (see Figure 7.1-left), engine type R9M, 1.6 L Diesel, with a maximum engine power of 160 kW, a maximum speed of 207 km/h, an automatic transmission, and a 0 to 100 km/h acceleration

7



Figure 7.1. The experimental vehicle, a Talisman phase 2 (left), with the VBOX GPS antenna (right)

time of 9.6 s. The vehicle was equipped with the Paris Initiale option, which included four-wheel steering, variable damping, and a Bose sound system comprising 13 speakers and a subwoofer. The experimental conditions and corresponding vehicle settings were switched using a mobile phone connected to a dSPACE MicroAutoBox. The CAN signals were recorded at frequencies between 10 Hz and 100 Hz. The GPS location and acceleration were recorded using a VBox at 100 Hz (see Figure 7.1-right) and calibrated each day. Finally, the same dashboard interface and blue ambient lighting colors were used for all conditions to prevent drivers from being informed about the used condition via visual information.

7.2.3. Independent variables and design

All participants drove in all of the following five conditions, where the first condition was identical to Renault's eco mode, the fifth condition was identical to Renault's sport mode, and Conditions 2, 3, and 4 represented a combination of eco- and sport-mode features.

1. Baseline
2. Modified throttle mapping (MTM)
3. Artificial engine sound enhancement (AESe)
4. Modified throttle mapping and artificial engine sound enhancement combined (MTM-AESe)
5. Modified throttle mapping, artificial engine sound enhancement, four-wheel steering, increased variable damping, and decreased power steering combined (MTM-AESe-4WS).

The MTM condition involved an altered throttle mapping, where a given driver's throttle depression ('throttle driver') resulted in a higher normalized requested engine torque ('throttle engine') (see Figure 7.2-left). Additionally, MTM increased the gear shift point in the rpm range (i.e., allowing a higher rpm before changing gears). For example, for a 'throttle driver' of 40%, the gear changed from 3rd to 4th at 35 km/h for Baseline, whereas for MTM, this was 43 km/h. The effect of this gear-changing strategy on the gear distribution for this experiment is shown in Figure 7.2-right. Finally, for the MTM condition, engine braking was done at higher engine speeds. The maximum engine power (160 kW) was the same for all conditions.

The AESe condition artificially amplified the natural engine sounds through the in-cabin speakers. More specifically, compared to Baseline, AESe increased the engine's second harmonic by 3 dB for engine speeds below 2000 rpm, by 7 dB for engine speeds between

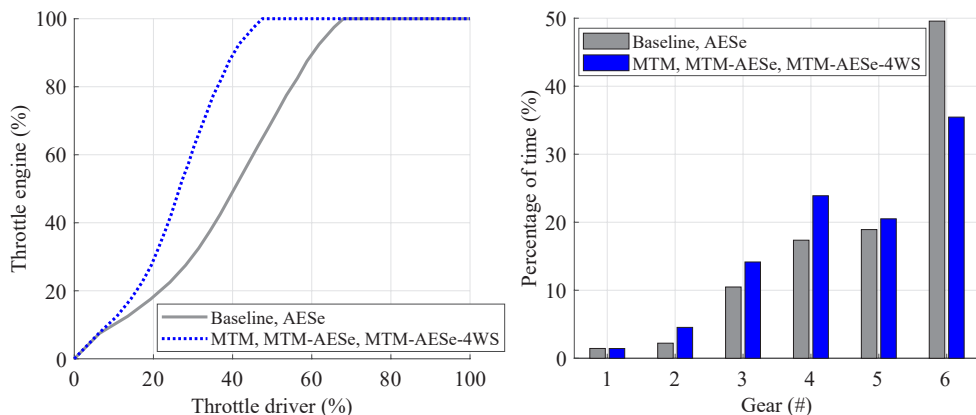


Figure 7.2. The modified throttle mapping (left) and the gear distribution during the driven route for all participants (right). Both graphs were created using the data recordings of the experiment.

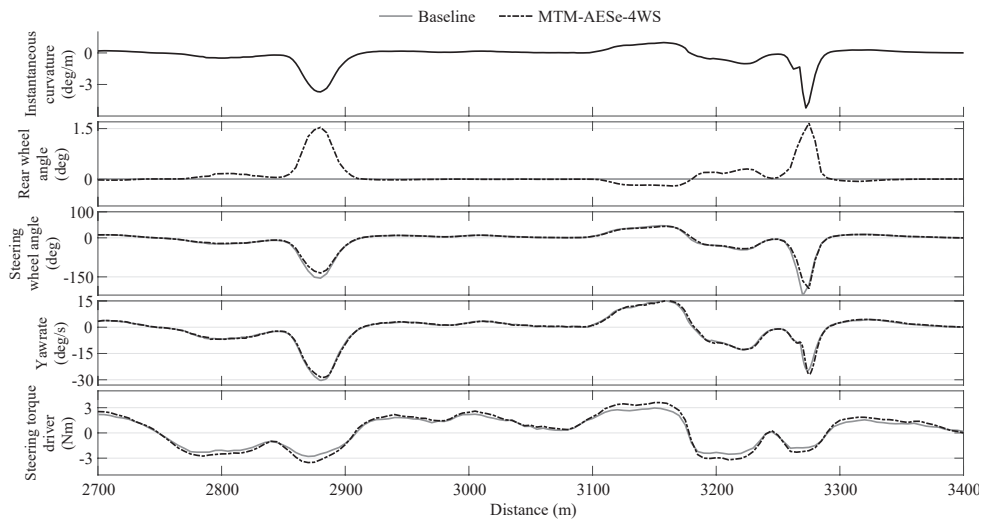


Figure 7.3. Illustration of four-wheel steering and power steering adjustments in the MTM-AESe-RWS condition versus the Baseline condition. The instantaneous curvature is calculated as the yaw rate/speed. The figure depicts two sharp curves (2880 m and 3270 m). The figure is made using the data recordings and shows the mean behavior averaged over all 31 participants.

2000 and 3500 rpm, and no enhancement was provided above 3500 rpm. The AESe setting was identical to the AESe setting used in Renault’s sport mode. Subjectively, this resulted in a roaring engine sound.

The MTM-AESe-4WS condition added four-wheel steering, increased vertical damping, and decreased power steering to the MTM and AESe conditions. The four-wheel steering system applied countersteering, where the rear wheels were turned in the opposite direction from the front wheels to increase the vehicle’s yaw response (i.e., a smaller steering wheel angle was required to drive through a curve). These effects are visualized in Figure 7.3 (see also Melman et al., 2021a, for more detailed information). The suspension damping coefficient increased about 3.5 times for MTM-AESe-4WS compared to Baseline (Melman et al., 2021a). The power steering assistance decreased, resulting in higher driver steering torques (see Figure 7.3).

It is noted that while 4WS involves dedicated hardware, MTM and AESe are software-based, i.e., these features aim to increase the perceived sportiness of the vehicle without requiring potentially costly hardware (Melman et al., 2021b). It is further noted that all five conditions offered the same dynamic envelope of the vehicle, i.e., if the throttle were fully depressed, the acceleration and gear-changing moments of the car would be identical. However, the presumed mechanisms of MTM and AESe on behavioral adaptation are quite different: MTM offers higher instantaneous acceleration capabilities than Baseline since, with MTM, the vehicle generally drives in a lower gear. Consequently, the driver can acquire a target speed more easily, without pressing the throttle deeply. In comparison, the AESe condition changes nothing to the responsiveness of the vehicle; any change in driving speed would be due to the illusion of driving a sportier vehicle (Melman et al., 2021b).

The participants each drove the five conditions in counterbalanced order. Because a complete permutation of the five conditions would require a very high number of participants ($5 \times 4 \times 3 \times 2 \times 1 = 120$), a more economical counterbalancing method was used, as defined by Williams (1949). For five conditions, Williams proposes a counterbalancing approach involving ten different orders. This was repeated three times for the first 30 participants in our

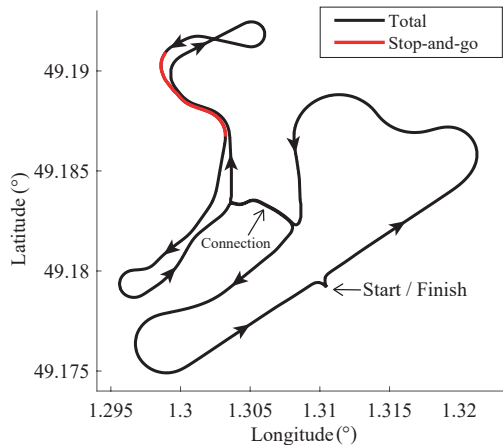


Figure 7.4. The experimental route on the Renault test track in Aubevoye, France. The driving direction is indicated by arrows, and the connection is driven in both directions.

experiment, with one additional order for the last participant.

7.2.4. Road Environment

The experiment was performed on Renault’s test circuit in Aubevoye, France. The participants drove on a 10.4 km route. The route consisted of a stop-and-go section (0.6 km; Figure 7.4), where drivers had to stop the vehicle and drive away from a standstill. The stop-and-go section was analyzed separately, resulting in a 9.8 km total route for the general analysis. The route consisted of a one-way two-lane road with a speed limit of 110 km/h and 90 km/h, except for the connection between two test tracks that consisted of a two-way single-lane road with a speed limit of 50 km/h (see Figure 7.4). Before entering the northern part of the test track, drivers had to stop in front of a stop sign and turn right. Very little traffic was encountered during the experiment; out of the 155 trials (5 conditions x 31 participants), only five trials encountered one or more vehicles. The experiment was conducted in dry weather for all drivers (the experiment was conducted in June 2021).

7.2.5. Procedure

The study was advertised, without stating the aim, in the general Renault newsletter that was sent to all employees. The participants read and signed a consent form and completed a questionnaire on their demographics, driving experience, and familiarity with the test track. The instruction sheet mentioned that the purpose of the study was to investigate their driving behavior and feelings while driving with different driving-experience enhancement systems. It also mentioned that the experiment consisted of five trials driven on the test track and that in each trial they would be supported by a different set of driving-experience enhancement systems. Participants were asked to drive as they usually do on the test track and adhere to the traffic rules indicated by road signs next to the road.

The first trial of the experiment was a familiarization run to let the driver become familiar with the route and the Baseline conditions. The participants were told that this trial would not be analyzed. During the first trial only, the experimenter, who was sitting next to the driver, gave navigation instructions, and the stop-and-go was practiced. After the familiarization trial, the car was parked, and the experiment started.

In each experimental trial, participants drove in one of the five conditions (Baseline, MTM, AESe, MTM-AESe, or MTM-AESe-4WS). The participants were not informed about

the settings of the conditions in this blinded experiment, and the dashboard did not give an indication of the vehicle settings that were currently active. After each trial, participants stepped out of the vehicle and completed a paper-and-pencil questionnaire about their driving experience. During the entire experiment, the experimenter was sitting next to the driver without talking. The entire experiment took approximately 75 minutes per participant. The consent form and the personal details questionnaire were written in French, and the post-trial questionnaire was written in English to replicate Melman et al. (2021b).

7.2.6. Dependent Measures

The dependent measures were categorized into self-reported experience and driving behavior, similar to the simulator study by Melman et al. (2021b). The driving behavior measures were calculated for the route excluding the stop-and-go section (9.8 km). Furthermore, for all measures (except the stop-and-go section), speeds below 10 km/h were excluded from the data to remove the influence of the stop sign on the measures.

Self-Reported Experience.

After each trial, participants completed a questionnaire containing 14 items on a five-point scale. The first four items investigated drivers' perceived effort for Q1 accelerating, Q2 steering, Q3 braking, and Q4 maintaining speed, from low to high. This was followed by four items that investigated whether the drivers perceived the vehicle settings: Q5 throttle responsiveness (low to high), Q6 brake responsiveness (low to high), Q7 engine sound (quiet to loud), and Q8 steering responsiveness (low to high). Finally, seven items polled whether participants had experienced the vehicle as Q9 not sporty/sporty, Q10 not likable/likable, Q11 not comfortable/comfortable, Q12 safe/dangerous, Q13 not agile/agile, and Q14 raising awareness/sleep-inducing. The two main items were Q9 (perceived sportiness) and Q12 (perceived danger).

Driving Behavior.

The following driving behavioral measures were calculated over the total track, excluding the stop-and-go section:

The speed measures below are the main measures of interest.

- *Mean speed (km/h)*. Mean speed is often used as an index of road safety: an increase in speed reduces the available time to respond in an emergency scenario and increases the probability of being involved in a crash (Aarts & Van Schagen, 2006; Pei et al., 2012).
- *Max speed (km/h)*. The maximum speed that was recorded.
- *Mean cornering speed (km/h)*. This measure shows the speeds driven during the cornering sections for instantaneous curvatures (calculated by the yaw rate/speed) greater than 0.7 deg/m. Using this threshold, 16% of the route was categorized as 'curve'.
- *Percentage above 110 km/h (%)*. The percentage of time above the 110 km/h speed limit was calculated as a percentage of the total time driven in the 110 km/h speed limit section.

In addition, we calculated nine longitudinal driver behavior measures that provide more insight into how drivers drove with the different combinations of sport mode components.

- *Mean absolute longitudinal acceleration (m/s^2)*. A high mean absolute longitudinal acceleration can be seen as sporty driving (Ericsson, 2001; Martinez et al., 2018).
- *Mean throttle driver (%)*. A measure of how deeply drivers pressed the accelerator on average. A lower value is expected for the three MTM conditions compared to AES

and Baseline, as less ‘throttle driver’ is needed to drive with a certain speed (see also the simulator study by Melman et al., 2021b).

- *Max brake pressure (bar)*. This measure indicates how hard the driver braked. Hard braking is an indication of sportive driving or approaching a curve at high speed.
- *Throttle driver release time (%)*. In the literature, this measure is also referred to as coasting and has been interpreted as indicative of uncertainty or a delay in decision-making (Houtenbos et al., 2017; Yeo et al., 2010). It is also a corollary of having accelerated too much, resulting in an overshoot of speed and a subsequent throttle release. This measure was previously found to be strongly affected by modifications in throttle mapping (Melman et al., 2021b).
- *Fuel consumption per km (cm³/km)*. An additional measure to quantify the impact of different sport mode components on fuel consumption. Higher fuel consumption is expected when driving with the MTM conditions compared to Baseline due to the altered gear-changing strategy (i.e., driving in a lower gear).
- *Mean gear*. A measure that captures the average used gear and is expected to be lower for the MTM than Baseline due to the more sportive gear changing strategy.

For the stop-and-go section, the following measure was calculated:

- *Mean acceleration during the first five seconds (m/s²)*. This measure indicates sporty driving. The start of each trial was determined based on the moment the throttle position exceeded 0%. A previous simulator study showed higher accelerations when driving with MTM compared to Baseline (Melman et al., 2021b).

7.2.7. Statistical Analyses

For each measure and each of the five experimental conditions, the mean and standard deviation (SD) across the 31 participants was computed. Pairwise comparisons between conditions were performed using paired-samples *t*-tests. Because of the large number of statistical comparisons made, a conservative alpha value of 0.005 was adopted (Benjamin et al., 2018). A reviewer noted that a conservative alpha value might cause Type II errors and

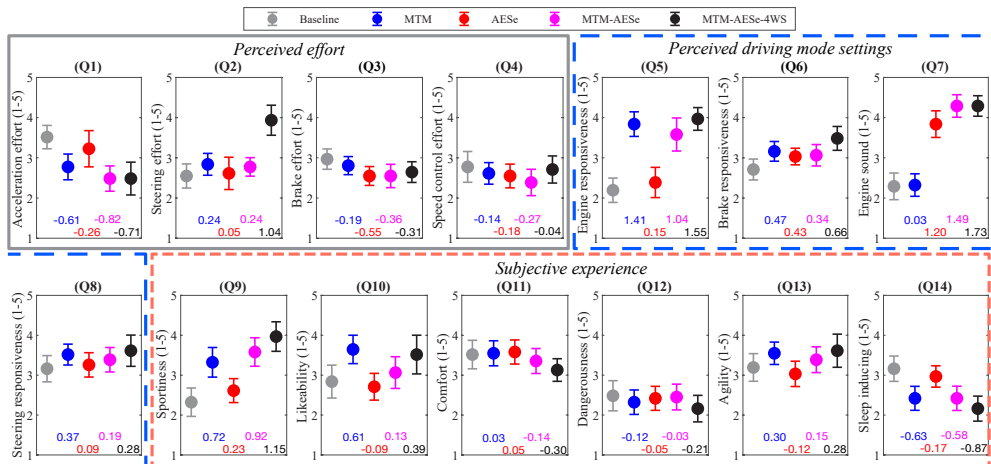


Figure 7.5. The questionnaire results per item and experimental condition. The figure depicts the means (circles) and within-subject 95% confidence intervals calculated according to Morey (2008). Q1–Q4 concern perceived effort, Q5–Q8 concern perceived driving mode features, and Q9–Q14 concern other aspects of subjective experience. The bottom of each figure shows the Cohen’s *d*_z for MTM, AESe, MTM-AESe, and MTM-AESe-4WS compared to Baseline ($|d_z| > 0.367$: $p < 0.05$, $|d_z| > 0.545$: $p < 0.005$).

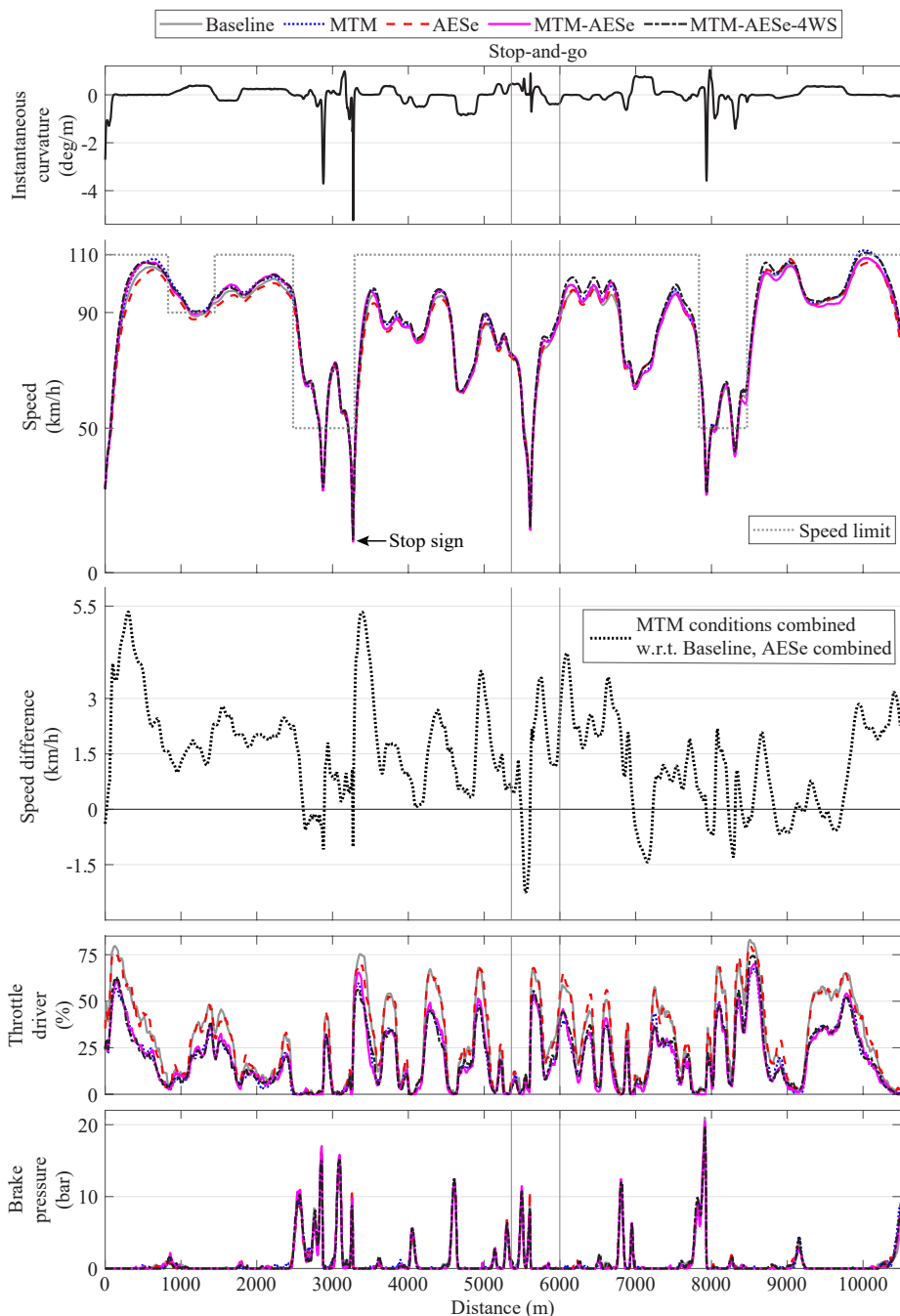


Figure 7.6. The mean driving behavior per condition averaged over all 31 participants (1) instantaneous curvature (yaw rate/speed), (2) driving speed, (3) driving speed of the three MTM conditions averaged relative to Baseline, AEsE averaged (positive values mean that participants drove faster with MTM compared to without), (4) throttle driver, and (5) brake pressure. Note that the vehicle speed does not drop to exactly 0 km/h during the stop-and-go and the stop sign (at 3300 m); this is because participants stopped their vehicles at slightly different positions on the road.

may therefore give the unfair impression that no behavioral adaptation exists. Therefore, we also report results for a more liberal alpha value of 0.05. We caution the reader that a number of the observed statistically significant effects could be false positives. Finally, within-subject effect sizes d_z were calculated according to Faul et al. (2007).

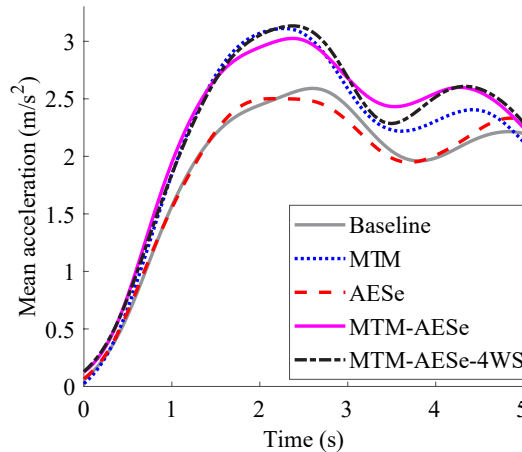


Figure 7.7. Mean vehicle acceleration after driving away from the stop-and-go section per condition, averaged over all participants during the first 5 s at the start and stop location.

Table 7.1. Means, standard deviation (in parenthesis), and pairwise comparisons for each dependent measure.

	Conditions					Pairwise comparisons			
	Baseline	MTM	AESe	MTM-AEsE	MTM-AEsE-4WS	1-2	1-3	1-4	1-5
Mean speed (km/h)	79.40 (5.63)	80.15 (5.40)	78.79 (5.45)	79.73 (5.88)	80.85 (5.85)	0.24	-0.23	0.08	<i>0.51</i>
Maximum speed (km/h)	115.01 (8.04)	116.92 (7.60)	114.03 (8.45)	116.12 (8.48)	116.84 (7.83)	0.35	-0.16	0.21	0.31
Mean cornering speed (km/h)	48.45 (3.55)	48.40 (3.31)	48.08 (3.73)	48.09 (3.71)	48.60 (3.93)	-0.03	-0.25	-0.15	0.09
Percentage above 110 km/h (%)	5.93 (9.45)	7.55 (9.36)	5.54 (9.04)	6.98 (9.51)	8.50 (12.02)	0.38	-0.12	0.27	<i>0.51</i>
Mean abs long acc (m/s ²)	0.727 (0.103)	0.772 (0.120)	0.727 (0.111)	0.773 (0.113)	0.783 (0.104)	0.72	0.01	0.61	0.96
Mean throttle driver (%)	27.88 (3.34)	18.59 (2.86)	28.02 (3.42)	18.60 (2.88)	19.12 (3.29)	-4.97	0.10	-4.08	-4.96
Max brake pressure (bar)	24.21 (4.75)	23.03 (3.95)	23.68 (4.73)	24.25 (4.98)	24.34 (3.45)	-0.35	-0.16	0.01	0.04
Throttle driver released time (%)	35.50 (5.66)	37.35 (6.44)	35.22 (6.38)	37.44 (6.22)	36.74 (5.92)	0.65	-0.10	0.63	0.62
Fuel consumption (cm ³ /km)	84.55 (11.00)	88.98 (12.14)	86.75 (13.53)	90.41 (13.08)	90.94 (10.45)	0.59	0.24	0.59	0.82
Mean gear (-)	5.10 (0.13)	4.76 (0.21)	5.07 (0.17)	4.74 (0.21)	4.77 (0.15)	-3.04	-0.49	-3.27	-4.57
Stop-and-go section									
Mean acceleration during the first five seconds (m/s ²)	1.92 (0.45)	2.20 (0.44)	1.91 (0.46)	2.28 (0.37)	2.28 (0.44)	0.74	-0.01	1.11	1.13

Note. The effect sizes are color-coded from -1.5 (red) to 0 (white) to 1.5 (green). $|d_z| > 0.367$: $p < 0.05$ (marked in italics), $|d_z| > 0.545$ (marked in boldface): $p < 0.005$.

7.3. Results

7.3.1. Self-Reported Experience

Figure 7.5 shows the means and 95% confidence intervals for the 14 self-report items described in the section 'dependent measures'. Compared to Baseline, MTM, MTM-AESe, and MTM-AESe-4WS resulted in significantly ($p < 0.005$) higher reported engine responsiveness (Q5) and reduced acceleration effort (Q1), while AESe, MTM-AESe, and MTM-AESe-4WS resulted in higher perceived engine sound (Q7). Furthermore, four-wheel steering (MTM-AESe-4WS) resulted in significantly ($p < 0.005$) higher perceived steering effort (Q2) but not a significant difference ($p > 0.05$) in steering responsiveness (Q8) and agility (Q13) compared to Baseline.

The perceived sportiness (Q9) was significantly ($p < 0.005$) higher for MTM ($M = 3.32$), MTM-AESe ($M = 3.58$), and MTM-AESe-4WS ($M = 3.97$) compared to Baseline ($M = 2.32$). Perceived danger (Q12) showed no significant differences ($p > 0.05$) from Baseline ($M = 2.48$) for MTM ($M = 2.32$), AESe ($M = 2.42$), MTM-AESe ($M = 2.45$), and MTM-AESe-4WS ($M = 2.16$). Additionally, it was found that likeability (Q10) was higher for MTM ($p < 0.005$) and MTM-AESe-4WS ($p < 0.05$) compared to Baseline. The MTM conditions (MTM, MTM-AESe, and MTM-AESe-4WS) resulted in significantly ($p < 0.005$) lower 'sleep inducing' ratings (Q14) than Baseline. No significant differences were found for the comfort (Q11) and speed control effort (Q4) ratings. Finally, it was interesting that the MTM, AESe, and MTM-AESe-4WS conditions increased perceived brake responsiveness (Q6) even though the brake pedal itself was not modified.

7.3.2. Driving Behavior

Table 7.1 shows the means, standard deviations, and results of the pairwise comparisons. The mean speed, maximum speed, and speed limit violation time for the three MTM conditions (MTM, MTM-AESe, MTM-AESe-4WS) were higher compared to Baseline, although often not statistically significant ($p > 0.05$). The mean cornering speed was equivalent for the five conditions and did not differ significantly ($p > 0.05$) from the Baseline condition.

On an absolute scale, the speed differences between conditions were rather small. Indicatively, participants' mean speed, maximum speed, mean cornering speed, and driving time above the speed limit were 0.75 km/h higher, 1.91 km/h higher, 0.05 km/h lower, and 1.63% higher in MTM compared to Baseline (see Table 7.1). For MTM-AESe-4WS compared to Baseline, the values for these four respective measures were 1.45 km/h, 1.84 km/h, 0.15 km/h, and 2.57% higher (see Table 7.1).

The lowest speed was found for AESe, but not significantly different from Baseline on any of the four speed-related measures. However, the mean gear was significantly ($p < 0.05$) lower for AESe compared to Baseline, suggesting that AESe evoked a cautious driving style. Table 7.1 further shows that participants adopted a more sporty driving style with MTM (MTM, MTM-AESe, and MTM-AESe-4WS) than Baseline, with higher mean absolute accelerations and more throttle fluctuations (higher throttle-release time).

Figure 7.6 shows the mean speed, throttle, and braking as a function of traveled distance. Furthermore, Figure 7.6 shows the speed difference for the three MTM conditions averaged (i.e., the average of MTM, MTM-AESe, and MTM-AESe-4WS) relative to Baseline and AESe averaged. Compared to Baseline/AESe, the largest speed differences (up to 5.5 km/h) were found when accelerating out of curves, after the stop sign, and after the stop-and-go section. In other words, the results indicate that it is during the acceleration phases that the difference between the MTM conditions and Baseline/AESe was largest.

Figure 7.7 shows the participants' mean acceleration during the first 5 s after driving away from the stop-and-go section per condition. This figure confirms that drivers adopted higher accelerations when driving with MTM, MTM-AESe, and MTM-AESe-4WS than with Baseline and AESe. After about 5 s, the accelerations were equivalent for all five conditions, in line with the simulator study by Melman et al. (2021b).

Finally, the fuel consumption was higher for MTM-AESe and MTM-AESe-4WS compared to Baseline. This is possibly the result of the gear-change strategy, where the vehicle stayed longer in lower gears (see Table 7.1).

7.4. Discussion

Two competing hypotheses regarding the effect of sport mode settings on behavioral adaptation were considered in this research: a speed increase due to increased perceived sportiness (cf. Horswill & Coster, 2002) and a speed reduction due to increased perceived danger (cf. Wilde, 1998). We tested these two hypotheses by means of a test-track experiment using an instrumented vehicle for different combinations of sport mode components. More specifically, we investigated five conditions: Baseline, Modified Throttle Mapping (MTM), Artificial Engine Sound enhancement (AESe), MTM and AESe combined (MTM-AESe), and MTM, AESe combined with four-wheel steering, increased damping, and decreased power steering (MTM-AESe-4WS).

The results suggest that the drivers, in the aggregate, noticed each sport mode setting. That is, compared to Baseline, participants reported increased engine responsiveness for MTM (Q5), a higher engine sound volume for AESe (Q7), and an increased effort required to steer (Q2) for the MTM-AESe-4WS condition. These findings suggest that necessary preconditions for behavioral adaptation were present.

The sport mode was hypothesized to increase perceived sportiness and thus encourage faster driving. The hypothesis of faster driving was not supported for the AESe condition; in fact, perceived sportiness was unaffected, and there were some tendencies for slower driving with AESe compared to Baseline. However, the hypothesis received mixed support for the MTM feature: compared to Baseline, the three MTM conditions yielded increased perceived sportiness ratings and caused increased speeds while accelerating out of curves (Figure 7.6) or while accelerating from a standstill (Figure 7.7). The MTM condition also caused, albeit with a small effect size, an elevated percentage of time driving above the 110 km/h speed limit. However, the MTM conditions did not cause statistically significant differences in cornering speed compared to Baseline. Thus, MTM appeared to cause increased accelerations but not faster cornering. Note that the higher mean speed of the MTM conditions compared to Baseline can directly be explained by the increased accelerations (in fact, achieving a higher mean acceleration while maintaining the same average speed is only possible if adopting a lower speed on the remaining part of the track). In conclusion, the findings suggest that behavioral adaptation was functional and opportunistic (i.e., increased acceleration to target speeds because of the given opportunity to accelerate more easily) rather than instigated by drivers feeling 'sporty' and hence adopting a riskier driving style. The current findings correspond to the examples cited in the introduction, where behavioral adaptation was said to be more likely when the technology offers a benefit to the driver.

The presumed cause of the increased acceleration is that, for a given throttle depression in the 10–60% range, the MTM conditions yielded higher instantaneous engine power compared to the Baseline condition (see Figure 7.2-left). In addition to the more sensitive pedal (and in contrast to the driving simulator study by Melman et al. (2021b), which simulated an electric engine without gears), more instantaneous engine power was available because the MTM conditions were driven in a lower gear (see Figure 7.2-right). Consequently, if the driver presses the pedal to a certain level, acceleration will be higher for MTM compared to Baseline. The driver, in turn, adapts to the sensitive pedal by pressing it less deeply (see 'throttle driver' in Figure 7.6 and see Melman et al., 2021b, for further explanation in the context of open-loop vs. closed-loop driver control). The present acceleration results replicate findings from an earlier simulator-based study by Melman et al. (2021b). However, in this driving simulator experiment, no effect of MTM was found on perceived sportiness,

which the authors attributed to the lack of vestibular feedback and large inter-driver variability in a driving simulator.

The competing hypothesis was that the sport modes would cause an increase in perceived danger, in turn causing drivers to compensate by adopting a lower speed compared to the Baseline condition. This hypothesis is rejected since the MTM feature did not cause a reduction but rather a small increase in driving speeds, as discussed above. In addition, the sport modes did not cause an increase in perceived danger. In fact, perceived danger was even slightly lower for the MTM-AESe-4WS condition than for the Baseline condition (2.16 vs. 2.48 on the 5-point scale).

A limitation of the current study was that it was conducted with predominantly experienced male drivers. They were familiar with the test track and may have driven faster than the average driver would. Another validity threat is that the daily work of most participants consisted of studying vehicle chassis behavior, as a result of which they may express socially desirable opinions about products of their own company. However, as we noticed in another study in which employees participated in a truck driving study in which they evaluated human-machine interface concepts (Bazilinskyy et al., 2019), the opposite may be the case. Our impression was that participants in the current experiment were open-minded, critical, and consciously tried to observe the differences between the vehicle conditions. Future studies should investigate how these results translate to different groups of drivers.

In the current study, there were speed limit signs next to the road, which may have produced a ceiling effect on driving speeds, although participants still drove faster than the 110 km/h speed limit for 5.5 to 8.5% of the time (see Table 7.1). Future research could replicate our findings on different types of roads and for different types of speed limits. In addition, it would be useful to repeat the current study as part of a field operational test, in which drivers may participate for a period of months and may tend to forget they are participating in an experiment. This would also allow for exploring other aspects of behavioral adaptation, such as the interaction with other road users. Finally, it should be noted that although the MTM condition was well-liked (Q10) relative to the Baseline condition, it caused an increase in fuel consumption of about 6%. In other words, the increased capabilities and likeability ratings come at the price of increased cost. The relatively low likeability score for the Baseline condition is consistent with a driving-simulator experiment by Allison et al. (2022), which found that asking drivers to engage in eco-driving behaviors had a negative impact on drivers' overall mood. It can therefore be expected that eco modes will be underutilized in real traffic.

7

7.5. Conclusions

The current study investigated behavioral adaptation in response to the sport driving mode. Two alternative hypotheses were tested: (1) increased speed due to increased perceived sportiness and (2) decreased speed due to increased perceived danger. The following conclusions are drawn:

- The sport mode setting that makes it easier for drivers to accelerate (i.e., modified throttle mapping) increases perceived sportiness, is well-liked, and causes increased speeds while accelerating out of curves or from a standstill. However, the MTM conditions did not cause detectable differences in mean cornering speed compared to Baseline. Thus, MTM seemed to cause increased accelerations but not riskier driving.
- The sport mode setting that alters the drivers' auditory experience (i.e., artificial engine sound enhancement) is perceived clearly but does not significantly affect perceived sportiness or perceived danger and does not cause drivers to drive faster.

These findings suggest that behavioral adaptation is a functional and opportunistic phenomenon (i.e., increased acceleration to target speeds because of the given opportunity to accelerate more easily) rather than mediated by drivers having the feeling of sportiness or dangerousness.

Apart from the theoretical contribution mentioned above, the present findings may have practical utility for vehicle manufacturers. This study replicates previous simulator-based research (Melman et al., 2021b) in that relatively simple software-based modifications to the vehicle, such as modified throttle mapping, can have a substantial impact on driver perception (e.g., perceived sportiness), and stimulate drivers to reach their target speed more quickly.

References

- Aarts, L., & Van Schagen, I. (2006). Driving speed and the risk of road crashes: A review. *Accident Analysis & Prevention*, *38*, 215–224.
- Allison, C. K., Stanton, N. A., Fleming, J. M., Yan, X., & Lot, R. (2022). How does eco-driving make us feel? Considering the psychological effects of eco-driving. *Applied Ergonomics*, *101*, 103680.
- Audi. (2021). *Driving dynamic. Audi drive select*. <https://ownersmanuals2.com/audi/q7-2020-owners-manual-75410/page-110>
- Bazilinsky, P., Larsson, P., Johansson, E., & De Winter, J. C. F. (2019). Continuous auditory feedback on the status of adaptive cruise control, lane deviation, and time headway: An acceptable support for truck drivers? *Acoustical Science and Technology*, *40*, 382–390.
- Benjamin, D. J., Berger, J. O., Johannesson, M., Nosek, B. A., Wagenmakers, E. J., Berk, R., ... & Johnson, V. E. (2018). Redefine statistical significance. *Nature Human Behaviour*, *2*, 6–10.
- BMW. (2021). *Drive modes in detail*. <https://ownersmanuals2.com/bmw-auto/x5-2021-owners-manual-80671/page-161>
- Cocron, P., Bühler, F., Franke, T., Neumann, I., & Krems, J. F. (2011). The silence of electric vehicles—blessing or curse. *Proceedings of the 90th Annual Meeting of the Transportation Research Board*.
- De Winter, J. C. F., & De Groot, S. (2012). The effects of control-display gain on performance of race car drivers in an isometric braking task. *Journal of Sports Sciences*, *30*, 1747–1756.
- Elvik, R., Høy, A., Vaa, T., & Sørensen, M. (2009). Basic concepts of road safety research. *The Handbook of Road Safety Measures* (pp. 81–98). Emerald Group Publishing Limited.
- Ericsson, E. (2001). Independent driving pattern factors and their influence on fuel-use and exhaust emission factors. *Transportation Research Part D: Transport and Environment*, *6*, 325–345.
- Evans, L. (1970). Speed estimation from a moving automobile. *Ergonomics*, *13*, 219–230.
- Evans, L. (1986). Risk homeostasis theory and traffic accident data. *Risk Analysis*, *6*, 81–94.
- Evans, L., & Herman, R. (1976). Note on driver adaptation to modified vehicle starting acceleration. *Human Factors*, *18*, 235–240.
- Faul, F., Erdfelder, E., Lang, A. G., & Buchner, A. (2007). G*Power 3: A flexible statistical power analysis program for the social, behavioral, and biomedical sciences. *Behavior Research Methods*, *39*, 175–191.
- Fosser, S., & Christensen, P. (1998). *Car age and the risk of accidents* (Report 386/1988). Oslo, Norway: Institute of Transport Economics. Retrieved from <https://rosap.ntl.bts.gov/view/dot/15605>
- Fuller, R. (2005). Towards a general theory of driver behaviour. *Accident Analysis & Prevention*, *37*, 461–472.
- Hellier, E., Naweed, A., Walker, G., Husband, P., & Edworthy, J. (2011). The influence of auditory feedback on speed choice, violations and comfort in a driving simulation game. *Transportation Research Part F: Traffic Psychology and Behaviour*, *14*, 591–599.
- Horswill, M. S., & Coster, M. E. (2002). The effect of vehicle characteristics on drivers' risk-taking behaviour. *Ergonomics*, *45*, 85–104.
- Horswill, M. S., & McKenna, F. P. (1999). The development, validation, and application of a video-based technique for measuring an everyday risk-taking behavior: Drivers' speed choice. *Journal of Applied Psychology*, *84*, 977–985.
- Horswill, M. S., & Plooy, A. M. (2008). Auditory feedback influences perceived driving speeds. *Perception*, *37*, 1037–1043.
- Kolekar, S., Petermeijer, B., Boer, E., De Winter, J., & Abbink, D. (2021). A risk field-based metric correlates with driver's perceived risk in manual and automated driving: A test-track study. *Transportation Research Part C: Emerging Technologies*, *133*, 103428.
- Krahé, B., & Fenske, I. (2002). Predicting aggressive driving behavior: The role of macho personality, age, and power of car. *Aggressive Behavior: Official Journal of the International Society for Research on Aggression*, *28*, 21–29.
- Martinez, C. M., Heucke, M., Wang, F. Y., Gao, B., & Cao, D. (2018). Driving style recognition for intelligent vehicle control and advanced driver assistance: A survey. *IEEE Transactions on Intelligent Transportation Systems*, *61*, 966–987.
- Melman, T., Abbink, D. A., Van Paassen, M. M., Boer, E. R., & De Winter, J. C. F. (2018). What determines drivers' speed? A replication of three behavioural adaptation experiments in a single driving simulator study. *Ergonomics*, *61*, 966–987.
- Melman, T., De Winter, J., Mouton, X., Tapus, A., & Abbink, D. (2021a). How do driving modes affect the vehicle's dynamic behaviour? Comparing Renault's Multi-Sense sport and comfort modes during on-road naturalistic driving. *Vehicle System Dynamics*, *59*, 485–503.
- Melman, T., De Winter, J. C. F., & Abbink, D. A. (2017). Does haptic steering guidance instigate speeding? A driving simulator study into

causes and remedies. *Accident Analysis & Prevention*, 98, 372–387.

- Melman, T., Visser, P., & De Winter, J. (2021b). Creating the illusion of sportiness: Evaluating modified throttle mapping and artificial engine sound for electric vehicles. *Journal of Advanced Transportation*, 2021, 4396401.
- Mercedes-Benz. (2021). *Driving modes*. https://moba.i.daimler.com/markets/ece-row/baix/cars/177.0_mbox-high_2020_a/en_GB/page/ID_9ec704d53993f553354ae365263f0b2f1d3ef3273993f563354ae36502733902-en-GB.html
- OECD. (1990). *Behaviour adaptations to changes in the road transport system*. Paris: OECD.
- Pei, X., Wong, S. C., & Sze, N. N. (2012). The roles of exposure and speed in road safety analysis. *Accident Analysis & Prevention*, 48, 464–471.
- Porsche. (2021). *Model overview. Panamera models*. <https://www.porsche.com/usa/models/panamera/panamera-e-hybrid-models/drivechassis/sport-mode>
- Reinmueller, K., Kiesel, A., & Steinhauser, M. (2020). Adverse behavioral adaptation to adaptive forward collision warning systems: An investigation of primary and secondary task performance. *Accident Analysis & Prevention*, 146, 105718.
- Renault. (2021). *Multi-sense*. <https://gb.e-guide.renault.com/eng/easy-link/MULTI-SENSE>
- Rudin-Brown, C., & Jamson, S. (Eds.). (2013). *Behavioural adaptation and road safety: Theory, evidence and action*. CRC Press.
- Rumar, K., Berggrund, U., Jernberg, P., & Ytterbom, U. (1976). Driver reaction to a technical safety measure—studded tires. *Human Factors*, 18, 443–454.
- Saad, F. (2006). Some critical issues when studying behavioural adaptations to new driver support systems. *Cognition, Technology & Work*, 8, 175–181.
- Sullivan, J. M., Flannagan, M. J., Pradhan, A. K., & Bao, S. (2016). *Literature review of behavioral adaptations to advanced driver assistance systems* (Technical Report). Washington, DC: AAA Foundation for Traffic Safety.
- Trimpop, R. M. (1996). Risk homeostasis theory: problems of the past and promises for the future. *Safety Science*, 22, 119–130.
- Underwood, G., Crundall, D., & Chapman, P. (2011). Driving simulator validation with hazard perception. *Transportation Research Part F: Traffic Psychology and Behaviour*, 14, 435–446.
- Vaa, T. (2007). The Risk Homeostasis Theory: Accept, reject or modify?—An opposition to Gerald Wilde’s RHT. *Proceedings of the 20th ICTCT Workshop*, Valencia.
- vlakveld, W. (2011). *Hazard anticipation of young novice drivers: Assessing and enhancing the capabilities of young novice drivers to anticipate latent hazards in road and traffic situations* (Doctoral dissertation). University of Groningen.
- Volvo. (2021). *V90 cross country. Drive modes*. <https://www.volvocars.com/en-th/support/manuals/v90-cross-country/2019w17/starting-and-driving/drive-modes/drive-modes>
- Wilde, G. J. (1998). Risk homeostasis theory: An overview. *Injury Prevention*, 4, 89–91.
- Wilde, G. J. S. (2013). Homeostasis drives behavioural adaptation. In C. M. Rudin-Brown & S. L. Jamson (Eds.), *Behavioural adaptation and road safety: Theory, evidence and action* (pp. 61–86). Boca Raton, FL: CRC Press.
- Williams, E. J. (1949). Experimental designs balanced for the estimation of residual effects of treatments. *Australian Journal of Chemistry*, 2, 149–168.
- Yeo, H., Shladover, S. E., Krishnan, H., & Skabardonis, A. (2010). Microscopic traffic simulation of vehicle-to-vehicle hazard alerts on freeway. *Transportation Research Record*, 2189, 68–77.

PART



ONLINE CHANGES IN VEHICLE SETTINGS

8

9

**Should Steering Settings be
Changed by the Driver or by the
Vehicle Itself?**



Introduction. Cars are increasingly computerized, and vehicle settings such as steering gain (SG) can now be altered during driving. However, it is unknown whether transitions in SG should be adaptable (i.e., triggered by driver input) or adaptive (i.e., triggered automatically). We examined this question for road segments expected to require different SG. **Objective.** This paper aimed to investigate whether SG mode changes should be made by the driver or automatically. **Methods.** Twenty-four participants drove under four conditions in a simulator: fixed low gain (FL), fixed high gain (FH), a machine-initiated steering system, which switched between the two SG levels at predetermined locations (MI), and a driver-initiated steering system, in which the SG could be changed by pressing a button on the steering wheel (DI). **Results.** Participants showed poorer lane keeping and reported higher effort for FH compared to FL on straights, while the opposite held true on curved roads. On curved roads, the MI condition showed better lane-keeping performance and lower subjective effort than the DI condition. However, a substantial portion of the drivers gave low preference rankings to the MI concept. **Conclusion.** Drivers prefer and benefit from a steering system with a variable rather than fixed gain. Furthermore, although automatic SG transitions reduce effort, some drivers reject this concept. **Application.** As the state of technology advances, MI transitions are becoming increasingly feasible, but whether drivers would want to delegate their decision-making authority to a machine remains a moot point.

Published as:

Melman, T., Weijerman, M. P. P., De Winter, J. C. F., & Abbink, D. A. (2022). Should steering settings be changed by the driver or by the vehicle itself? *Human Factors*. <https://doi.org/10.1177/00187208221127944>

8.1. Introduction

A vehicle's steering gain (SG), also known as steering ratio or steering sensitivity, is a key parameter that determines how much the front wheels turn for a given steering wheel input (Gross, 1977; Reuter & Saal, 2017). Until the late 1990s, steering systems in production vehicles were designed with a fixed SG. A drawback of a fixed SG is that it cannot accommodate differences in desired sensitivity for different driving situations (Black et al., 2014; Jamson et al., 2007). If the SG is high, it may be more challenging to control the vehicle precisely when driving on a straight road at high speed (e.g., highway driving), as high control gains amplify motor noise (e.g., Chapanis & Kinkade, 1972; De Winter & De Groot, 2012). On the contrary, a low SG would enable more precise control but requires larger steering movements, which would be effortful when parking or driving through sharp curves (Kroes, 2019; Olson & Thompson, 1970; Reuter & Saal, 2017; Shoemaker et al., 1967).

Cars are becoming increasingly computerized, and vehicle settings that were once fixed can now be altered during driving (e.g., Melman et al., 2021a; Shibahata, 2005). Two ways of implementing variable steering settings can be distinguished: changes can be initiated based on vehicle-state variables such as speed (e.g., Jamson et al., 2007; Millsap & Law, 1996; Shimizu et al., 1999) or as part of a driving mode, such as the sport mode (e.g., BMW, 2022; Koehn & Eckrich, 2004; Renault, 2022). However, a yet-unanswered question is whether changes in SG mode should ideally be initiated by the driver (e.g., via the press of a button) or automatically by the car. This question has important implications since literature suggests that large changes in SG may, in some cases, negatively impact driver safety and acceptance. In particular, in a study on lane changing, Russell et al. (2016) found that drivers needed several trials to get used to a new SG.

The effects of machine-initiated and human-initiated mode changes (also referred to as adaptive vs. adaptable automation) have previously been investigated in various human-automation interaction studies (e.g., Hancock, 2007; Li et al., 2013; Sauer et al., 2012). In a review, Kaber and Prinzel (2006) concluded that *“there is a substantial body of research on adaptive automation demonstrating performance and workload benefits over manual systems control and traditional, technology-centered approaches to automation. Unfortunately, the same cannot be said for adaptable systems ...”*. In the same vein, it can be expected that driver-initiated SG changes will increase workload since there is an increase in the driver's responsibility for system supervision. However, others have noted that human-initiated mode changes have benefits in terms of improving operators' confidence and sense of control and reducing unpredictability (Kidwell et al., 2012; Miller & Parasuraman, 2007). It is also noted that machine-initiated mode changes will be ineffective if the triggers are inappropriate. Sauer et al. (2012), for example, found that performance-based mode changes yielded a higher workload than event-based mode changes and human-initiated mode changes. A possible explanation was that their performance-based trigger was not sensitive enough, resulting in infrequent adaptations (Sauer et al., 2012). In the same vein, Li et al. (2013) found that machine-initiated mode changes yielded a higher workload and lower preference ratings than human-initiated mode changes as participants considered the triggering criteria confusing or inappropriate. In comparison, in the human-initiated mode-change condition, where operators were in charge of setting the level of automation, operators often selected the highest level of automation in which they had little to do.

The current study aimed to examine the effects of machine-initiated and driver-initiated changes in SG on lane-keeping performance, perceived effort, and system preference. Participants completed four conditions: fixed low SG (FL), fixed high SG (FH), machine-initiated steering that switched between the two SG at predetermined locations (MI), and driver-initiated steering in which the SG setting could be changed by pressing a button on the steering wheel (DI). It is noted that, technologically, the DI and MI concepts seem feasible on real roads, since these concepts require hardware such as steer-by-wire and a location-

specific triggering mechanism. The latter is already part of intelligent speed assistance/adaptation (ISA), for example (Ryan, 2019).

To investigate MI and DI, three comparisons were prerequisites: First, FL was compared to FH to examine whether drivers indeed benefit from different SG in different parts of the road. More specifically, participants drove a route containing three driving-task segments—overtaking, driving on a straight road, and curve-driving— that were hypothesized to require different SG. For the overtaking and curve-driving segments, the FH condition was expected to produce more favorable outcomes (better lane-keeping, low effort) than FL, whereas, for the straight segment, the opposite was expected. Second and third, the DI and MI conditions were compared with the ‘inappropriate’ fixed-SG condition to examine whether the variable-SG conditions offer an overall benefit compared to FL and FH. Finally, we compared the MI and DI conditions, the primary topic of this work. Based on the above literature, it was expected that the MI condition would be less effortful for drivers than the DI condition, in which they had to change SG themselves.

8.2. Method

8.2.1. Participants

This research complied with the American Psychological Association Code of Ethics and was approved by the Human Research Ethics Committee of the TU Delft. Informed consent was obtained from each participant. Twenty-four participants (4 female) between 22 and 30 years old ($M = 24.9$, $SD = 2.0$) with a valid driving license and normal or corrected-to-normal vision participated in this study. In response to the question of how often they drove in the last 12 months, 1 participant drove less than once a month, 8 drove less than once a week, 13 drove 1–3 days a week, and 2 drove 4–6 days a week. Regarding mileage in the last 12 months, 6 participants drove 1–1000 km, 8 drove 1000–5000 km, 7 drove 5000–10000 km, 2 drove 10000–15000 km, and 1 drove 15000–20000 km.



Figure 8.1. A participant driving in the driving simulator. The dashboard display shows the steering gain (SG) currently active (here colored blue, indicating low SG). The arrow next to the depicted speed indicates the advised SG level (available in the DI condition only). In this figure, participants are advised to switch ‘up’, from low SG to high SG. The left-bottom inset shows the button at the back of the steering wheel that was used to initiate SG transitions. Participants wore headphones that displayed regular driving sounds (Melman et al., 2021b).

8.2.2. Apparatus

The experiment was conducted in a fixed-base driving simulator at the Cognitive Robotics laboratory at the Faculty of Mechanical Engineering of the Delft University of Technology. The simulation was developed using JOAN (Beckers et al., 2021), an open-source software framework developed at the Delft University of Technology, which builds on the CARLA open-source simulator (Version 0.9.8; Dosovitskiy et al., 2017). A 65-inch 4K screen was used to show the vehicle environment (Figure 8.1) with a refresh rate of 60 Hz. A SensoDrive® steering provided self-aligning torques with a fixed steering stiffness of 2.20 Nm/rad and a damping ratio of 0.60 Nms/rad. An Audi S4 (wheelbase 281 cm, width 185 cm, mass 1705 kg) was used to simulate the vehicle dynamics. The data was recorded at 100 Hz, and the update rate of the vehicle environment was 80 Hz. A mouse was attached to the back of the steering wheel for providing inputs to the driver-initiated steering system (left bottom corner Figure 8.1).

8.2.3. Driving Tasks

All participants drove each trial on the same one-way two-lane road in one of the four conditions. The road was 14.3 km long, had lanes of 3.5 m wide, and consisted of three segments of approximately equal length: an overtaking segment, followed by a straight segment and a curved road segment.

The participant's car had a fixed speed of 100 km/h throughout each trial to ensure that the steering demands were the same for all participants. Driving is normally a self-paced task (De Winter et al., 2007; Taylor, 1964), and previous research in the same driving simulator showed that if drivers can choose their own speed, large individual differences in speed arise (Melman et al., 2021b). These individual differences would complicate the comparisons between conditions because driving speed strongly affects lane-keeping performance (Godthelp et al., 1984).

In the overtaking segment, participants, who drove at a constant speed of 100 km/h, needed to swerve through traffic on a straight road. The other cars were driving 60 km/h and were alternately positioned in the left and right lanes (see Figure 8.1). Traffic density gradually increased from low (i.e., longitudinal spacing of 80 m, or 12.5 cars/km) to high (i.e., longitudinal spacing of 40 m, or 25 cars/km), and then gradually reduced back to low (longitudinal spacing of 80 m, or 12.5 cars/km). A higher traffic density can be expected to require a higher SG as the driver needs to provide faster steering inputs to fulfill the task. When the traffic density was high, the driver would have to make a lane change for every 100 m traveled, that is, every 3.6 seconds. In total, participants made 34 lane changes in the overtaking segment.

The second segment was a straight road without traffic, where the driver was instructed to stay in the right lane. The third and final segment consisted of a road with curves of different radii (between 100 and 200 m) without traffic.

8.2.4. Independent Variables

All the participants drove in all of the following four conditions according to a counterbalanced within-subject design.

- Fixed low SG (FL)
- Fixed high SG (FH)
- Machine-initiated SG transitions (MI)
- Driver-initiated SG transitions (DI)

The FL condition featured a fixed steering ratio between the steering wheel and the front wheels of 25:1 throughout the entire track, whereas the FH condition used a fixed steering ratio of 12.5:1. These SG levels correspond to the literature. For example, Millsap and Law

(1996) performed simulation studies with SGs of 24:1 and 14:1, where the latter was regarded as “consistent with a vehicle that is perceived by drivers to be ‘darty’ or difficult to maintain directional control during highway driving” (p. 1157).

The MI condition automatically switched between the two SG levels at predefined locations. During the overtaking segment, the settings changed from low SG to high SG when the traffic density became high (after 6 of 34 lane-change maneuvers) and from high SG to low SG when the traffic density became low again (after 28 of 34 lane-change maneuvers). Finally, 100 m before the curved road segment, the machine switched to high SG.

The DI condition allowed the driver to switch between low and high SG by clicking the left and right buttons of a horizontally-oriented mouse (see Figure 8.1). If the right (i.e., upper) mouse button was pressed, the steering system switched to high SG, and if the left (i.e., lower) mouse button was pressed, the steering system switched to low SG. All participants started the DI trial with the low SG setting. It was reasoned that to enable a meaningful comparison between the DI and MI conditions, participants in the DI condition should have access to the same knowledge about SG switches as available in the MI condition. Accordingly, participants in the DI condition were provided with switching advice, the locations of which were identical to the switching locations of the MI condition. The advised SG setting was displayed to the driver by an arrow: a downward facing arrow to suggest moving to low SG and an upward facing arrow to suggest moving to high SG (see Figure 8.1 for the upward arrow). If the driver already used the same steering setting as the machine would, no arrow was shown.

During a steering setting transition in the MI and DI conditions, the SG was linearly changed in 3.5 s. The current steering setting was visually communicated to the driver through a dashboard display which was either blue for low SG or red for high SG (Figure 8.1). The transition was visualized by changing the color of the dashboard display with a gradient between blue and red (from low to high SG) or between red and blue (high to low SG).

8.2.5. Procedure

First, participants received a combined information sheet and consent form, which detailed the purpose, driving tasks, instructions, and procedures of the study. More specifically, the study was introduced as follows: “*the purpose of this study is to look into the effect of changing steering ratios initiated by the driver (you) or the machine itself. Two steering ratio settings (a slow steering and a fast steering mode) are tested in a machine-initiated steering system and a human-initiated steering system (where the driver can adapt the steering modes), and the designs are compared with two different passive steering systems (passive slow steering and passive fast steering). The effect of these systems is measured in terms of performance, safety margins, driver workload, and system acceptance.*” The document also mentioned the expected experiment duration of 1 hour, that the simulated car had a constant speed and only the steering wheel had to be controlled, that there were practice trials before each main trial, that participants had to complete four trials (FL, FH, MI, DI), and that each trial consisted of three segments (overtaking slow-driving vehicles, straight road without vehicles, curved road without vehicles). The consent form further explained that in the DI condition, participants could press the mouse buttons to change the SG level.

After reading and signing the informed consent form, the participants were requested to sit in the simulator. They first drove two 2.5-minute familiarization trials, one trial with low SG and one trial with high SG, on a curvy road without other vehicles. The experiment was then started. Participants drove four trials, each trial in one of the four conditions (FL, FH, DI, or MI).

Before each experimental trial, a separate 2-minute practice trial was performed to let the participants experience the upcoming condition. The practice trial consisted of two straight-road segments and two curved-road segments. In the case of the DI condition, participants were encouraged to switch between high SG and low SG, and it was mentioned that they

could switch whenever they wanted and that the advice displayed could also be ignored. In the practice trial of the MI condition, the SG switched automatically to low for straights and to high for curves.

Through the information sheet, participants were instructed to drive as follows: “*During the real trials you are asked to drive as you normally would with the emphasis on safe and controlled driving. The test track consists of three sections i.e. overtaking traffic vehicles which have a constant speed on a straight road, following a straight road without traffic vehicles and following a curved road without traffic vehicles. After the experiment you are asked to fill out a questionnaire. ... Task instructions: During the entire track drive as you normally would. You are expected to drive on the right lane unless the traffic situation requires you to drive on the left lane.*” After each trial, the participants stepped out of the simulator and completed a questionnaire about the trial that was just completed. Finally, at the end of the experiment, participants completed a questionnaire about their overall experiences and preferences. The experiment took approximately 75 minutes per participant.

8.2.6. Dependent Measures

The steering wheel angle and steering wheel speed from the SensoDrive were filtered with a zero-phase 2nd-order Butterworth filter for the data analysis. Dependent measures were calculated per participant for the following three road segments: overtaking (the part where the traffic density was maximal, between a traveled distance of 1963 m and 3464 m), straight (between a traveled distance of 5500 m and 9618 m), and curves (between a traveled distance of 9758 and 14345 m).

- *Mean absolute front wheel angle (deg)* describes the variability in steering output, where a higher value was considered poorer lane-keeping behavior. The front-wheel angle is the output of the driver’s steering wheel input after the conversion of the steering gain.
- *Mean absolute lateral velocity (m/s)*. This is a measure of lane-keeping behavior, where a high lateral velocity can be seen as indicative of having to provide extra input to keep the car on the track.
- *Range of lateral position (m)*. This measure, which is defined as the maximum lateral position minus the minimum lateral position, is an index of lane-keeping performance. A higher range implies that the participant made larger lateral excursions and therefore exhibited less safe driving behavior.
- *High SG (0 to 1)*. The proportion of time that was driven with high SG. This measure was always 0 (i.e., low SG) for the FL, and always 1 (i.e., high SG) for the FH condition. For the MI condition, it was 1, 0, and 1, for the overtaking, straight, and curve segments, respectively. For the DI condition, participants could decide whether to drive with the low or high SG setting, and so the value could take any number from 0 to 1. Steering gain settings were considered from the moment the button was pressed, that is, the 3.5-s transition period was not taken into account in computing the *High SG* gain measure.

Additionally, the following measures were obtained from the self-report questionnaire after each trial:

- *Subjective effort per segment (1 to 7)* was used to quantify the perceived effort of the driver per segment. After each trial, the participant was asked to answer for each of the three segments the question “*During the test, it took me little effort to overtake the traffic vehicles (follow the lane on the straight road / follow the lane on the curved road)*,” coded on a seven-point scale from 1 (*Fully agree*), 4 (*Neutral*), to 7 (*Disagree*).
- *Subjective workload (0 to 100)*. The NASA-TLX questionnaire was used to determine participant workload on six facets: mental demand, physical demand, temporal

demand, performance, effort, and frustration (Hart & Staveland, 1988). The items were rated on a 21-point scale from *Very low / Perfect* to *Very high / Failure*, and the overall score was determined as the mean of the six items and converted to a scale from 0 to 100.

Finally, the following measures were extracted from the post-experiment questionnaire:

- *Overall steering system ranking.* The participants were asked “Which steering system do you prefer? Rank the four systems from 1 to 4 (1 most, 4 least)”. Each number could only be used once.
- “When overtaking the traffic vehicles (driving on a straight road / driving on a curved road) I prefer the slow steering response”, coded on a seven-point scale from 1 (*Fully agree*), 4 (*Neutral*), to 7 (*Disagree*).
- *Driver-initiated versus machine-initiated preference.* The participants were asked “Do you prefer letting the machine change the steering modes or changing the steering modes yourself (MI vs HI)?”, with response options machine-initiated and human-Initiated.

8.2.7. Statistical Analysis

Mean differences between the experimental conditions were examined using paired-samples *t*-tests. A total of four paired comparisons per dependent measure were made. First, FL was compared with FH. For the overtaking and curve-driving segments, the FH condition was expected to yield more favorable outcomes (better lane-keeping, low effort) than FL, whereas, for the straight segment, the opposite was expected. Second and third, the DI and MI conditions were compared with the ‘inappropriate’ fixed-SG condition for that segment to examine whether the variable-SG conditions offer a benefit compared to a static SG. Thus, for the overtaking and curve-driving segments, the comparison of DI and MI was made with FL, whereas for the straight segment, the comparison was made with FH. Finally, the DI and MI conditions were compared with each other.

Within-subject effect sizes d_z were calculated according to Faul et al. (2007). A Bonferroni correction was applied, which means that the alpha value of 0.05 was reduced by a factor of four (i.e., $\alpha = 0.0125$).

8.3. Results

Figure 8.2 shows the mean steering wheel angle, mean lateral position, and mean absolute lateral velocity for the FL and FH conditions. The steering wheel angles in the FL condition were higher than those in the FH condition due to the factor-two difference in SG. More specifically, the mean absolute steering wheel angle for FL and FH, respectively, was 7.33 and 3.84 deg in the overtaking segment, 0.41 and 0.30 deg in the straight segment, and 27.96 and 13.99 deg in the curve segment. For the curved road segment, some participants in the FL condition had difficulty driving through sharp curves, as reflected by large lateral excursions and high absolute lateral velocity.

Figure 8.3 shows the mean steering wheel angle, mean absolute lateral velocity, and number of participants driving with high SG for the MI and DI conditions. The steering angles were relatively similar for MI and DI, which can be explained by the fact that participants in the DI condition tended to follow the depicted advice and, accordingly, mostly drove with similar SG as the MI condition.

However, as can be seen in the bottom panel of Figure 8.3, not all participants followed the advice, as some made intermediate switches. More specifically, in the MI condition, there were always three transitions between SG levels, while in the DI condition, the mean number of switches per participant was 5.50 ($SD = 2.23$, min = 3, max = 12). One participant drove

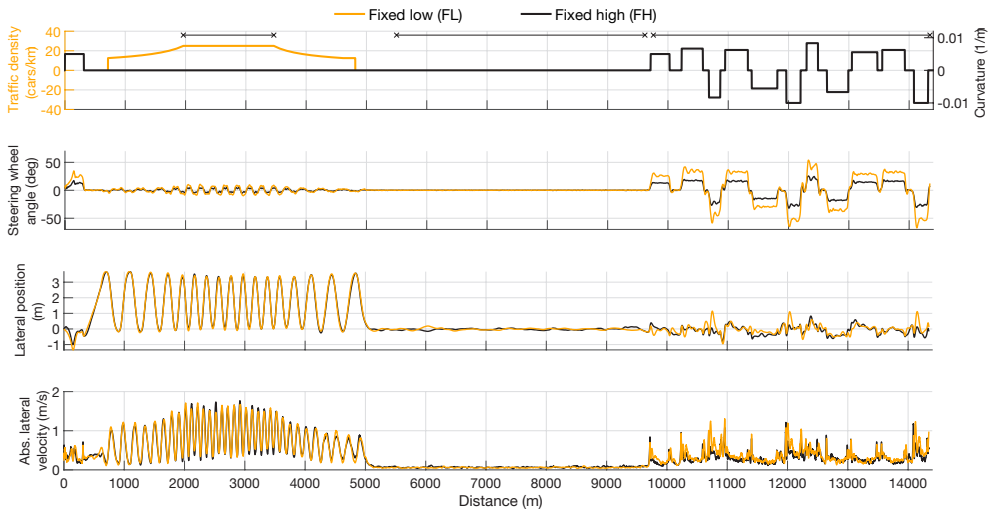


Figure 8.2. The mean steering wheel angle (second panel), mean lateral position with respect to the center of the right lane (third panel), and mean absolute lateral velocity (fourth panel) for the fixed low (FL) and fixed high (FH) conditions. Positive values indicate a left curve, steering, and lateral movement. The first (top) panel shows traffic density, road curvature, and three horizontal line segments that demarcate the three segments used in the analysis: overtaking, straight, and curves.

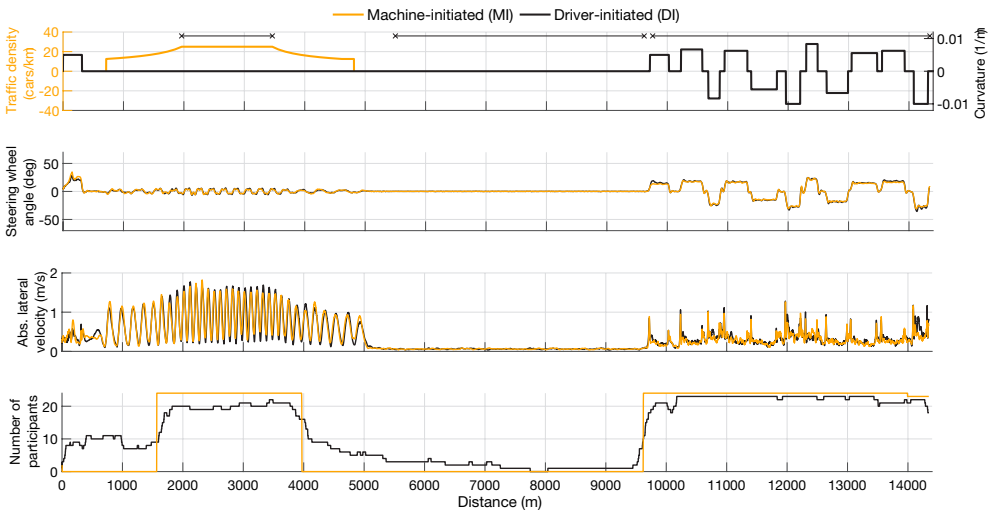


Figure 8.3. The mean steering wheel angle (second panel), mean absolute lateral velocity (third panel), and the number of participants driving with high steering gain (SG) (fourth panel) for the machine-initiated (MI) and driver-initiated (DI) conditions. Positive values indicate a left curve, steering, and lateral movement. The first (top) panel shows traffic density, road curvature, and three horizontal line segments that demarcate the three segments used in the analysis: Overtaking, straight, and curves.

Table 8.1. Means (*M*), standard deviations (*SD*), and effect sizes (*d_z*) per dependent measure and experimental condition.

Overtaking segment	Mean				Standard deviation				Effect size (<i>d_z</i>)					
	FL	FH	MI	DI	FL	FH	MI	DI	FL-FH	FL-MI	FL-DI	FH-MI	FH-DI	MI-DI
Subjective effort (1 to 7)	2.54	1.96	2.25	1.83	1.50	1.00	1.48	1.24	0.42	0.16	0.40			0.22
Mean abs. front wheel angle (deg)	0.293	0.307	0.324	0.295	0.051	0.084	0.091	0.063	-0.22	-0.46	-0.03			0.41
Mean abs. lateral velocity (deg/s)	1.015	0.976	0.976	0.962	0.118	0.117	0.113	0.128	0.41	0.53	0.64			0.15
Lateral position range (m)	4.46	4.30	4.45	4.25	0.55	0.62	0.71	0.57	0.22	0.02	0.40			0.30
Mean SG (0 to 1)	0.00	1.00	1.00	0.83	0.00	0.00	0.00	0.31						
Straight segment														
Subjective effort (1 to 7)	1.42	2.21	1.46	1.63	0.78	1.50	0.658	0.92	-0.56			0.55	0.47	-0.30
Mean abs. front wheel angle (deg)	0.016	0.024	0.016	0.016	0.006	0.014	0.007	0.007	-0.77			0.85	0.63	-0.16
Mean abs. lateral velocity (deg/s)	0.059	0.069	0.062	0.060	0.018	0.029	0.019	0.018	-0.44			0.36	0.42	0.09
Lateral position range (m)	1.14	1.16	1.21	1.08	0.36	0.41	0.37	0.26	-0.06			-0.13	0.27	0.41
Mean SG (0 to 1)	0.00	1.00	0.00	0.07	0.00	0.00	0.00	0.14						
Curve segment														
Subjective effort (1 to 7)	3.75	2.71	2.29	2.92	1.48	1.23	0.81	1.28	0.73	1.14	0.67			-0.62
Mean abs. front wheel angle (deg)	1.118	1.119	1.122	1.119	0.014	0.014	0.017	0.016	-0.10	-0.30	-0.07			0.20
Mean abs. lateral velocity (deg/s)	0.374	0.319	0.312	0.332	0.114	0.082	0.071	0.085	0.95	1.01	0.66			-0.57
Lateral position range (m)	3.31	2.84	2.81	3.27	1.02	0.76	0.88	1.08	0.66	0.58	0.05			-0.60
Mean SG (0 to 1)	0.00	1.00	1.00	0.93	0.00	0.00	0.00	0.20						
Overall subjective ratings														
NASA TLX overall (0 to 100)	33.1	31.81	28.75	31.01	15.87	13.52	10.70	12.71	0.15	0.42	0.32	0.30	0.10	-0.30

Note. The effect sizes are color-coded for visual clarity purposes. The color-coding ranges from -1.5 (red) to 0 (white) to 1.5 (green). $|d_z| > 0.553$: $p < 0.0125$ (marked in boldface), $|d_z| > 0.769$: $p < 0.001$. For the overtaking and curve segments, comparisons between DI/MI and FL are shown, and for the straight segment, comparisons between DI/MI and FH are shown, (i.e., to test whether variable SG provides benefits compared to the fixed SG level for that was inappropriate for that road segment.).

the entire curve segment with low SG. It can also be seen that about five participants took a long time to switch back to low SG settings in the overtaking segment; that is, they appeared to have initially missed or ignored the presented advice and waited until they had overtaken all cars and drove on the straight, before switching to low SG. The switch back to high SG for the curve segment was more immediate, with about 10 participants even switching before the advice was displayed.

Table 1 shows the means, standard deviations, and effect sizes for the dependent measures per segment.

FH vs. FL. In the curve-driving segment, participants' subjective effort, mean absolute lateral velocity, and lateral position range were higher for FL than for FH. For the overtaking segment, differences between FL and FH were nonsignificant, but of the same sign. On the straight road, where high SG was expected to be detrimental, FH led to higher subjective effort than FL. Furthermore, the mean absolute front wheel angle was lower for FL compared to FH, suggesting that it was more difficult to drive accurately on a straight road with FH compared to FL. In summary, the comparison of FH and FL indicates that participants benefited from high SG in curves and from low SG on straights.

MI & DI vs. FL/FH. As seen in Table 1, participants benefited from variable settings (MI & DI) in comparison to the fixed steering sensitivity. More specifically, on the straight segment, MI and DI yielded lower subjective effort than FH, and in the curve segment, MI and DI yielded lower subjective effort than FL. In the same vein, participants showed improved lane-keeping (lower lateral velocities during overtaking and curves, smaller absolute front wheel angles on straights) with MI and DI compared to the fixed SG levels.

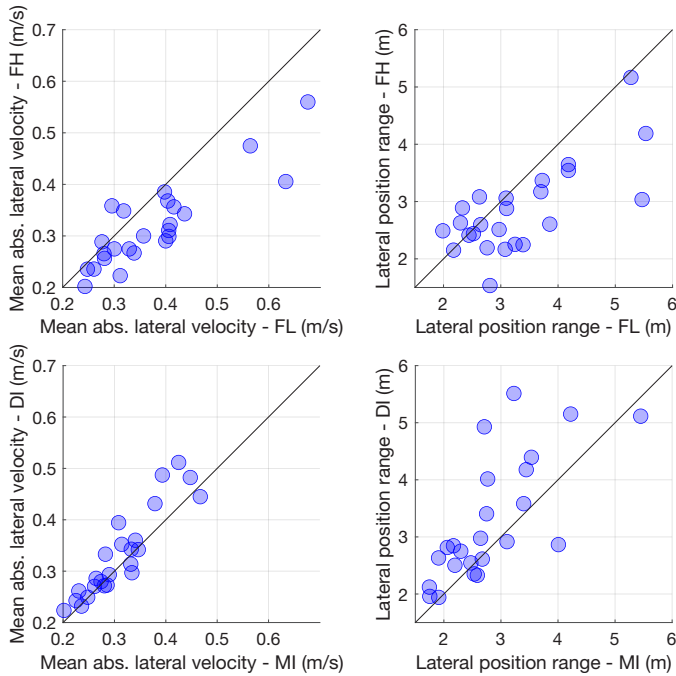


Figure 8.4. Mean absolute lateral velocity and lateral position range for the fixed high (FH) vs. fixed low (FL) conditions, and for the driver-initiated (DI) vs. machine-initiated (MI) conditions, for the curve-driving segment. Each marker represents a participant. The diagonal line is the line of unity.

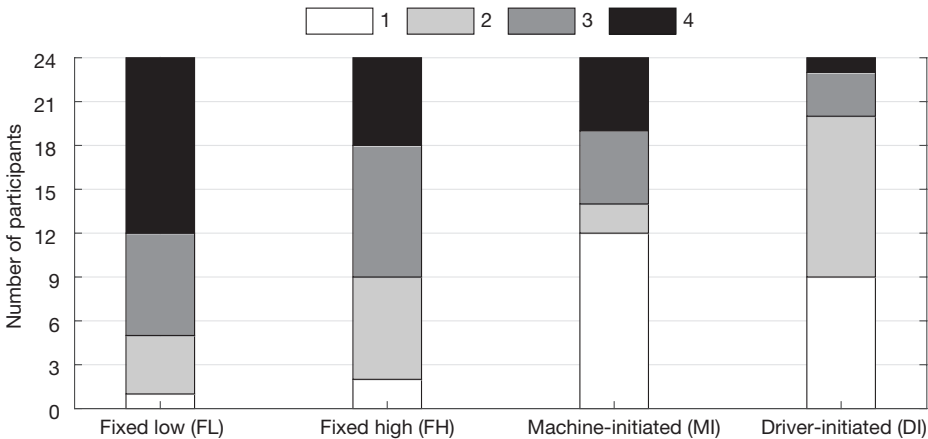


Figure 8.5. Ranking of the steering systems, with 1 representing the most preferred and 4 the least preferred.

MI vs. DI. In the curve segment, a lower subjective effort was found for MI compared to DI. Also, participants showed poorer lane-keeping (larger range and velocity of lateral position) for the DI condition compared to the MI condition.

Table 1 provides numerical information and does not elucidate how the experimental effects manifest themselves at the individual level. Therefore, a scatter plot is provided for several key

comparisons of interest. More specifically, Figure 8.4 shows lane-keeping measures related to the curve-driving segment for FH versus FL (top two figures) and DI versus MI (bottom two figures). It can be seen that most points lie below or above the diagonal line, consistent with the statistically significant effects shown in Table 1. At the same time, individual differences are substantial, as could also be inferred from the large standard deviations in Table 1.

Overall Ratings of Conditions. The NASA-TLX showed the lowest workload for MI and the highest for FL; however, these effects were not statistically significant. The post-experiment ranking showed that MI and DI were significantly better-ranked than FL, and DI better than FH. Interestingly, although 12 participants ranked MI as the most preferred, 10 participants ranked it third or fourth (Figure 8.5). In comparison, for the DI condition, 9 participants ranked it first, and only 4 participants ranked it third or fourth. To the question, “Do you prefer letting the machine change the steering modes or changing the steering modes yourself?” 11 participants reported preferring MI, and 13 preferred DI.

Finally, in response to the question: “I prefer the slow steering response”, means (SDs) on the 7-point scale from 1 (Fully agree) to 7 (Disagree) were 4.54 (1.93), 1.38 (0.65), and 6.08 (0.97), for overtaking, straight-line driving, and curve-driving, respectively. These findings are consistent with the above results in that different driving environments require different SG levels.

8.4. Discussion

This study aimed to examine the effects of adaptive and adaptable transitions in steering gain (SG) on perceived effort, lane-keeping behavior, and system preference. In a simulator experiment, we compared two fixed SG levels and two systems that could switch between the low and high SG, either in an adaptable manner, that is initiated by the driver via a press of a button (DI) or in an adaptive manner, that is automatically by the car and triggered based on the location of the vehicle (MI). A test road was designed with segments that were hypothesized to require different SG settings. Based on the literature, we expected that machine-initiated transitions would reduce workload since the machine controls the adaptation and the driver is able to focus on the driving task.

In accordance with the intended experimental design, different SG levels were found to be appropriate for different road segments: Compared to a fixed low steering gain (FL), driving with a fixed high steering gain (FH) was perceived by participants as more effortful and resulted in poorer lane-keeping behavior on straights, while the opposite held in curves and to a lesser extent during overtaking maneuvers. A possible explanation for the relatively small differences between FL and FH in the overtaking segment is that the required steering angles were not as large as in the curve driving segment (see Figures 2 and 3, Table 1). That is, although high SG was the recommended setting for the overtaking segment, the overtaking segment could also be comfortably driven with low SG. Literature indicates that the relationship between control-output gain and task performance follows a U-curve that results from the benefits of high gain in terms of movement amplitude and benefits of low gain in terms of precise control (Chapanis & Kinkade, 1972; MacKenzie, 2013, p. 81). Our steering sensitivity levels were selected based on realistic values (Millsap & Law, 1996) and a pilot study (Kroes, 2019). The observed SG \times road-type interaction suggests that drivers may benefit from a steering gain that is adjusted or adjustable. The experimental results concur that the MI and DI conditions yielded favorable outcomes compared to driving with the SG level that was inappropriate for that road segment.

The literature indicates that, compared to adaptable automation, adaptive automation reduces workload at the possible cost of unpredictability: “Doing tasks directly costs more workload, but the payoff is greater awareness of how the task is being done” (Miller &

Parasuraman, 2007, p. 60). The current study also found a workload reduction for adaptive automation. More specifically, on curved roads, the MI condition produced lower effort ratings combined with better lane-keeping performance than the DI condition. The explanation for these findings is two-fold: (1) In the DI condition, there are at least some participants who drove with the "wrong" setting for some of the time (i.e., low SG instead of high SG), making them susceptible to the same performance deficits as observed in the FL condition, and (2) in the DI condition, drivers had to spend some effort to determine if and when a switch can be made and press a button (usually participants did so when driving in between curves).

In the overtaking segment, however, there were no significant differences in effort ratings between MI and DI. This lack of effort reduction for MI in the overtaking segment may be explained by unpredictability: the automatic SG switch occurred while the participants were still overtaking cars (in comparison, for the curve segment, the switch occurred 100 m before the first curve). This explanation is supported by the fact that some participants in the DI condition did not readily respond to the low SG advice after the overtaking segment, suggesting that this advice was ignored or missed.

The ranking of the four conditions showed that the MI and DI steering systems were more preferred than the fixed steering gains. However, despite the improved performance for MI, a substantial portion of the participants gave low preference rankings to the MI condition. Possible explanations are that drivers in the MI condition disliked its unpredictability and the inability to choose the steering gain themselves. More generally, literature in aviation automation suggests that automation-mode confusions may arise if mode changes are not initiated by the human operator but by an external trigger (Sarter & Woods, 1995). Similarly, it can be expected that, despite the colored SG mode display on the dashboard, some drivers in the MI condition had difficulty understanding why an SG switch had occurred. Future research should examine whether the SG setting should be displayed to drivers, such as in the current study, or whether this information should remain hidden. The latter solution may have some benefits as it minimizes visual distraction, but it may also exacerbate mode confusion.

In comparison to the MI condition, the DI condition gave drivers flexibility. In essence, if drivers in the DI condition preferred low (high) SG, they could select the low (high) SG setting at the start of their drive. That is, the DI condition can deliver what FL and FH can also deliver, which can explain why the DI condition was hardly ranked third or fourth (see Figure 8.5). This observation is in line with a study on adaptable automation by Sauer and Chavaillaz (2018), which concluded that the primary advantage of adaptive automation is that it supports diverse types of operators, who differ in their preferences. A correlation analysis provided support for the notion that the DI condition facilitated individual preferences: participants who ranked the FL condition higher (i.e., more preferred) were more likely to select a low SG in the DI condition (see Supplementary Material). Even though MI delivered better driving performance than DI, it can be argued that driver preference is just as important, or as noted by De Waard and Brookhuis (1999): "*A system may function perfectly in the technical sense, if it is not accepted by the public, it will not be used*" (p. 50). An additional advantage of the DI system compared to the MI system is that the DI system is easier to implement, as it does not rely on GPS and maps that define which SG level should be selected.

As shown in Figure 8.3, participants in the DI condition drove with approximately the same SG level as in the MI condition. That is, the great majority of participants in the DI condition switched to high SG when overtaking cars, to low SG on the straight, and back to high SG in curves. The high similarity may be due to the fact that the trigger locations of the MI system were chosen appropriately, that is, in such a way that they correspond to the participants' preferred SG setting. However, the high similarity just as well be caused by the strong tendency of participants to follow the switching advice displayed in the DI condition. Possibly, participants' reliance on the advice in the current experimental setting was stronger

than it would be when driving a real car, where disuse of feedback systems is a known concern (Kidd et al., 2017). On the other hand, about half of the participants made the switch *before* the high-SG advice was displayed, suggesting that these participants anticipated the upcoming steering demands and were not just relying on the advice.

A limitation of our experiment was that it was conducted with young and predominantly male students with a relatively low yearly driving mileage. Future research is needed with other population groups, such as expert and older drivers. Based on earlier literature on ADAS and older drivers (Classen et al., 2019; Young et al., 2017), it can be expected that older drivers may benefit from automation support, such as offered by the MI condition. At the same time, older drivers may have more difficulty driving while simultaneously processing other visual information, such as mode status and mode-changing advice.

Another limitation is that the machine-initiated transitions occurred at preprogrammed locations. Future studies could consider the current steering angle and driver state to determine safe moments for machine-initiated transitions. Note that, in the current study, abrupt and potentially dangerous SG transitions were prevented by smoothly changing the SG smoothly over a period of 3.5 s. Future research should also examine whether our findings replicate for different types of HMIs and advice in the DI condition or no displayed advice at all, and conditions in which the driver can choose from a range of SG levels. Furthermore, future studies could explore the potential benefits of variable SG for specific situations, such as understeer or oversteer prevention (e.g., Heathershaw, 2004) and lane changes (e.g., Wang et al., 2017).

This study found that different driving tasks (e.g., overtaking and curve driving vs. straight-line driving) benefit from different SG levels and that a flexible SG (DI & MI) reduces subjective effort and yields better lane-keeping than a static SG (FL or FH). In turn, the MI condition yielded lower effort and better lane-keeping performance in curves than the DI condition but was disliked by some drivers. Whether the same driving behaviors would be elicited on real roads, on which drivers can be expected to be 'satisficers' (Hancock, 1999), and speed is not kept constant, remains unknown. Although simulators have been found to exhibit relative validity in short-lasting experiments such as ours (e.g., Klüver et al., 2016), how drivers would respond to MI and DI systems in the long term is unknown. An analysis of learning trends showed that participants demonstrated slightly smaller steering angles as the experiment progressed, indicating more stable control (see Supplementary Material). With prolonged driving experience, underutilization and disuse of technology can become factors to be considered, as indicated above. Test track studies and field operational tests would be required to examine whether DI and MI are viable and safe solutions for future traffic.

Data Availability

Raw data, MATLAB scripts used for the analyses, and a demonstration video can be accessed here: <https://doi.org/10.4121/20484999>

References

- Beckers, N., Siebinga, O., Giltay, J., & Van der Kraan, A. (2021). *JOAN, a human-automated vehicle experiment framework* (Version 1.0) [Computer software]. <https://github.com/tud-hri/joan>
- Black, J., Freeman, P. T., Wagner, J. R., Iyasere, E., Dawson, D. M., & Switzer, F. S. (2014). Evaluation of driver steering preferences using an automotive simulator. *International Journal of Vehicle Design*, 66, 124–142.
- BMW. (2022). *Drive modes in detail*. <https://ownersmanuals2.com/bmw-auto/x5-2021-owners-manual-80671/page-161>
- Chapanis, A., & Kinkade, R. G. (1972). Design of controls. In H. P. van Cott & R. G. Kinkade (Eds.), *Human engineering guide to equipment design* (pp. 345–379). Washington, DC: American Institute for Research.
- Classen, S., Jeghers, M., Morgan-Daniel, J., Winter, S., King, L., & Struckmeyer, L. (2019). Smart in-vehicle technologies and older drivers: a scoping review. *OTJR: Occupation, Participation and Health*, 39, 97–107.

- De Winter, J. C. F., & De Groot, S. (2012). The effects of control-display gain on performance of race car drivers in an isometric braking task. *Journal of Sports Sciences*, *30*, 1747–1756.
- De Winter, J. C. F., Wieringa, P. A., Kuipers, J., Mulder, J. A., & Mulder, M. (2007). Violations and errors during simulation-based driver training. *Ergonomics*, *50*, 138–158.
- Dosovitskiy, A., Ros, G., Codevilla, F., Lopez, A., & Koltun, V. (2017). CARLA: An open urban driving simulator. *Proceedings of Machine Learning Research*, *78*, 1–16.
- Faul, F., Erdfelder, E., Lang, A. G., & Buchner, A. (2007). G*Power 3: A flexible statistical power analysis program for the social, behavioral, and biomedical sciences. *Behavior Research Methods*, *39*, 175–191.
- Godthelp, H., Milgram, P., & Blaauw, G. J. (1984). The development of a time-related measure to describe driving strategy. *Human Factors*, *26*, 257–268.
- Gross, F. G. (1977). *The measurement and comparison of relative workloads under several driving conditions using a simulator* [Doctoral dissertation]. Virginia Polytechnic Institute and State University.
- Hancock, P. A. (2007). On the process of automation transition in multitask human-machine systems. *IEEE Transactions on Systems, Man, and Cybernetics-Part A: Systems and Humans*, *37*, 586–598.
- Hart, S. G., & Staveland, L. E. (1988). Development of NASA-TLX (Task Load Index): Results of empirical and theoretical research. *Advances in Psychology*, *52*, 139–183.
- Heathershaw, A. (2004). Matching of chassis and variable ratio steering characteristics to improve high speed stability. *SAE Technical Paper Series*, 2004-01-1103.
- Jamson, A. H., Whiffin, P. G., & Burchill, P. M. (2007). Driver response to controllable failures of fixed and variable gain steering. *International Journal of Vehicle Design*, *45*, 361–378.
- Johnson, M., Bradshaw, J. M., Feltovich, P. J., Jonker, C. M., Van Riemsdijk, M. B., & Sierhuis, M. (2014). Coactive design: Designing support for interdependence in joint activity. *Journal of Human-Robot Interaction*, *3*, 43–69. <https://doi.org/10.5898/JHRI.3.1>.
- Kaber, D. B., & Prinzl, L. J., III (2006). *Adaptive and adaptable automation design: A critical review of the literature and recommendations for future research* (NASA/TM-2006-214504). Hampton, VI: National Aeronautics and Space Administration, Langley Research Center.
- Kidd, D. G., Cicchino, J. B., Reagan, I. J., & Kerfoot, L. B. (2017). Driver trust in five driver assistance technologies following real-world use in four production vehicles. *Traffic Injury Prevention*, *18*, S44–S50.
- Kidwell, B., Calhoun, G. L., Ruff, H. A., & Parasuraman, R. (2012). Adaptable and adaptive automation for supervisory control of multiple autonomous vehicles. *Proceedings of the Human Factors and Ergonomics Society Annual Meeting*, *56*, 428–432.
- Koehn, P., & Eckrich, M. (2004). Active steering—the BMW approach towards modern steering technology. *SAE Technical Paper Series*, 2004-01-1105.
- Kroes, R. (2019). *The impact of steering ratio variability to road profiles on driver acceptance and driving behaviour* [Master's thesis]. Delft University of Technology. <http://resolver.tudelft.nl/uuid:057dda58-f06c-4e89-8744-e14b267a94a5>
- Li, H., Sarter, N., Wickens, C., & Sebok, A. (2013). Supporting human-automation collaboration through dynamic function allocation: The case of space teleoperation. *Proceedings of the Human Factors and Ergonomics Society Annual Meeting*, *57*, 359–363.
- Melman, T., De Winter, J., Mouton, X., Tapus, A., & Abbink, D. (2021a). How do driving modes affect the vehicle's dynamic behaviour? Comparing Renault's MultiSense sport and comfort modes during on-road naturalistic driving. *Vehicle System Dynamics*, *59*, 485–503.
- Melman, T., Visser, P., Mouton, X., & De Winter, J. C. F. (2021b). Creating the illusion of sportiness: Evaluating modified throttle mapping and artificial engine sound for electric vehicles. *Journal of Advanced Transportation*, 4396401.
- Miller, C. A., & Parasuraman, R. (2007). Designing for flexible interaction between humans and automation: Delegation interfaces for supervisory control. *Human Factors*, *49*, 57–75.
- Millsap, S. A., & Law, E. H. (1996). Handling enhancement due to an automotive variable ratio electric power steering system using model reference robust tracking control. *SAE Technical Paper Series*, 960931.
- Olson, P. L., & Thompson, R. R. (1970). The effect of variable-ratio steering gears on driver preference and performance. *Human Factors*, *12*, 553–558.
- Renault. (2022). *MULTI-SENSE*. <https://gb.e-guide.renault.com/eng/easy-link/MULTI-SENSE>
- Reuter, M., & Saal, A. (2017). Superimposed steering system. In M. Harrer & P. Pfeffer (Eds.), *Steering handbook* (pp. 469–492). Cham: Springer.
- Russell, H. E., Harbott, L. K., Nisky, I., Pan, S., Okamura, A. M., & Gerdes, J. C. (2016). Motor learning affects car-to-driver handover in automated vehicles. *Science Robotics*, *1*.
- Ryan, M. (2019). Intelligent speed assistance technologies: A review. Proceedings of the Irish Transport Research Network (IRTN) Conference. Retrieved from: https://www.researchgate.net/profile/Margaret-Ryan-8/publication/335722660_Proceedings_of_the_IRTN2019_5_th_-6_th_September_QUB_Margaret_Ryan_Intelligent_Speed_Assistance_Technologies_A_review_Intelligent_Speed_Assistance_Technologies_A_Review/links/5d779695299bf1cb80956e6b/Proceedings-of-the-ITRN2019-5-th-6-th-September-QUB-Margaret-Ryan-Intelligent-Speed-Assistance-Technologies-A-review-Intelligent-Speed-Assistance-Technologies-A-Review.pdf

- Sauer, J., Kao, C. S., & Wastell, D. (2012). A comparison of adaptive and adaptable automation under different levels of environmental stress. *Ergonomics*, 55, 840–853.
- Shoemaker, N. E., Dell'Amico, F., & Chwalek, R. J. (1967). A pilot experiment on driver task performance with fixed and variable steering ratio. *SAE Technical Paper Series*, 670508.
- Shibahata, Y. (2005). Progress and future direction of chassis control technology. *Annual Reviews in Control*, 29, 151–158.
- Shimizu, Y., Kawai, T., & Yuzuriha, J. (1999). Improvement in driver-vehicle system performance by varying steering gain with vehicle speed and steering angle: VGS (Variable Gear-ratio Steering system). *SAE Technical Paper Series*, 1999-01-0395.
- Taylor, D. H. (1964). Drivers' galvanic skin response and the risk of accident. *Ergonomics*, 7, 439–451.
- Wang, W., Xi, J., Liu, C., & Li, X. (2017). Human-centered feed-forward control of a vehicle steering system based on a driver's path-following characteristics. *IEEE Transactions on Intelligent Transportation Systems*, 18, 1440–1453.
- Young, K. L., Koppel, S., & Charlton, J. L. (2017). Toward best practice in Human Machine Interface design for older drivers: A review of current design guidelines. *Accident Analysis & Prevention*, 106, 460–467.

Appendix 8A

Table 8A. Means (*M*), standard deviations (*SD*), and effect sizes (*d_z*) per dependent measure and order of presentation (1 = first trial, 2 = second trial, 3 = third trial, 4 = fourth trial).

Overtaking segment	Mean				Standard deviation				Effect size (<i>d_z</i>)					
	1	2	3	4	1	2	3	4	1-2	1-3	1-4	2-3	2-4	3-5
Subjective effort (1 to 7)	2.38	2.13	2.04	2.04	1.44	1.30	1.20	1.43	0.18	0.22	0.16	0.06	0.05	0.00
Mean abs. front wheel angle (deg)	0.322	0.305	0.302	0.291	0.053	0.081	0.069	0.090	0.30	0.44	0.39	0.08	0.18	0.13
Mean abs. lateral velocity (deg/s)	1.017	0.982	0.968	0.963	0.109	0.137	0.112	0.117	0.37	0.70	0.55	0.17	0.22	0.05
Lateral position range (m)	4.53	4.28	4.34	4.31	0.55	0.66	0.61	0.63	0.38	0.39	0.31	-0.12	-0.04	0.05
High SG (0 to 1)	0.46	0.45	0.48	0.45	0.49	0.50	0.50	0.50	0.01	-0.03	0.01	-0.04	0.00	0.04
Straight segment														
Subjective effort (1 to 7)	1.625	1.667	1.833	1.583	1.13	1.20	1.167	0.65	-0.04	-0.14	0.03	-0.17	0.08	0.24
Mean abs. front wheel angle (deg)	0.018	0.018	0.018	0.018	0.007	0.010	0.006	0.015	-0.01	0.18	-0.01	0.13	0.00	-0.07
Mean abs. lateral velocity (deg/s)	0.059	0.063	0.065	0.062	0.017	0.022	0.021	0.027	-0.23	-0.40	-0.16	-0.15	0.02	0.12
Lateral position range (m)	1.114	1.142	1.22	1.113	0.30	0.38	0.31	0.41	-0.09	-0.37	0.00	-0.26	0.09	0.29
High SG (0 to 1)	0.021	0.026	0.024	0.003	0.07	0.11	0.08	0.01	-0.04	-0.03	0.27	0.01	0.20	0.26
Curve segment														
Subjective effort (1 to 7)	3.33	2.96	2.79	2.58	1.31	1.12	1.41	1.38	0.26	0.31	0.43	0.12	0.30	0.22
Mean abs. front wheel angle (deg)	1.125	1.120	1.119	1.115	0.018	0.015	0.011	0.015	0.45	0.41	0.71	0.07	0.50	0.30
Mean abs. lateral velocity (deg/s)	0.333	0.327	0.337	0.341	0.091	0.083	0.096	0.099	0.12	-0.05	-0.13	-0.11	-0.27	-0.05
Lateral position range (m)	3.17	3.03	2.98	3.07	1.27	0.75	0.74	1.01	0.15	0.18	0.11	0.07	-0.07	-0.10
High SG (0 to 1)	0.49	0.45	0.50	0.50	0.50	0.50	0.51	0.51	0.04	-0.01	-0.01	-0.05	-0.05	0.00
Overall subjective ratings														
NASA TLX overall (0 to 100)	33.06	30.80	30.63	30.21	11.47	13.60	15.23	12.94	0.34	0.22	0.31	0.02	0.09	0.05
Preference rank (1 to 4)	2.5	2.46	2.25	2.79	1.14	0.93	1.33	1.06	0.03	0.11	-0.16	0.11	-0.20	-0.29

Note. The effect sizes are color-coded for visual clarity purposes. The color-coding ranges from -1 (red) to 0 (white) to 1 (green). $|d_z| > 0.553$: $p < 0.0125$ (marked in boldface), $|d_z| > 0.769$: $p < 0.001$.

A Proactive Method to Assist Eco-driving



Eco-driving has the potential to substantially reduce energy consumption, but empirical evidence suggests the potential benefits are transient. A more direct approach to stimulate eco-driving is through an eco mode, which adapts powertrain settings. In practice, however, this feature tends to be underutilized, mostly due to a lack of acceleration performance. This paper describes the design and preliminary testing of a proactive eco mode that assists drivers in driving eco-friendly without being limited by the vehicle's acceleration performance. The system uses a pre-recorded database of location-specific driving behavior and road topology, in order to proactively increase powertrain settings at locations where acceleration is needed. Additionally, the system mitigates conflicts in case of misalignment with actual driver needs by overruling the proactive eco mode settings. The proactive eco mode was implemented in a Renault Talisman and tested with nine drivers driving on French roads. When driving with the proactive eco mode, the participants reached their target speed significantly faster while having similar energy consumption over the same distance compared to the non-adaptive eco mode. Moreover, all nine drivers rated the proactive eco mode as 'adding value' and rated the system as 'easier to reach a target speed' compared to the conventional non-adaptive eco mode. This study suggests that eco-driving (and its beneficial effects on energy consumption) can be stimulated by location-specific triggering of powertrain settings that facilitate acceleration.

Published as:

Melman, T., Beckers N. W. M., De Winter J. C. F., Mouton, X., & Abbink, D. A. (2022). *A proactive method to assist eco-driving*. Manuscript submitted for publication

Patented as:

Beckers N. W. M., Melman, T., Abbink, D. A., & Mouton, X. (2022). *ProActive Driving Mode* (French Patent No. FR2200162). Renault SAS

9.1. Introduction

Stimulating a driver to drive economically has the potential to substantially reduce energy consumption and emissions compared to normal driving (Barkenbus, 2010). Successful eco-driving behavior includes maintaining a uniform throttle position, minimizing speed oscillations while cruising, and avoiding excessive speed; in other words, it requires the driver to anticipate oncoming road situations (Alam & McNabola, 2014; Ericsson, 2001; Huang et al., 2018; Melman et al., 2021a; Sanguinetti et al., 2017).

An approach to stimulate eco-driving behavior is to provide drivers with the option to select an eco mode. An eco mode sets powertrain characteristics related to reducing energy consumption, including adopting an earlier gear-switching strategy and modifying the throttle mapping (i.e., the relation between throttle driver and normalized requested engine torque; Melman et al., 2021c). As a result, an eco mode helps to keep the engine speed and corresponding engine power low and thereby reduce energy consumption (Melman et al., 2021b).

In practice, eco modes do not necessarily lead to the promised reduction in energy consumption because drivers can adapt their behavior to the eco mode, in particular during acceleration phases. Based on real-world driving behavior, Kutzner et al. (2021) found that drivers that drove with an eco mode resulted in similar fuel consumption compared to drivers without the eco mode engaged. Drivers with eco mode engaged accelerated just as quickly as drivers without an eco mode, adapting their behavior to compensate for the limited acceleration performance imposed by the eco mode by pressing the throttle pedal more deeply than needed to smoothly accelerate, negating the likely intention of the eco mode (Melman et al., 2022). An eco mode can also result in driver frustration due to the lower acceleration performance, possibly hampering eco mode acceptance (e.g., Allison et al., 2022).

The limited benefits of an eco mode might be because it reduces the vehicle's acceleration performance all the time for every driving situation, whereas energy-efficient driving in different driving situations requires different acceleration performance. Literature suggests that 'slow' accelerations are energy-efficient for small speed differences, whereas 'stronger' accelerations to quickly reach a target speed is optimal for large speed differences (Dib et al., 2014; Mensing et al., 2013; Saerens & Van den Bulck, 2013). As a result, a conventional eco mode lacks the power when stronger accelerations are needed for large speed differences, for example, when accelerating onto a highway. Ideally, to improve driver acceptance and eco mode usage, an eco mode should adapt the powertrain settings based on the driving situation.

Such an adaptive eco mode system could anticipate when more acceleration performance is needed and adapt the powertrain settings just *before* the start of an acceleration phase. Likewise, an eco mode could predict cruising phases and select the powertrain setting that facilitates low engine speed and power as soon as the target speed is reached. In other words, an adaptive eco mode that proactively adapts the powertrain settings based on the demands of the oncoming driving situation.

The situational demands can be described by the predicted power that the driver requires for the oncoming driving situation, for example high power to strongly accelerate or low power to maintain speed or to make small speed adjustments. We, therefore, base the proactive powertrain adaptations on the predicted power. In a recent study, we observed that variability in driving behavior is predominantly dictated by the location where you drive rather than who is driving (Melman et al., 2021a). This allows us to predict power based on a location-specific driving behavior database in which relevant behavior (velocity, acceleration) are linked to geographical location through GPS tracking - a common approach in driving behavior studies and various commercial services for navigation (Grengs et al., 2008; Hofmann-Wellenhof et al., 2003)

However, the power predictions can be inaccurate, for example due to dynamic road situations such as other traffic and can lead to incorrect adaptations. If conflicts due to incorrect predictions persist, it is likely to lead to system frustration, increased workload (Kaber & Endsley, 2004) and could ultimately lead to disuse (Parasuraman & Riley, 1997). We, therefore, follow a human-centered automation design approach, in which conflicts between driver and automation are minimized by keeping the driver primarily in charge of the driving task and through monitoring the current driver behavior and ensuring the driver can influence or override the automation at any time (Abbink et al., 2018; Johnson et al., 2014).

In this study, we aim to design, implement, and test a proactive eco mode that – while conserving low energy consumption – assists the driver to reach a target speed by temporarily improving the vehicle’s acceleration performance compared to a non-adaptive eco mode. First, we present the proactive eco mode method (Sec. 9.2). Second, the functionality of the proactive eco mode was demonstrated in a real-world test vehicle in an urban traffic setting in France using 12 Renault experts with different fields of expertise (Sec. 9.3). We show that the proactive eco mode can locally improve acceleration performance while maintaining energy consumption compared to the conventional non-adaptive eco mode. In addition, we illustrate how conflicts can be mitigated inherently in the design for two examples: an unexpected strong acceleration (an overtake maneuver), and an unexpected stop-and-go.

9.2. Design of the Proactive Eco Mode System

Figure 9.1 shows a schematic representation of the proactive eco mode system: a method that automatically switches powertrain settings based on predicted location-specific data and current driver behavior. The powertrain settings (PWT) determine the acceleration response of the vehicle given the throttle pedal input. Specifically, the proactive eco mode switches between the two predefined powertrain settings: a ‘low’ setting corresponding to powertrain settings used in Renault’s MultiSense® eco-driving mode (PWT_{low} ; Renault, 2022), and a ‘normal’ setting corresponding to the powertrain settings used in the normal driving mode (PWT_{normal} ; see section 9.3.2 for more detail about the underlying settings). In general, the proactive eco mode method consists of two main paths: (1) a proactive path (Figure 9.1 – highlighted in green) that predicts the powertrain settings using a location-specific database and current driving behavior and (2) a conflict mitigation path that infers driver’s intention and proposes a powertrain setting for two specific examples: a speed-based PWT proposal and a throttle-based powertrain setting proposal (Figure 9.1 – block 2, highlighted in blue). An arbitrator decides which proposed powertrain setting from the proactive, speed-based, or throttle-based paths are ultimately applied to the vehicle (section 9.2.3, Figure 9.1 – block 3). The settings are finally communicated to the driver (Figure 9.1 – block 4). The two paths and the arbitrator will be explained in more detail in sections 9.2.1, 9.2.2 and 9.2.3, respectively.

9.2.1. The Proactive Path (1)

Proposed predicted powertrain setting (1c)

The powertrain settings are switched using a threshold-based decision logic (Equation 9.1, Figure 9.2):

$$\text{Proactive powertrain setting} = \begin{cases} PWT_{normal} & \text{if } \bar{P} > \tau_{normal}(P) \\ PWT_{low} & \text{if } \bar{P} < \tau_{low}(P) \ \& \ P_c < \tau_{low}(P) \end{cases} \quad (9.1)$$

where \bar{P} is the average predicted power in kW estimated using a location-specific database averaged over a prediction window ahead of the vehicle (see next section), P_c is the current measured vehicle power in kW, $\tau_{normal}(P)$ is 20 kW, and $\tau_{low}(P)$ is 10 kW. The lower threshold is chosen such that PWT_{low} is selected at a cruising speed of 100 km/h without accelerations

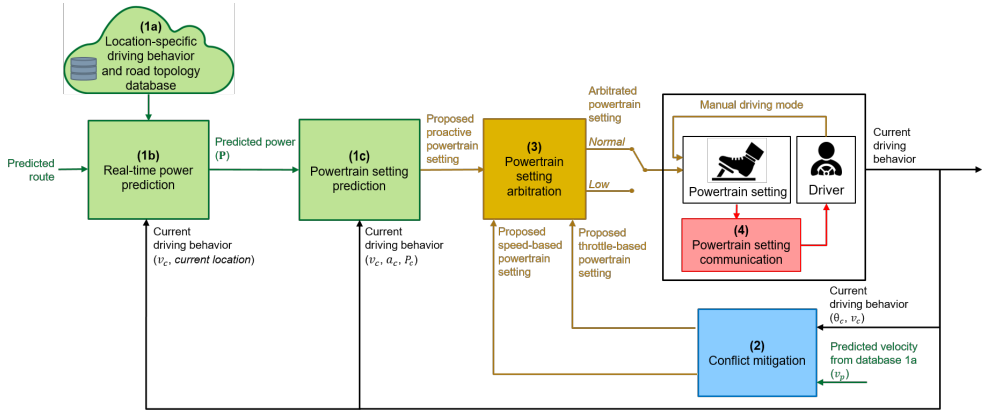


Figure 9.1. A schematic representation of the proactive eco mode that switches between two sets of powertrain settings. It contains two main paths: a proactive path (in green) and a conflict mitigation path (in blue) that are evaluated at 1000 Hz. (1) The proactive path predicts power by extracting pre-recorded location-specific data using the current location, current speed, and predicted route. (2) The conflict mitigation path continuously monitors for potential conflicts between the proactive predictions and the current driving behavior (block 2). An arbitrator (block 3) decides if and what settings are ultimately applied. The applied settings are communicated to the driver (block 4).

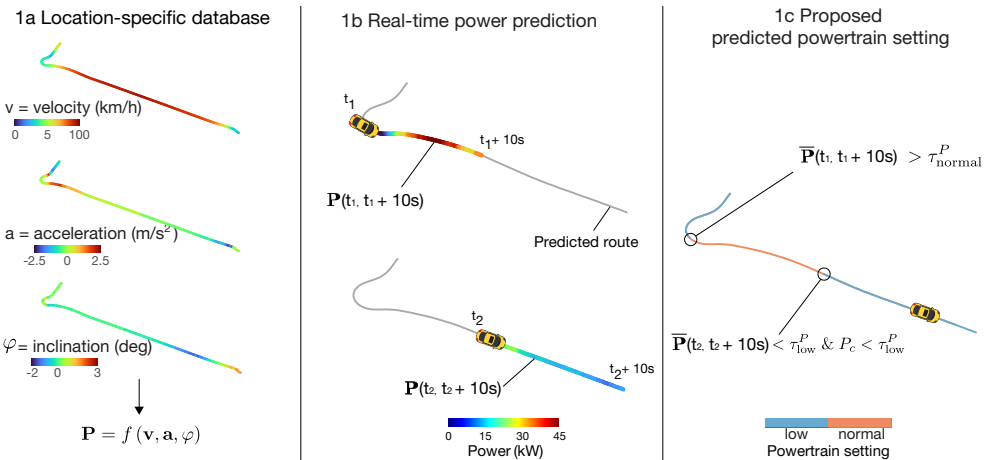


Figure 9.2. Overview of the proactive path steps for time instances t_1 and t_2 (1a to 1c corresponding to Figure 9.1). The proactive path predicts the power demand over a prediction horizon and adapts the powertrain settings accordingly. 1a. The traces show part of the a-priori recorded location-specific database. 1b. The predicted power ahead of the current position along the predicted route is calculated at each time step based on location-specific data extracted for a 10-second prediction window. 1c. The powertrain setting results for the two time instances.

(our test vehicle requires 9.6 kW at 100 km/h without considering external influences). The high threshold is heuristically tuned, such that the normal settings are selected during acceleration above 2 m/s² for speeds below 25 km/h and 0.8 m/s² for speeds above 80 km/h. In other words, during strong predicted accelerations – as signaled when the mean predicted power exceeds an upper power threshold – the system switches to PWT_{normal}. Conversely, the PWT_{low} is selected during cruising phases (i.e., when the mean predicted power and

current power are below a lower power threshold).

Real-time power prediction (1b)

The predicted power \bar{P} is estimated using the following equations:

$$\bar{P} = \frac{1}{N} \sum_{i=1}^N P_i, \text{ with} \quad (9.2)$$

$$P_i = \left(\frac{1}{2} \rho A C_d v_i^2 + m a_i + m g \sin \varphi_i \right) v_i \quad (9.3)$$

where $N = 50$ is the number of data points in the 10-second prediction window (i.e., time steps of 0.2 s), P_i is the power at prediction time step i , v_i the speed, a_i the acceleration or deceleration, and φ_i road inclination, ρ the mass density of air (1.225 kg/m³), m the vehicle mass (1430 kg), A the vehicle frontal area (2.73 m²), and C_d the vehicle's drag coefficient (0.27).

The 10-second prediction window was heuristically chosen because most acceleration phases with a speed difference of 50 km/h lasted approximately 10 seconds based on pilot tests. Moreover, averaging the power demand over the 10-second window filtered our small accelerations or short pulses in power demand, resulting in powertrain setting adaptations for relatively strong anticipated power demands.

To prevent switching powertrain settings too often, the algorithm checks whether consecutive powertrain setting switches would occur in a short time span over the near future. Therefore, the moment the system decides to switch to PWT_{low}, the algorithm temporarily shifts the prediction window another 10 seconds in the future. If the shifted prediction window would result in PWT_{normal} following Equation 9.1, the powertrain settings are not switched to PWT_{low}, but would remain PWT_{normal}.

Location-specific database (1a)

The database consists of the speed, acceleration, and road inclination per GPS location over a predicted route (see section 9.3.1. for a detailed description of the test route) sampled every 5 m. The algorithm extracts the location-specific behavior over the 10-second prediction window along the anticipated route ahead of the current location.

Real-time localization is performed by searching for the minimal Euclidean distance between the current GPS location to the nearest database GPS location using the last-known location as a starting point for the search. The velocity, acceleration, and inclination over the prediction horizon were then extracted from the location-specific database by iteratively predicting the future locations over the prediction window per 0.2 s time step. The first location is calculated using the current location and current speed v_c . The following locations are calculated from their previous location and the speed extracted from the database at the previous location. This resulted in predicted location-specific data for velocity $\mathbf{v} = [v_1 \dots v_N]^T$, acceleration $\mathbf{a} = [a_1 \dots a_N]^T$, and inclination $\varphi = [\varphi_1 \dots \varphi_N]^T$ linked to GPS positions $\mathbf{p} = [p_1 \dots p_N]^T$

The location-specific database for our demonstration was recorded a-priori based on three laps of the route with one driver and was stored locally on the real-time system running the proactive eco mode algorithms. Supplementary Figure 9.A shows the location-specific database for the complete test route.

Conflict mitigation path (2)

The algorithm continuously monitors the driver's throttle input and vehicle speed for potential conflicts between the proactive adaptation path predictions and the current driving behavior. The powertrain settings are adapted if a conflict is observed, which we illustrate using two representative examples.

Example 1: speed-based conflict mitigation for an unexpected stop-and-go

An example of a conflict between predicted speed and measured speed is a stop-and-go at a location where the reference driver in the location-specific database maintains speed, hereafter referred to as 'unexpected stop-and-go'. This situation represents a situation where a driver may stop for a pedestrian crossing and needs to accelerate back to cruising speed afterward and which cannot be predicted by the location-specific database. To demonstrate the predictive power that lies in the difference between predicted vehicle state and measured vehicle state, we implemented a rule-based algorithm that proposes the normal powertrain settings if the difference in current speed and expected speed exceeds a threshold:

$$\text{Speed-based powertrain setting} = \begin{cases} \text{PWT}_{\text{normal}} & \text{if } v_p - v_c > \tau(v) \\ \text{PWT}_{\text{low}} & \text{otherwise} \end{cases} \quad (9.4)$$

where v_p is the predicted speed based on the nearest location-specific database location, v_c is the current speed, and $\tau(v)$ is the speed difference threshold of 36 km/h.

Example 2: throttle-based conflict mitigation for an unexpected strong acceleration

A driver's intention to accelerate can depend on dynamic obstacles, such as other vehicles. Because a location-specific driving behavior database does not account for dynamic road situations, this could lead to situations in which the proactive path does not propose to select the normal powertrain settings while the driver would want to use it to reach a target speed. An example of this is an overtaking scenario. In this example, immediate acceleration intention is inferred from the driver's throttle rate (i.e., the speed of the throttle depression), implemented as follows:

$$\text{Throttle-based powertrain setting} = \begin{cases} \text{PWT}_{\text{normal}} & \text{if } \dot{\theta} > \tau(\dot{\theta}) \\ \text{PWT}_{\text{low}} & \text{otherwise} \end{cases} \quad (9.5)$$

Where $\dot{\theta}$ is the throttle pedal rate and $\tau(\dot{\theta})$ is the rate threshold of 90 %/s. The throttle-based $\text{PWT}_{\text{normal}}$ is applied until the current power P_c is below 10 kW. High throttle rates indicate that the driver requires higher power immediately, such as when preparing to overtake another vehicle. The throttle rate is estimated by fitting a first-order regression to the last 0.5 s of the measured throttle input.

9.2.3. Arbitrator (3)

An arbitrator decides which proposed powertrain setting from the proactive, speed-based, or throttle-based paths to apply to the vehicle. The arbitrator applies $\text{PWT}_{\text{normal}}$ to the powertrain if any of the three paths proposes the $\text{PWT}_{\text{normal}}$. Otherwise, the PWT_{low} settings of the proactive path are selected by default. Moreover, the proactive powertrain settings are only applied the moment the current throttle input angle is smaller than 30 deg. This way, no settings are changed when the driver has a large throttle input to assure smooth transitions between PWT settings. The speed-based PWT settings and throttle-based PWT settings are applied immediately.

9.3. Real-world Evaluation

9.3.1. Method

Instrumented vehicle and equipment

The proactive eco mode system was implemented in a Renault Talisman Phase 2 (see Figure 9.3). The vehicle had a 1.6 L diesel engine (type R9M), an automatic transmission, with a maximum engine power of 160 kW, a maximum speed of 207 km/h, and a 0 to 100 km/h acceleration time of 9.6 s. The vehicle was instrumented with a Dassault Systems dSpace

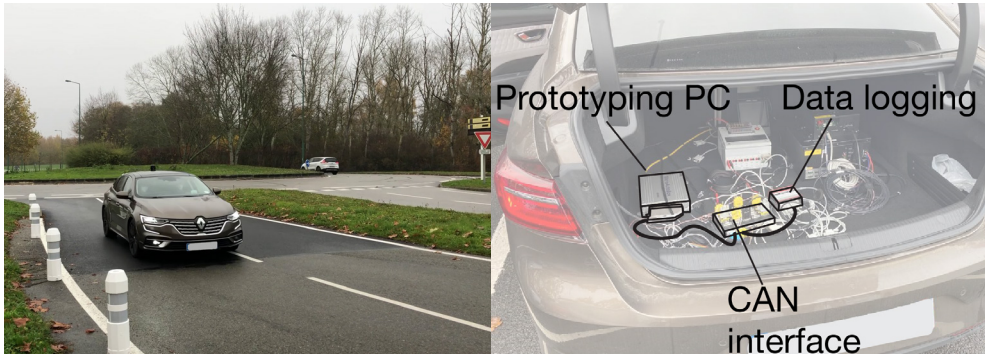


Figure 9.3. The test vehicle (left) with the prototyping PC, the CAN bus interface, and data acquisition interface in the trunk (right).

DS1401 prototyping PC connected to the vehicle's CAN bus. The proactive eco mode was implemented in Simulink and compiled to run on the prototyping PC at a frequency of 1000Hz. The vehicle's CAN signals, including the current vehicle state (speed, acceleration, power), vehicle settings, and current driver behavior were transmitted to the prototyping PC in real-time and recorded with RTmaps. A VBOX Automotive 3i GPS sensor provided the vehicle's GPS location to the prototyping PC at a 100 Hz update rate with a 50 cm position accuracy.

Participants

Nine Renault experts in vehicle dynamics, driving experience, or human factors participated in the demonstration. All participants were licensed to drive. No further personal information (such as age, gender, or average mileage a year) was gathered during this demonstration.

Powertrain settings

The proactive eco mode switches between two predefined powertrain settings: a 'low' setting identical to the powertrain settings used in Renault's MultiSense® eco mode (Renault, 2022; PWT_{low}), and a 'normal' setting identical to the powertrain settings used in Renault's normal mode (PWT_{normal}). Compared to PWT_{low} , PWT_{normal} involved an alteration in the throttle mapping, where a given driver's throttle depression ('throttle driver') resulted in a higher normalized requested engine torque ('throttle driver') (see Figure 9.4a). Additionally, PWT_{normal} increased the gear shift point in the rpm range (i.e., allowing a higher rpm before changing gears). For example, for a 'throttle driver' of 70%, the gear changed from 3rd to 4th at 55 km/h for PWT_{low} , whereas for PWT_{normal} this was 57 km/h. The powertrain settings were communicated to the driver through the visual cockpit interface (see Figure 9.4b). Selecting PWT_{normal} will likely lead to stronger accelerations according to Melman et al. (2021b), who showed that increased throttle mapping and powertrain settings can increase acceleration performance.

Route and scenario selection

During the demo, participants drove on a predefined 8.0 km long route that took approximately 10 minutes to complete (Figure 9.5). The speed limit was 50 km/h unless stated otherwise in Figure 9.5. The route contained three scenarios along the route: an expected stop-and-go, an unexpected stop-and-go, and an overtake maneuver. The first scenario (expected stop-and-go) was used to quantitatively evaluate the effect of the proactive eco mode on driving behavior and energy consumption for a controlled scenario. Scenarios 2 and 3 are used to demonstrate how conflicts can be mitigated.

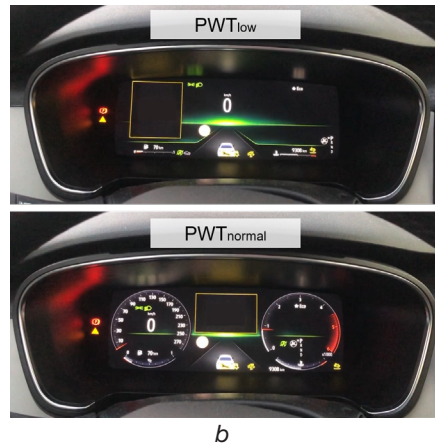
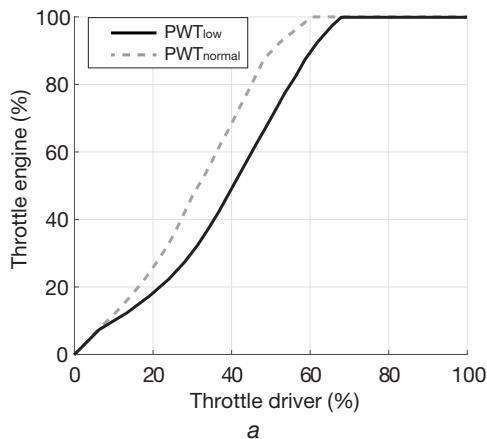


Figure 9.4. a. The throttle map for the low (PWT_{low}) and normal powertrain setting (PWT_{normal}), created using test data. b. The visual interface on the test vehicle cockpit for PWT_{low} (top) and PWT_{normal} (bottom).

Scenario 1, the expected stop-and-go (310 m), took place on Renault’s premises and experienced low traffic volumes, allowing participants to stop and accelerate unhindered by traffic. Specifically, drivers were asked to stop at a designated location and accelerate from 0 km/h to a target speed (speed limit of 50 km/h), which was predicted by the location-specific data (i.e., speed was 0 km/h for the stop and strong acceleration was predicted).

Scenario 2, the unexpected stop-and-go, demonstrates how conflicts can be mitigated by continuously comparing the driver’s actual behavior and the predicted behavior (see section 9.2.2.1. for more detail). During the unexpected stop and acceleration, drivers were requested to safely stop anywhere at a 500 m long straight road (see Figure 9.5), and accelerate back to the road (speed limit of 50 km/h). This scenario represents acceleration phases that are not predicted by the location-specific database, such as a stop for a crosswalk and subsequent acceleration.

Scenario 3, the overtaking maneuver, demonstrates how the system could deal with scenarios that were not predicted by the location-specific database, for example, when additional power is desired to overtake, but PWT_{low} settings are selected. Participants were asked in scenario 3 to safely perform overtaking maneuvers on two segments of a dual lane national road, see Figure 9.5. These segments were chosen because the proactive path would recommend PWT_{low} while PWT_{normal} would make overtaking easier. The resulting segments for scenario 3 were 1.1 km long and are visualized in Figure 9.5. This scenario demonstrates that the system can infer the additional power request through the driver’s throttle behavior and adapts the powertrain settings accordingly (see section 9.2.2. for more detail).

Procedure

At the start of the demonstration participants were asked to drive as they usually would and adhere to the traffic rules indicated by road signs next to the road. The participants drove three trials with different eco mode configurations in the same order: (C1) non-adaptive eco mode, (C2) proactive eco mode without throttle-based adaptation (i.e., see section 9.2.2.), and (C3) proactive eco mode with throttle-based adaptation. The first trial was driven in the non-adaptive eco mode and the participants were not explicitly instructed about the used vehicle settings. Next, the participants were informed they drove the non-adaptive eco mode and the proactive eco mode functionality driver before driving condition C2 and C3. After trial C2 and C3, participants completed a short questionnaire. All nine drivers completed scenario

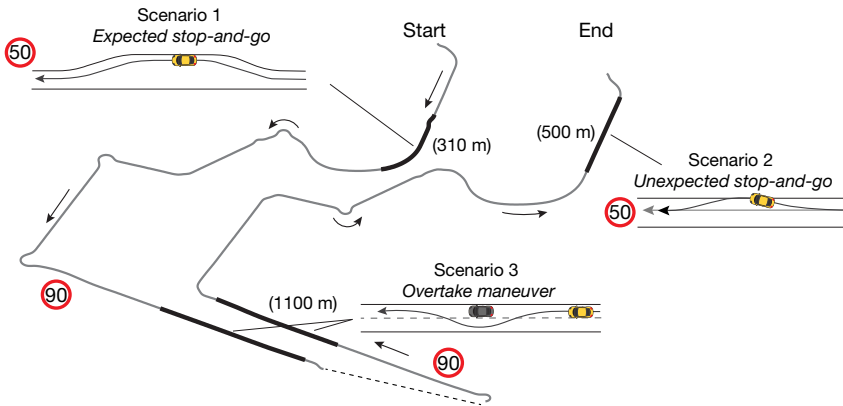


Figure 9.5. The experiment route, the to –and from– legs separated spatially for clarity. The driving direction is indicated by arrows. The route consisted of primarily dual lane roads with roundabouts and one traffic light. Scenarios 1, and 2 were on roads with low traffic volumes on the premises of Technocentre Renault at Aubevoye. Scenario 3 was on public roads with varying degrees of traffic.

1 for both the non-adaptive eco mode and proactive eco-mode; 7 performed scenarios 2 and 3.

Dependent measures and data analysis

We describe and analyze overall system performance, driving behavior data, and self-reported ratings for the non-adaptive eco mode and proactive eco mode, for the complete route and more detailed analysis of the expected stop-and-go (scenario 1). The conflict mitigation scenarios 2 and 3 are not evaluated but merely illustrate the functioning of the proactive eco mode using the data from one driver.

Proactive eco mode performance. To assess the accuracy of the proactive powertrain setting adaptations, we compare if the proactive eco predictions indeed were followed by strong accelerations ($\bar{P} < \tau_{normal}(P)$). Specifically, we simulate the mean predicted power (\bar{P} ; section 9.2) over the complete route using each driver’s measured driving behavior as the location-specific data. This results in mean predicted power specific to each driver’s own data, which allows us to assess whether the actual setting adaptations during the demonstration were correctly applied.

Driving behavior. Data including the vehicle state (vehicle speed, acceleration, motor torque delivered to the wheels), vehicle settings (e.g., throttle map, driving mode), and driver input (throttle pedal angle) were recorded from the vehicle’s CAN bus at 10 or 100 Hz and subsequently resampled to 100 Hz in post-processing. Specific to the expected stop-and-go (scenario 1), five dependent measures are calculated for each participant.

- *Mean energy consumption (kJ/km).* The energy consumption per kilometer is calculated by integrating the actual power over time divided by the total distance of the stop-and-go segment (310 m). Power is calculated by calculating the resultant force of the measured delivered motor torque to the wheels on the road using the tyre radius, and multiplying this force with the measured vehicle speed.
- *Fuel consumption (cm³/km).* The measured fuel consumption during the stop-and-go segment divided by the total distance of the stop-and-go segment (310 m).
- *Time to 95% target speed (s).* The time it takes to reach 95% of the driver’s own target

speed relative to the start of the acceleration. Each driver's target speed is based on their mean speed over the last 10 seconds in scenario 1. The start of the acceleration is determined when the speed exceeds 0.5 m/s after the full stop.

- *Mean acceleration to 95% target speed (m/s^2)*. The mean acceleration to reach the 95% target speed (see above). Compared to non-adaptive eco, the proactive eco is expected to increase the mean acceleration while adopting the same mean throttle.
- *Mean throttle to 95% target speed (%)*. Mean throttle to reach the 95% of the target speed.

Parameters are reported using the mean and 95% confidence interval of the mean, which is determined using bootstrapping ($n = 10,000$ samples; the 2.5% and 97.5% percentiles are selected). Within-subject differences between the non-adaptive and proactive eco mode are calculated and bootstrapped to determine significance per dependent variable. A difference is significant if the 95% confidence interval of the within-subject difference does not include zero (Tibshirani, & Efron, 1993).

Self-reported ratings. Participants rated on a seven-point Likert scale to what degree the proactive eco mode helps to reach a target speed easily and whether the proactive eco mode adds value compared to the non-adaptive eco mode after trials C2 and C3.

9.3.2. Results

Overall driving behavior and system performance

Figure 9.6 shows the average speed, throttle, delivered power, and most used powertrain setting versus the traveled distance of the full route. The route consisted of multiple acceleration phases with varying differences in start and target speed (see the speed profile in Figure 9.6). Overall, note that the averaged speed and power over the participants are substantially lower compared to the database speed and power. The proactive powertrain setting adaptation switches the powertrain from PWT_{low} to PWT_{normal} just before large peaks in power demand (see the vertical lines in Figure 9.6). Moreover, please note that there is large inter-driver variability when the proactive system switches back to PWT_{low} (Figure 9.6 bottom). This can be explained by the fact that some drivers accelerated stronger and longer and thus it took longer before the current power was below $\tau_{low}(P)$. Moreover, Figure 9.6 shows that the unexpected stop-and-go was executed over a 500 m long segment resulting in a large variability of PWT switch locations.

The proactive eco mode, excluding the throttle-based adaptation in scenario 3, switched 79 times to the normal powertrain settings across the nine participants during run 2 (average of nine times per lap per participant). Of these switches, 47 (59%) were indeed followed by an acceleration phase with a measured mean power demand larger than 20 kW ($\bar{P} > \tau_{normal}(P)$), 26 switches were followed by an acceleration phase with mean power demand smaller than 20 kW and larger than 10 kW ($\tau_{low}(P) < \bar{P} < \tau_{normal}(P)$), and 4 switches followed by an acceleration phase of below 10 kW ($\bar{P} < \tau_{low}(P)$). The proactive adaptations were indeed also proactive: only 1 out of a total of 79 adaptations was too late due to a single GPS sensor misread.

The PWT_{low} settings are selected when the expected and current power demand is below our power decision threshold (< 10 kW), which corresponds to phases when the speed is expected to be relatively constant over the 10 s prediction window. 68.5% of the time drivers drove with PWT_{low} applied (CI: (66.8%, 70.0%)), compared to 31.5% of the time in PWT_{normal} (CI: (30.0%, 33.2%)).

Scenario 1 - Expected stop-and-go

The mean speed, throttle, power, energy consumption and powertrain setting as a function of time for the expected stop-and-go (scenario 1) are shown in Figure 9.7. Note that the

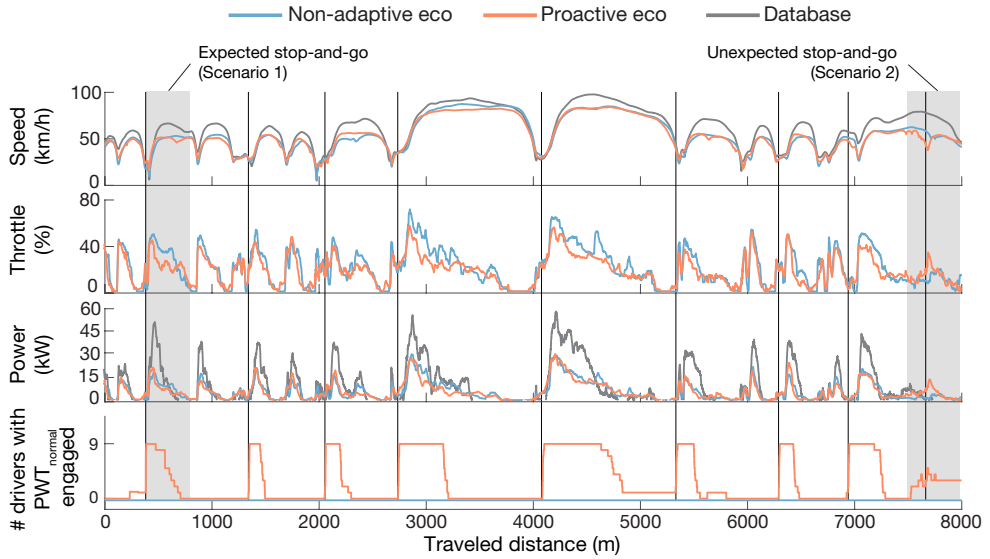


Figure 9.6. The mean speed, mean throttle, mean power and the number of participants driving with PWT_{normal} for the proactive eco and non-adaptive eco condition. While all participants stopped ($v = 0$ km/h) at the stop-and-go scenarios, the mean speed is not zero because participants stopped at slightly different locations.

powertrain settings PWT_{normal} are already proactively applied before the acceleration starts at $t = 0$ s. Once each driver’s acceleration phase is over, the powertrain settings are automatically switched to the low settings. The variation in moments in time when the system switches to PWT_{low} is because the system switches back once the predicted power demand and the current power demand are below a threshold (see section 9.2.1.). In other words, drivers who accelerate longer remain longer in PWT_{normal} and can be seen in Figure 9.7.

Proactively adapting the powertrain settings helps drivers to reach their target speed significantly quicker while keeping energy consumption and fuel consumption similar to the non-adaptive eco mode (see Table 9.1 and Figure 9.7). Mean acceleration during the acceleration phase is significantly higher, and subsequently time to target speed is significantly shorter for the proactive eco mode. Participants provide similar mean throttle input with the proactive eco mode engaged, resulting in initially more power demand compared to the non-adaptive eco. The power demand subsequently drops below the non-adaptive eco mode once the target speed is reached, compensating for the initial higher power demand. As a result, energy consumption over the 310 m long scenario is similar between both modes. A strong correlation was found between energy consumption and fuel consumption ($\rho = 0.96$).

Example 1: speed-based conflict mitigation for an unexpected stop-and-go

Figure 9.8 demonstrates how powertrain settings can be adapted proactively when a mismatch occurs between the driver’s current speed and the expected speed in the location-specific database. While the driver decelerates, the system selects PWT_{normal} in anticipation of the acceleration to the expected cruising speed. The normal settings are applied until the acceleration phase is done, which is determined based on the measured current power demand P_c . Please note that this did mean that the system automatically switched to PWT_{normal} when speed = 0 km/h. During the demo, drivers stopped in total 15 times outside the two stop-and-go scenarios (e.g., a stop for a traffic light), 14 of these stops did not trigger a speed-based PWT setting switch using the current thresholds because the predicted speed

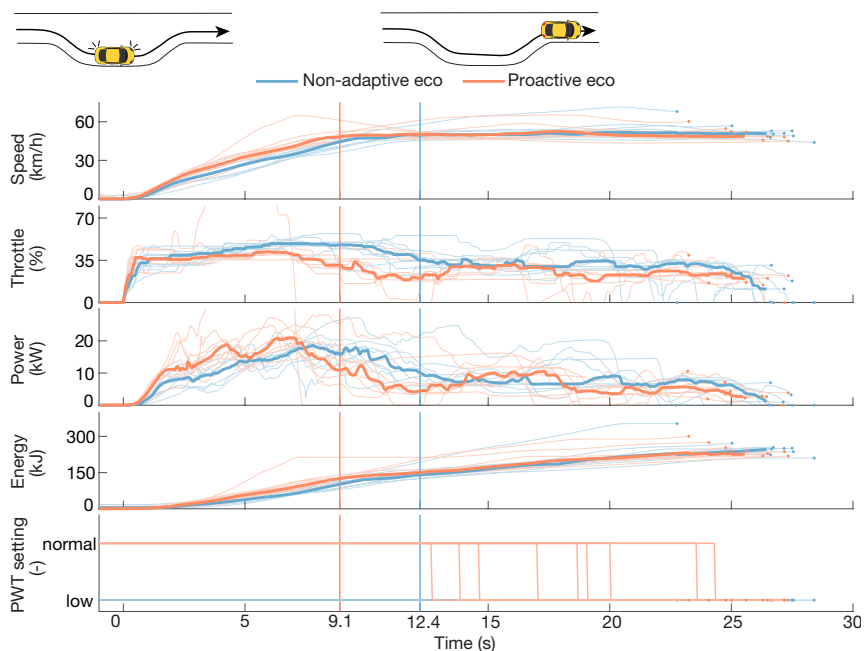


Figure 9.7. Time traces of the individual drivers ($n = 9$; thin lines) and mean (thick line) of the expected stop-and-go (scenario 1) for the non-adaptive eco and proactive eco mode. Compared to the non-adaptive eco, proactive eco yields a shorter time to target speed (indicated by the vertical lines), yet the energy consumption over the full scenario segment is similar. The proactive proposed PWT settings are arbitrated based on each driver's current power demand, resulting in driver-dependent moments in which settings are switched from PWT_{normal} to PWT_{low} . Dots indicate the time to drive the 310 m scenario segment for each driver.

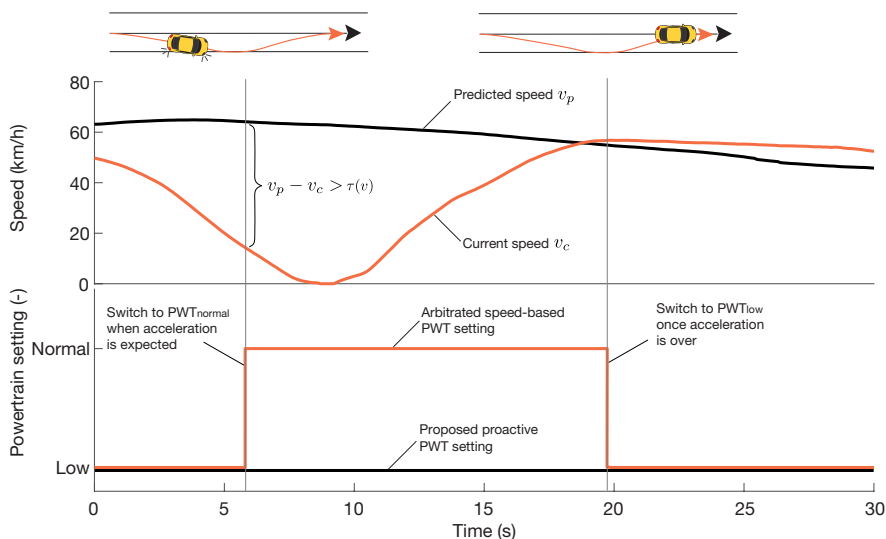


Figure 9.8. An example of a speed-based powertrain setting switch. The speed and the powertrain setting for one participant performing an unexpected stop-and-go (orange) versus the predicted speed in the location-specific database (black).

Table 9.1. The mean (M) and the upper and lower bounds of the 95% confidence interval (CI) of the mean for Scenario 1 (Expected stop-and-go, $n = 9$). Parameters are either calculated for the full scenario segment or the acceleration phase. Significant differences based on within-subject differences are shown in bold.

	Non-adaptive eco M (CI)	Proactive eco M (CI)	Within-subject M (CI)
Energy consumption (kJ/km)	823.0 (755.0, 916.5)	801.7 (748.0, 863.6)	-21.4 (-63.2, 18.1)
Fuel consumption (cm ³ /km)	151.6 (141.7, 165.5)	150.6 (142.1, 160.0)	-1.0 (-7.9, 5.4)
Time to 95% target speed (s)	12.4 (10.4, 14.6)	9.1 (7.2, 11.2)	-3.3 (-5.9, -1.4)
Mean acceleration to 95% target speed (m/s ²)	1.42 (1.27, 1.55)	1.85 (1.57, 2.16)	0.43 (0.17, 0.81)
Mean throttle to 95% target speed (%)	42.3 (40.2, 44.4)	39.4 (36.0, 44.4)	-2.9 (-6.6, 2.9)

in the database at those locations was lower than $\tau(v)$. The one that did trigger a speed-based PWT setting switch was a stop located at the 90 km/h road segment (Figure 9.5).

Conflict mitigation example 2: An unexpected strong acceleration

Figure 9.9 shows a driver overtaking a slower vehicle. Because the location-specific driving behavior database does not capture dynamic traffic situations, the powertrain settings are not adapted proactively. Instead, we adapt the powertrain settings to PWT_{normal} based on a rapid throttle pedal depression, and switch back to PWT_{low} once the measured power is below $\tau_{low}(P)$. Hence, to account for unforeseen or difficult to predict situations, the adaptive system should also reactively adapt the settings based on the current driver input.

Subjective ratings

In response to the question ‘Compared to the non-adaptive eco (C1), the proactive eco mode (C2) helps to easily reach a target speed’ 3 participants very strongly agreed, 4 participants strongly agreed, and 2 participants agreed. In response to the question ‘Compared to the

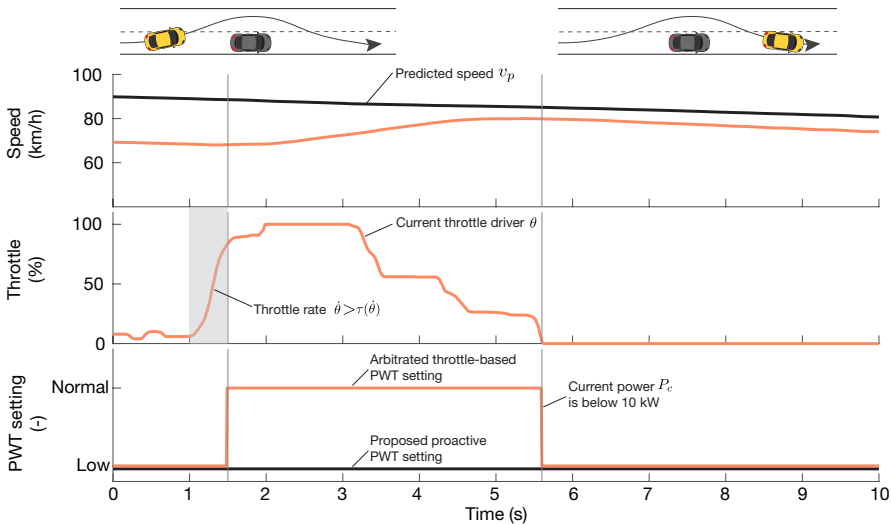


Figure 9.9. An example of a throttle-based powertrain setting switch. One participant during an overtake maneuver which was not predicted in the database. The system switches to normal powertrain (PWT) setting due to the high throttle speed (estimated over the last 0.5 s throttle; indicated with a gray box) and returns to low PWT setting once the current power is below 10 kW.

non-adaptive eco (C1), the proactive eco mode (C2) adds value' 2 participants very strongly agreed, 4 participants strongly agreed, 2 participants agreed, and 1 participant was neutral. Lastly, adding functionality such as throttle-based adaptations (C3) resulted in similar results compared to C2. Compared to non-adaptive eco (C1), C3 makes it easier to reach a target speed ($M = 2$, range = [1 3]), and adds value ($M = 1.75$, range = [1 3]).

9.4. Discussion / Conclusion

We designed and demonstrated a proactive eco mode that aimed to stimulate eco-driving by helping the driver to quickly and efficiently reach a target speed, with the aim of improving eco mode acceptance and usage compared to a non-adaptive eco mode. We discuss the most important observations below.

Energy-efficient driving can include stronger accelerations for large speed differences

As expected, the proactive eco mode that temporarily switched to PWT_{normal} for strong acceleration phases resulted in drivers significantly reaching their target speed faster *with similar energy consumption* compared to the non-adaptive eco mode. These real-world results complement simulation studies that argue 'strong' accelerations followed by constant cruising speed for optimal energy efficiency (Mensing et al., 2013; Saerens & Van den Bulck, 2013). Although this study provides evidence that temporarily switching from PWT_{low} to PWT_{normal} during acceleration phases does not hamper energy efficiency, we did not test whether driving only with PWT_{normal} would harm energy consumption on a trip level. Still, evidence shows that powertrain settings with a higher throttle map and later gear changes, such as in PWT_{normal}, lead to higher fuel consumption, mainly due to an average higher engine speed (Melman et al., 2021b, 2022; Sanguinetti et al., 2017). Hence, selecting PWT_{low} for cruising and *low acceleration phases* can be argued to be beneficial to improve energy efficiency.

The proactive eco mode switched too often but was still well-received by the drivers

For scenario 2, all the PWT_{normal} setting adaptations were predicted using an a-priori measured location-specific database. Using this database, the system predicted 79 times strong accelerations in total for all drivers. Of these predictions, 47 were indeed followed by a strong acceleration with a power demand higher than 20 kW. Nevertheless, the system also switched for acceleration phases that were followed by lower power demands (i.e., 26 switches were followed by a power demand between 10 kW and 20 kW and 4 switches followed by a power demand below 10 kW). The primary parameter that could be the cause for this 'over-adaptation' is the location-specific database, which showed to be atypical compared to the average driving behavior of the participants (see Figure 9.6). This suggests that the database should be based on average driving behavior of a larger population, or could be tailored to specific driving styles.

Despite this 'over-adaptation', participants rated the system positively: all nine drivers rated the proactive eco mode to add value and rated the proactive eco mode to facilitate reaching higher target speeds, compared to the non-adaptive eco mode. This suggests that the current method of combining proactive predictions while taking current driving behavior into account is promising in reducing conflicts. Moreover, it could be argued that our system that switched often to more responsive powertrain settings (i.e., having more power available than needed) inherently causes less conflict than a system that switches too little (i.e., wanting more power but not getting it). Future studies could systematically induce conflicts in vehicle settings to investigate conflict mitigation.

Location-specific data can provide sufficiently accurate driving behavior predictions

Although our database captured more acceleration-prone behavior compared to the participant pool, a location-specific database proved useful in predicting acceleration phases, supporting our previous observations that variability in driving behavior is more impacted by changes in the environment than by inter-driver variability (Melman et al., 2021a). Relying on a-priori measured behavior has the potential to simplify behavior predictions, alleviating the reliance on often complex computational models that need to sense and interpret the environment in order to predict behavior, and require rich datasets to train and may lack generalizability to untrained environments. However, we realize that our approach is not a one-stop solution. For example, the dependence on predicted route navigation, the influence of traffic, and other external factors such as weather, are challenges that need to be addressed in future work to make predictions more robust.

The proactive eco mode can mitigate conflicts when they occur

Making adaptive systems that are accepted is not self-evident, especially because system acceptance is hampered by incorrect predictions that will occur eventually (Johnson et al., 2014; Melman et al., 2020). Our aim was to demonstrate that continuously tracking driver behavior and inferring driver intention is important to create an adaptive system that is accepted by drivers.

We described a methodology (Figure 9.1) where the driver's current behavior is closely monitored to improve proactive predictions (block 1a), decide when to switch modes based on current throttle behavior (block 3), and mitigation when conflicts occur (block 2). The first two prevented inappropriate powertrain switches, such as not switching to PWT_{normal} when releasing the throttle, and not switching back to PWT_{low} when still accelerating. The latter (block 2) showed how conflicts between the proactive adaptation path predictions and the current driving behavior could be mitigated for two examples. Although the first subjective results are promising, the two scenarios and our implementations of our algorithms are simplified and have limitations. For example, the speed-based PWT setting algorithm in its current implementation will trigger an (undesired) switch to PWT_{normal} during a traffic jam.

9.4.1. Future Considerations and Limitations

We focus our energy analysis on short strong acceleration phases in which likely the largest differences in energy efficiency would be visible if any difference would exist (Melman et al., 2021a). Although no significant differences between the proactive eco mode and the non-adaptive eco mode were found, future work should systematically investigate if this holds for longer trips that include extensive cruising phases.

The results show that the switches were mostly location-specific and the same for all drivers. The driver mostly determined *when* the switch would be initiated rather than *if* a switch would occur. This suggests that the proactive method could be simplified. Specifically, the online extraction of the database (block 1a and 1b; Figure 9.1), and online calculation of mode switch (block 1c) could be replaced by a connected service that provides location-specific information of when to switch powertrain settings up and down. In other words, the proposed proactive powertrain settings (output of block 1c) are then directly provided from the cloud, where the arbitrator still decides when to execute based on the current driving behavior. Although this will likely improve simplicity, the downside of this approach is that it will not allow for a comparison between predicted behavior and expected driving behavior in the proactive calculation (block 1c). Future studies should investigate the practical benefits and limitations of this online and offline strategy.

Several technologies exist that stimulate eco-driving, including providing feedback based on the eco-friendliness of past driving behavior, yet their benefits on energy consumption

are transient (Af Wåhlberg, 2007; Beusen et al., 2009; Kutzner et al., 2021; Lauper et al., 2015; Rolim et al., 2014). This can partially be explained by the observation that drivers can show unforeseen behavioral adaptation. For example, Kutzner et al. (2021) found that drivers adapted their behavior to the reduced acceleration performance of the eco mode, negating the potential energy benefits. While we did not aim to investigate such behavioral adaptation in the long term in the current study, we found no behavioral adaptation in the short term; drivers seem to use similar throttle behavior during the proactive eco mode compared to the non-adaptive eco mode. Still, the question remains whether a proactive eco mode can encourage sustained energy efficient driving combined with high driver acceptance in the long term.

Finally, we are aware of the limitations in terms of generalizability and scientific robustness. First, while our participants were all Renault employees that specialize in assessing novel vehicle technology, their views can be biased. A proactive eco mode should also be tested with naive drivers from the general public. Moreover, our conditions were neither counterbalanced nor were the participants naive to the system's functionality. Lastly, human-factors-related challenges such as mode confusion, system acceptance and driver behavioral adaptation due to the proactive eco mode need to be systematically assessed in future studies.

Despite these limitations, this study provides valuable insights for the design of future adaptive eco driving technology. Until now, eco-driving techniques are considered to have negative psychological effects on drivers (Allison et al., 2022); our work demonstrates the potential for adaptive technology that uses preview to induce eco-friendly driving that is accepted by drivers.

References

- Abbink, D. A., Carlson, T., Mulder, M., De Winter, J. C. F., Aminravan, F., Gibo, T. L., & Boer, E. R. (2018). A topology of shared control systems—finding common ground in diversity. *IEEE Transactions on Human-Machine Systems*, 48, 509-525.
- Af Wåhlberg, A. E. (2007). Long-term effects of training in economical driving: Fuel consumption, accidents, driver acceleration behavior and technical feedback. *International journal of industrial ergonomics*, 37, 333-343.
- Alam, M. S., & McNabola, A. (2014). A critical review and assessment of Eco-Driving policy & technology: Benefits & limitations. *Transport Policy*, 35, 42-49.
- Allison, C. K., Stanton, N. A., Fleming, J. M., Yan, X., & Lot, R. (2022). How does eco-driving make us feel? Considering the psychological effects of eco-driving. *Applied Ergonomics*, 101, 103680.
- Barkenbus, J. N. (2010). Eco-driving: An overlooked climate change initiative. *Energy policy*, 38, 762-769.
- Beusen, B., Broekx, S., Denys, T., Beckx, C., Degraeuwe, B., Gijssbers, M., ... & Panis, L. I. (2009). Using on-board logging devices to study the longer-term impact of an eco-driving course. *Transportation research part D: transport and environment*, 14, 514-520.
- Dib, W., Chasse, A., Moulin, P., Sciarretta, A., & Corde, G. (2014). Optimal energy management for an electric vehicle in eco-driving applications. *Control Engineering Practice*, 29, 299-307.
- Ericsson, E. (2001). Independent driving pattern factors and their influence on fuel-use and exhaust emission factors. *Transportation Research Part D: Transport and Environment*, 6, 325-345.
- Grengs, J., Wang, X., & Kostyniuk, L. (2008). Using GPS data to understand driving behavior. *Journal of urban technology*, 15, 33-53.
- Hofmann-Wellenhof, B., Legat, K., & Wieser, M. (2003). *Navigation*. Springer Science & Business Media.
- Huang, Y., Ng, E. C., Zhou, J. L., Surawski, N. C., Chan, E. F., & Hong, G. (2018). Eco-driving technology for sustainable road transport: A review. *Renewable and Sustainable Energy Reviews*, 93, 596-609.
- Johnson, M., Bradshaw, J. M., Feltovich, P. J., Jonker, C. M., Van Riemsdijk, M. B., & Sierhuis, M. (2014). Coactive Design: Designing Support for Interdependence in Joint Activity. *Journal of Human-Robot Interaction*, 3, 43.
- Kaber, D. B., & Endsley, M. R. (2004). The effects of level of automation and adaptive automation on human performance, situation awareness and workload in a dynamic control task. *Theoretical issues in ergonomics science*, 5, 113-153.
- Kutzner, F., Kacperski, C., Schramm, D., & Waenke, M. (2021). How far can we get with eco driving tech?. *Journal of Environmental Psychology*, 76, 101626.
- Lauper, E., Moser, S., Fischer, M., Matthies, E., & Kaufmann-Hayoz, R. (2015). Psychological predictors of eco-driving: A longitudinal study. *Transportation research part F: traffic psychology and behaviour*, 33, 27-37.
- Melman, T., Abbink, D., Mouton, X., Tapus, A., & De Winter, J. (2021a). Multivariate and location-specific correlates of fuel consumption: A test track study. *Transportation Research Part D: Transport and Environment*, 92, 102627.
- Melman, T., Beckers, N., & Abbink, D. (2020). *Mitigating undesirable emergent behavior arising between driver and semi-automated*

vehicle. arXiv preprint arXiv:2006.16572

- Melman, T., De Winter, J., Mouton, X., Tapus, A., & Abbink, D. (2021b). How do driving modes affect the vehicle's dynamic behaviour? Comparing Renault's Multi-Sense sport and comfort modes during on-road naturalistic driving. *Vehicle System Dynamics*, 59, 485–503.
- Melman, T., Tapus, A., Jublot, M., Mouton, X., Abbink, D., & De Winter, J. (2022). Do sport modes cause behavioral adaptation? Submitted to Journal
- Melman, T., Visser, P., & De Winter, J. (2021c). Creating the illusion of sportiness: Evaluating modified throttle mapping and artificial engine sound for electric vehicles. *Journal of Advanced Transportation*, 2021, 4396401.
- Mensing, F., Bideaux, E., Trigui, R., & Tattégrain, H. (2013). Trajectory optimisation for eco-driving taking into account traffic constraints. *Transportation Research Part D: Transport and Environment*, 18, 55–61.
- Parasuraman, R., & Riley, V. (1997). Humans and automation: Use, misuse, disuse, abuse. *Human factors*, 39, 230–253.
- Renault. (2022). *Multi-sense*. <https://gb.e-guide.renault.com/eng/easy-link/MULTI-SENSE>
- Rolim, C. C., Baptista, P. C., Duarte, G. O., & Farias, T. L. (2014). Impacts of on-board devices and training on light duty vehicle driving behavior. *Procedia-social and behavioral sciences*, 111, 711–720.
- Saerens, B., & Van den Bulck, E. (2013). Calculation of the minimum-fuel driving control based on Pontryagin's maximum principle. *Transportation Research Part D: Transport and Environment*, 24, 89–97.
- Sanguinetti, A., Kurani, K., & Davies, J. (2017). The many reasons your mileage may vary: Toward a unifying typology of eco-driving behaviors. *Transportation Research Part D: Transport and Environment*, 52, 73–84.
- Tibshirani, R. J., & Efron, B. (1993). An introduction to the bootstrap. *Monographs on statistics and applied probability*, 57, 1–436.

Appendix 9A

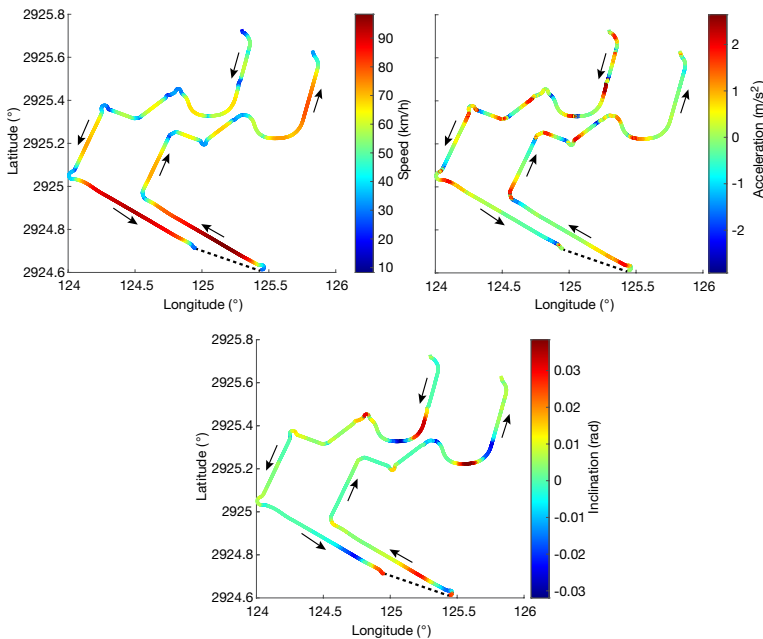


Figure 9A. The database for the experimental route at Renault's test track in Aubevoye, France. The driving direction is indicated by arrows.

***CONCLUSIONS AND
DISCUSSION***

10

This thesis contains multiple chapters, each of which describes its own individual scientific challenges, results, limitations and conclusions. In this conclusion chapter, the individual contributions are integrated towards overarching conclusions, limitations, and future work.

10.1. Recapitulation of Research Goal and Approach

This dissertation aims to provide new quantitative and qualitative insights into the underlying principles to design a system with proactive adaptive vehicle settings: A system that automatically changes the vehicle settings to fit the individual and context-dependent needs of the driver.

Figure 10.1 depicts the three main parts in which this thesis is organized. Since our aim was to develop a system that adapted according to what the human driver would want, the first step was to understand how and why humans adapt their driving behavior. For this reason, the first part of this thesis investigates the fundamental mechanisms behind driver adaptations to environmental changes and to vehicle characteristics. The second part investigates the effect of offline vehicle setting changes on the vehicle's dynamic behavior, driver's perception and driving behavior. In this part, mode changes were performed offline, meaning that changes only occurred between driving trials and not while driving. In this way, the impact of transient effects in the data was minimized. Finally, the more complex question of a online adaptive system, in which vehicle settings proactively change while driving, is considered. The third part ends with a proposed proactive eco mode method, which was implemented in a real vehicle and tested on real roads.

Each part contains multiple chapters, each of which describes its individual results, limitations, and conclusions. In this conclusion chapter, the aim is to integrate the individual contributions towards overarching conclusions, limitations, and future work.

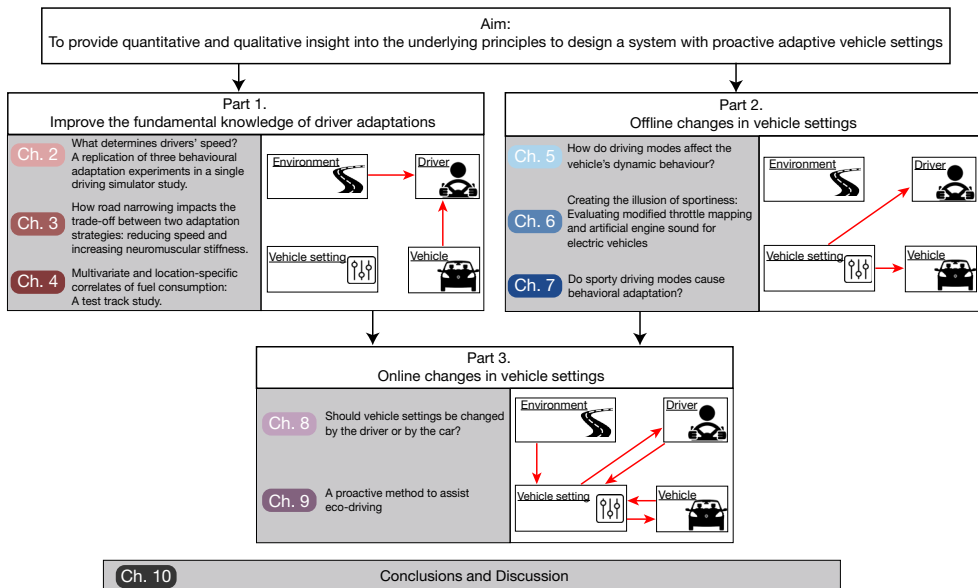


Figure 10.1. Schematic overview of the three main research parts of this thesis, and their respective chapters. Note that the theoretical and empirical knowledge obtained in Parts 1 and 2 was used to develop the prototypes in Part 3.

10.2. Key Conclusions

Conclusion 1. Motivational driving models that use emotions or experiences as a construct are theoretically insightful but impractical; driving behavior could better be predicted by car state or location-specific variables.

A substantial part of this thesis investigates how people adapt to different road environments (road width and curvatures; Chap 2 and 3), task instructions (Chap 4), and car characteristics (Chap 4, 6, and 7). This kind of knowledge would help improve the understanding of why drivers drive as they do in case the location (where they drive), the target (i.e., eco vs. normal vs. sport) and the driving mode (sound, powertrain settings, steering settings) changes. The results showed that the above mentioned conditions had a strong impact on driving behavior. However, there is a lack of strong evidence for the predictive capabilities of moderating psychological constructs such as perceived risk, sportiness, or effort. Driver adaptations have turned out to be mainly opportunistic rather than driven by emotions or experience (as motivational models suggest; cf. Trimpop, 1996). For example, a wider road results in an increased driving speed (Chap 2 and 3), an increased powertrain setting is used to reach a target speed sooner (Chap 6 and 7) and amplifying the engine sound is used to improve speed control (Chap 6). Chapter 2 found strong speed adaptations for varying road widths; however, none of the three well-cited homeostatic measures (i.e., experienced risk, experience effort, and safety margins) offered persuasive evidence for speed adaptation because they failed either the sensitivity criterion (i.e., the measure should increase/decrease if speed was held constant) or the constancy criterion (i.e., the measure should homeostatically be held constant if speed adaptations occurred). An additional measure for control activity, the steering reversal rate, outperformed the other three measures regarding sensitivity and constancy, prompting a further evaluation of the role of a physical measure (such as steering reversal rate) in speed adaptation. It is likely that subjective measures (i.e., perceived risk) and physiological measures are too distant from the real driving task and generally suffer from a low signal-to-noise ratio to be practically useful. From a practical point of view, the need for models that can predict driver adaptations has been reduced as cars become more intelligent and equipped with sensors that can measure the surroundings and the driver directly. Such a data-driven approach has led to the final proof-of-concept (Chap 9) that makes power predictions based on measured (location-specific) driving behavior data.

Conclusion 2. A large part of the variability in driving behavior can be explained by location; location should be included in the design of an adaptive vehicle setting system.

Multiple chapters (Chap 2-4 and 6-9) demonstrated the importance of considering *location-specific* information (e.g., curvature, road width, speed advice, and inclination) on variability in driving behavior. Chapter 4 provided evidence that to predict fuel consumption, it is more important to know *where* someone is driving than *who* is driving. Ninety-one drivers drove a total of 4617 laps, in two vehicles, on two test-track routes, and with two driving instructions. Although a strong predictive value for fuel consumption was found for metrics related to speed, RPM, and throttle position, the largest variance was attributable to the route type (highway vs. country road). A subsequent location-specific analysis showed that the inter-driver variability in fuel consumption for the entire trip could already be predicted by measuring the instantaneous speed just after a single curve (i.e., the speed measured at a single curve had a good correlation with the fuel consumption of the total trip). Following this conclusion, throughout this thesis location-specific information has been accounted for in the analysis before investigating the intended effect of the conditions on driving behavior. For example, when investigating the effect of vehicle settings on driving behavior, the total driven routes are always analyzed per different road segments, such as straights and curves (Chap 6 and 8), highway or mountain roads (Chap 4 and 5), specific acceleration segments (Chap

6), segments with varying road widths (Chap 2 and 3). Additionally, to make the influence of the environment apparent, driving behavior is consistently visualized as a function of traveled distance and road topology (Chap 2-8), rather than time. Finally, the importance of location-specific information on driving behavior has led to a proactive eco mode that makes predictions by checking if the *location-specific* power requirement is high (Chap 9).

Conclusion 3. The tested sport mode led to objectively more 'sporty' vehicle dynamics.

The current sport mode in the commercially available Renault Multi-Sense consists of several active components that jointly affect vehicle dynamic behavior (see Introduction). This thesis provides empirical methodologies, metrics, and models to quantify this joint impact on longitudinal, lateral, and vertical vehicle dynamics. Before this thesis, their combined effect on the total vehicle's dynamic behavior for naturalistic driving on actual roads was unavailable (Hilgers et al., 2009; Jeon et al., 2016). Chapter 5 and 7 showed strong vehicle dynamic behavioral differences in rear-wheel angle, engine torque, longitudinal acceleration, and vertical motion when driving with different vehicle settings. This goes beyond knowledge from literature, where the working principle of individual vehicle dynamical components is generally tested in a simulated environment or on test tracks. However, no empirical studies investigate how these individual active components are affected by driving modes. Furthermore, for actual roads, the impact of driving modes on the vehicle's dynamic behavior was unknown.

Conclusion 4. Sport mode settings are clearly perceived but do not cause speeding behavior.

Different *offline* variations of sport mode settings are clearly perceived by drivers, but do not lead to an increased speed. Experiments in this thesis did not provide any evidence for the hypothesis from literature (and concerns from company experts) that riskier driving might occur when presenting drivers with sport mode. Chapter 6 and Chapter 7 tested various combinations of individual vehicle settings in an instrumented vehicle (Chap 7) and in a driving simulator study (Chap 6). Both chapters found increased sportiness perception when combining artificial engine sound and modified throttle mapping (a system that increases the acceleration performance given the driver's throttle input), and when presenting drivers with more agile four-wheel steering settings (a system that changes the steering responsiveness of the vehicle). Yet, both in simulation and in real-world the increased sportiness perception did not result in any changes in speed. However, other adaptations in driving behavior were observed, for example, drivers opportunistically used the increased available acceleration performance to accelerate more strongly to reach their target speed sooner (but the average speed remained the same). This insight was used to improve the design of the prototype in Chapter 9 (i.e., by dynamically changing the powertrain settings all drivers intuitively accelerate faster and smoother without fuel efficiency degradation).

Conclusion 5. Proactive adaptations of vehicle settings can objectively improve acceleration performance, lane-keeping, and steering performance, but are not always accepted by drivers.

Online adapting vehicle settings can improve steering performance (Chap 8) and acceleration performance (Chap 9) compared to fixed vehicle settings, but the acceptance of these adaptations depends on the way the proactive system interacts with the driver. Chapter 8 tested two interaction designs to adapt vehicle steering dynamics (driver-initiated and machine-initiated). This study showed that different driving situations (e.g., overtaking and curve driving vs. straight-line driving) require different steering dynamics. Both interaction designs objectively led to benefits for the driver over the entire route, compared to a non-

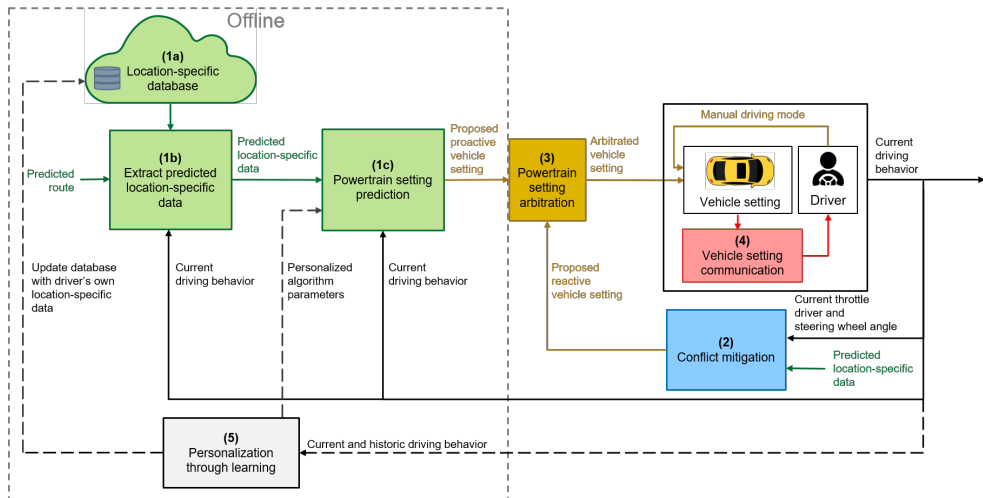


Figure 10.2. Future work towards an *offline learning* proactive *vehicle setting* method. Note that this is based on Figure 9.1, but with three adjustments: (1) an added learning loop (box 5: personalisation through learning) to mitigate misalignments, (2) offline calculation of the proposed vehicle setting and (3) generalization to vehicle settings. The learning loop illustrates two ways that could mitigate conflicts: learning the driver's own location-specific driving behavior, and learning the desired proactive algorithm parameter.

adaptive, fixed steering sensitivity. Interestingly, some drivers preferred the driver-initiated system, even when these led to more effort and objectively less performance increase than a machine-initiated system. A likely explanation is that the driver-initiated condition gives drivers the freedom to choose, whereas they give away their freedom in the machine-initiated condition. In essence, if drivers want low (high) steering gain, they can select the low (high) steering gain setting at the start of their drive. That is, the driver-initiated condition can deliver what a fixed low and fixed high steering gain can deliver as well, and so theoretically should not be rated worse than a fixed steering gain.

This illustrates that developing machine-initiated adaptations in vehicle dynamics is very difficult, especially when considering that system acceptance is hampered by incorrect predictions that will inevitably occur (Johnson et al., 2014; Melman et al., 2020), and even if predictions are correct the moment of transition can be perceived as incorrect (i.e., see Chapter 8). Chapter 9 demonstrated the proactive method can help cope with conflicts induced by incorrect predictions. Specifically, conflicts between driver and automation are minimized by keeping the driver primarily in charge of the driving task and by closely monitoring the current driver behavior and ensuring the driver can influence or override the automation at any time. Despite by two induced conflicts (i.e., the unexpected stop-and-go and overtake example), and proactive predictions based on a single atypical driving profile (which undoubtedly reduced the accuracy of the power predictions), the results showed that the 9 drivers unanimously indicated that the proactive eco system added value and made it easier to reach a target speed compared to non-adaptive eco mode.

10.3. Overarching Limitations and Considerations

In the previous section, results of multiple chapters were combined to consolidate the overarching conclusions. However, some results of chapters were contradictory rather than complementary and will be addressed in this section. Two main potential causes are highlighted: driving simulator studies versus real-world studies, and the (limited) generalizability of the participants' pool.

Opposite results in terms of sportiness perception and speed control of modified throttle mapping (MTM) and artificial engine sound enhancement (AESe) were found in Chapter 6 and Chapter 7. Compared to baseline, in Chapter 6, a driving simulator study mainly using students as participants, a strong effect on perceived sportiness was found for AESe, but not for MTM. Conversely, in Chapter 7, a test track study with 31 drivers, reported a strong effect on perceived sportiness for MTM, but not for AESe, compared to baseline.

The AESe in the driving simulator study (Chap 6) was designed as a function of driving speed and thus added relevant speed information to the driver. A plausible explanation for the improved speed control and increased sportiness perception would be that, due to the more rapid change in virtual RPM for AESe compared to Baseline, changes in engine torque were more readily noticed, which in turn improved speed control (see also Hellier et al., 2011 for the influence of engine sound on driving behavior). For the test track study, the reduced impact of additional sound on sportiness perception and speed control could be explained by the fact that AESe did not add relevant speed-related information to the already present (real) engine sound. To improve acceptance and speed control, it is therefore recommended to focus on functional benefits when designing sound characteristics in electric vehicles or sport modes, in addition to sound characteristics, such as loudness, roughness, sharpness, and tonality (Krüger et al., 2004; Kwon et al., 2018).

For MTM, a likely explanation for the reduced acceleration performance perception could be the lack of vestibular feedback when driving in the fixed driving simulator. The changes in acceleration performance could only visually be perceived (i.e., which also results in drivers braking less hard for curves in driving simulators; De Groot et al., 2011; Reymond et al., 2001). On the same note, one could argue that the driving simulator studies in Chapter 2 and 3 lacked physical risk, and thus unrealistic driver adaptations may have occurred. This raises the question whether fixed-based (or even moving-based) driving simulators are sufficient to test driving behavioral adaptations and perception for conditions that affect the vehicle's dynamic behavior and/or road topology. However, in general, the relative validity (i.e., the effect sizes between the pairwise comparisons) is high for simulators and real-world experiments (Klüver et al., 2016), and even studies argue that risk is well perceived in simulation (Walker et al., 2019). In other words, driving simulators can be argued to be useful to test driving behavior and motivation models (cf. Hoyes & Glendon, 1993), however, they are not always sufficient as the results of Chapter 6 and Chapter 7 suggest. Still, many simulator results correlated with real-world results: strong speed adaptations were found between the wide and narrow road sections in both Chapter 2 and 3, similar to adaptations found in on-road experiments (De Waard et al., 1995; Fitzpatrick et al., 2000), and the same throttle driver adaptation was found for Chapter 6 (driving simulator) and Chapter 7 (test-track). For now, it is recommended that future studies on the perception of *longitudinal* vehicle dynamics will be conducted in settings that allow for vestibular feedback such as real vehicles or high-end moving-based simulators (i.e., Reymond & Kemeny, 2000).

Another important limitation of the human factors studies performed in this thesis is that all test track studies (Chap 4, 7, 9) were performed primarily with expert drivers, and all driving simulator studies primarily with students (Chap 2, 3, 6, 8). The student drivers might show little variability compared to a group consisting of students, elderly, or expert drivers together (Carsten & Nilsson, 2001; Wood & Mallon, 2001). Similarly, for Renault expert drivers, there is a risk that this is a sample who was being asked to evaluate a product produced by their

own company, and hence might be biased (even if just subconsciously) in their assessments. Moreover, all experts and students had an engineering background, which might be a population that is more likely to be favorable to technological innovations compared with the average member of the population. Future studies need to test the adaptive driving modes with a larger distribution in participants.

10.4. Extending the Scientific Contributions Towards Design Guidelines for Product Development

The current thesis focussed on location-specific advice and vehicle setting changes in steering gain and powertrain settings. The proactive eco mode (Chap 9) has been patented and is currently being developed further by Renault. Challenges that are being addressed include making the location-specific predictions more robust by investigating the dependence on predicted route navigation (and thus accurate GPS) and the inference of the most likely route. Also, the real fuel benefits of the proactive eco mode compared to normal driving are mapped out for various routes and driving styles.

However, the journey does not end here; there is a big potential for location-specific information, calibrated using the populations driving behavioral data, in future product development. The use of location-specific data allows for adjustments in vehicle settings *before* the setting is required (i.e., by increasing the powertrain settings before the start of the acceleration phase; Chap 9). The use of intelligent location detection systems, and relying on a-priori measured location-specific data has the potential to simplify behavior predictions. Such data alleviate the reliance on often complex computational models which need to sense and interpret the environment in order to predict behavior, and which require rich datasets to train (with the potential lack of generalizability to untrained environments). The proactive method could be extended for other vehicles settings such as: adaptations in steering responsiveness (e.g, Chap 8), vertical dynamics (e.g., to proactively adjust damping parameters for speed bumps), cockpit ambiance settings (e.g., changing the dashboard information when driving offroad), or to provide adaptive route navigation assistance in the vehicle.

Specifically, some follow-up suggestions could be considered for future product development based on the results of this thesis. First, an important challenge with adaptive systems is to keep driver acceptance high even when conflicts occur between the predicted setting and the driver's desired setting, a challenge often highlighted in literature (e.g., Johnson et al., 2014; Kaber & Endsley, 2004; Parasuraman, 2000). Chapter 9 demonstrates how conflicts can be coped with through continuously tracking driver behavior and inferring driver's intention (e.g., in case of a sudden -unpredicted- acceleration request). In future work repeated conflicts could be avoided by *learning* the driver's own location-specific driving behavior (Melman et al., 2020), and learning the desired proactive algorithm parameters. Both tuning the algorithm parameters and personalized location-specific data greatly influence the setting predictions. Figure 10.2, visualizes the future proactive method including learning (box 5). Previous ADAS literature has shown that systems that learn from conflicts can increase driver acceptance (Biondi et al., 2019; Sun et al., 2019).

Second, the results of the proactive eco mode (Chap 9) showed that all drivers received the same PWT settings changes given the location with small variation in start and end position. This is because the arbitrator (box 3; Figure 10.2) decides the appropriate moment to switch to PWT_{normal} (i.e., if the driver's throttle input was low) and to switch back to PWT_{low} (i.e., when current power is low). This suggests that the proactive method could be simplified. The extraction of the database (box 1a and 1b; Figure 10.2), and the calculation of the mode switch (box 1c) could be calculated offline and stored in the cloud. In other words, the proposed proactive powertrain settings (output of box 1c) are then directly provided from

the cloud, where the arbitrator (box 3; Figure 10.2) still decides when and if to execute the proposed proactive vehicle setting. This would reduce computational power, and make the system implementable in almost all vehicles that already have navigation systems. Future studies should investigate the practical benefits and limitations of this online and offline strategy.

Third, this thesis did not look into the influence of the design of the switch between one setting to the other on acceptance of an adaptive driving mode. There is a large design space for how to proactively switch (vehicle) settings, such as the timing (i.e., when to proactively switch the mode), the speed of change, the size of change, the smoothness of change (see also Hou et al., 2015 for an overview of adaptive design considerations). For example, in a study on lane changing, Russell et al. (2016) found that drivers needed several trials to get used to a new steering gain. Future studies should investigate the underlying mechanisms of the transition between vehicle settings while driving.

Fourth, the observed dominant impact of route and vehicle type on fuel consumption (see Conclusion 2) suggests that eco-driving predictors / scores should be normalized to the road environment. Ideally, an eco-score or eco-driving predictor should correlate strongly with fuel consumption and should be interpretable in different road environments and for different vehicles. In other words, when driving in an energy-demanding environment (e.g., mountain), drivers should *not* receive a notification that they drive eco-unfriendly. Of course, such information might still be valid if drivers need to be informed that they selected an eco-unfriendly route, but in practice, drivers may not be able to adjust their route. Similar statements were made by Andrieu and Saint Pierre (2012), Shi et al. (2015), and Dib et al. (2014), who proposed normalizing fuel consumption to the road environment.

10.5. Outlook and Future Research

Apart from future product development, some future research directions might be considered based on the results of this thesis.

The literature on behavioral adaptations typically focuses on the negative adaptations rather than positive behavioral adaptations (cf. Rudin-Brown & Jamson, 2013). For example, the term ‘risk compensation’ (introduced by Elvik et al., 2009 and 17.900 hits on google scholar) is a common way to describe decreased safety, such as faster driving or driving with shorter headways. Rather than focusing on negative behavioral changes a posteriori (e.g., speeding), future research should investigate how adaptive vehicle settings can be used to induce positive behavioral adaptations a-priori. This thesis shows the potential to induce positive behavioral adaptation using adaptive vehicle settings. For example, in Chapter 6 and Chapter 7 drivers used the improved acceleration performance of a vehicle opportunistically: when provided with a better acceleration performance drivers accelerate stronger. In Chapter 9 we used this result in the proactive eco method to accelerate faster and smoother without fuel efficiency degradation over the entire segment. To induce positive behavioral adaptations, requires a good understanding of driver adaptation, and a shift in system design thinking: from optimal vehicle behavior to optimal *joint* human-vehicle behavior. For example, Melman et al. (2018) showed that the safest lane-keeping system does not necessarily be the safest when the driver is in the loop (i.e, drivers tend to increase speed, and diminish the safety benefits). In other words, the safest stand-alone system is not the safest when considering the joint human-vehicle behavior. In theory, an intuitive approach that induces positive behavioral adaptations has the potential to improve long-term behavioral benefits and is considered an important future research direction.

In Chapter 2 and 3, we tested qualitative models and concluded they could not readily be used to predict speed adaptations (see section 10.2.). Alternatively, we could have tested computational models that use large datasets to estimate the model parameters, but have

the potential to quantitatively predict driving behavior. An important reason to not investigate computational models was they often poorly generalize to previously unseen scenarios, and collecting the required training data to parametrize these models can be costly. Despite these limitations, better models are needed that can quantitatively explain the underlying mechanisms of driver adaptations.

Finally, an important issue that can hamper system acceptance of adaptive systems, mentioned in literature, is predictability (Johnson et al., 2014; Chap 8). Please note that in theory, a proactive adaptive system can still allow the driver to make an internal model, as long as the vehicle behaves the same *given the situation*. This is illustrated by Formula 1 designer Adrian Newey (Formula 1 car designer) when he introduced the active suspension, a system that optimizes the ride heights before every corner and straight for the optimal downforce, to his two F1 drivers (Nigel Mansell and Riccardo Patrese). “Both reported that it felt uncommunicative and ... they had to trust it had grip rather than knowing” (Newey, 2017, p. 153). At a point that Nigel Mansell said “I don’t want to race this car, I want to race the passive car” (Newey, 2017, p. 153). In the end, the engineers made sure it was reliable at every corner, and they dominated F1 for two consecutive years (1992 and 1993) until active suspension was banned in 1994.

To conclude, I hope this thesis has contributed to a better insight into the underlying principles of human adaptations, the impact of vehicle dynamic adaptation, and made the first step towards proactive adaptive vehicle settings that makes driving safer, more eco-friendly and more accepted. Regardless of how the future looks, driver acceptance should be central in the development of any driver assistance system. Without acceptance, any technology development will have a smaller impact than desirable or needed.

References

- Andrieu, C., & Saint Pierre, G. (2012). Using statistical models to characterize eco-driving style with an aggregated indicator. In *2012 IEEE Intelligent Vehicles Symposium*. 63-68. IEEE.
- Barendswaard, S. (2021). *Modelling Individual Driver Trajectories to Personalise Haptic Shared Steering Control in Curves* (Doctoral dissertation). <https://doi.org/10.4233/uuid:7292e35d-d45a-4ad1-9663-ae2b5c5a9f16>
- Biondi, F., Alvarez, I., & Jeong, K. A. (2019). Human-vehicle cooperation in automated driving: A multidisciplinary review and appraisal. *International Journal of Human-Computer Interaction*, *35*, 932-946.
- Carsten, O. M. J., & Nilsson, L. (2001). Safety assessment of driver assistance systems. *European Journal of Transport and Infrastructure Research*, *1*, 225-243.
- De Groot, S., de Winter, J. C., Mulder, M., & Wieringa, P. A. (2011). Nonvestibular motion cueing in a fixed-base driving simulator: Effects on driver braking and cornering performance. *Presence*, *20*, 117-142.
- De Waard, D., Jessurun, M., Steyvers, F. J., Reggatt, P. T., & Brookhuis, K. A. (1995). Effect of road layout and road environment on driving performance, drivers' physiology and road appreciation. *Ergonomics*, *38*, 1395-1407
- Dib, W., Chasse, A., Moulin, P., Sciarretta, A., & Corde, G. (2014). Optimal energy management for an electric vehicle in eco-driving applications. *Control Engineering Practice*, *29*, 299-307.
- Elvik, R., Vaa, T., Høy, A., & Sørensen, M. (Eds.). (2009). *The handbook of road safety measures*. Emerald Group Publishing.
- Fitzpatrick, K., Carlson, P. J., Woolridge, M. D., & Brewer, M. A. (2000). *Design factors that affect driver speed on suburban arterials*, (No. FHWA/TX-00/1769-3).
- Hellier, E., Naweed, A., Walker, G., Husband, P., & Edworthy, J. (2011). The influence of auditory feedback on speed choice, violations and comfort in a driving simulation game. *Transportation Research Part F: Traffic Psychology and Behaviour*, *14*, 591-599.
- Hilgers, C., Brandes, J., Ilias, H., Oldenettel, H., Stiller, A., & Treder, C. (2009). Active air spring suspension for greater range between adjusting for comfort and dynamic driving. *ATZ Worldwide*, *111*, 12-17.
- Hou, M., Banbury, S., & Burns, C. (2015). Intelligent adaptive systems: An interaction-centered design perspective. CRC Press.
- Hoyes, T. W., & Glendon, A. I. (1993). Risk homeostasis: issues for future research. *Safety Science*, *16*, 19-33.
- Jeon, B. W., Kim, S. H., Jeong, D., & Chang, J. Y. I. (2016). *Development of Smart Shift and Drive Control System Based on the Personal Driving Style Adaptation* (No. 2016-01-1112). SAE Technical Paper.
- Johnson, M., Bradshaw, J. M., Feltovich, P. J., Jonker, C. M., Van Riemsdijk, M. B., & Sierhuis, M. (2014). Coactive Design: Designing Support for Interdependence in Joint Activity. *Journal of Human-Robot Interaction*, *3*, 43.
- Kaber, D. B., & Endsley, M. R. (2004). The effects of level of automation and adaptive automation on human performance, situation awareness and workload in a dynamic control task. *Theoretical Issues in Ergonomics Science*, *5*, 113-153.
- Klüver, M., Herrigel, C., Heinrich, C., Schöner, H. P., & Hecht, H. (2016). The behavioral validity of dual-task driving performance in fixed and moving base driving simulators. *Transportation research part F: traffic psychology and behaviour*, *37*, 78-96.
- Krüger, J., Castor, F., & Müller, A. (2004). Psychoacoustic investigation on sport sound of automotive tailpipe noise. *Fortschritte der Akustik-DAGA* (pp. 233-234). Strasbourg, France.
- Kwon, G., Jo, H., & Kang, Y. J. (2018). Model of psychoacoustic sportiness for vehicle interior sound: Excluding loudness. *Applied Acoustics*, *136*, 16-25.
- Melman, T., Beckers, N., & Abbink, D. (2020). *Mitigating undesirable emergent behavior arising between driver and semi-automated vehicle*. arXiv. <https://arxiv.org/abs/2006.16572>
- Melman, T., De Winter, J. C. F., & Abbink, D. A. (2018). Does haptic steering guidance instigate speeding? A driving simulator study into causes and remedies. *Accident Analysis & Prevention*, *98*, 372-387.
- Newey, A. (2017). *How to build a car*. Harper Collins.
- Parasuraman, R. (2000). Designing automation for human use: empirical studies and quantitative models. *Ergonomics*, *43*, 931-951.
- Reymond, G., & Kemeny, A. (2000). Motion cueing in the Renault driving simulator. *Vehicle System Dynamics*, *34*, 249-259.
- Reymond, G., Kemeny, A., Droulez, J., & Berthoz, A. (2001). Role of lateral acceleration in curve driving: Driver model and experiments on a real vehicle and a driving simulator. *Human factors*, *43*, 483-495.
- Rudin-Brown, C., & Jamson, S. (Eds.). (2013). *Behavioural adaptation and road safety: Theory, evidence and action*. CRC Press.
- Russell, H. E., Harbott, L. K., Nisky, I., Pan, S., Okamura, A. M., & Gerdes, J. C. (2016). Motor learning affects car-to-driver handover in automated vehicles. *Science Robotics*, *1*, eaah5682.
- Shi, B., Xu, L., Hu, J., Tang, Y., Jiang, H., Meng, W., & Liu, H. (2015). Evaluating driving styles by normalizing driving behavior based on personalized driver modeling. *IEEE Transactions on Systems, Man, and Cybernetics: Systems*, *45*, 1502-1508.
- Sun, Q., Zhang, H., Li, Z., Wang, C., & Du, K. (2019). ADAS acceptability improvement based on self-learning of individual driving characteristics: a case study of lane change warning system. *IEEE Access*, *7*, 81370-81381.
- Trimpop, R. M. (1996). Risk homeostasis theory: problems of the past and promises for the future. *Safety Science*, *22*, 119-130.
- Walker, F., Hausbauer, A. L., Preciado, D., Martens, M. H., & Verwey, W. B. (2019). Enhanced perception of risk in a driving simulator. *International journal of human factors modelling and simulation*, *7*, 100-118.
- Wood, J. M., & Mallon, K. (2001). Comparison of driving performance of young and old drivers (with and without visual impairment) measured during in-traffic conditions. *Optometry and Vision Science*, *78*, 343-349.

CURRICULUM VITAE

Education

- 2018 – 2022 Ph.D. Cognitive Robotics
Delft University of Technology, Group Renault, Ensta Paris
Thesis title: Towards Proactive Adaptive Vehicle Settings
- 2013 – 2016 M.Sc. Mechanical Engineering (**Cum Laude**)
Delft University of Technology
Thesis title: Does haptic steering guidance instigate speeding?
- 2011 – 2013 B.Sc. Mechanical Engineering (**Cum Laude**)
Delft University of Technology
- 2010 – 2011 Propadeuse (**Cum Laude**)
Delft University of Technology
- 2004 – 2010 Voorbereidend Wetenschappelijk Onderwijs (VWO)
Het Veenlanden College, Mijdrecht

Experiences

- 2016 – 2018 Research Engineer
Delft University of Technology
- 2015 Traineeship USA
Entropy Control Inc., San Diego

LIST OF PUBLICATIONS

Journal Publications

1. **Melman, T.**, Abbink, D. A., Van Paassen, M. M., Boer, E. R., & De Winter, J. C. F. (2018). What determines drivers' speed? A replication of three behavioural adaptation experiments in a single driving simulator study. *Ergonomics*, 61, 966–987. <https://doi.org/10.1080/00140139.2018.1426790> (Chapter 2)
2. **Melman, T.**, Abbink, D. A., Mouton, X., Tapus, A., & De Winter, J. C. F. (2021). Multivariate and location-specific correlates of fuel consumption: A test track study. *Transportation Research Part D: Transport and Environment*, 92, 102627. <https://doi.org/10.1016/j.trd.2020.102627> (Chapter 4)
3. **Melman, T.**, De Winter, J. C. F., Mouton, X., Tapus, A., & Abbink, D. A. (2021). How do driving modes affect the vehicle's dynamic behaviour? Comparing Renault's MultiSense sport and comfort modes during on-road naturalistic driving, *Vehicle System Dynamics*, 59, 485–503. <https://doi.org/10.1080/00423114.2019.1693049> (Chapter 5)
4. **Melman, T.**, Visser P. J. D., De Winter, J. C. F. (2021). Creating the Illusion of Sportiness: Evaluating Modified Throttle Mapping and Artificial Engine Sound for Electric Vehicles. *Journal of Advanced Transportation*, 2021, 4396401. <https://doi.org/10.1155/2021/4396401> (Chapter 6)
5. **Melman, T.**, Tapus, A., Jublot, M., Mouton, X., Abbink, D. A., & De Winter, J. C. F. (2022). Do sport modes cause behavioral adaptation? *Transportation Research Part F: Traffic Psychology and Behaviour*. <https://doi.org/10.1016/j.trf.2022.07.017> (Chapter 7)
6. **Melman*, T.**, Weijerman*, M. P. P., De Winter, J. C. F., & Abbink, D. A. (2022). Should steering settings be changed by the driver or by the vehicle itself? *Human Factors*. <https://doi.org/10.1177/00187208221127944> (Chapter 8)
7. **Melman*, T.**, Beckers*, N. W. M., De Winter J. C. F., Mouton, X., & Abbink, D. A. (2022). A proactive method to assist eco-driving. Manuscript submitted for publication (Chapter 9)
8. **Melman, T.**, De Winter, J. C. F., & Abbink, D. A. (2018). Does haptic steering guidance instigate speeding? A driving simulator study into causes and remedies. *Accident Analysis & Prevention*, 98, 372–387. <https://doi.org/10.1016/j.aap.2016.10.016>
9. Van Gent, P., **Melman, T.**, Farah, H., Van Nes, N., & Van Arem, B. (2018). Multi-level driver workload prediction using machine learning and off-the-shelf sensors. *Transportation Research Record*, 2672, 141–152. <https://doi.org/10.1177/0361198118790372>

Peer-Reviewed Conference Papers

10. **Melman*, T.**, Kolekar*, S. B., Hogerwerf, E. W. M., & Abbink, D. A. (2020). How road narrowing impacts the trade-off between two adaptation strategies: Reducing speed and increasing neuromuscular stiffness. *Proceedings of the 2020 IEEE International Conference on Systems, Man, and Cybernetics* (pp. 3235–3240). Toronto, Canada. <https://doi.org/10.1109/SMC42975.2020.9283172> (Chapter 3)

Workshop Papers

11. **Melman*, T.**, Beckers*, N. W. M., & Abbink, D. A. (2020). Mitigating undesirable emergent behavior arising between driver and semi-automated vehicle. *arXiv*. <https://arxiv.org/abs/2006.16572>

Patents

12. Beckers* N. W. M., **Melman*, T.**, Abbink, D. A., & Mouton, X. (2022). *ProActive Driving Mode* (French Patent No. FR2200162). Renault SAS

*Equal contribution

ACKNOWLEDGEMENTS

Saturday, September 24th, 2022 - the last part of my journey called “PhD”.

When I started four years ago, I could not have imagined all the amazing highs (and lows) I would experience when David finally convinced me of doing a PhD (after first 2 years of being a research engineer in his lab). During all these highs and lows, many people have been essential to keep me on the right path. I have made friends for life and have seen the best in people during my serious struggles with my French-Dutch contract (hereafter called “struggles”). This is my moment to thank you all.

First, I would like to thank my Promotor **David**. David, you have been an inspiration to me since I started my MSc back in 2016. During my struggles, you have proven to be more than just a great scientist but mostly a great person. You stepped forward to help me without limits. Your advice to not think in terms of output but in terms of what would make me happy, resulted in the amazing collaboration with Niek and resulted in me realizing how much I love science. The evening we celebrated the successful demo at Renault together is a memory I hold dear. I truly thank you for everything David, it was an amazing ride that would not have ended this way if it wasn't for your people skills and devotion to your PhD students.

Second, I owe a lot to my Promotor **Joost**. Your amazing drive to deliver high-quality research has motivated me greatly. You showed me the eye for detail it takes to become a good researcher. The best advice during my PhD came from you: ‘Maybe it is time to stop making these fuzzy schemes and start writing a paper’. Your input helped me to find the balance between deep thinking and writing throughout the four years. Without your devotion to this thesis, I would not have managed to finish it in four years. I also thank you for your openness when we agreed to disagree. We had several scientific “fights” but I have the feeling this brought us closer to publishing and always improved our mutual understanding.

Xavier, you initiated this collaboration and are therefore the fundament of this thesis. You have always given me the warmest welcome when I visited Renault. From organizing creative sessions (sometimes you had 30 new ideas in one day) to a walk around Versailles with your wife Karline – you made me feel at home. I have seen your belief in this PhD and dedication to assure that people throughout Renault were involved with proMEX. I am proud we worked on a patented product that hopefully will be integrated into future Renault cars. Moreover, I also want to use this moment to thank all the engineers and researchers that have helped me prepare the experiments and cars. Merci beaucoup! (Good thing I did a French course for three years).

Finally, from my supervising team, I would like to thank my co-promotor **Adriana**. Due to COVID-19, I was less able to visit ENSTA in person, but despite this, you were always willing to provide feedback when needed. Your presence during the test of the self-adapting driving mode at Renault was a memorable way to celebrate the tri-party collaboration.

Niek and **Sarvesh**, whom I both consider more as friends than colleagues. Niek, this thesis owes you a lot. Without you, Chapter 10 would not have been possible. The speed of discussions and prototyping we did was addictive. I sometimes wish you could see yourself through my eyes. You are the cleverest and most modest person I have met (you probably read this and think ‘Ah that is not true’). ‘The big friendly giant’ has a face from now on. The “almond joke” is something that we pulled your leg over, but I quickly learned that you are often right in what you say, so I better keep listening.

Then Mr. S. Despite winning from me with ping-pong in the lab (sorry to my other colleagues), I really enjoyed our time in the lab. Your practical jokes, the many coffee breaks, walks, and the lunches on the haptic hill (often with a 100 points croissant for you) are one of the many memories I hold dear. You are someone I can always rely on for a quick talk. Even now, while you are 7000 km away, you kept on asking how my PhD and life were going and were involved. Unexpectedly, these informal talks often ended in useful brainstorming or

recently getting me into a new job at TomTom. I look forward to what we will come up with in our future talks! Before you know: world peace.

I also would like to thank my MSc students whom I had the pleasure to supervise: **Peter, Mark, Rik, Ellen, Roderick, and Sam**. You all have an important (direct or indirect) contribution to this thesis. Peter and Mark, your MSc theses are the fundament for Chapters 6 and 8, respectively. Thank you all for your collaboration and enthusiasm. It gives me great pleasure to see you are doing so well. Ellen even won an Olympic medal, although I do admit that I probably had nothing to do with that part.

Joris ‘handyman’ Giltay. On a serious note, I want to thank you for your essential work with the new driving simulator in which Mark, Peter, and Sam conducted their studies. On a less serious note, I want to thank you for your superpower: talking without listening. Since you joined the lab, I became more productive during my 45 min train ride than during the rest of the day. Nevertheless, I could always count on you. You even visited me when I was a candidate for the “Mekel prize“. I didn’t win but fortunately, there was a musical interlude of 45 min and a speech of 2h, and I quote ... end quote.

Rosanne and Hanneke, I want to thank you for being so passionate about the well-being of the entire group. Rosanne, you have helped me tremendously during my “struggles” and Hanneke you made me feel part of the COR group, even though I had a French contract. Please do not underestimate how much the gesture meant to also receive the small gift during Christmas.

Finally, too many people have been around in the lab that assured me that I went with a big smile to my work and came home with an even bigger one. To name a few: **Bastiaan, Sarah, Marco, Gaia, Hugo, Elco, Sjors, Marijke, Karlijn, Stijn, Dirk, Arkady, Olger, Wietske, Tom**, and many more! You people have been essential to a culture in which doing a PhD did not feel like a lonesome job anymore. From participating in a pattern recognition course with Sarah to being on the first row when our cuckoo bird Elco made an inappropriate joke; I enjoyed every moment of it.

From the lab to my friends and family at home. **Vincent**, my big nephew. This thesis would have finished much sooner if it were not for you. We both found out during COVID-19 that we have the skill to talk endlessly about nothing in particular. Our 10 o’clock coffee talks about Ajax, the farm of our family, and our personal lives have become part of a great weekly routine.

I also want to thank all my friends who have the ability to take me out of my academic bubble with one single joke. A special thanks to my dear friends **Pascal, Robin, Wester, and Bob** who extensively asked about the PhD and always supported me during the highs and lows of this journey. I also want to thank **Jean, Mathilde, and Mitchell** for being my second family and home.

Chardé deserves a special place in this acknowledgment. When I asked Studio CB to help me with the design, I could not have imagined the countless hours we would spend deciding about font type/size/spacing, and many more. It opened my eyes to the difficulty of graphical design and what a talented person you are. Thank you for this great design.

Pap, Mam en Nadine, jullie zijn onbeschrijfelijk belangrijk voor mij. Nadine – mijn grote zus – wij hebben iets speciaals wat niet te beschrijven is in één zin. Ik weet je te vinden als ik zoekende ben en jij mij. Pap en Mam, zonder jullie basis en onvoorwaardelijke liefde had ik hier nooit gestaan. Mam, jij weet als geen ander wat het betekent om een PhD-thesis te schrijven. Ik ben trots dat ik in jouw voetsporen mag treden, al zal mijn thesis nooit dezelfde impact hebben. Van jouw dankwoord weet jij als geen ander de echte impact van deze woorden: *“Wat ben ik blij dat jullie dit moment mee kunnen maken”*.

Dan als laatste mijn Melis. Zonder jouw support en overtuiging was ik niet aan een PhD begonnen. Je zag het helemaal niet zitten dat ik zoveel naar Frankrijk zou moeten reizen, maar was toch de eerste die zei dat ik het moest doen. Je hebt een ongelooflijk groot hart en ik ben dankbaar dat daarin zo'n groot plekje voor mij is gereserveerd. De wederzijdse liefde en support is er altijd zonder dat we het expliciet hoeven te zeggen. Echter wil ik dit moment gebruiken om dat toch eens te doen: Ik hou van je. Ik zie jou als ik naar Siem kijk en dat maakt mij de gelukkigste persoon op aarde.

Bien amicalement,

Timo